Design and Synthesis of Novel Compounds to Inhibit CSF-1R

&

Evaluation of Novel Substrates and Reactivities in NHC Catalysis

A thesis submitted by:

Robert Wen Ming Davidson

In partial fulfilment of the requirements for the degree of:

Doctor of Philosophy

November 2014

Department of Chemistry
Imperial College London
South Kensington
London
SW7 2AZ

Declaration of Originality

I, Robert Davidson, confirm that the work presented within this thesis is entirely my own, conducted at Imperial College London, Department of Chemistry under the supervision of Dr Matthew J. Fuchter, unless otherwise stated. All work not performed by the author has been acknowledged within the text and has been appropriately and adequately cited.



Robert W. M. Davidson

London, 1st November 2014

Copyright Declaration

The copyright of this thesis rests with the author and is made available under a Creative Commons Attribution Non-Commercial No Derivatives licence. Researchers are free to copy, distribute or transmit the thesis on the condition that they attribute it, that they do not use it for commercial purposes and that they do not alter, transform or build upon it. For any reuse or redistribution, researchers must make clear to others the licence terms of this work.

Abstract

Chapter I describes work undertaken on a Medicinal Chemistry project studying the small molecule inhibition of the protein CSF-1R. Initial computational work, using the Cresset software package, involved modeling the key steric and electrostatic properties of compounds known to bind to the active site of the target enzyme, CSF-1R. The subsequent use of a virtual (computational) screen, provided new chemotypic scaffolds, which were used as starting points for structure activity relationship (SAR) exploration. Synthetic chemistry routes were designed and optimised towards analogues of promising compound "hits" focusing on the potential to introduce diversified structural features and the diminution of synthetic steps. This included the construction of an uncommon heterocyclic core motif and efforts to understand and control the regioselectivity of its formation.

Chapter II concerns a synthetic methodology project in the area of N-heterocyclic carbene (NHC) catalysis. Work on this project included the development of a novel methodology for the formation of amide bonds using an internal redox approach. This involved the activation of an α-reducible aldehyde with an NHC to form an acyl azolium and subsequent trapping of this intermediate with amine nucleophiles. The hypothesis to be studied was that previous attempts at performing similar transformations with these substrates had been hampered by incompatibility of the aldehyde and amine reagents leading to unwanted condensation side reactivity; thus the main focus of this work was to provide an *in situ* slow release of the amine nucleophile by masking it as a carbamate that would gradually extrude CO_2 under the reaction conditions releasing the amine. The other project discussed in this chapter involves the use of hemiacetals as masked aldehydes, in particular within carbohydrates, due to their natural abundance, making them a cheap source of fixed stereocentres.

Acknowledgements

I would like to thank Dr Matt Fuchter for the opportunity to carry out the work contained within this thesis as a member of his group. I am extremely grateful for his enduring support, patience and guidance over the past four years as well as the freedom and enthusiasm given to pursue ideas which I found interesting during my studies.

I am also thankful for the generous funding granted by Cancer Research UK

Importantly, I wish to recognise the contributions of my collaborators for the FMS work: Dr Caroline Low, Rakhee Chauhan & Dr Nick Dibb, Dr Olan Dolezal, Dr Bin Ren & Dr Tom Peat. Without their expertise, it would not have been possible to undertake such a project.

For their invaluable help and assistance, I would like to thank the analytical staff Dr Lisa Haigh, Pete Haycock and Dick Sheppard.

My time at Imperial College would not have been the same without the people I've shared the experiences with. For all the memories, I'd like to thank all of the past and present members of the Fuchter and Barrett groups that I've had the chance to work with, starting with a great lab 742 – Fanny, Paolo, Marko and Jez, the guys who helped me get up and running – Dr Christmas, Matty Baud, Dil & Tom, Miss Dirtee JoJo & Nico, Hideki, Jullien, Marianne, Christine, Okanya, Jensy, Malte, Brian, Liz, Jenny, Dr Batt, Alex Bandle, Andy Bayly, Albert, Geoffrey B. More recent excellent people Ken, Kate, Claire, Thom, Dan, Nicole, Jamie G, Dr Daniel Craig (Elliott), Josh, Sandeep, Jochen, Rob "the oracle" Richardson, the China crew Rosa and James. Special mentions to Big Bro DrAP, Bhav, Dr Matthew Matthew Penny, Dr Brookes, Dr Cordier, Dr Andreas Doepner who is a great organic chemist and a great human being by any standard, and the one's who I started and finish with, Lauriane (Dr Bubajeon), President Joe, Lee (sort of but we'll count it) and co-founder of the superbay Dr Pete Blencowe – we've been through a lot together!

Thanks again to my proofreaders Paul, Matt and Jochen and previous mentors Carmen and Hawa.

Outside the lab, Andy, Alex, Little Pete and Jo, Nick and Liz, Stolli, Ryan and Dave, you will understand this about as much as I understand what you do for a living (apart from Dave who does spying).

My family - Mum, Dad, Grandma, Mama, Mike & Sarah (+ 1) thanks for your love and support, I hope this makes you proud.

Stef, I don't want to embarrass you – you're great and thanks for everything.

This thesis is dedicated to Tan Hock Sai

Contents

Abstract **4**

Acknowledgements **5**

Abbreviations **11**

Chapter I – Design and Synthesis of Novel Compounds to Inhibit CSF-1R **14**

1 Introduction **14**

1.1 FMS – Colony Stimulating Factor 1 Receptor **14**

1.2 Tumour Associated Macrophages **15**

1.3 Targeting FMS with Small Molecule Inhibitors **17**

1.3.1 Kinases as Drug Targets 17

1.3.2 Active vs. Inactive conformers 18

1.3.3 Kinase Inhibitor Types 19

1.3.4 Binding sites in FMS 19

1.4 Computer-Aided Drug Design (CADD) **21**

1.4.1 Docking & Schrödinger Suite 21

1.4.2 Cresset Field Point Templating & Virtual Screen 21

1.5 Biological assays **23**

1.5.1 Cell Growth Assay 23

1.5.2 Phosphorylation Assay 24

1.6 Project Plan **24**

2 Results & Discussion **26**

2.1 Reference compounds **26**

2.1.1 DFG-in reference compound **1** 26

2.1.2 Synthesis of DFG-out compound **2** 29

2.1.3 Cresset Search molecule **3** 30

2.2 Virtual Screening **31**

2.2.1 FieldPoint Templating 31

2.2.1.1 Generation of template from de novo computationally calculated binding pose 32

2.2.1.2 Assignment of FieldPoints to the existing 3-D structure 34

2.2.2 Cresset Search Template 36

2.3 Selection of Lead Series **36**

2.4 Sulfonamide Series **38**

2.4.1 Orientation of sulfonamide series structures 39

2.4.2 Retrosynthetic analysis of sulfonamide series 41
2.4.3 Preparation of sulfonamide series analogues 42
2.4.3.1 General synthesis of compounds of the sulfonamide series 42
2.4.3.2 Analogue selection for SAR generation 42
2.4.4 Synthesis of chiral amine motifs 45
2.4.5 Summary of sulfonamide series 48
2.5 Triazolopyrimidone series 49
2.5.1 Orientation of triazolopyrimidone analogues 49
2.5.2 Disconnection and synthesis of heterocyclic core 50
2.5.3 Regiochemistry of triazolopyrimidone structures 51
2.5.4 Triazolopyrimidone core synthesis 51
2.5.4.1 Synthesis and assignment of heterocyclic regioisomers 51
2.5.4.2 Incorporation of functional handle onto heterocyclic core 53
2.5.4.3 Use of diethyl (ethoxymethylene)malonate as alternative Michael acceptor 55
2.5.5 Summary of triazolopyrimidone series 56
2.6 Biological Assessment 57
2.7 X-ray crystallographic data 59
3 Conclusions and Future Work (Chapter I) 60
Chapter II – Evaluation of Novel Substrates and Reactivities in NHC Catalysis 62
4 Introduction 62
4.1 Background 62
4.1.1 Triplet Carbene vs. Singlet Carbene Multiplicity 63
4.1.2 Stabilised Singlet Carbenes 64
4.1.2.1 Bertrand's Phosphinosilyl Carbene 64
4.1.2.2 Wanzlick's N-Heterocyclic Carbenes 65
4.1.2.3 Arduengo's Stable N-Heterocyclic Carbene 66
4.1.3 Electronic Stabilisation of NHCs 66
4.1.4 Carbene vs. Ylide Representation 67
4.1.5 Generation of N-Heterocyclic Carbenes 69
4.1.6 NHCs as Nucleophilic Carbenes 70
4.2 Synthetic Applications of N-Heterocyclic Carbenes 70
4.2.1 NHC Coordination to Transition Metals 70
4.2.2 NHC–Non-Metallic Element Adducts 71
4.3 Organocatalysis with NHCs 72

4.3.1 Reactive Species Formed from the Breslow Intermediate 74
4.3.1.1 Acyl anion 74
4.3.1.2 Acyl Azolium 75
4.3.1.3 Azolium Enolate 77
4.3.1.4 Azolium Homoenolate 77
4.3.2 Carbonyl Containing Electrophilic Substrates 78
4.4 Redox Acylation 80
4.5 Project Aims 81
5 NHC-Catalysed Redox Amidation 82
5.1 Background 82
5.2 Current Redox Amidation Approaches 84
5.2.1 Co-catalyst Relay Redox Amidations 84
5.2.1.1 Use of Functionalised Aldehydes as NHC-Catalysed Redox Active Substrates 85
5.2.1.2 Use of α'-Hydroxyenones as Substrates 86
5.2.2 Kinetic Resolution of Amines 87
5.2.2.1 Chiral NHC with Achiral Co-catalyst 88
5.2.2.2 Achiral NHC with Chiral Co-catalyst 88
5.3 Proposed Direct Redox Amidation Approach 88
5.3.1 Masked Nucleophile Hypothesis 89
5.4 Results and Discussion – NHC-catalysed Redox Amidation 90
5.4.1 Assessment of α-*O*-Carbamoyl Aldehyde Substrates 90
5.4.1.1 Proposed Catalytic Cycle with α-*O*-Carbamoyl Aldehyde Substrates 92
5.4.1.2 Preparation of 2° α-*O*-Carbamoyl Aldehyde Substrates 93
5.4.1.3 Preparation of 3° α-*O*-Carbamoyl Aldehyde Substrates 94
5.4.2 NHC-Catalysed Reactivity of α-*O*-Carbamoyl Aldehyde Substrates 97
5.4.2.1 Base and Triazolium Compatibility 97
5.4.2.2 Synthesis of Alternative Triazolium Precatalysts 99
5.4.2.3 Optimisation of Formal Intramolecular NHC-catalysed Redox Amidation 100
5.4.2.4 Formation of Hydrolysis Products 102
5.4.2.5 Summary 107
5.4.3 Intermolecular NHC-Catalysed Redox Amidation 107
5.4.3.1 Redox amidation reactions using α,α-Dichlorohydrocinnamaldehyde (**137**) 109
5.4.3.2 Amine Substrate Scope 112
5.4.3.3 Synthesis and Reactions of α-Chloroaldehyde Substrate **238** 114
5.4.3.4 Synthesis of α-Aroyloxyaldehyde Substrate **243** 115

5.4.3.5 Summary of Intermolecular NHC-catalysed Redox Amidation 117

6 Activation of Carbohydrates for NHC-catalysed Redox Acylation 118

6.1 Carbohydrate Lactols as Masked Aldehydes 118

6.2 Reactions of NHCs with Masked Aldehydes 119

6.3 Redox Esterification of Carbohydrate Monosaccharide Lactols using NHCs 120

6.3.1 Attempted Reactions with 2,3,4,6-tetra-*O*-Substituted Glucose derivatives 121

6.4 Summary of NHC-catalysed Reactions with Carbohydrate Lactol Substrates 126

7 Conclusions and Future Work (Chapter II) 127

8 Experimental 128

8.1 General Comments 128

8.2 Experimental Procedures – Chapter I 129

8.3 Experimental Procedures – Chapter II 155

References 180

Abbreviations

Δ	Heat
Ac	Acetyl
AD-mix	Asymmetric dihydroxylation mixture
Alloc	Allyloxycarbonyl
aq	Aqueous
Asp (D)	Aspartatic acid
ATP	Adenosine Triphosphate
Bn	Benzyl
Boc	*tert*-Butyloxycarbonyl
Bu	Butyl
c-	Cyclo-
CADD	Computer-aided drug design
Cbz	Carboxybenzyl
CDI	*N*,*N*'-Carbonyldiimidazole
CSF-1	Colony Stimulating Factor 1
CSF-1R	Colony Stimulating Factor 1 Receptor
Cys (C)	Cysteine
DABAL-Me_3	DABCO-trimethylaluminium adduct
DABCO	1,4-Diazabicyclo[2.2.2]octane
DBU	1,8-Diazabicyclo[5.84.0]undec-7-ene
DCM	Dichloromethane
$(DHQ)_2PHAL$	Hydroquinine 1,4-phthalazinediyl diether
$(DHQD)_2PHAL$	Hydroquinidine 1,4-phthalazinediyl diether
DiPEA	Diisopropylethylamine
DMAP	4-Dimethylaminopyridine
DMDO	3,3-Dimethyldioxirane
DME	1,2-Dimethoxyethane
DMF	*N*,*N*-Dimethylformamide

DMSO	Dimethylsulfoxide
dppf	1,1'-Bis(diphenylphosphino)ferrocene
EDCI	1-Ethyl-3-(3-dimethylaminopropyl)carbodiimide
eq.	Equivalents
Et	Ethyl
FLP	Frustrated Lewis pair
Fmoc	Fluorenylmethyloxycarbonyl
FMS	See CSF-1R
Gly (G)	Glycine
Hex	Hexyl
HFIP	1,1,1,3,3,3-Hexafluoro-2-propanol
HOAt	1-Hydroxy-7-azabenzotriazole
HOBt	1-Hydroxybenzotriazole
i-	*iso*-
IC_{50}	Half-maximum inhibitory concetration
IR	Infrared
µWave	Microwave (irradiation)
m-	*meta*-
M-CSF	Macrophage Colony Stimulating Factor
M-CSFR	Macrophage Colony Stimulating Factor Receptor
*m*CPBA	*meta*-Chloroperbenzoic acid
Me	Methyl
Mes	Mesityl (2,4,6-trimethylphenyl)
MS	Mass spectrometry
NCS	*N*-Chlorosuccinimide
NHC	N-Heterocyclic carbene
NIS	*N*-Iodosuccinimide
NMP	*N*-Methyl pyrrolidinone
NMR	Nuclear magnetic resonance
o-	*ortho*-

p-	*para*-
PBM	Petasis-borono-Mannich
PDB	Protein Data Bank
PE	Petroleum ether
Pent	Pentyl
Ph	Phenyl
Phe (F)	Phenylalanine
PhMe	Toluene
piv	Pivaloyl (trimethylacetyl)
PMA	Phosphomolybdic acid
PMB	*para*-Methoxybenzyl
PMP	*para*-Methoxyphenyl
PNP	*para*-Nitrophenyl
Pr	Propyl
RTK	Receptor tyrosine kinase
SAR	Structure activity relationship
SKI	Small kinase inhibitor
SPR	Surface plasmon resonance
t- or *tert*-	Tertiary
t-BSA	*tert*-Butylsulfinamide
TCP	2,4,6-Trichlorophenyl
TEMPO	(2,2,6,6-Tetramethylpiperidin-1-yl)oxy
THF	Tetrahydrofuran
Thr (T)	Threonine
TKI	Tyrosine kinase inhibitor
TMS	Trimethylsilyl

Chapter I – Design and Synthesis of Novel Compounds to Inhibit CSF-1R

1 Introduction

This chapter details the targeting of the macrophage colony stimulating factor (colony stimulating factor 1) receptor. As this protein has been implicated in the aetiology of a number of diseases including several forms of cancer, there is a clear therapeutic benefit to be gained through understanding the effects of inhibiting its activity.[1] The approach taken uses computational techniques from Cresset and Schrödinger to enable identification of new chemotypes that inhibit CSF-1R and would allow expansion of initial hits into libraries of analogues for structure activity relationship (SAR) data generation and analysis.

1.1 FMS – Colony Stimulating Factor 1 Receptor

The colony stimulating factor 1 receptor (CSF-1R or FMS), encoded by the *c-fms* protooncogene[2] (the cellular homologue of the *v-fms* oncogene product of the Feline McDonough Sarcoma virus)[3] is predominantly found in hematopoietic cells and cells in the female reproductive tract.[4,5] It is a type III transmembrane receptor tyrosine kinase (RTK) and as such is of the same family as PDGF, c-KIT and FLT-3 kinases.[6]

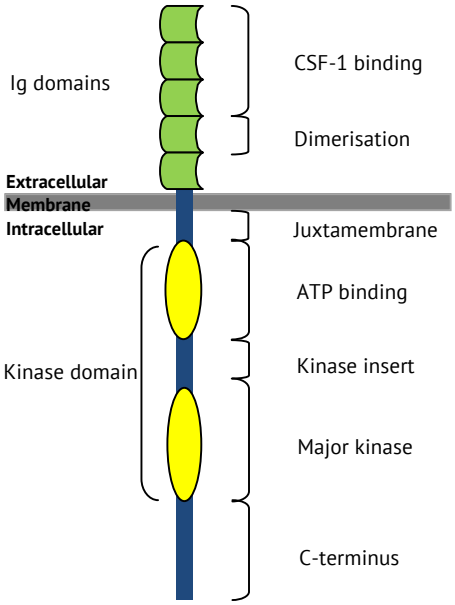


Figure 1. Representation of CSF-1R structural domains. (Adapted graphic)[1]

Structurally it is typical of type III RTKs comprising 5 extracellular immunoglobulin (Ig) domains which bind to the CSF-1 ligand, a transmembrane domain and a juxtamembrane domain joining the transmembrane segment to the intracellular tyrosine kinase domain which is divided in two by a kinase insert domain (Figure 1).[2,6] When folded into its tertiary

structure, the protein is arranged into two lobes. The N lobe is primarily made up of α strands with one β helix while the larger C lobe is predominantly helical. A short strand creates a flat cleft between the two lobes known as the hinge region where the cofactor adenosine triphosphate (ATP) binds in order to phosphorylate key residues through transfer of its terminal phosphate group to the protein (Figure 2).[7]

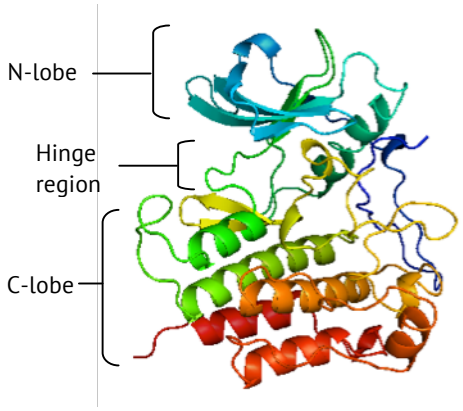


Figure 2. Crystal structure of FMS highlighting N- and C- lobes and ATP-binding cleft. (PDB code: 2OGV).

FMS also contains a C-terminal regulatory domain. CSF-1 is also known as macrophage colony stimulating factor (M-CSF) and when bound to FMS induces homodimerisation and trans-autophosphorylation of several tyrosine residues in the receptor's intracellular kinase domain which upon conformational changes enables docking and phosphorylation of downstream signalling molecules including the MAPK (mitogen-activated protein kinase) and PI3K (phosphoinositide 3-kinase) pathways which are involved in cancer if improperly regulated.[8] FMS and CSF-1 are responsible for regulating the key functions for macrophage proliferation, survival and action, including differentiation of the monocyte-macrophage series.[9,10]

1.2 Tumour Associated Macrophages

Macrophages can be differentiated into two classes of "polarised" macrophages: activated (M1) and alternatively activated (M2) macrophages.[11] M1 macrophages are biased towards an inflammatory response and are microbicidal by means of generation of reactive oxygen species and nitric oxide (NO), which enables the destruction of pathogens and cells. M2 macrophages have immunomodulator characteristics tending towards wound healing and antibody production; as such they are poorly microbicidal.[12] These properties involved in healing are thought to predispose M2 macrophages to stimulate tumour progression, therefore the M2 phenotype is generally considered to be the polarisation of tumour

associated macrophages (TAMs).[13,14] As M2 polarisation is induced by CSF-1, this makes FMS an interesting potential target for anti-cancer therapeutic agents. There is growing evidence that TAMs can aid tumour growth and survival through production of growth signals and by angiogenesis such as during the "angiogenic switch", a rapid increase in blood vessel production from benignity to malignancy in tumours.[15,16] Both "self-sufficiency in growth signals" and "sustained angiogenesis" should be noted as being two of the "Hallmarks of Cancer" as laid out in the seminal publications by Hanahan and Weinberg.[17,18] Studies have also seen that CSF-1 is expressed in many tumours at high levels and correlates with poor prognosis.[19,20] It is also known that tumor cells themselves synthesise M-CSF in order to stimulate macrophage production.[15] As well as tumourigenisis, CSF-1 derived cells are implicated in a number of other inflammation based disease pathways such as rheumatoid arthritis and osteoporosis which has been supported with biological studies using M-CSF deficient mice which makes the targeting of the CSF-1 receptor promising in terms of therapeutic benefit.[21] In addition, Imatinib, a tyrosine kinase inhibitor (TKI) of the bcr-abl protein, was reported to deactivate osteoclast function by off-target inhibition of FMS, leading to a suppression of breast cancer metastasis to bones which adds weight to the opinion that FMS is a viable target for anti-cancer treatment by small molecule inhibition.[22,23]

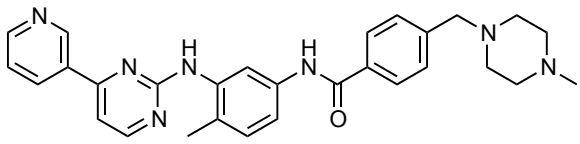


Figure 3. Imatinib – Glivec®.

1.3 Targeting FMS with Small Molecule Inhibitors

1.3.1 Kinases as Drug Targets

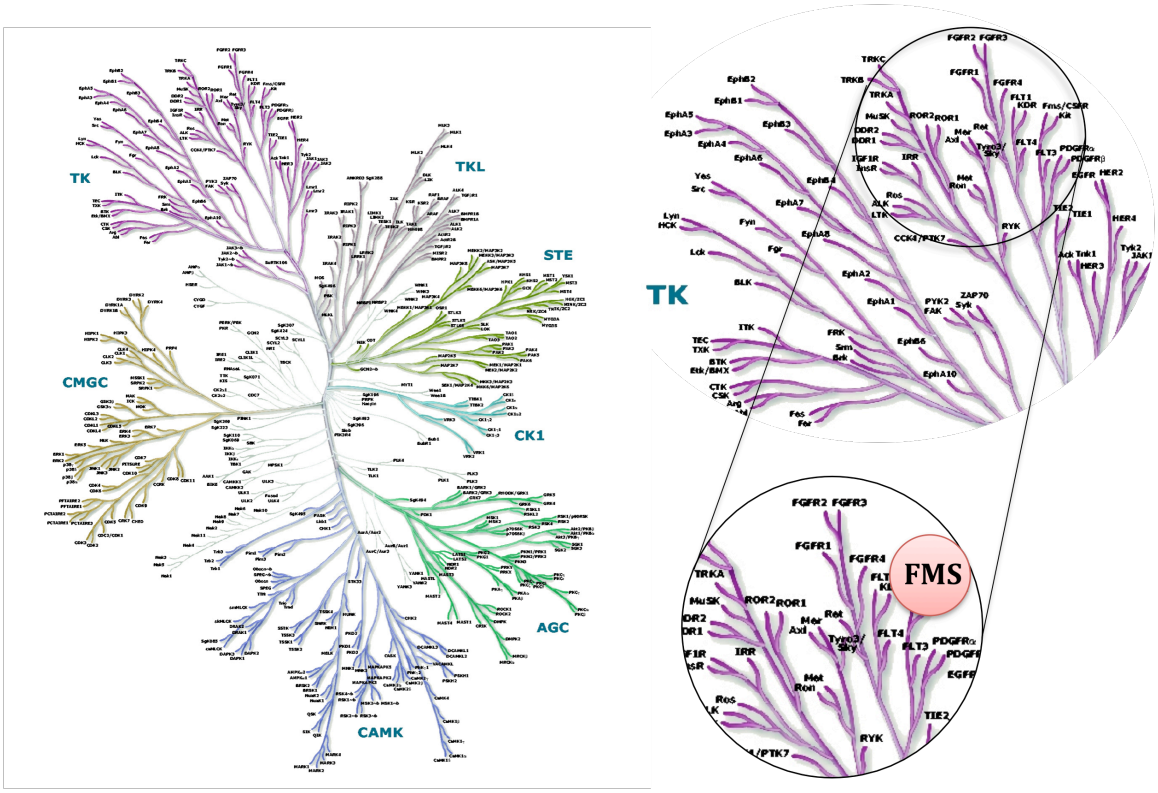


Figure 4. Human kinome with FMS (CSF-1R) highlighted within the Tyrosine Kinase family.[24]

There are 518 predicted kinases in the human genome which are expressed ubiquitously throughout the body (Figure 4).[24] Due to their key involvement in many cell proliferation and survival pathways, kinases have become widely targeted in oncology.[25] Kinase activity is caused by phosphotransfer reactions from ATP to residues within the protein. This makes the ATP binding site a primary target area for small kinase inhibitors.

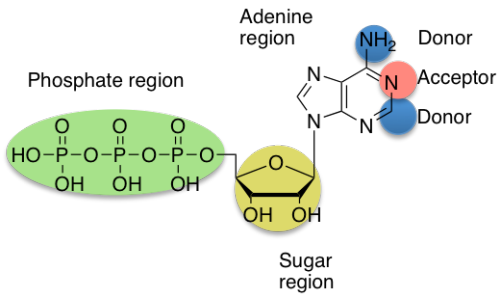


Figure 5. ATP showing hydrogen bond (H-bond) donor, acceptor, donor functionality in the adenine motif.

As the ATP binding cleft is so well conserved between most kinases, ATP-mimic inhibitors tend to have very similar structural features; H-bond donor-acceptor-donor functionality to interact with the hinge residues, largely hydrophobic in the adenine and sugar regions, and

very flat to be accommodated in the narrow interlobal cleft (Figure 5).[26] This template for general kinase inhibition means that one of the main challenges in developing a small molecule inhibitor for binding to a kinase is finding selectivity for the desired kinase over the large number of possible kinases available whilst at the same time occupying novel chemical space.

1.3.2 Active vs. Inactive conformers

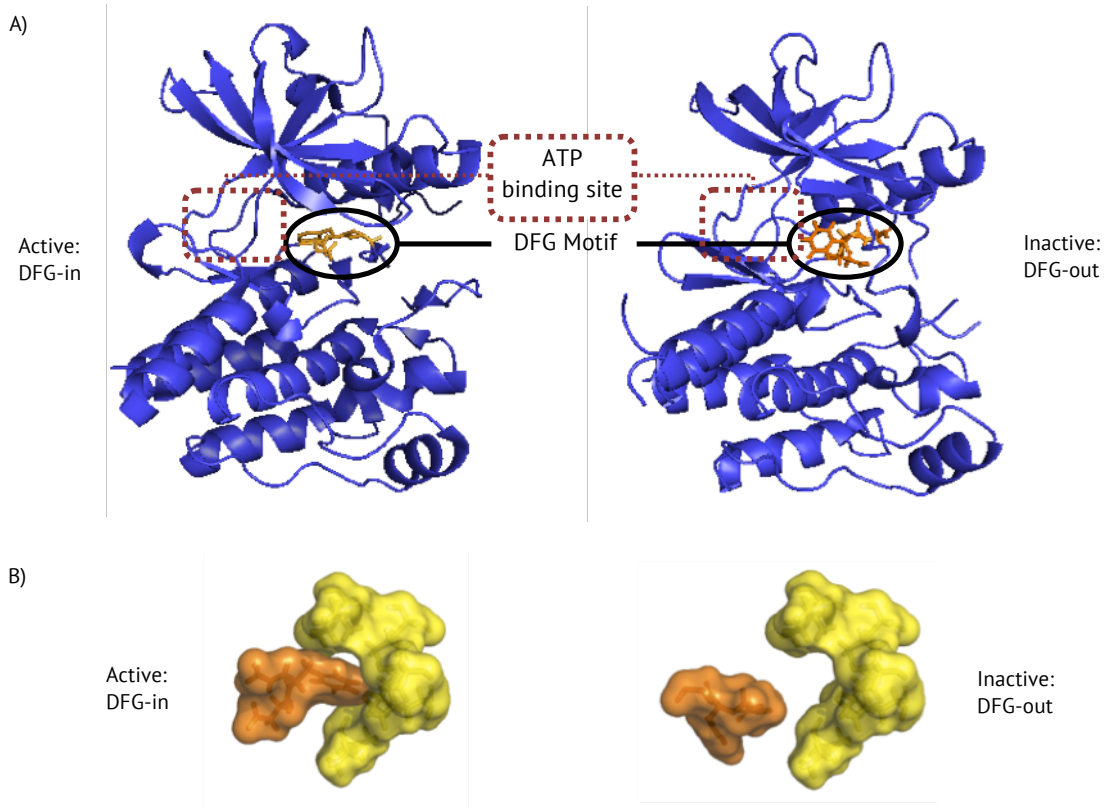


Figure 6. A) DFG-in (PDB: 3LCD) and DFG-out (PDB: 3LCO) conformers of FMS; B) Expanded views of DFG motif (orange) position in relation to allosteric pocket (yellow) in active vs. inactive conformations of the kinase.

There are a number of features within kinases that, although conserved, are flexible and can expose less well conserved parts of the protein allowing a degree of selectivity to be gained, the main one of these being the DFG motif. This Asp-Phe-Gly (DFG) trio of residues makes up part of the activation loop of the kinase, which dictates whether the protein is in an open active or closed inactive conformation. As seen above, in the active conformation, the DFG motif is buried within the protein in an hydrophobic pocket leaving the ATP binding cleft open for binding of the substrate whereas the DFG in the inactive conformation closes off the pocket entrance and prevents nucleotide and protein binding (Figure 6A).[27] In this second conformation however, additional allosteric sites are accessible that were previously occupied by the DFG motif (Figure 6B).[28]

1.3.3 Kinase Inhibitor Types

Kinase inhibitors fall broadly into classes depending on how they bind to the protein, the main two classes being Type I & Type II. These two classes differ in that they bind preferentially to different conformers of the protein, active (DFG-in) or inactive (DFG-out).[29] This is also true in the case of FMS inhibition. Type I inhibitors bind to the active FMS conformer where the DFG motif occupies a region close to the gatekeeper residue Thr633. Due to the fact that they occupy the ATP binding site, this leads to binding competition between Type I inhibitors and the high levels of ATP found in cells. Selectivity over other kinases is harder to achieve for ATP-competitive ligands due to the high level of conservation in this area between kinases. Type II inhibitors also bind at the ATP site using the same interactions with hinge residues but also occupy an allosteric site nearby which is only revealed when the DFG motif is in the "out" position in the inactive conformer. This can be of use as the allosteric site residues are less well conserved between kinases and this may be exploited to aid the design of a more selective molecule. The major drawback in allosteric binding is that mutations in the allosteric residues can lead to reduced affinity and while with Type I binding, mutations preventing the inhibitor binding may also prevent the ATP substrate binding, with Type II inhibition non-ATP site mutations may lead to drug resistance without reducing the activity of the kinase.[28]

1.3.4 Binding sites in FMS

The key binding regions in FMS are typical for proteins in the RTK family and kinases in general.[30] As shown previously (Figure 5) ATP has a number of structural features and these are complemented by the binding sites within the kinase. The hydrogen bonding motif of ATP interacts with a the hinge region of the protein with the adenine ring itself sitting in a flat cavity adjacent; there is a largely hydrophobic sugar binding pocket containing a small number of more polar residues to accommodate the ribose unit of the adenosine; and moving beyond this is a solvent exposed area for the phosphate tail to occupy. In addition to this is the hydrophobic back pocket region that is occupied by the DFG-motif in the active conformer but is accessible in the DFG-out, inactive conformer of the kinase.

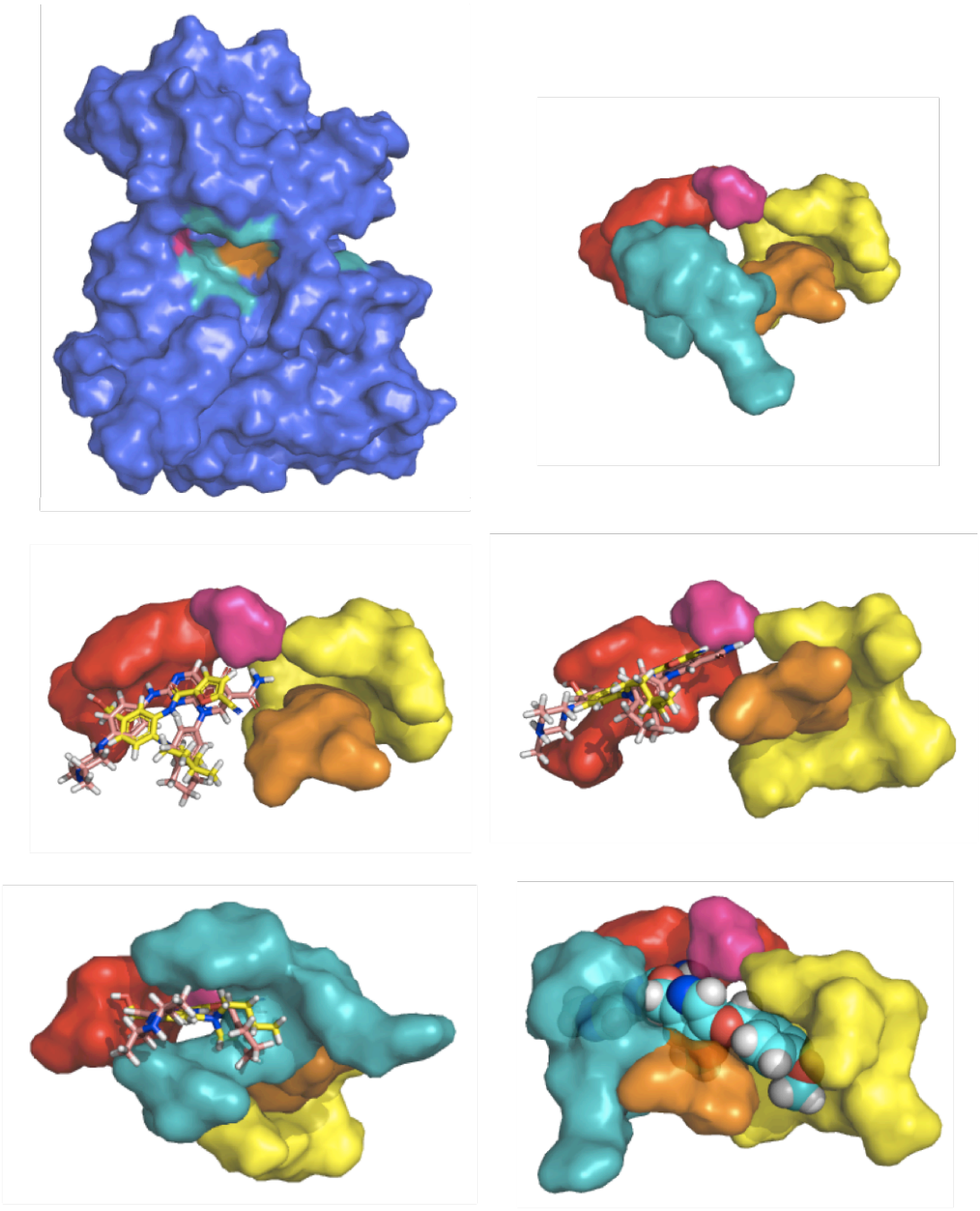


Figure 7. Surface representation of FMS (dark blue) and internal binding regions (Hinge region : red; Gatekeeper residue : pink; Backpocket : yellow; DFG motif : orange; Sugar region : light blue) showing interactions with active ligands in both DFG-out and DFG-in conformations.

To illustrate these regions, a composite model of protein-ligand co-crystal structures was generated by overlaying a series of solved structures (PDB codes: 3LCO; 3LCD; 3BEA; 2I1M; 2I0V; 3DPK) using Schrödinger Maestro (see **1.4.1**) before using PyMOL (Schrödinger) to highlight the specific residues that comprise the different pockets and motifs (Figure 7).

1.4 Computer-Aided Drug Design (CADD)

The use of i*n silico* techniques in drug discovery has been made possible by the rapid progression of computing power over recent decades and the subsequent accumulation of data generated around molecular interactions. When combined with developments in X-ray crystallography, and the vast libraries of solved protein crystal structures,[31,32] this has led to the production of invaluable if not essential computational tools for use in drug development programs, such as docking, virtual screening & structural overlays.

1.4.1 Docking & Schrödinger Suite

Recent computational advancement and development of algorithms that better describe protein flexibility have led to increased reliability and trust in docking results.[33] Docking is a computational technique primarily used to aid the prediction of binding conformations of ligands both when protein–ligand crystal structures cannot be obtained and for a preliminary indication of affinity to streamline the process of designing and synthesising new analogues.[34] The Schrödinger Suite comprises a number of useful programs including Glide for docking,[35] as well as its interface software Maestro, which may be used to overlay protein structures for ease of conformational comparison.[36] It is worth noting that, whilst accuracy of docking predictions have increased substantially in the previous decades, there can still be a great deal of discrepancy between different docking softwares as well as between the computational data and physical biological data meaning that docking results should always be treated with caution and backed up wherever possible with robust biological data.[37]

1.4.2 Cresset Field Point Templating & Virtual Screen

The Cresset field point templating system was developed using the knowledge that two seemingly structurally diverse molecules may interact at the same receptor if they share common electrostatic and van der Waals' properties which are impartially recognised by the binding site.[38] The original usage was for membrane bound G-protein coupled receptors whose structures were not known. Through analysis of inhibitors with similar biological activities a pharmacophore template could be built up for an active binding conformation at the target.[39]

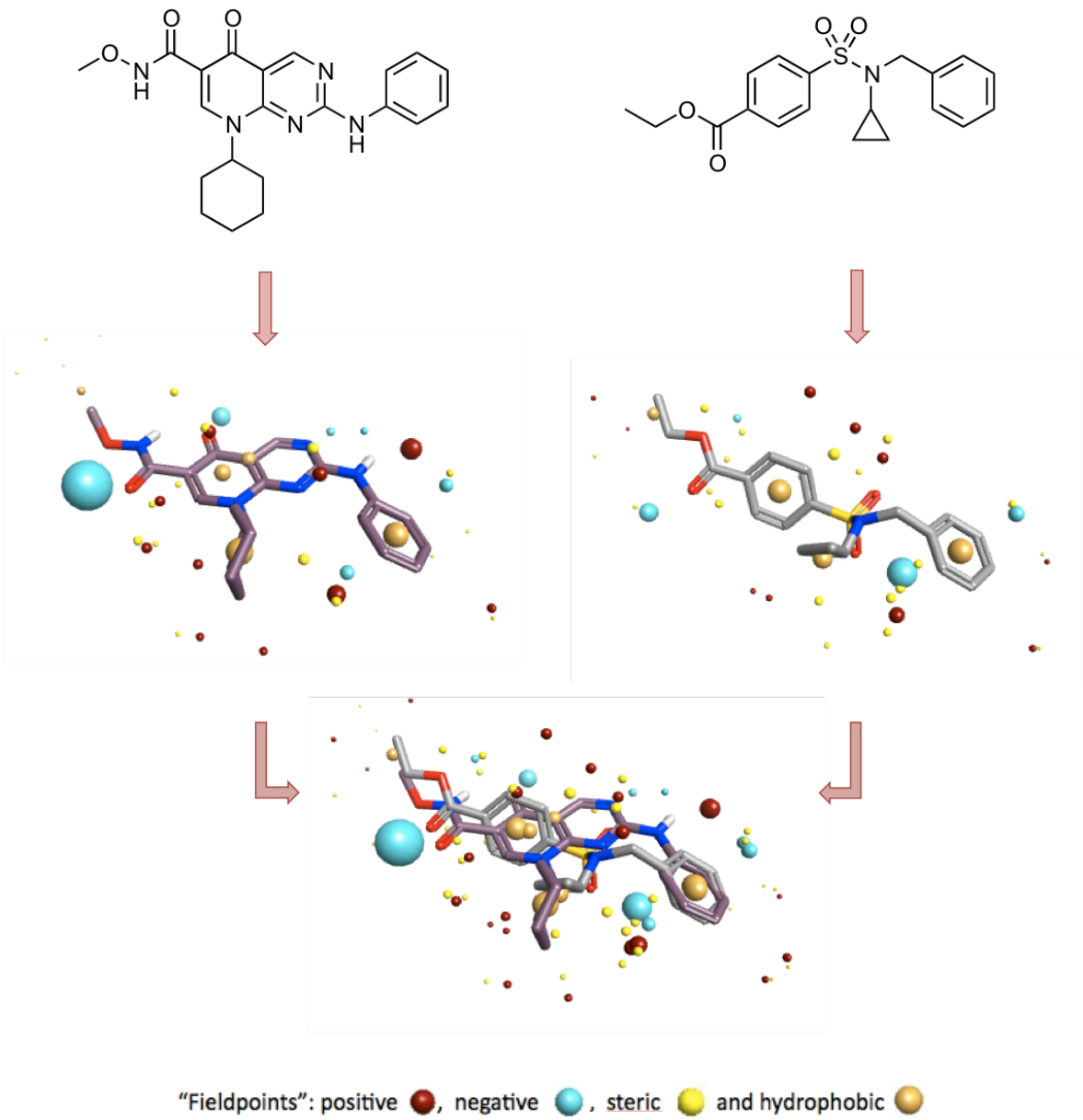


Figure 8. Overlay of 3-D generated conformations from 2-D structure inputs using Fieldpoints.

This may be achieved by finding the low energy conformers of the known inhibitors, using molecular mechanics with the XED (eXtended Electron Distribution) forcefield, and assigning electrostatic field values to the molecules minimized to their "local extrema or 'field points'". Molecules are then compared on the basis of overlaying FieldPoints rather than structural elements (Figure 8). There are four types of fields generated by the Cresset software; a positive field defined by favourable interactions with a negatively charged probe; a negative field generated using a positive probe; a surface field defined by steric interactions with a neutral probe; and a hydrophobic field calculated by an empirical density function weighted towards nonpolar atoms.[40] In a FieldScreen search, the field point template is compared to 100 low energy conformations of each molecule in the FieldScreen database and the results are scored for the best overlaid match of conformations on the basis of field point similarity.[41]

These techniques of docking and virtual screening combined can be used as a preliminary means of reducing the number of compounds to be tested *in vitro* as opposed to conventional high-throughput screening of compound libraries containing upwards of 10^5 compounds to as little as <100 molecules, greatly improving the time and cost efficiency of identifying new hits and lead series.

1.5 Biological assays

The two preliminary cell based assays on this project are based on cell growth and phosphorylation readouts. The assays were performed by Rakhee Chauhan and Dr Nick Dibb at Imperial College London, Hammersmith Hospital campus.

1.5.1 Cell Growth Assay

The cell growth assay is used to assess whether the molecule administered reduces the rate of cell proliferation. This type of assay can be used to work out IC_{50} values for the compounds. The compound is added to cultured cells in growth media in a serial dilution along with a negative control (DMSO) and a positive control (Dasatinib - Figure 10). The cell lines used are FDvFMS, FDD2V (Figure 11) which are both active without the need to add any CSF-1 ligand and are both dependant on FMS for growth.

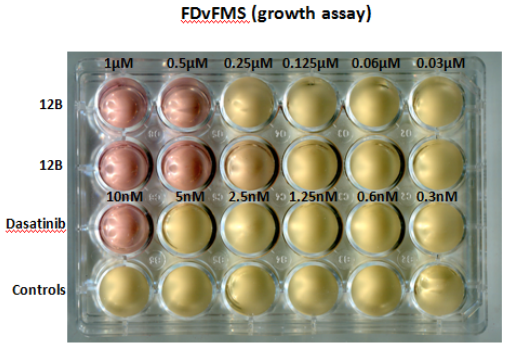


Figure 9. Cell growth assay

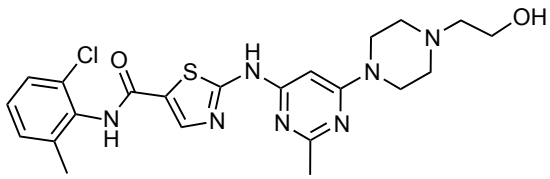


Figure 10. Dasatinib – Sprycel®.

Red media such as that in the top left above (Figure 9) shows inhibition of cell proliferation, yellow media such as towards the right and for the negative control shows cell growth (RPMI media used: indicator – phenol red).

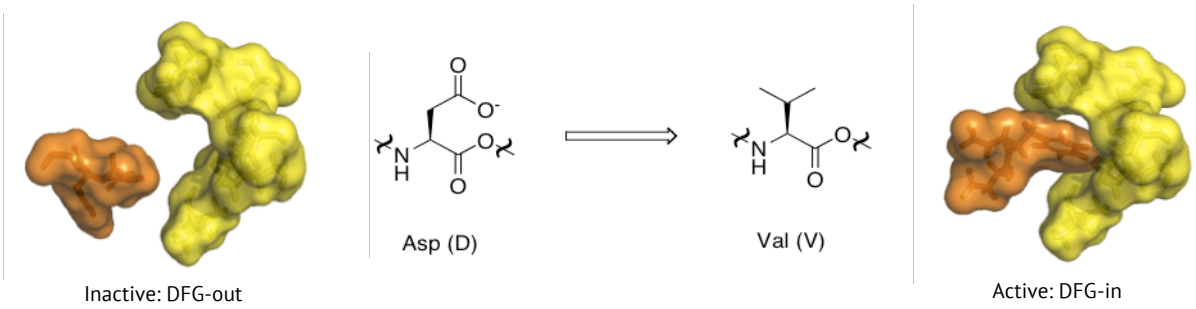


Figure 11. D2V mutation of charged aspartate to hydrophobic valine residue greatly increases the affinity of the activation loop for the hydrophobic back pocket, locking the protein in the active form.

1.5.2 Phosphorylation Assay

This assay was performed on cFMS, vFMS, T633i cell lines. The T633i cells contain a mutation at the gatekeeper residue (threonine 633 to an isoleucine) to disrupt interactions in the nearby hinge reaction and which also prevents access to the allosteric pocket. The assay is designed to show the extent of phosphorylation of key residues in the protein as this is a good sign of whether ATP is able to bind or whether it is being inhibited. The cell lines are incubated with ATP and varying concentrations of the inhibitor molecules, then lysed and the released FMS protein analysed for the degree of phosphorylation by Western blot analysis. In this assay a decrease in phosphorylation should be seen at high drug molecule concentrations (Figure 12).

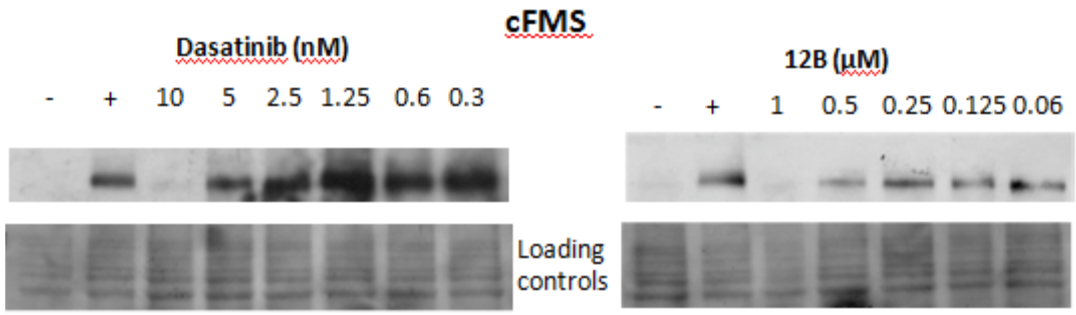


Figure 12. Preliminary results for the phosphorylation assay showing decreased phosphorylation of cFMS at higher inhibitor concentrations – Western blot electrophoresis.

1.6 Project Plan

The main aim of this project is to design a FMS-selective kinase inhibitor – although there is an argument for "selectively promiscuous" kinase inhibitors (i.e. molecules which show activity at multiple kinase targets) being of greatest therapeutic benefit through inhibition of numerous pathways with only a single xenobiotic molecule,[42] a highly selective inhibitor for CSF-1R would give valuable biological insight into the role of FMS with fewer off-target complicating factors. A large part of the strategy involves investigating both the active and

inactive conformers of FMS to provide a convergent approach to a novel small kinase inhibitor (SKI). Type I and type II inhibitors each have their advantages. Type I inhibitors can bind to both inactive and active conformers of the protein, are less vulnerable to mutative resistance and can be selective although selectivity is usually low. Type II inhibitors will only bind to the inactive protein conformer and are more sensitive to resistance both in the ATP site and in allosteric sites, but they have the potential to be a lot more selective. In addition, the chemical space around type II inhibitors is a lot more open. There are examples of both type I (Dasatinib) and type II (Imatinib) inhibitors with FDA approval used in cancer therapy (specifically chronic myelogenous leukemia or CML). Therefore, it was decided that it would be most interesting to pursue both strategies at the start of the project. This is helped by the fact that the mutated FMS proteins (described in **1.5**), can aid differentiation between the two types of binding.

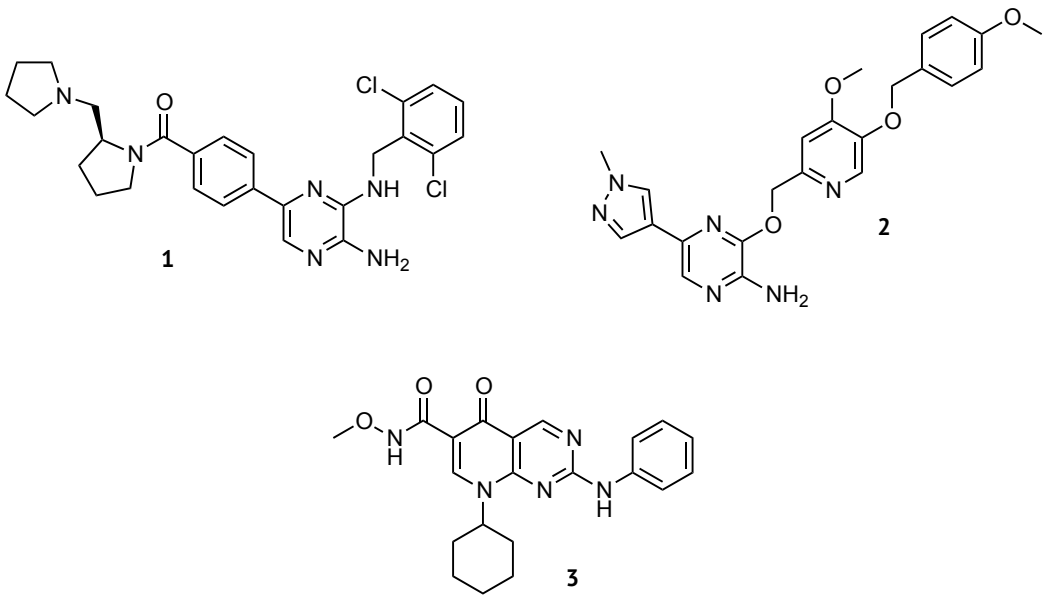


Figure 13. Reference compounds from Pfizer Type I binder **1** & Type II binder **2** and search molecule for virtual screen **3**.

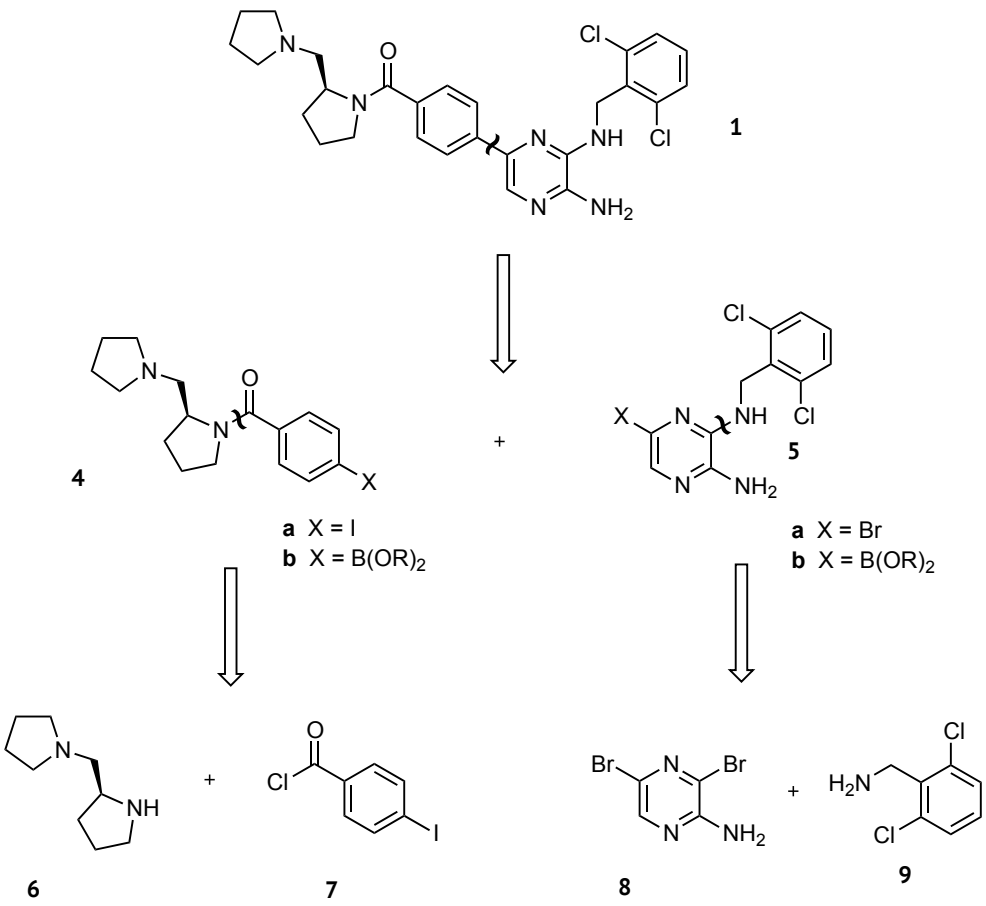
To this end, computational studies including a virtual screening process was used to identify new scaffolds for lead optimisation. Routes were designed to these general scaffolds focusing on a combinatorial chemistry approach towards synthetic route design to allow rapid generation of analogues. In addition, a number of reference compounds were synthesised to validate both the biological assays and the virtual screen (Figure 13). The first two reference molecules to be synthesised were Pfizer compounds, DFG-in **1** and DFG-out **2**, with known binding modes due to the fact that both have been co-crystallised with FMS.[43] The third reference molecule **3** was used as the seed molecule for the virtual screen, it is a truncated version of a Johnson & Johnson compound which also has a solved co-crystal structure.[44]

2 Results & Discussion

2.1 Reference compounds

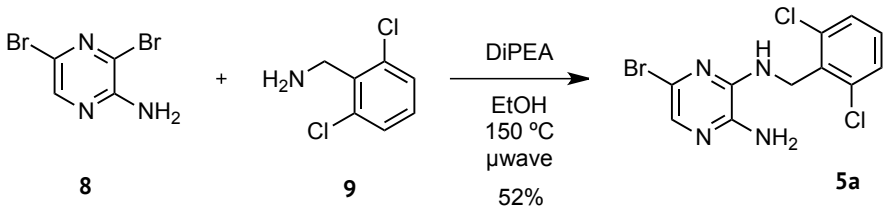
2.1.1 DFG-in reference compound 1

The compound co-crystallised with FMS in the DFG-in conformation, **1** (PDB: 3LCD) was the starting point of a Pfizer project aimed at converting a Type I kinase binder into a Type II binder that would target the DFG-out FMS conformer.[43] Although the structure of the complete molecule **1** is referenced, its synthesis is unreported apart from the formation of intermediate **5a**.[43] Furthermore this single synthetic step that was included, the S_NAr reaction between 2-amino-3,5-dibromopyrazine (**8**) and 2,6-dichlorobenzylamine (**9**), had not been optimised to a synthetically useful standard. Thus a retrosynthesis was proposed, providing a convergent approach towards **1** (Scheme 1).



Scheme 1. Retrosynthetic analysis of DFG-in compound **1**.

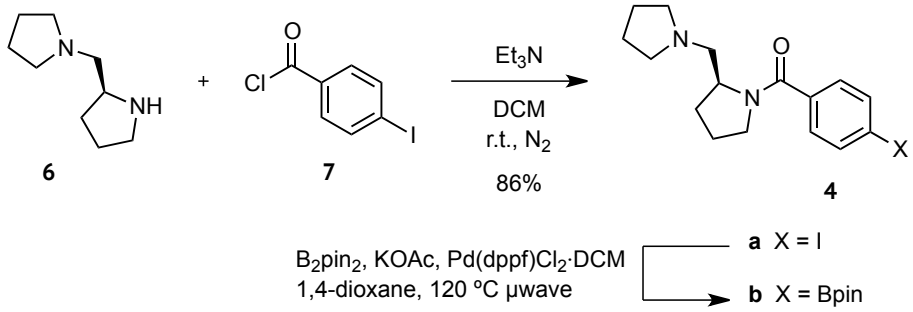
The route above hinges around assembly of the two components for a key Suzuki–Miyaura cross-coupling between known compound **5a** and corresponding aryl boronic ester **4b**.



Scheme 2. Formation of bromopyrazine **5a** via an S_NAr reaction between **8** & **9.**

To form the aryl bromide coupling partner **5a**, the conditions reported by Pfizer use Na_2CO_3 as the base and NMP as solvent;[43] however, this largely resulted in poor conversion and the formation of polymeric byproducts. It was found that compounds similar to the desired **5a** had been formed by using diisopropylethylamine (DiPEA) in ethanol under microwave heating at 180 °C.[45] Optimisation of these conditions led a moderate yield (52%) being achieved using sealed tube microwave irradiation at the slightly lower temperature of 150 °C (Scheme 2).

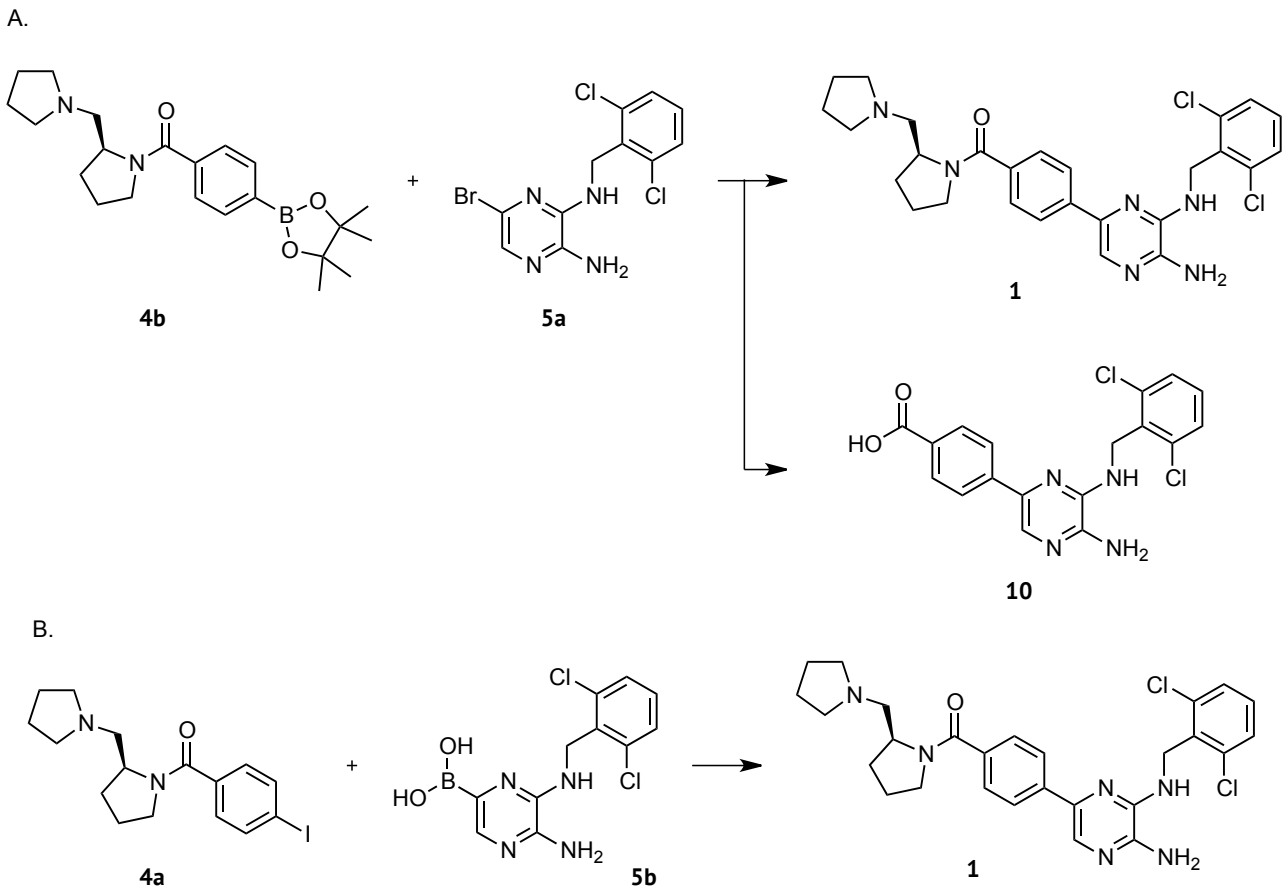
The boronic ester **4b** was obtained by acylation of (*S*)-(+)-1-(2-pyrrolidinylmethyl)pyrrolidine (**6**) with 4-iodobenzoyl chloride (**7**), followed by a Miyaura borylation reaction with bis(pinacolato)diboron (B_2pin_2) to give the desired coupling partner as the boronic acid pinacol ester (Bpin) as shown below (Scheme 3).



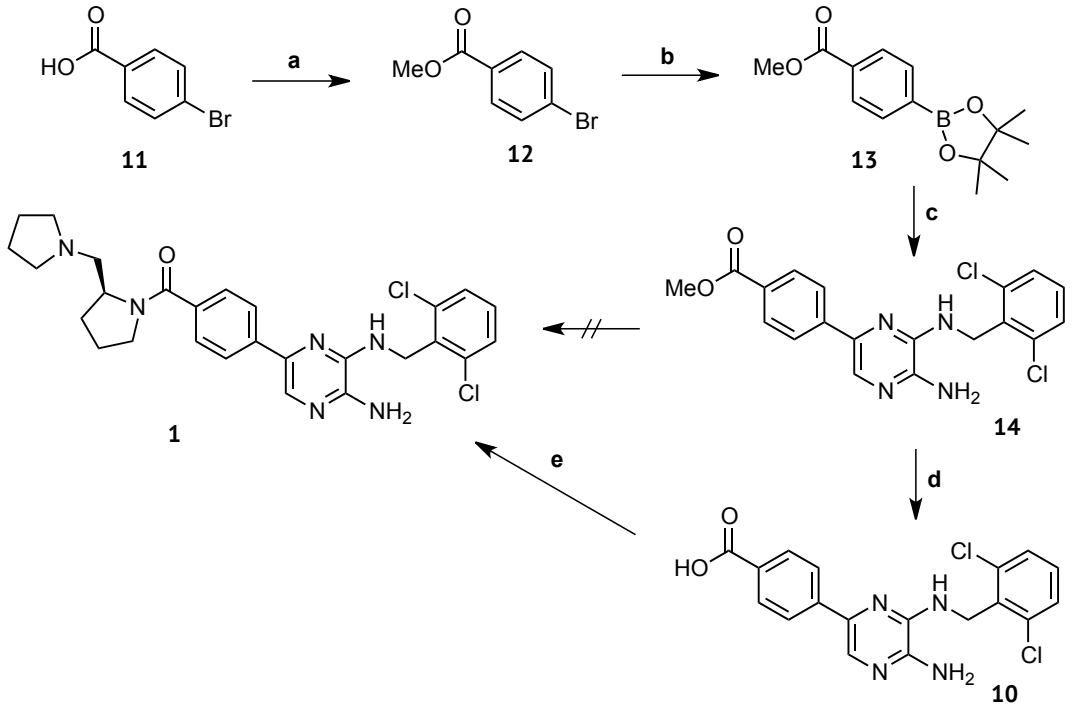
Scheme 3. Formation of boronic ester **4b**.

The Suzuki–Miyaura cross-coupling reaction between **4b** and **5a** was undertaken using a number of different palladium sources and bases with limited success exemplified below (Scheme 4A). Poor conversion was exacerbated by hydrolysis of the amide bond to carboxylic acid **10** under the reaction conditions as well as difficulty isolating the final product which displayed sensitivity towards photodegradation. Reversing the coupling partners to **4a** and **5b** led to a slightly increased yield making isolation of the product easier (Scheme 4B). **5b** was prepared using the same Miyaura borylation reaction conditions as in Scheme 3, which under the reaction conditions underwent hydrolysis of the pinacol ester to give the boronic acid. The Suzuki coupling proceeded best when using phosphine ligands; unfortunately this led to

organophosphine oxide contaminants in the products. The desired compound **1** could never be isolated with sufficient purity *via* this method.



Scheme 4. Suzuki–Miyaura cross-coupling attempts. Reagents and conditions: $Pd(OAc)_2$, PPh_3, 2 M $Na_2CO_{3(aq)}$, 1,4-dioxane, 80 °C led to <10% yields and impure products.



Scheme 5. Reagents and conditions: (a) $TMSCHN_2$, PhMe / MeOH, r.t., 85%; B_2pin_2, KOAc, $Pd(dppf)Cl_2$·DCM, 1,4-dioxane, 120 °C μwave, 73%; (c) **5a**, $Pd(OAc)_2$, PPh_3, 2 M $Na_2CO_{3(aq)}$, 1,4-dioxane, 80 °C, 60%; (d) LiOH, THF / H_2O, r.t.; (e) **10**, EDCI, DCM, r.t., 44% (2 steps).

The main issues with these syntheses was the difficulty of purification for any intermediate containing the strongly basic bispyrrolidine unit and additionally, in removing the byproducts of the Suzuki reaction. These issues were both addressed by undertaking a linear synthetic route to the target, incorporating the biaryl cross-coupling earlier in the sequence and introducing the bispyrrolidine amide in the final step (Scheme 5).

The synthesis starts with the methyl esterification of 4-bromobenzoic acid (**11**) with *in situ* generated diazomethane – using $TMSCHN_2$ under Aoyama–Shioiri conditions.[46,47] The resulting methyl ester **12** underwent Miyaura borylation using the previously described conditions to give the aryl boronic ester **13**, which was subsequently coupled with aryl bromide **5a**. Direct amidation of ester **14** was attempted using a number of known conditions (e.g. activation with $AlMe_3$,[48] DABAL-Me_3,[49] or *i*-PrMgCl)[50] but was not achievable. Completion of the synthesis was achieved by conversion of the ester to the carboxylic acid **10** and a final EDCI coupling with the bispyrrolidine unit. It was found that the esterification of **11** and subsequent ester hydrolysis were necessary additional steps to ensure successful purification of the intermediate aryl boronic ester and improve the efficiency of the Suzuki–Miyaura cross-coupling step.

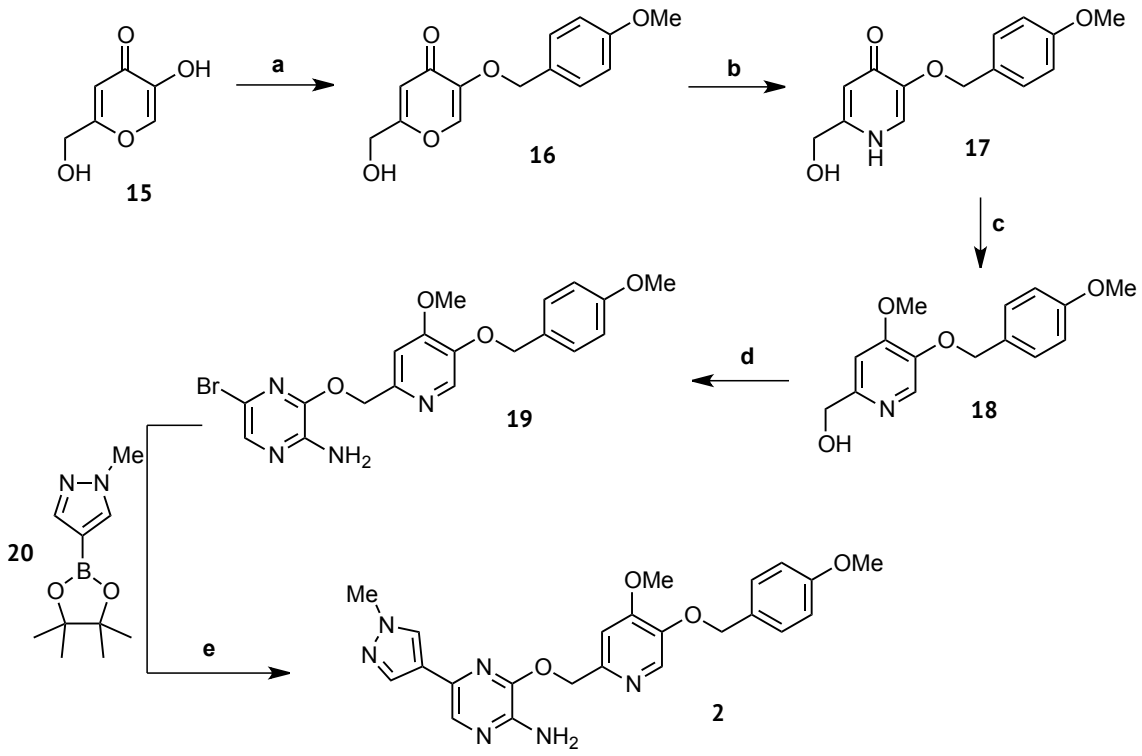
With this revised synthetic route, the compound **1** could be isolated in sufficient quantity and purity to be used in the biological assays.

2.1.2 Synthesis of DFG-out compound 2

The next compound to be synthesised was another Pfizer compound, co-crystallised with FMS in the inactive (DFG-out) conformer of the protein (PDB: 3LCO). The synthetic route to this compound has been outlined by Pfizer,[43] using a known GlaxoSmithKline sidechain **18** (Scheme 6).[51]

This synthesis starts with 4-methoxybenzylation of Kojic acid (**15**), followed by conversion of the resulting pyranone **16** to the pyridone **17** using ammonium hydroxide solution in ethanol. The methylation of **17** with $TMSCHN_2$ is selective for *O*– over *N*–alkylation and the phenolic oxygen over the carbinol, but this reaction was hindered by poor solubility of the starting material under the reaction conditions. A nucleophilic aromatic substitution of **18** onto known fragment **8** gave the penultimate intermediate to be used for a final Suzuki coupling

with methylpyrazole boronic ester **20**. Following the published conditions (Scheme 6e), the Suzuki coupling did proceed, albeit slowly, to give **2** with a maximum conversion of 4%.



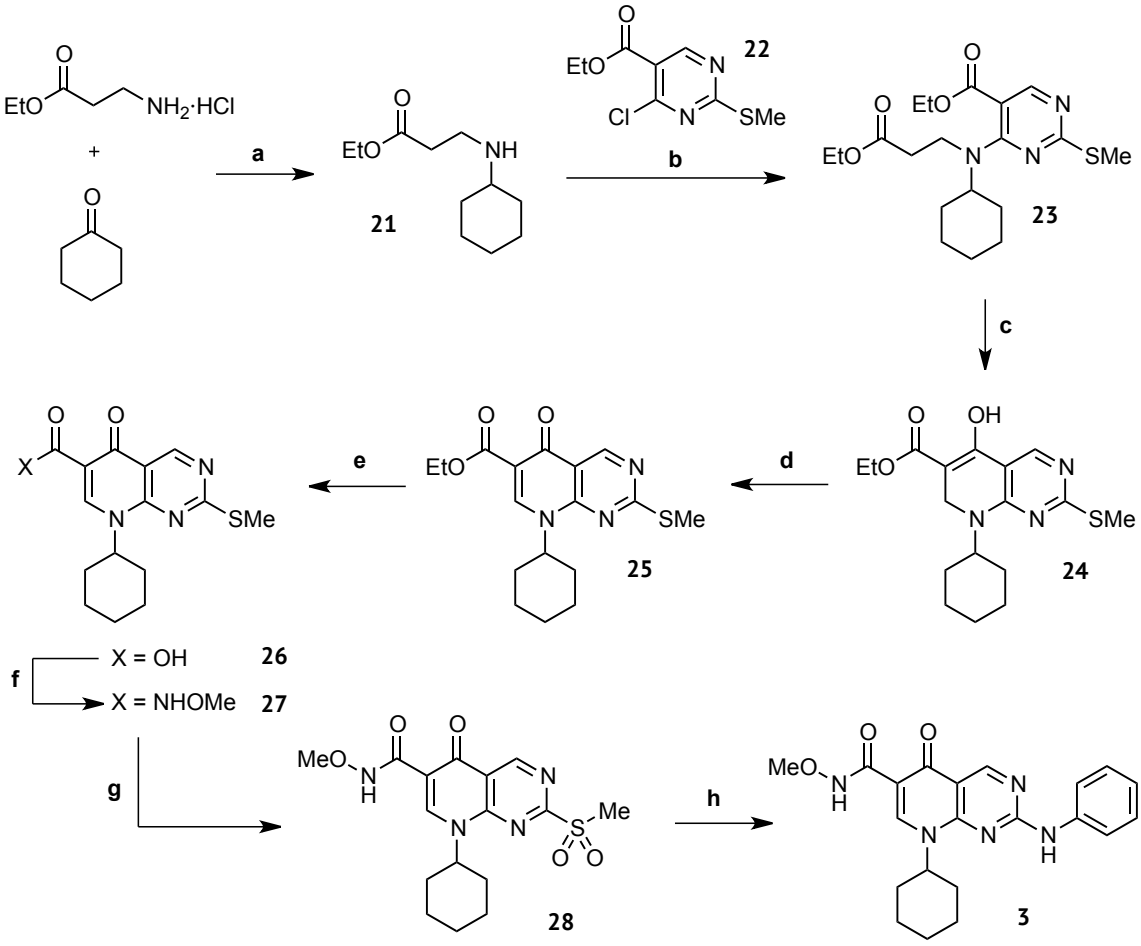
Scheme 6. Synthesis of **2**. Reagents and conditions: (a) PMB-Cl, K_2CO_3, DMF, 80 °C, 76%; (b) NH_4OH, EtOH, 100 °C, sealed tube, 70%; (c) $TMSCHN_2$, PhMe, MeOH, r.t., 38%; (d) **8**, KO*t*-Bu, THF, 60 °C, 69%; (e) **20**, $Pd(PPh_3)Cl_2$, 2 M Na_2CO_3, DME, 80 °C, 4%. PMB = *p*-methoxybenzyl.

Even with the low yielding final step, the DFG-out reference compound **2** could be obtained *via* this synthetic route and was submitted for biological testing.

2.1.3 Cresset Search molecule 3

The last reference molecule to be synthesised was a truncated version of a Johnson & Johnson ligand co-crystallised with FMS (PDB: 3DPK) (see **2.2.2**).[44] This compound was needed as a verification that the structure used as the seed template for the computational compound screen was valid as this structure had no previously reported biological data. The synthesis of **3** is adapted from published syntheses of a series of analogues of this structure (Scheme 7).[44,52,53] Reductive amination of cyclohexanone with β-alanine methyl ester (as its hydrochloride salt) yielded the secondary amine **21** which underwent an S_NAr reaction with the functionalised pyrimidine **22** to give intermediate **23**. A Dieckmann cyclisation gave the "dihydro" core precursor **24**, which was oxidised to the completed core motif **25** through addition and elimination of bromine. Acid catalysed hydrolysis of **25** followed by one-pot conversion to the acyl chloride and amidation formed the *O*-methyl hydroxamate **27**. Finally,

oxidation of the methyl sulfide to the sulfone **28** facilitated the S_NAr reaction with aniline to yield the desired final compound **3** in good yield and purity for the biological assays.



Scheme 7. Synthesis of Cresset search molecule **3**. Reagents and conditions: (a) NaOH, $NaBH(OAc)_3$, DCM, MeOH, r.t., 94%; (b) **22**, DiPEA, DCM, r.t., 95%; (c) KO*t*-Bu, PhMe, 90 °C, 45%; (d)(i) Br_2, DCM, r.t.; (ii) DiPEA, r.t., 60% (2 steps); (e) 1 M $HCl_{(aq)}$, 1,4-dioxane, 105 °C μwave, 72%; (f)(i) $(COCl)_2$, DMF (cat.), DCM; (ii) $MeONH_2$·HCl, Et_3N, 0 °C – r.t., 97% (2 steps); (g) mCPBA, DCM, 0 °C – r.t., 95%; (h) $PhNH_2$, *i*PrOH, 90 °C μwave, 46%.

2.2 Virtual Screening

Due to the small scale of this project and lack of an available compound library, a high-throughput biological assay was not a viable option to identify a new start-point. As mentioned previously (see **1.4**), computational methods can be helpful tools for providing structures that occupy new chemical space for defined protein targets and this was the approach taken for the identification of new hits with activity at FMS.

2.2.1 FieldPoint Templating

The virtual screening required the generation of a FieldPoint template which is a 3-D map of the key steric and electronic properties of one or more small molecules with known biological activity at the target protein (i.e. a ligand-based pharmacophore).[39] This template

must take into account the binding conformation of the ligand or ligands within the protein and may be generated in a number of ways – primarily either by *de novo* generation of a binding pose and/or by assigning a FieldPoint template to a known active conformation of a ligand.

2.2.1.1 Generation of template from de novo computationally calculated binding pose

The first method described above is particularly useful where there is a lack of crystallographic data available for ligands binding at the specified active site of the protein target.

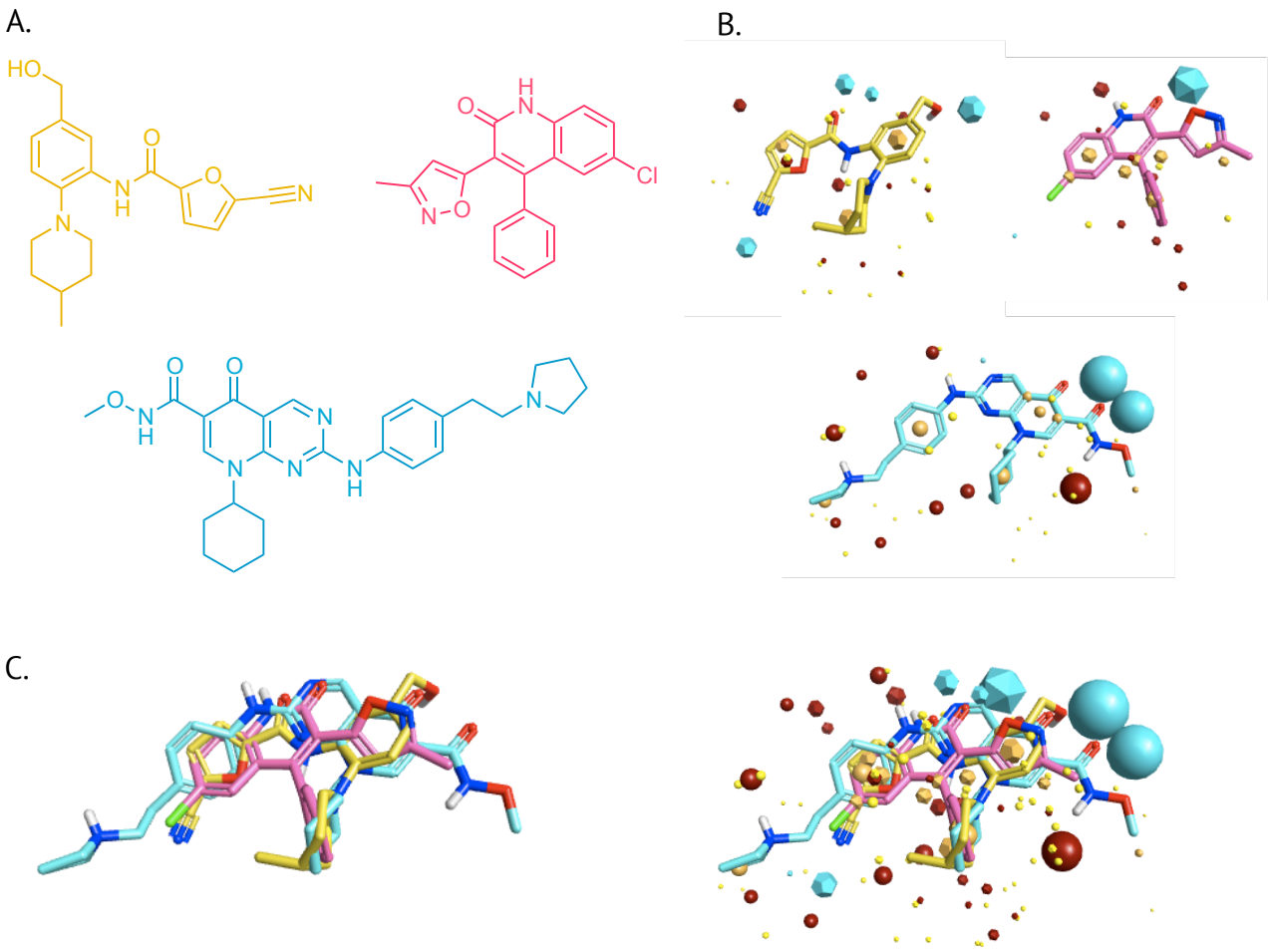


Figure 14. Overlay template generation using Cresset FieldAlign software. A) 2-D structures of known FMS ligands – PDB IDs: 5CN – yellow; 6C3 – pink; 8C5 – blue; B) Generation of low energy conformers and assignment of FieldPoints (one representative example shown for each ligand); C) Alignment of FieldPoints to generate overlay template (shown with and without FieldPoints).

Using the FieldAlign software, three or more 2-D structures of compounds with verified biological activity at the protein are entered into the program and a number of low energy 3-D conformers are generated for each molecule and assigned FieldPoints. These sets of conformers are then aligned against each other and scored for best similarity, leading to a

template that should best describe the important steric and electronic interactions made by each of the molecules and thus those which are recognised by the protein (Figure 14).

For this project it was useful to have the additional crystal structure information due to the fact that, as mentioned previously (see **1.3.2**), ligands tend to bind to kinases preferentially in the DFG-in and DFG-out conformers. In these different conformations, the ligand binding site and therefore points of interaction presented, can be significantly different – thus it was important to choose ligands which had been shown through their protein–ligand co-crystal structures to be able to bind to the same site in the protein. Of the available crystal structures at the time, only one of the ligands was co-crystallised with the DFG-out (inactive) form (PBD: 3LCO:LCO) of the protein compared to 5 that were co-crystallised with the DFG-in (active) conformer (PDB codes: 3BEA: IXH; 2I1M:5CN; 2I0V:6C3; 3DPK:8C5; 3LCD:BDY – taking the form protein:ligand) (N.B. although the ligands are shown to be co-crystallised with one form of the protein, this does not necessarily preclude them from also binding to other conformations). A number of molecules are needed for the alignment to increase the validity of the result, which meant that the selection had to come from the set of ligands that bound to the DFG-in FMS conformer. A further restriction for this computational experiment is that results are improved when using less flexible molecules. It is quite common for the saturated sidechains of small molecules inhibitors to occupy areas in which their rotational freedom is less restricted, e.g. further outside the main binding site (Figure 15). Aligning overlays to such sidechains may therefore miss key binding interactions and overstate less significant interactions, producing a less accurate template.

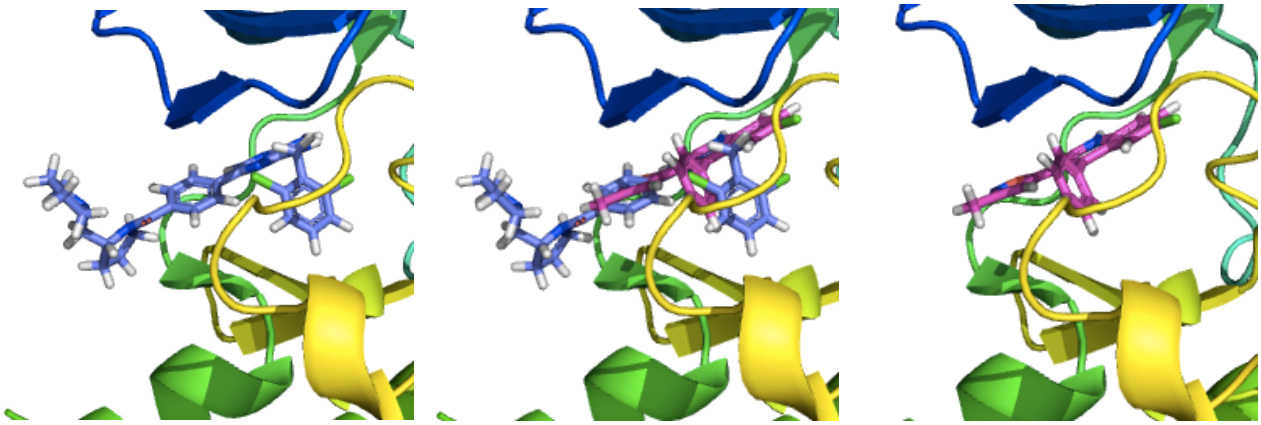


Figure 15. Comparison of positioning of ligand BDY (blue) with saturated sidechain compared to 6C3 (pink) without – from overlaid crystal structures PDB: 3LCD & 2I0V. For 2-D structures of ligands, see **Figure 14**.

Information from the available protein–ligand co-crystal structures allowed a more informed selection of the structures to be used for the overlay template (8C5, 5CN & 6C3).

A further benefit of the crystal structure data available was that the reliability of the *in silico* generated FieldPoint template could be assessed through direct comparison with the overlaid co-crystal structures.

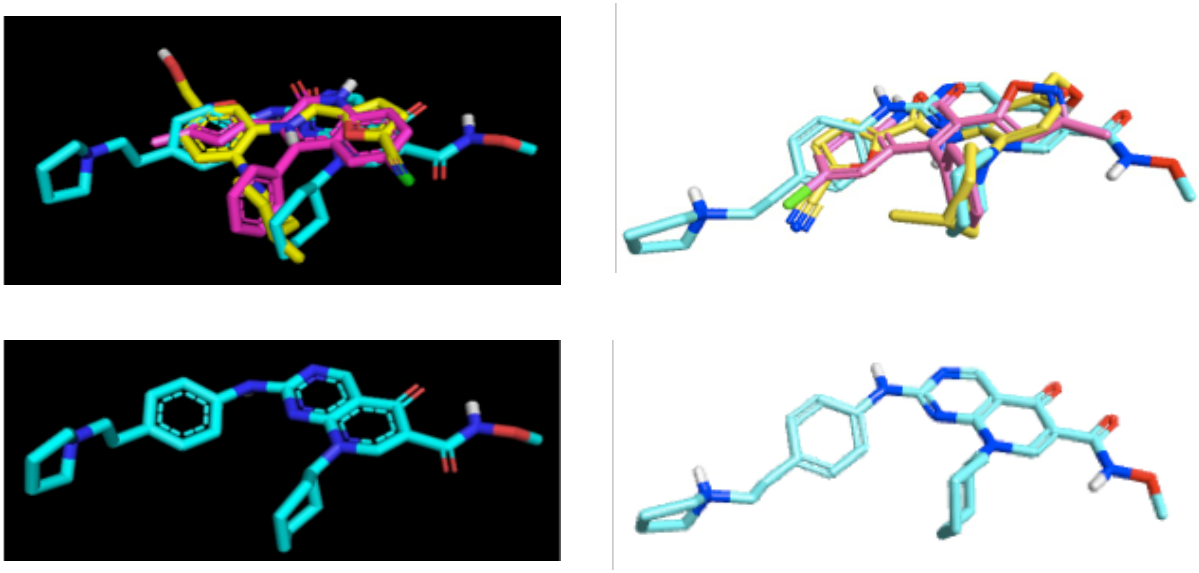


Figure 16. Comparison of overlays and predicted binding conformations generated from protein–ligand co-crystal structures (black background) *vs.* overlays generated *in silico* by FieldAlign (white background) – ligand PDB IDs: 8C5, 5CN & 6C3 (for 2-D structures see **Figure 14**).

When overlaid computationally using the FieldAlign software, the two smaller ligands (5CN & 6C3 – yellow & pink) are reversed in their orientation compared to that seen in the crystal structure overlay (Figure 16). Upon closer inspection it is seen that the two carbonyl groups of ligand 8C5 (blue) are aligned instead of opposed meaning that once the FieldPoints are assigned, there is a heavy bias for negatively charged electrostatic interactions in this region for the overlay, possibly rendering most of the other interactions negligible. Importantly the computationally generated conformation of 8C5 is lacking a structurally defining intramolecular hydrogen bond between the hydroxamate and the C-5 carbonyl on the heteroaromatic core.[44] The knowledge of this inaccuracy through the crystal structure data was valuable and helped to inform the degree to which the generated templates could be relied upon (these structural features will be discussed in further detail in section **2.6**).

2.2.1.2 Assignment of FieldPoints to the existing 3-D structure

An alternative method for generating a FieldPoint template for use in the computational compound screening is to take a 3-D conformation of a molecule and assign FieldPoints to it (Figure 17).

When compared to the method outlined in the previous section (**2.2.1.1**), there are a number of advantages and disadvantages. The main advantage of this method is that obtaining the active conformer of the ligand is easily achievable by taking a co-crystal structure of the ligand bound to the protein and in viewing software such as PyMOL or Maestro removing the data for the protein structure (Figure 17A). Another advantage is that the conformational structure obtained will be one known to provide interactions with the protein – although it is worth stating that it would be difficult to discern whether or not this binding mode is the primary source of the ligand's activity in solution (cf. in biological systems) from just crystallographic data (as noted in **2.2.1.1**).

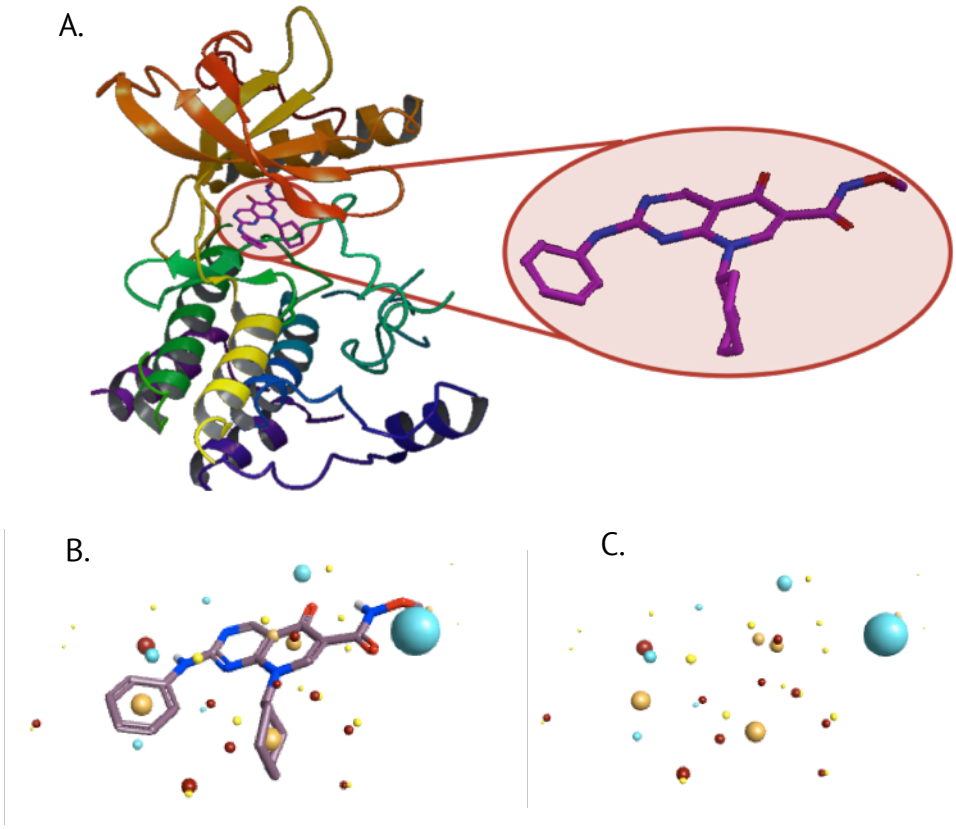


Figure 17. Generation of seed template for virtual screen *via* A) Extraction and truncation of ligand binding conformation (ligand PDB ID: 8C5) from protein–ligand co-crystal structure (PDB: 3DPK); B) Assignment of FieldPoints to the 3-D molecule in fixed conformation; C) Removal of molecular scaffold to obtain FieldPoint template.

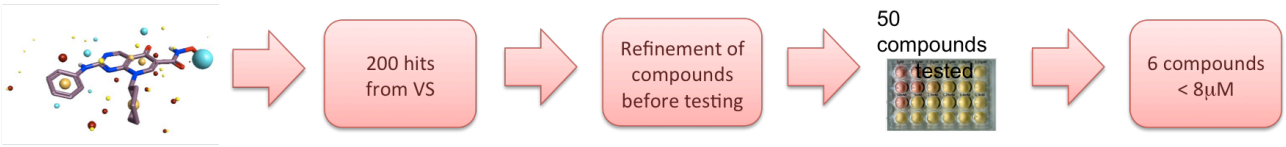
This method also allows greater predictability over the effects of modifications to the structure, for instance removal of solvent exposed flexible sidechains. If these are removed from the fixed conformation of the structure, they will not affect the FieldPoints generated elsewhere in the molecule whereas if they are removed prior to running an alignment experiment, the overlays could be skewed. In this case the pyrrolidine ethyl substituent of 8C5 is clearly solvent exposed and does not form significant bonding interactions with the protein. Removing this group prior to assigning FieldPoints meant that the resulting

pharmacophore was weighted towards interactions responsible for binding to the ATP-binding site of the kinase, but as there were no modifications made to the conformational pose, the original 3-D conformational information from the co-crystal structure was retained. Conversely the use of a single structure for template generation is disadvantaged by the fact that because just one molecule is being used, greater importance might be given to FieldPoints generated for this molecule that do not actually correspond to interactions with the protein (i.e. the molecule chosen is not an optimal ligand) – leading to redundant interactions being given significance in the results generated. If the multiple-molecule overlaying approach were to be employed, these artifacts would largely be averaged out and features that do not correspond to good interactions with the protein would be downplayed. In addition, on a more fundamental level, this approach may only be used where the 3-D structural information of the molecule in an active conformation can be obtained (e.g. with a protein–ligand co-crystal structure).

2.2.2 Cresset Search Template

This work was performed with the help of Dr Caroline Low. The template chosen for use in the virtual screen was that generated from the co-crystallised conformation of 8C5 that had been truncated to remove its flexible sidechain (Figure 4C), to maximise potential overlays with interactions within the key binding site of the kinase. In addition, it was hoped that by entering a smaller structure into the virtual screen, lower molecular weight (MW) results would be returned and these would have greater potential for modification and extension.[54] This was influenced by the knowledge that, recently, lower-affinity small molecule leads with lower molecular weight have gained favour as "hit molecules" relative to molecules that have higher absolute binding affinity if they contain greater relative binding efficiency (i.e. higher activity to MW ratio).[55–57] The computational screen was run by the Cresset Group.

2.3 Selection of Lead Series



Scheme 8. Process for identification of new molecular structures with FMS activity starting from a FieldPoint template.

The purpose of undertaking a virtual screen was to identify new scaffolds in novel chemical space and this is performed in a series of steps (Scheme 8). In this virtual screen, the input

seed field was compared to commercially available drug-like molecules from a database curated by the Cresset Group. The field point pattern was compared to 100 conformations from each of the 3.7 x 10^6 molecules, totalling 3.7 x 10^8 field patterns. The seed template is compared in turn to each conformation of any one molecule. Initial alignments are generated on the basis of distances, sizes and types of field point and grouped into 'cliques'. These are assigned scores reflecting both the size of the clique and the field points within it. For top scoring alignments, the field points of one conformation are used to sample the full field of the second molecule and the process then repeated for the second on the first. The average of the two scores is taken as the overall score for that pair and normalized to give a Dice field similarity metric. The scoring function reflects the electrostatic and steric similarity of compounds within the database to those of the seed pharmacophore and is used to rank the 'virtual hits'. The 200 hits with the highest similarity were defined as the virtual screening 'hitlist'.

As 200 was still a relatively large number of compounds to purchase from commercial sources or make purely for the purpose of a primary biological screen, the number of compounds had to be further reduced. Fortunately this was simplified by applying well precedented medicinal chemistry principles, such as removal of known toxicophoric functionality (e.g. nitro groups, electrophiles / Michael acceptors, unsubstituted anilines etc.),[58–61] lowering molecular weight and lipophilicity,[62,63] and guidelines such as Lipinski's "rule of five" (Ro5) which also take into account polar functionality such as numbers of hydrogen bond donors & acceptors.[64] This pre-selection led to 50 compounds being purchased from commercial screening compound libraries, which were then tested for FMS activity in the cell based assays described previously (see **1.5**); of these, 6 compounds were seen to have IC_{50} (concentration at which half of the maximum inhibition is obtained) measurements in the low micromolar concentrations (<8 μM) – seen below (Figure 18). In this case this inhibition refers to suppression of cell proliferation.

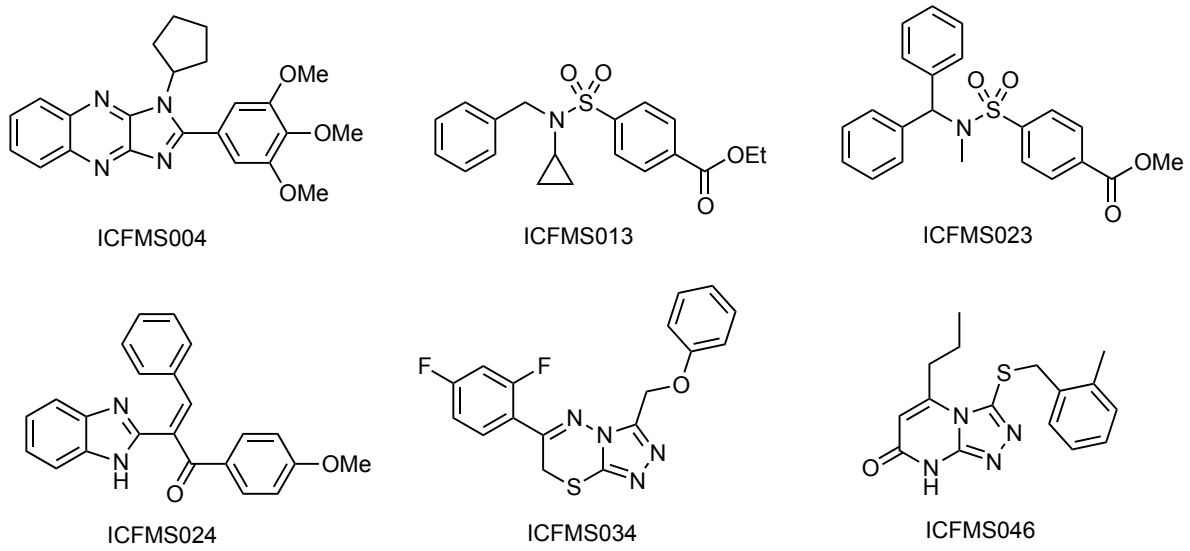


Figure 18. Structures of compounds identified in the cell based biological assays. ICFMS reference codes are in-house numbering system.

From the structures above, ICFMS013, ICFMS023 & ICFMS046 were chosen to populate two classes of compounds to be developed into lead series – the sulfonamide series and triazolopyrimidone (formally 7-oxo-7,8-dihydro-1,2,4-triazolo[4,3-*a*]pyrimidine) series. The former was chosen due to the fact that it is an atypical structure for a kinase inhibitor. Two molecules of this structure showed FMS activity and considering that these hits were modeled from an ATP-binding pharmacophore, it was hoped that this series could provide novel and distinct structural features in the crowded chemical space of kinase inhibitors. The second series contains more obvious kinase inhibitor characteristics such as a flat heteroaromatic bicyclic core with hydrogen bond donor and acceptor motifs to interact with the hinge region in the ATP-site (see **1.3.1**). This series was chosen owing to its potential for derivatisation as well as the fact that the construction of the heterocyclic core appeared to provide some interesting synthetic challenges.

2.4 Sulfonamide Series

To gain a better understanding of how to build up the SAR around each series and the impact this would have on potential disconnection strategies, a rational hypothesis had to be formed as to the potential positioning of the new ligands in the binding site. This was primarily done through comparison of the overlaid conformations provided by the Cresset screen – how the ligand with unknown binding aligned to the ligand with known binding from the crystal structure (Figure 19).

2.4.1 Orientation of sulfonamide series structures

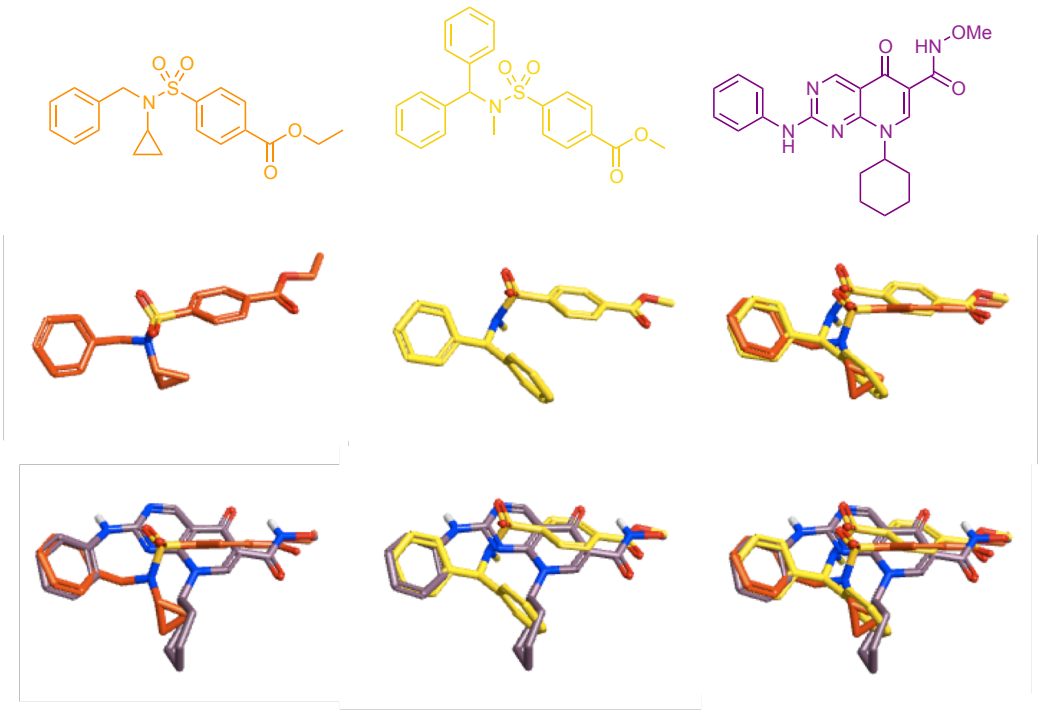


Figure 19. Conformational results of virtual screen for compounds ICFMS013 (orange) & ICFMS023 (yellow) aligned to the seed molecule **3** (purple).

Although the aryl ester portions of the new series of molecules overlaid well with the hydroxamate of the seed molecule, the sulfonamide portions were seen to occupy slightly different spatial areas with respect to the protein; however, by studying the crystal structure data, it was seen that this hydrophobic region within the protein was substantially open and therefore should not obstruct molecules positioned in these conformations (Figure 20). On top of this, the hydrophobic motifs present in these sulfonamide molecules overlaid well with those of the search molecule.

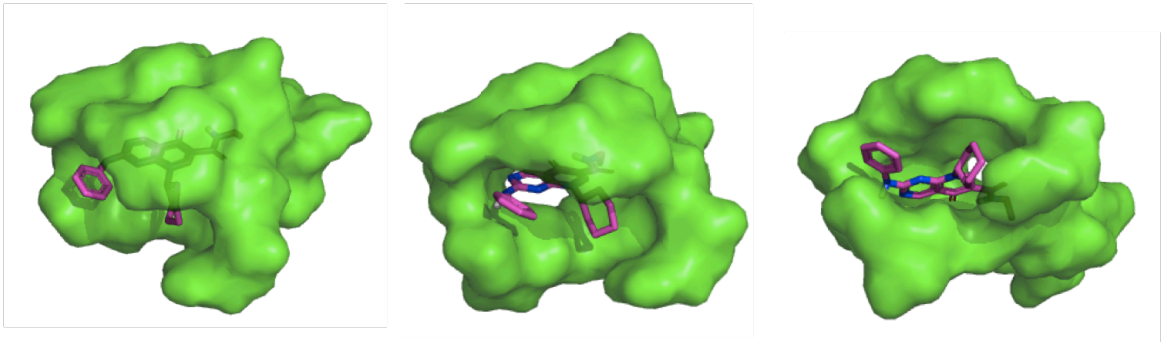


Figure 20. Different perspective views of the search molecule **3** in the open hydrophobic region of the binding site.

Through comparison of these overlays and knowledge of the orientation of the seed molecule in the crystal structure, preliminary vectors were tentatively assigned to the new molecular series (Figure 21 & Figure 22). Ultimately, these data helped guide logical SAR development

from the base series and provided a platform for the exploration of new chemical space, in line with the aforementioned drug development guidelines.

The main vectors assigned were aimed towards known important interactions within the binding pocket (Figure 21 & Figure 22). The ester motif may be extended into the back pocket by introducing further hydrophobic groups to homologate the aliphatic substituent. As this ester functionality is also located in the hinge-binding region, the use of an amide rather than the ester may help to provide a hydrogen-bonding interaction to the protein. The aromatic rings on the sulfonamide portion of ICFMS023 are directed towards both the sugar pocket and the solvent exposed entrance of the binding site. In the absence of the second aromatic ring such as in ICFMS013 a sufficiently extended hydrophobic motif can replace one of these interactions.

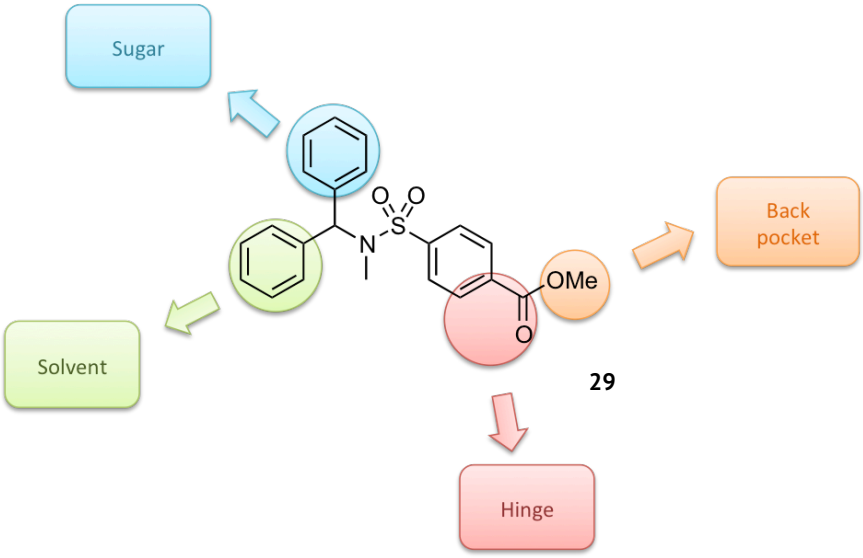


Figure 21. Assigned vectors on the 2-D structure of ICFMS023 **29**.

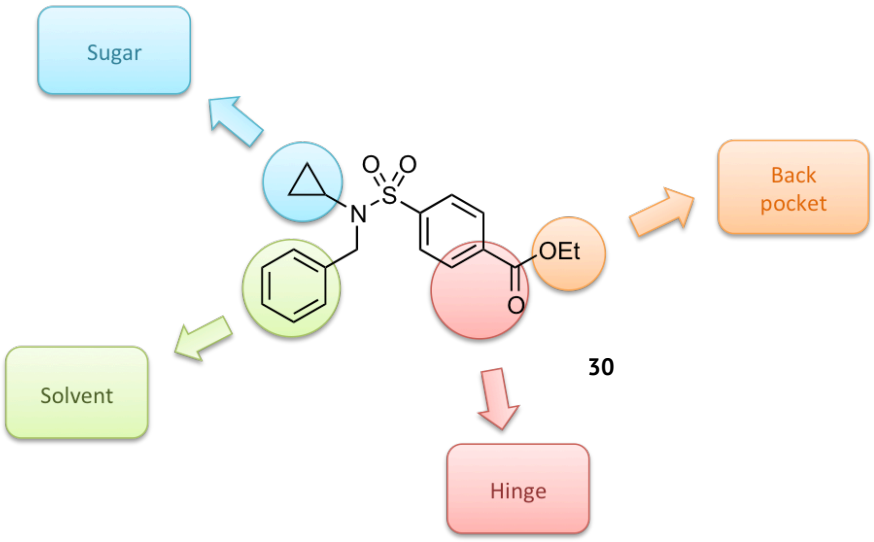


Figure 22. Assigned vectors on the 2-D structure of ICFMS013 **30**.

It is worth noting that in the case of the benzhydryl structure of ICFMS023 **29**, any differentiation in the structure of one of the phenyl substituents (e.g. *via* replacement with an alternative aryl group or alkyl chain) leads to the creation of a stereocentre alpha to the sulfonamide nitrogen. Adding 3-D complexity in this manner has the potential to enhance the targeting of these interactions towards their proposed binding pockets and therefore increase the selectivity of these molecules for a particular kinase target.

2.4.2 Retrosynthetic analysis of sulfonamide series

The retrosynthetic approach was designed to allow the installation and variation of the features mentioned in section **2.4.1** utilising robust chemistry and a minimisation of required synthetic steps.

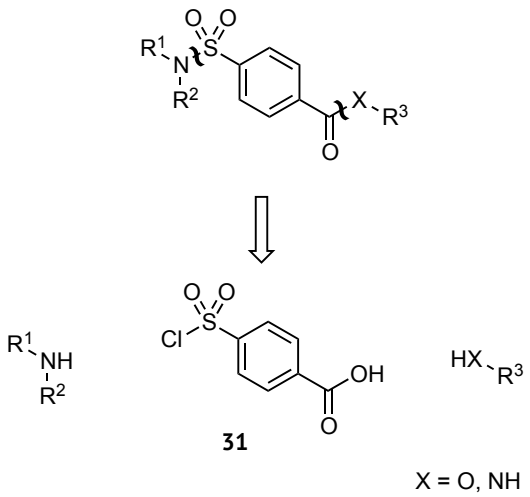
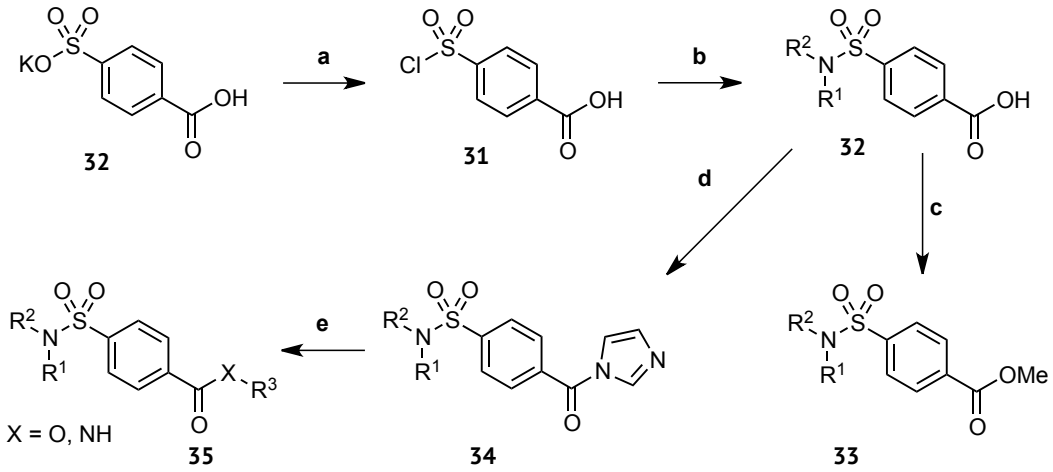


Figure 23. Disconnections to key building blocks for sulfonamide series.

The fundamental disconnections gave rise to three key building blocks, centring around the *p*-carboxybenzenesulfonyl chloride **31** (Figure 23).

2.4.3 Preparation of sulfonamide series analogues

2.4.3.1 General synthesis of compounds of the sulfonamide series



Scheme 9. General synthetic scheme to sulfonamide series analogues. Reagents and conditions: (a)(i) HSO_3Cl (neat), r.t.; (ii) ice, 90%; (b) R^1R^2NH (3.5 eq), DCM, r.t., 87-94%; (c) $TMSCHN_2$, PhMe, MeOH, r.t., 44-69%; (d) CDI, DCM, r.t.; (e) HXR^3, DCM, r.t., 41-63% (2 steps).

The analogues of this series were synthesised according to the route above (Scheme 9). The syntheses started with the monopotassium salt of the aryl diacid **32** which was converted to the arylsulfonyl chloride using chlorosulfonic acid presumably *via* an *in situ* hydrolysis of the acyl chloride of the corresponding dichlorinated intermediate.[65] Direct methyl esterification of intermediate **31** using reported conditions ($TMSCHN_2$ in toluene and methanol) was unsuccessful and led to a major product of methyl 4-(methoxysulfonyl)benzoate.[66] This necessitated the formation of the sulfonamide to be the proceeding step which was achieved using the required amine in sufficient excess to sequester any HCl generated, as well as giving rise to the desired products **32**. The acids were derivatised to the methyl esters **33** for a direct comparison of the effect of varying the amine portion compared to the original hits from the virtual screen. Once these methyl esters were synthesised, it was possible to then study the SAR through variation of the acyl group in addition to the new amine units. These acylations were achieved by converting the acids to their acyl imidazoles **34** using *N,N'*-carbonyldiimidazole (CDI; Staab's reagent)[67] and subsequent reaction of these imidazolides with alcohol or amine nucleophiles to provide the new analogues **35**.

2.4.3.2 Analogue selection for SAR generation

The analogues prepared by this route were selected to answer some important questions around basic SAR tolerances for this scaffold.

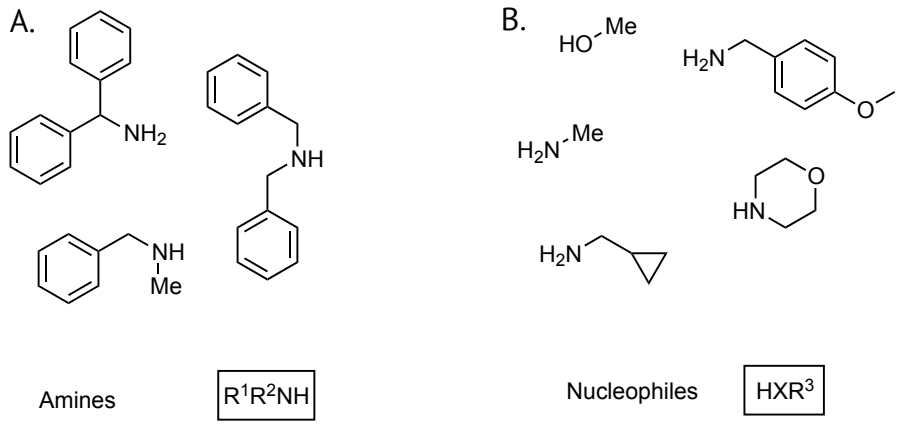


Figure 24. Variations to the amine and nucleophile building blocks for SAR generation.

A number of amines (Figure 24A) were chosen to test the steric and electronic interactions around the sulfonamide moiety. One of the most interesting differences in the FieldPoint templates between the seed molecule **3** used in the Cresset search and the compounds of the sulfonamide series (e.g. ICFMS023 **29**) is that the latter compounds do not make use of a potential hydrogen-bonding interaction that is seen to be given by the aniline in the seed molecule (Figure 25) – this interaction is made between the N–H of **3** and the carbonyl oxygen of the residue Cys666 situated in the FMS hinge region.[44]

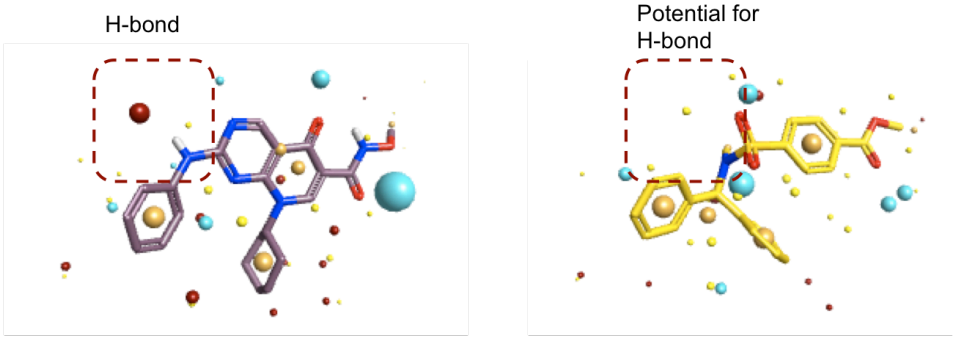
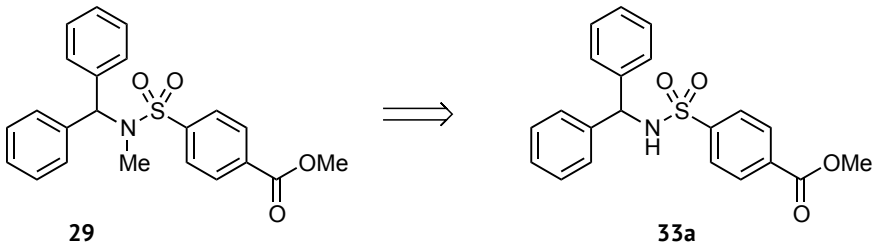


Figure 25. Hydrogen-bond donating interaction (positive electrostatics – red FieldPoint) seen in search molecule **3** (purple) not present for ICFMS023 **29** (yellow).



Scheme 10. Structure of ICFMS023 **29** *vs.* de-methylated analogue **33a**.

Using benzhydrylamine, ICFMS023 **29** would be converted to **33a** (Scheme 10), which could present a hydrogen-bond donating motif, similar to that of the aniline N–H in the computational search molecule **3**, importantly in an approximately equivalent position.

The remaining amines chosen for the sulfonamide moiety were selected to examine the effects of altering the steric properties around the substituted nitrogen.

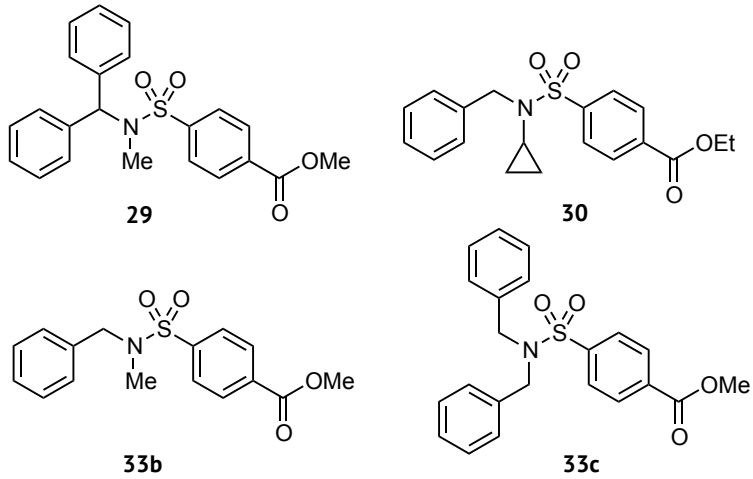


Figure 26. Sulfonamide analogue: commercially available **29** & **30** with synthesised compounds **33b** & **33c**.

These properties may be studied through comparison of the *N*-methylbenzylamine, *N*-cyclopropylbenzylamine, *N*-methylbenzhydrylamine and dibenzylamine analogues **33b**, **30**, **29** and **33c** respectively (Figure 26).

The variations made to the ester portion of the series investigated the conversion of this functionality to an amide – known to have greater stability under biological conditions and the additional capability of being able to perform hydrogen-bond donor and acceptor roles (in the cases of primary and secondary amides). In addition, the substituents chosen (Figure 24B) were aimed at potentially extending this motif towards the back-pocket region and the possible differentiation of the DFG-in and DFG-out binding modes. The below compounds (Figure 27) were synthesised *via* the route shown in **2.4.3.1**. The molecules produced were biased towards derivatives containing the *N*-methylbenzylsulfonamide motif as the least sterically bulky and the *N*-benzhydrylsulfonamide motif to probe the effect of the potential sulfonamide hydrogen bond donation. These analogues were submitted to biological assays to test their FMS activity (see section **1.6**).

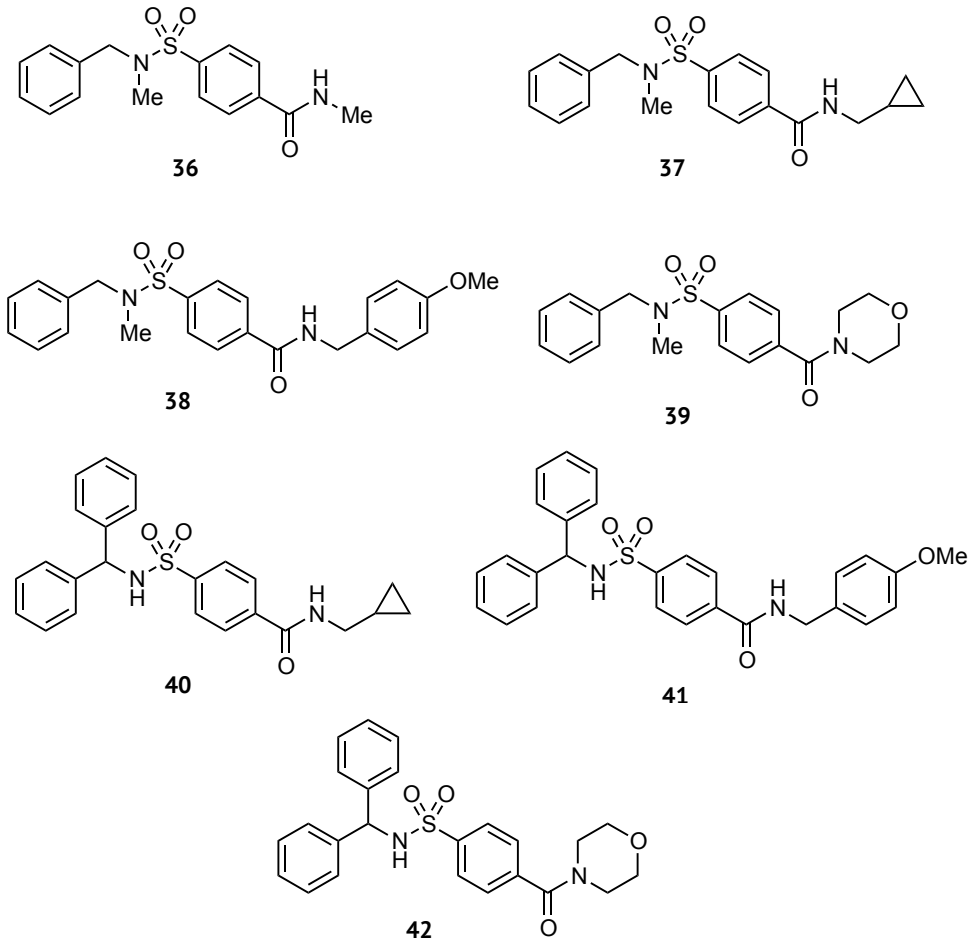
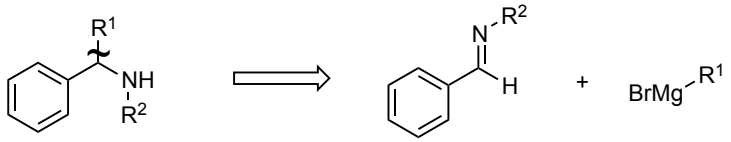


Figure 27. Analogues of the sulfonamide series synthesised for preliminary SAR analysis.

2.4.4 Synthesis of chiral amine motifs

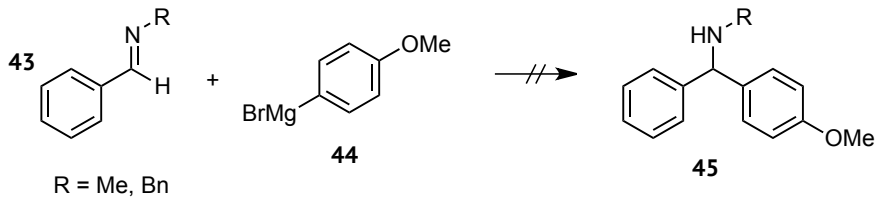
One of the remaining synthetic areas of this series was the construction of the chiral amines that would be incorporated into the sulfonamide moiety. The most convenient disconnection to produce these amines leads back to the addition of an organometallic reagent to an imine (Scheme 11).



Scheme 11. Retrosynthetic analysis of amine motif.

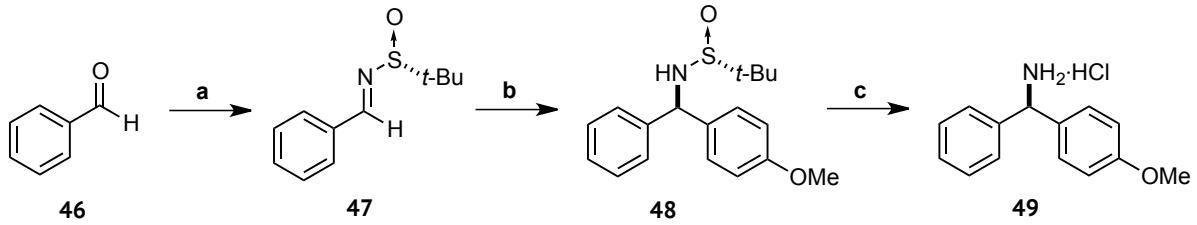
Initial attempts to add 4-methoxyphenylmagnesium bromide (**44**) to *N*-alkyl benzaldimine derivatives (**43**; R = Me, Bn) showed no reaction (Scheme 12). To increase the electrophilicity of the imine, an *N*-sulfinyl group was introduced – specifically through the condensation of *t*-butylsulfinamide (*t*-BSA; Ellman's auxiliary) with the required aldehyde (benzaldehyde). In

addition to the increase in reactivity, these *N*-sulfinyl auxiliaries are well precedented in their ability to direct diastereoselective addition of nucleophiles to the imine functionality.[68,69]



Scheme 12. Unsuccessful Grignard addition to unactivated imines.

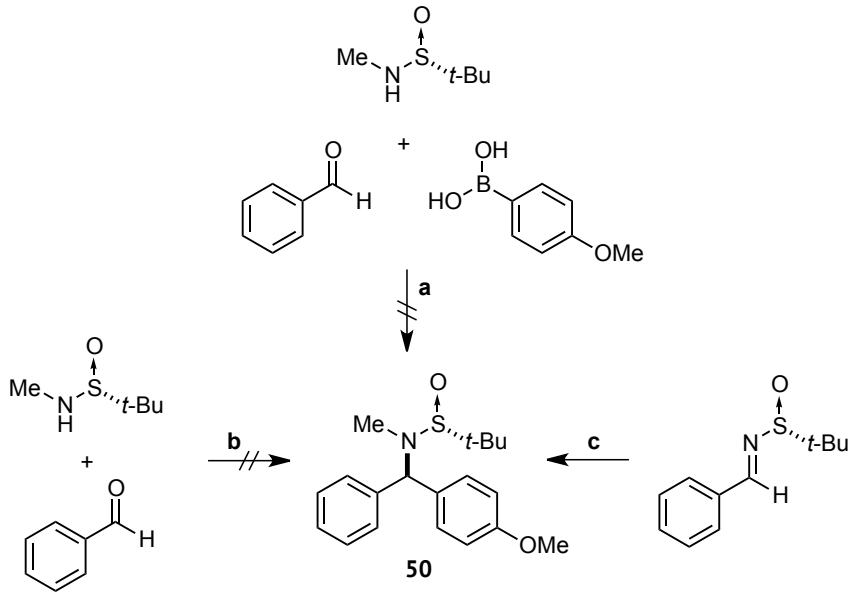
Pleasingly it was found that the Grignard additions to the *N*-sulfinylimine **47** (e.g. Scheme 13) gave yields and diastereoselectivities in good agreement with literature precedent.[68] Typical of a medicinal chemistry project, the synthesis was carried out in a racemic fashion to be later adapted to an asymmetric synthesis if there was promising activity shown by the racemate through the use of a single enantiomer of the Ellman auxiliary.



Scheme 13. Racemic synthesis of chiral amine moiety. Reagents and conditions: (a) *t*-BSA, Cs_2CO_3, DCM, reflux, 91%; (b) **44**, PhMe, –40 °C, 73%; (c) 4.0 M HCl in 1,4-dioxane, Et_2O, r.t., 90%.

For the structures required in this analogue series, the synthesis started through condensation of the *t*-butylsulfinamide auxiliary with benzaldehyde (**46**) to give the *N*-sulfinyl imine **47**. After the addition of the Grignard reagents, the sulfinamide products (e.g. **48**) were treated with anhydrous HCl to remove the sulfinyl auxiliary and yield the bench stable amine hydrochloride salts (e.g. **49**).

Attempts were also made to utilise this auxiliary in the direct synthesis of secondary amines (i.e. disubstituted after removal of the auxiliary) to try and improve the step economy for production of these moieties.



Scheme 14. Approaches towards the construction of tertiary sulfinamide **50**. Reagents and conditions: (a) DCM, r.t. - reflux; (b)(i) $TiCl_4$, DCM, 0 °C – r.t.; (ii) **44**; (c)(i) **44**, PhMe, –40 °C; (ii) CuI (0.6 eq), DMSO:THF (1:1), –40 °C –0 °C; (iii) MeI, 0 °C – r.t., 62%.

These attempts included three component Petasis-borono-Mannich (PBM) reactions using secondary sulfinamides (Scheme 14a), the addition of a Grignard reagent to *N*-sulfinyl iminium species (Scheme 14b), and the alkyl halide trapping of the intermediate of a Grignard addition to an *N*-sulfinyl imine (Scheme 14c).

The PBM reaction has been previously reported using the Ellman auxiliary;[70] however, the reported aldehyde and sulfinamide substrates were glyoxylic acid and *t*-BSA which would be more reactive than the reagents shown (Scheme 14a) under conventional uncatalysed conditions. It was found that, as expected, the selected starting materials did not react at room temperature or elevated temperatures. Lewis acids have commonly been used to aid iminium formation in the PBM reaction through enhancement of the *in situ* dehydration, including the use of $BF_3{\cdot}Et_2O$ with hemiaminals derived from amides and carbamates.[71,72] It is possible that the use of similar conditions may have improved this reaction although this was untested – as the published literature reported that the use of the Ellman auxiliary in the PBM reaction did not provide any stereoinduction, it was decided that optimisation of this reaction would not be valuable if the reactivity could not be extended to an asymmetric synthesis.

Another strategy towards the construction of this motif was the addition of a Grignard reagent to an *N*-sulfinyliminium species (Scheme 14b). As with the previously mentioned

Petasis-borono-Mannich reaction, the key obstacle to this was seemingly formation of the iminium itself. Dehydration attempts through the use of oxophilic Lewis acids such as $TiCl_4$, or increased equivalents of the Grignard reagent even at elevated temperatures were unsuccessful.

The final method considered was the *in situ* trapping of the *N*-sulfinylimine–Grignard addition intermediate with alkyl halides. The mono- and dialkylation of sulfinamides under basic conditions is known reactivity,[73,74] therefore it was proposed that it should be possible to perform similar reactions with the anionic intermediate generated once the Grignard reagent had reacted with the *N*-sulfinylimine. Initially the addition of alkyl halides (MeI, EtBr, BnBr) to the reaction mixture after complete consumption of the imine did not lead to any further reaction, and the only product isolated was that corresponding to protonation of the Grignard addition product. The use of organocuprates, generated from Grignard reagents and copper salts is well precedented for S_N2 alkylation using alkyl halides.[75,76] Through the addition of CuI (0.6 eq) to the reaction mixture prior to the addition of the alkyl halide as well as a DMSO:THF (1:1) solvent mixture to increase solvation and reactivity,[77] the methylation of the intermediate was seen to proceed smoothly and cleanly to give the methylated product **50** in moderate yield (62%) along with unmethylated **48** (20% yield). Varying the equivalents of copper did not lead to an increase in the yield of the reaction; in fact, when 1.0 eq or more of CuI was used, an unreactive precipitate was formed which was thought to be a polymeric metal amide aggregate.

2.4.5 Summary of sulfonamide series

With the syntheses described in the two preceding sections (**2.4.3** & **2.4.4**), it was possible to prepare and assemble the building blocks to construct the series analogues with a focus on step economy. The general synthetic route was planned so that modifications to test the SAR around this series could be installed without the need to alter the synthesis on a case-by-case basis. Initial analogues to investigate the SAR were chosen through analysis of protein–ligand co-crystallisation data as well as computationally generated data and were synthesised to analyse their biological activity (see **1.6**).

2.5 Triazolopyrimidone series

The other series investigated were the triazolopyrimidone analogues, the desired structures contain 7-oxo-7,8-dihydro-1,2,4-triazolo[4,3-*a*]pyridine moieties as their core, and as such present much more common kinase inhibitor qualities (i.e. the flat heteroaromatic bicyclic unit, presenting hydrogen-bond donating and accepting features – similar to the adenine in ATP).

2.5.1 Orientation of triazolopyrimidone analogues

As with the previous series, the available computational and physical data already obtained for these molecules meant that it was possible to assign a prediction to the binding mode of this structure.

As can be seen below (Figure 28), the new structure was predicted to fit well when aligned to the seed molecule in the Cresset screen, picking up both the important electrostatic interactions in the hinge-binding region as well as overlaying well with the hydrophobic regions.

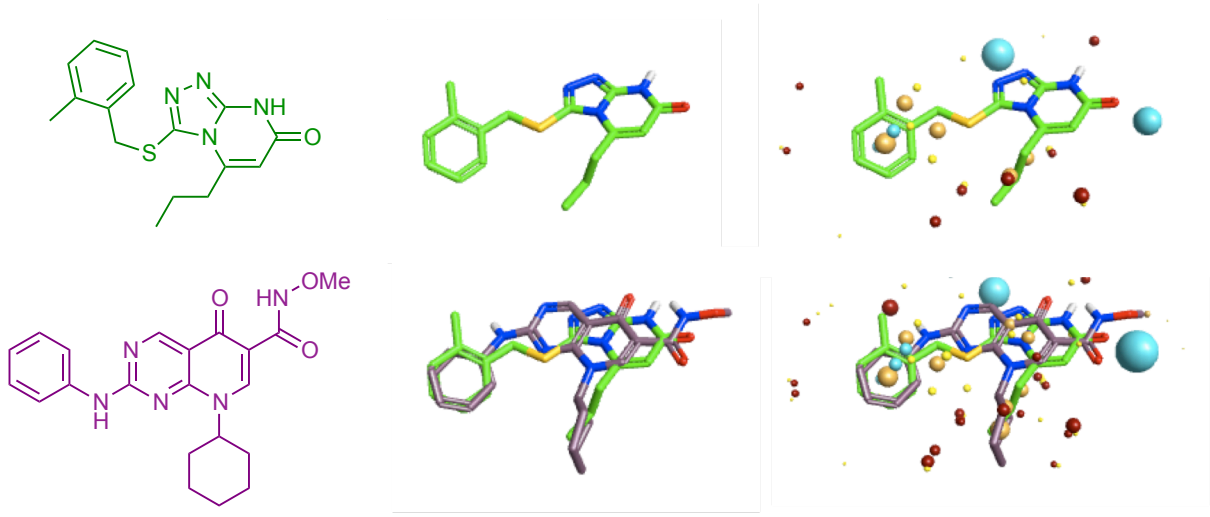


Figure 28. Cresset overlay of ICFMS046 (green) and search molecule (purple), with and without FieldPoints.

When considered in this orientation, it can be seen that functionalisation of the carbonyl (or possibly C–6) would allow targeting of the back pocket region through extension of the core structure. Further substitution of the heteroaromatic nitrogens would likely disrupt the hydrogen-bonding interactions and would therefore be unfavourable. Additionally, the C–5

and *S*– substituents could be modified to understand the nature and tolerances of the hydrophobic regions (Figure 29).

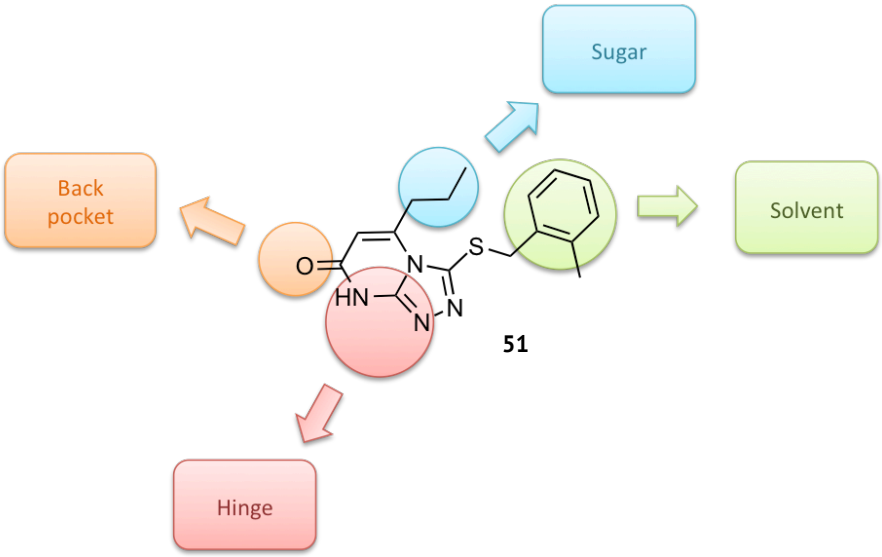


Figure 29. Assigned vectors on 2-D structure of ICFMS046 **51**.

Interestingly some preliminary SAR was available through consideration of the structures similar to **51** that did not show activity in the original assays (e.g. Figure 30, **52** & **53**).

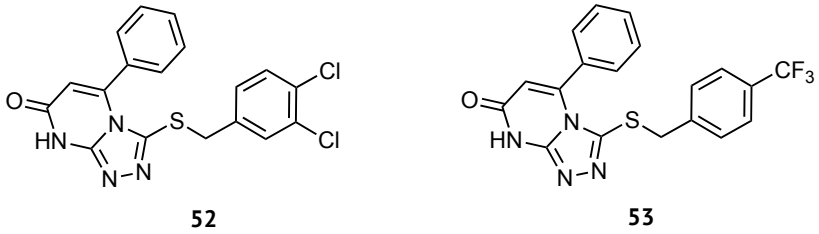


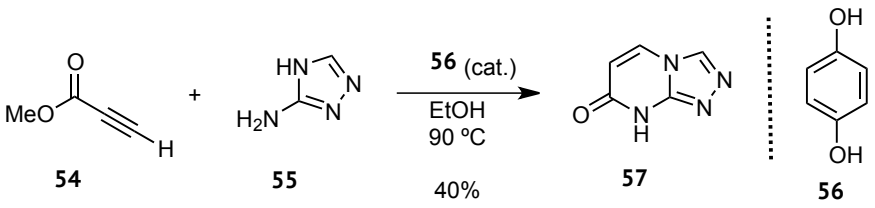
Figure 30. Inactive triazolopyrimidone series analogues.

Taking into account the above results and the chemical similarity between the structures, it would seem that an alkyl substituent is preferable to an aryl substituent at the C–5 position.

2.5.2 Disconnection and synthesis of heterocyclic core

The first aim was to understand the formation of the unsubstituted heterocyclic core as well as how simple functional handles may be incorporated into the core precursors to allow downstream derivatisation. There are limited examples in the published literature of the formation of the unsubstituted heterocycle **57**,[78–82] of which the only method that yields the desired regioisomer as a single product is that shown below (Scheme 15). The authors report starting from 3-amino-1,2,4-triazole and methyl propiolate with hydroquinone used as a radical inhibitor.[81] This reaction presumably proceeds *via* a 1,4-addition to the unsaturated

ester of one of the nitrogens from the triazole ring, followed by formation of the 6-membered ring through a condensation reaction of the exocyclic nitrogen with the methyl ester.



Scheme 15. Synthesis of heterocyclic core **57**.

2.5.3 Regiochemistry of triazolopyrimidone structures

The issue of regioselectivity in the construction of this heterocyclic motif presented the greatest challenge encountered. There are four regioisomeric variants of the oxo-dihydro-1,2,4-triazolopyrimidine structure, shown below (Figure 31).

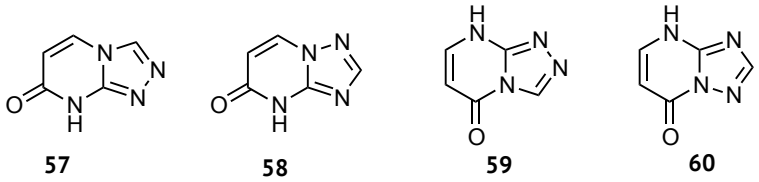


Figure 31. Regioisomeric forms of the heterocyclic core. In order: **57** 7-oxo-[4,3-*a*], **58** 5-oxo-[1,5-*a*], **59** 5-oxo-[4,3-*a*], **60** 7-oxo-[1,5-*a*] dihydrotriazolopyrimidines.

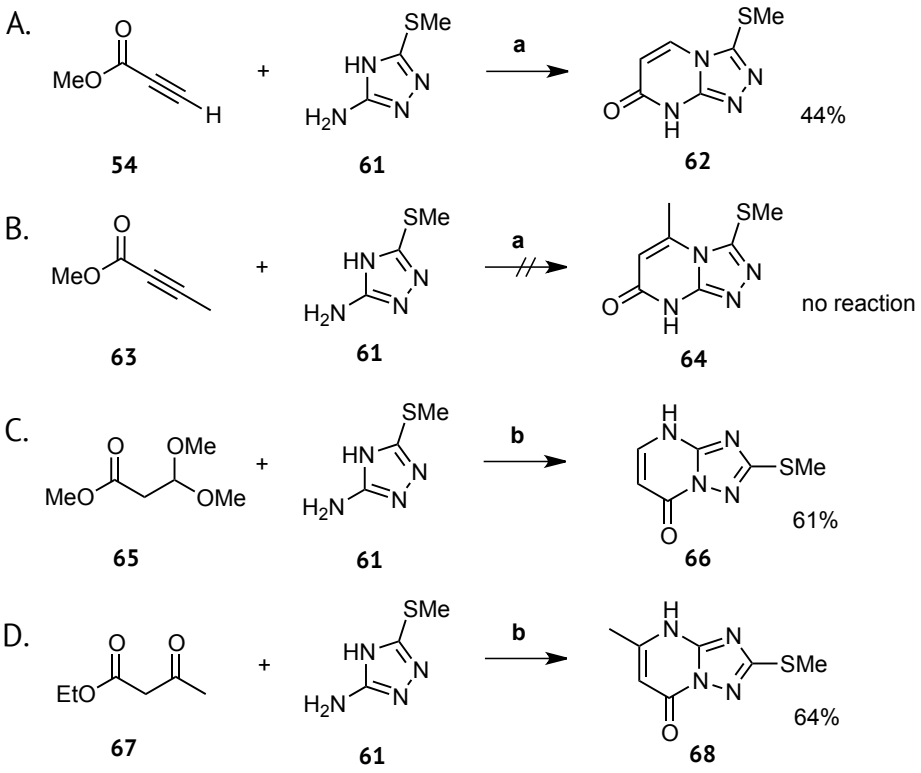
It was hoped that by using a methylsulfide substituted aminotriazole **61**, this substituent would be incorporated as a functional handle on the core to produce an intermediate for analogue synthesis; however, it was necessary to investigate whether or not this additional functionality would affect the regiochemical outcome of the reaction.

2.5.4 Triazolopyrimidone core synthesis

2.5.4.1 Synthesis and assignment of heterocyclic regioisomers

To properly assess the regiochemistry of the core formation it was necessary to attempt the synthesis under conditions reported to yield differing regioisomeric products.

In addition to the method shown above (Scheme 15) which was predicted to form the 7-oxo-[4,3-*a*]-fused structures, conditions were found that had been reported to form the 5-oxo-[1,5-*a*] regioisomers (e.g. analogues of **60**).



Scheme 16. Syntheses of regioisomers for analytical comparison. Reagents and conditions: (a) Hydroquinone (cat.), EtOH, 90 °C; (b) AcOH, 130 °C.

The reactions to yield **62** & **68** (Scheme 16A & D) were the most similar to the literature precedents and pleasingly only a single regioisomer was obtained in each one. **62** was synthesised using the same conditions as seen for the unfunctionalised core (Scheme 15), coupling methyl propiolate (**54**) with 3-amino-5-methylthio-1,2,4-triazole (**61**) (Scheme 16A). Under these conditions **62** was formed in a comparable yield (44%). To form **68**, the same methylthiotriazole **61** underwent acid-catalysed condensation with ethyl acetoacetate giving the product in moderate yield (64%) (Scheme 16D). Unfortunately it was found in the attempted synthesis of **64** that adding an alkyl substituent to the alkyne reagents (i.e. methyl butynoate (**63**)) led to a complete loss of reactivity (Scheme 16B). As a result, **66** was synthesised to present a direct isomeric comparison to **62**. This was achieved through the reaction of methyl 3,3-dimethoypropionate (**65**) and 3-amino-5-methylthio-1,2,4-triazole (**61**) under the same acidic condensation conditions used for the previous 1,3-dicarbonyl substrate **67**, again in a comparable yield for these conditions (61%) (Scheme 16C).

It was apparent that **62** & **66** had different regioisomeric structures, as expected. Correlation to the literature structures with NMR & IR spectroscopic analysis provided strong evidence that these corresponded to the predicted regioisomer assignments.[78,81,82] In addition, ^{1}H NMR spectroscopy NOE experiments provided correlations that reinforced these assignments.

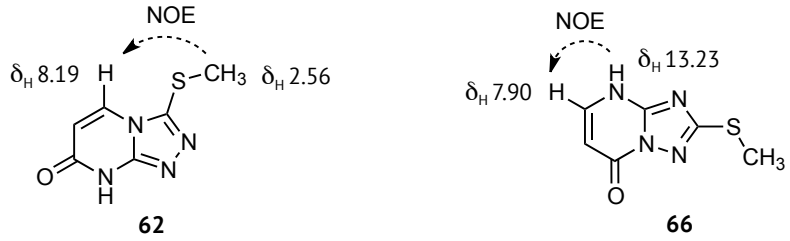


Figure 32. Observable NOE correlations for **62** & **66**.

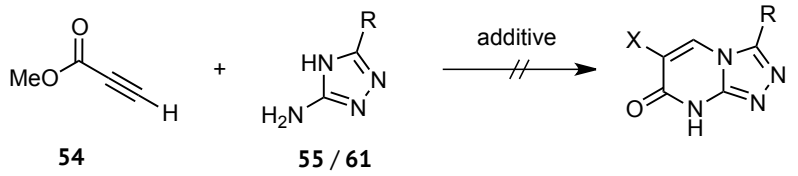
With this valuable information regarding regioselective heterocycle synthesis in hand and one functional handle introduced onto the core molecule, the focus was shifted to improving the yield of the reaction to assess the scope for the possible introduction of a second functional group on the 6-membered ring.

2.5.4.2 Incorporation of functional handle onto heterocyclic core

The first two approaches taken towards the improving the core formation investigated the activation of the alkyne in either a mono- or bimolecular approach. Additives such as I_2, *N*-iodosuccinimide (NIS) in combination with transition-metal π-acids were also screened, in an attempt to install a second functional handle in the molecule.

The bimolecular approach uses the conditions seen previously (Scheme 16A) with methyl propiolate, 3-amino-1,2,4-triazole (**55**) or 3-amino-5-methylthio-1,2,4-triazole (**61**) and the additive (with and without hydroquinone).

Under the attempted reaction conditions below (Table 1), it was not possible to obtain any of the desired heterocyclic products. Typically the decomposition products were polymeric in nature and for the reactions with I_2 and NIS, occurred both with and without the use of hydroquinone. The Ag(I)NTf_2 and [Ph_3PAu(I)Cl] catalysed reaction conditions were adapted from published reactions which included an iodo-demetallation to turnover the catalyst – installing the iodine as a potential point of derivatisation.[83–85] Unfortunately, though these reactions (Table 1 entries 5-9) showed a trace of heterocycle formation *via* MS analysis, the majority of the isolated material was again polymeric in nature. Attempts to isolate the heterocycle product from these mixtures through separation or derivatisation (through alkylation or acylation of the amide) were unsuccessful. Lowering the reaction temperature to 0 °C resulted in no reaction.

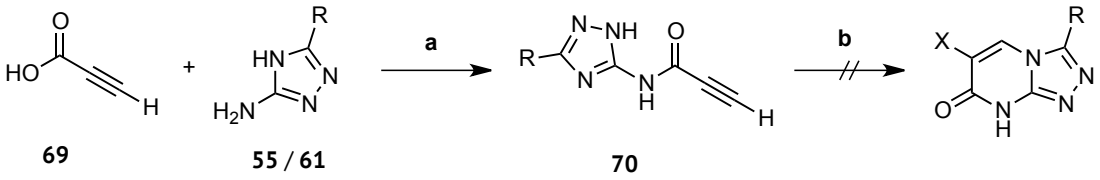


Scheme 17. Attempted use of additives to improve cyclisation.

Entry	Additive	R	X	Result (r.t.)	Result (40 °C)	Result (0 °C)
1.	I_2	SMe	I	No reaction	Decomposition	-
2.	NIS	H	I	No reaction	Decomposition	-
3.	NIS	SMe	I	No reaction	Decomposition	-
4.	Cu(I)OTf	H	H	No reaction	-	-
5.	Ag(I)NTf_2	H	H	Decomposition	-	No reaction
6.	Ag(I)NTf_2 / NIS	H	I	Decomposition	-	No reaction
7.	Ag(I)NTf_2 / NIS	SMe	I	Decomposition	-	No reaction
8.	[Ph_3PAu(I)Cl] / NIS	H	I	Decomposition	-	No reaction
9.	[Ph_3PAu(I)Cl] / NIS	SMe	I	Decomposition	-	No reaction

Table 1. Conditions and results for bimolecular cyclisations with additives to activate the alkyne. DCM was used as solvent.

The monomolecular approach investigates pre-formation of the adduct **70** prior to cyclisation through amidation of propiolic acid with the aminotriazole *via* an activated ester (e.g. acid chloride or EDCI coupling), then completion of the cyclisation either thermally or with the additives seen previously.



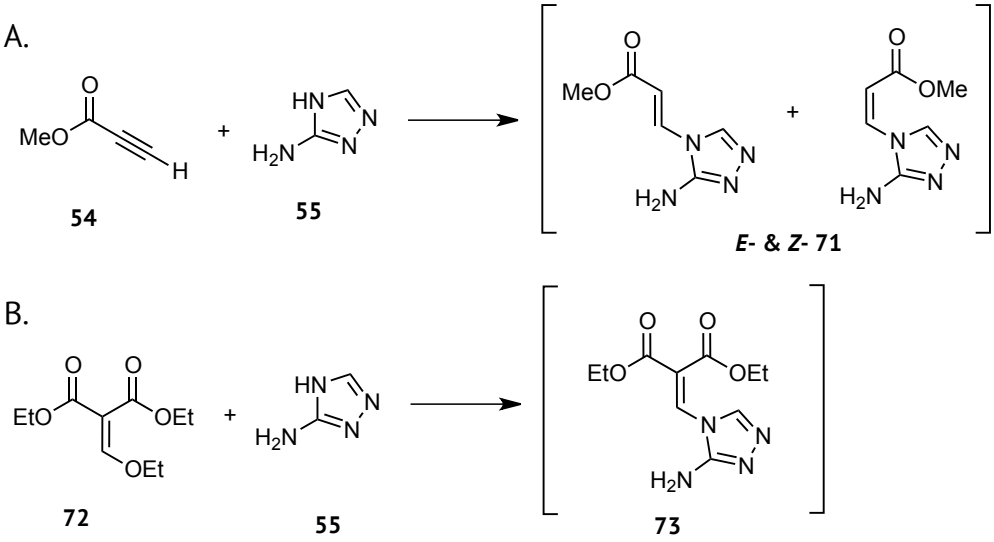
Scheme 18. Two-step cyclisation *via* formation of acylated aminotriazole **70**. Reagents and conditions: (a) acylation reaction (e.g. EDCI coupling or acyl chloride formation); (b) heat or alkyne activation.

This route was not successful in terms of producing the desired heterocycles. It was not clear if this was due to problems in the cyclisation step or the prior amide formation. It is possible that the acylated aminotriazole **70** is not very stable as an intermediate, as it is structurally similar to the acyl imidazole functionality. Furthermore the regiochemical outcome of this approach is not clear as the initial adduct may form through one of the endocyclic nitrogens

or the exocyclic nitrogen, and the cyclisation of the desired adduct **70** would be possible by either of the triazole nitrogens.

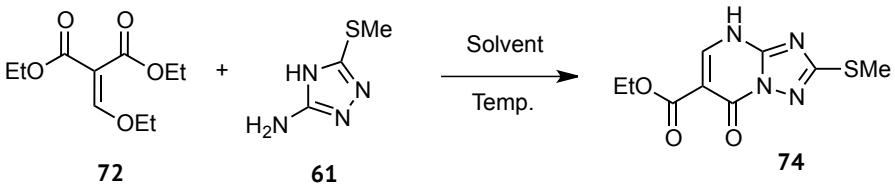
2.5.4.3 Use of diethyl (ethoxymethylene)malonate as alternative Michael acceptor

It was not clear for the successful cyclisations (Scheme 16A), whether the initial adduct from the Michael addition gave the *E* or *Z* form of the olefin, and what impact this would have on the subsequent cyclisation (Scheme 19A). To remove the potential bias from this initial addition, an alternative Michael acceptor unit, diethyl (ethoxymethylene)malonate (**72**), was proposed that would only give a single intermediate form **73**.



Scheme 19. Intermediates from the use of methyl propiolate *vs.* diethyl (ethoxymethylene)malonate as the Michael acceptor.

The reaction was initially attempted in EtOH at reflux, which led to the precipitation of the heterocyclic product **74** in 10% yield (Table 2, entry 1). As the EtOH may have been acting as a competing nucleophile, alternative solvents were investigated. It was also deemed necessary to remove the EtOH generated during the reaction, so toluene was chosen as an azeotrope for this purpose, leading to a 3.5-fold increase in yield (35%) (Table 2, entry 2). The aminotriazole was sparingly soluble in PhMe and as the product formed, it precipitated around the unreacted starting material. This led to an approximate 10% recovery of starting material that was inseparable from the product. The most successful solution to this issue was to increase the reaction temperature above the melting point of 3-amino-5-methylthio-1,2,4-triazole (130–133 °C) using xylenes. Pleasingly this led to product formation in 58% yield as a single regioisomer (Table 2, entry 3).



72 61 74

Scheme 20. Formation of heterocycle **74**.

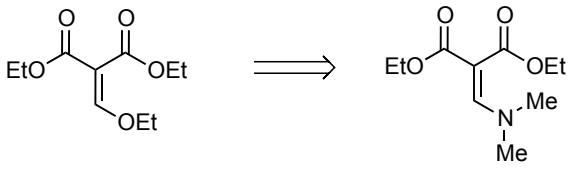
Solvent	Temp. (°C)	Time (h)	Yield (%)
EtOH	90	12	10
PhMe	100	12	35 (+ 10 S.M.)
Xylenes	140	12	58

Table 2. Conditions for synthesis of heterocycle **74**.

Analysis of the products of the above reactions (Table 2) revealed that they all yielded the same regioisomeric product. Unfortunately it was found to be the 7-oxo-7,8-dihydro-1,2,4-triazolo[1,5-*a*]pyrimidine regioisomer **74** which upon further inspection of the literature, corresponds well with similar systems without the methylsulfide substituent.[78] Subsequently, it was found that this regioisomer **74** had previously been formed using these reagents in trichlorobenzene solvent at reflux and under acid-catalysed conditions.

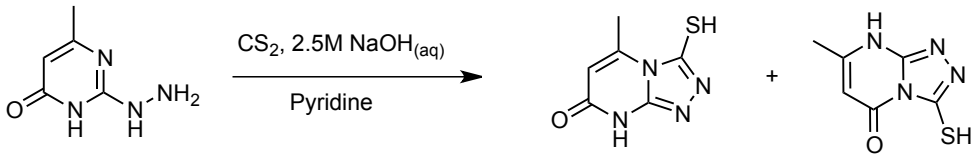
2.5.5 Summary of triazolopyrimidone series

For this series of compounds, promising results were made with the synthesis and regiochemical analysis of the desired core with a methylsulfide functionalisable handle. Although the synthesis using the alternative Michael acceptor moiety **72** resulted in the formation of an incorrect regioisomer, it may be possible to modify this reactivity to favour the desired regioisomer. Initial efforts would focus upon adjusting the protonation state of the aminotriazole, altering the reversibility of the Michael addition step by using less nucleophilic polar solvents (e.g. *t*-BuOH) instead of EtOH, or introducing alternative conjugated leaving groups (e.g. (Scheme 21) R = NMe_2 instead of R = OEt) on the Michael acceptor.



Scheme 21. Modification of Michael acceptor leaving group.

An alternative approach to the synthesis of this core would be formation of the pyrimidone ring first (as a 2-hydrazinopyrimidine) with subsequent formation of the triazole.[79]



Scheme 22. Formation of triazolopyrimidones from hydrazinopyrimidone.

The cyclisation reaction above (Scheme 22) has been performed under a number of conditions including using CS_2 to install a sulfide onto the triazole.[79] Without substitution on one or the other of the pyrimidine nitrogens, a mixture of the two possible regioisomers is obtained. In addition, this route was initially discounted due to the extra steps required to prepare the starting materials.

2.6 Biological Assessment

Compounds from both series were submitted for testing in cell based assays identical to those used in the biological evaluation of the initial virtual screening molecules. Unfortunately it was found that these assays failed to provide robust reproducible data and therefore it was impossible to identify any SAR trends. The reason for the lack of reproducibility for these results is yet to be determined.

In order to obtain better data on the activity of these compounds, they were tested along with all of the original commercial stock compounds and the seed molecule in the cell free SPR assay run by Dr Olan Dolezal at CSIRO. This assay was performed using a Biacore T200 SPR instrument with a streptavidin coated sensor chip. CSF-1R and RET (a related protein kinase) were "minimally" biotinylated and captured onto the streptavidin surfaces as well as a negative control of biotinylated USP7-CD and a reference surface blocked with D-biotin, giving a total chip configuration comprising four flow cells. ICFMS compounds were directly diluted from 100 mM in DMSO to 100 µM in the running buffer (pH 7.5), then the diluted compounds were sequentially injected over immobilized target proteins. Binding data obtained was processed using Scrubber software.

From this alternative assay, it was apparent that the molecules from commercial sources expected to show FMS activity, as well as those synthesised in house (for both series) did not have activity at FMS (Figure 33).

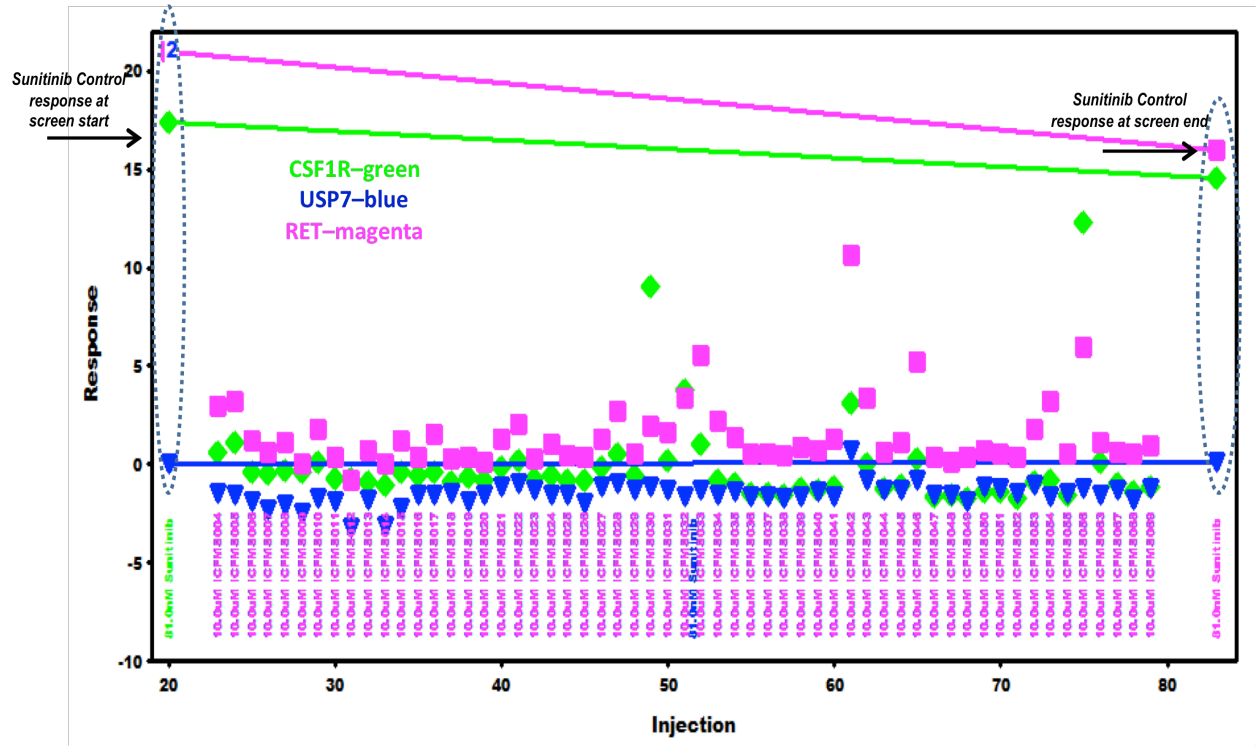
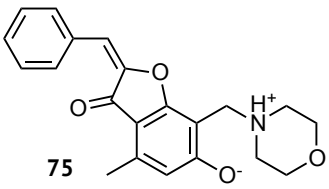


Figure 33. Data from SPR assay for original stock compounds, synthesised compounds and seed molecule.

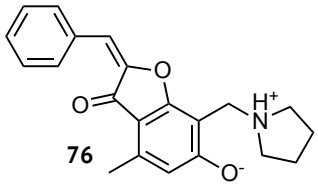
The compounds that did show activity are shown below (Figure 33), of these, the compounds with the highest activity (besides the search molecule ICFMS056 **3**) are ICFMS030 **75** and ICFMS032 **76**, which due to their charged nature could have resulted in poor cell permeability – explaining why they may not have been active in the cell based assays.



75

ICFMS030

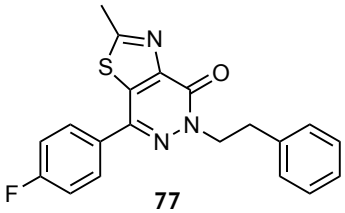
KD = 4.9 μM



76

ICFMS032

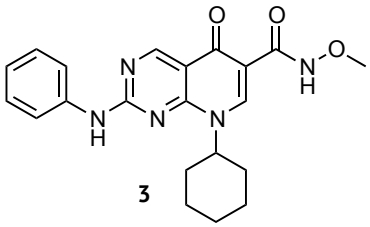
KD = 18.9 μM



77

ICFMS042

KD = 390 μM



3

ICFMS056

KD = 25 nM

Figure 34. Active compounds from cell free assay.

2.7 X-ray crystallographic data

The new data obtained from the SPR assay led to attempts being made to co-crystallise the four compounds shown (Figure 34) by Dr Bin Ren at CSIRO. Of these, protein–ligand co-crystal structures were obtained for the seed molecule **3** (ICFMS056) and **75** (ICFMS030). These protein–ligand co-crystal structures were obtained from apo crystals, soaking in compounds at ~0.7 mM concentration for 30 h at 4 °C. The structures for the ligand in both cases could be modeled onto the data obtained in multiple orientations giving two sets of coordinates for each small molecule. When the co-crystal structures were compared to the structure which had been used to generate the search template (PDB:3DPK) as well as the alignments from the virtual screen, good correlation could be seen in each case to one of the corresponding coordinates. In both cases, the set of coordinates that best agreed with the previous computational experiments also were the ones with lower Free R-factors, implying that the models fit better with the experimental diffraction data.

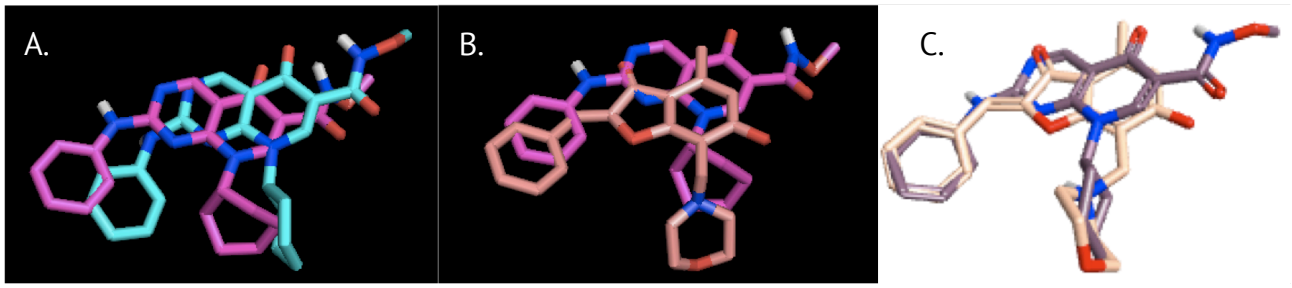


Figure 35. Co-crystal structure overlays (black background) and comparison with Cresset virtual screen alignment (white background): A.) Truncated 8C5 (blue) from PDB:3DPK overlaid with in-house synthesised search molecule **3** (purple); B.) **3** overlaid with ICSFMS030 **75** (beige) – both crystal structures obtained at CSIRO; C.) Conformational result of Cresset alignment of seed molecule **3** (purple) and ICFMS030 **75** (beige). For 2-D structures see (**Figure 34**).

It was pleasing to see that the newly generated crystal structure data corresponded well with both the original co-crystal structure conformation and the predicted overlay from the Cresset software (Figure 35). The latter comparison was particularly important and was recognised as being a good validation of this choice of method for accessing new chemical structures.

3 Conclusions and Future Work (Chapter I)

This work covers the initiation of a medicinal chemistry project investigating the use of a computational screen to identify new scaffolds that showed FMS activity. This method led to an initial biological assay of only fifty compounds, of which three were found to be active in the cell free SPR binding assay, which is a high return rate when compared to a standard high-throughput screen. In addition, a high-throughput screen would typically require the screening of 10^5–10^6 compounds which makes this method much more efficient in terms of consumption of time and materials.

The use of the Cresset software in the virtual screen also provided alignments of the new molecules onto the structure of a compound in a known binding mode. This computationally generated data, along with the available crystal structure data for this protein was a powerful combination in terms of understanding the positioning of the newly identified active compounds within the binding pocket – confirmed by the similarity of the co-crystallised ICFMS030 **75** and ICFMS056 **3** when compared to their Cresset alignment. This exemplified the potential for the use of these data for its predictive capabilities.

The syntheses in this project were focused around step-economy. The sulfonamide series was disconnected to allow targeting of the various binding regions within the FMS ATP-site in as few as four steps. The introduction of a chiral amine moiety into the sulfonamide unit was also investigated and it was found that the stereocentre and a second *N*-alkyl group could be installed in a simple one-pot procedure (Scheme 14c). The triazolopyrimidone series synthesis prioritised the regioselective synthesis of the core molecule with an interest in introducing a functional group that may provide opportunities for derivitisation. Through the synthesis of multiple regioisomeric forms of the heterocyclic core, a better understanding was gained as to the use of 3-amino-5-methythio-1,2,4-triazole in the cyclocondensation reactions described (Scheme 16). For both series, disappointing biological results meant that no SAR could be identified but the preliminary synthetic work undertaken in this project should allow re-entry into these series if new interactions can be identified with the aid of predictive computer modeling.

This project highlights the caution that must be taken with regards to the use of cell-based assays as the primary biological test. Although cell permeability is an important factor for

many biologically active therapeutic molecules, by using a cell-based assay at the start of a project, compound structures active at the desired target protein that lack cell permeability may be overlooked. Furthermore, cell growth assays measure activity through secondary readouts (cell death) that may or may not be independent of the specific activity of the small molecule at the target protein, leading to false positive results. In addition, the lack of reliability in the cell-based assays meant that the differentiation of type I and type II kinase inhibition activity was not possible and the hypotheses and compound modifications along these lines were untested. The earlier introduction of the cell-free assay would have provided better validation in the original biological testing and may have impacted on the future development of one or more of the lead series.

The generation of the template from a single binding pose of a protein-ligand co-crystal structure proved to be a viable approach to performing the virtual screen; however, as stated previously (**2.2.1.1**), it carries the possibility of inappropriate bias towards idiosyncratic points of interaction from the search molecule. This in fact may not be a problem of itself, especially if there is structural data available that would allow more careful selection of the seed molecule (for subsequent conversion into the FieldPoint template) – e.g. choosing a molecule that strongly displays interactions known to be important such as hinge-binding interactions in kinase inhibitors. It would also be necessary to assess the results of the virtual screen to take into account these intrinsic biases when viewing the alignment results, and to favour selection of compounds showing strong alignment to known kinase pharmacophore interactions and disfavour the compounds whose alignments are tending towards interactions more unique to the search molecule. In future work, it may be worth considering the use of several virtual screens using multiple templates extracted from protein-ligand co-crystal structures and then conducting a comparison of the results to prioritise the new compound structures that are returned in multiple virtual screens. Through this approach, the benefits of averaging the weighting of the FieldPoints (cf. generating the screening template through an alignment of multiple molecules) are retained, combined with the fact that the templates have been generated from known (*vs.* calculated) binding conformations.

Chapter II – Evaluation of Novel Substrates and Reactivities in NHC Catalysis

4 Introduction

This chapter describes work undertaken to investigate the reactivity of underused substrates in organocatalysis with N-heterocyclic carbenes (NHCs), with a particular focus on amide bond formation and the use of carbohydrates as masked aldehyde functionality.

4.1 Background

Carbenes are neutral, divalent carbon species i.e. two-coordinate with no formal charge on the carbon;[86] as such they are coordinatively unsaturated and contain an electron sextet in their valence shell of which two are non-bonding. These highly reactive species have been implicated as reaction intermediates since as early as the mid-19th century – dichlorocarbene was the suggested product of alkali induced elimination of HCl from chloroform and a proposed intermediate in the Reimer–Tiemann and Ciamician–Dennstedt reactions.[87] The high reactivity of these species however, meant that for a time they were regarded as transient reactive intermediates that may not be isolable.[88,89]



Figure 36. Representations of carbenes with paired and unpaired non-bonding electrons.

N-Heterocyclic carbenes (NHCs) represent a class of carbenes where this reactive functionality is stabilised through its incorporation onto a nitrogen-containing heterocyclic scaffold (Figure 37).[90]

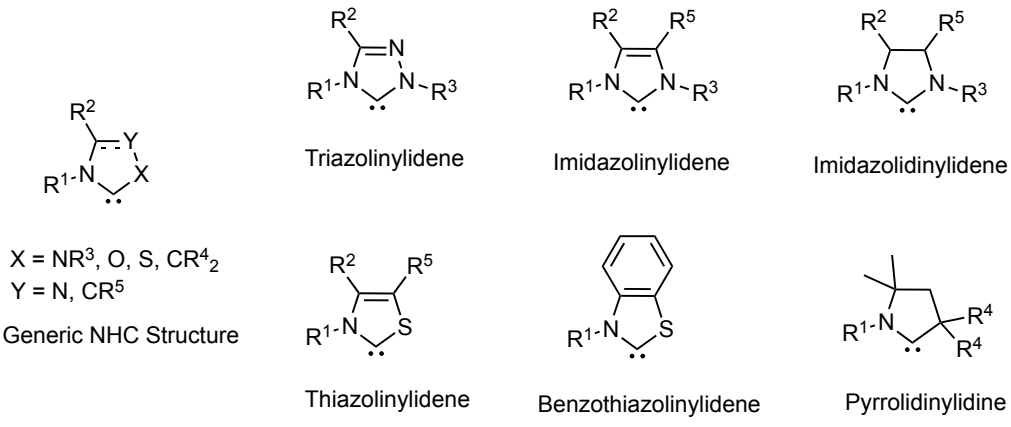


Figure 37. Generic NHC structure with representative examples of substitution patterns.

Typically in these systems, the carbene is flanked by two heteroatoms, at least one of which is a nitrogen atom, the other heteroatom being nitrogen, oxygen, sulfur etc. but is not strictly required.[91]

4.1.1 Triplet Carbene vs. Singlet Carbene Multiplicity

The geometry of the two substituents on carbenes may be broadly defined as linear or bent, these terms being more practically described by their orbital hybridisation and arrangement.

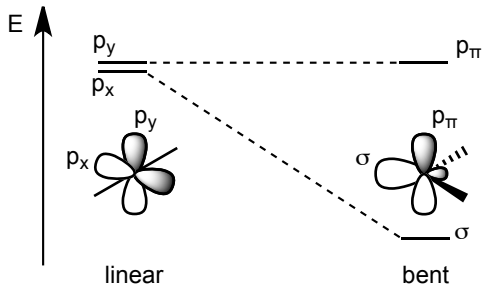


Figure 38. Stabilisation of orbitals through transition towards bent sp^2-type structure.[92]

The transition from the linear geometry with two degenerate p orbitals (p_x and p_y) to the bent form breaks the degeneracy of these orbitals, as the hybridisation at the carbon changes from linear sp-hybridised to trigonal (bent) sp^2-type hybridised. In the bent form, one p orbital remains largely unchanged in character and is referred to as p_π whereas the other p-type orbital acquires partial s-character for stabilisation and is labeled the σ orbital (Figure 38).[92]

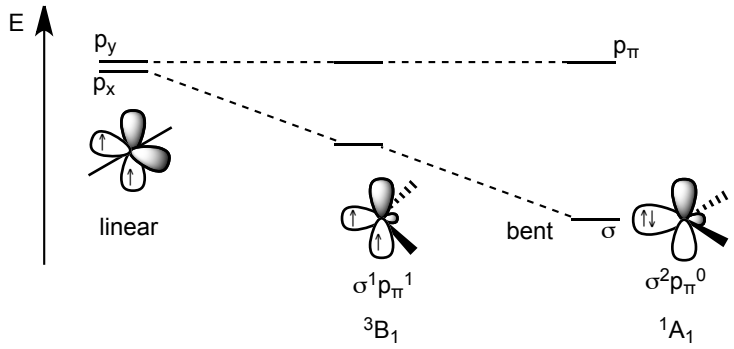


Figure 39. Possible orbital occupancy for triplet and singlet carbenes.[93]

The two non-bonding electrons may be assigned singly to separate orbitals or paired to one orbital. The triplet state of the carbene refers to the unpaired electrons with parallel spin – in this state the electronic stabilisation is maximised when these electrons occupy degenerate orbitals, hence linear geometries will favour the triplet carbene.[92] When triplet carbenes are non-linear they can be described as having a $\sigma^1p_\pi^1$ electron configuration ($^3B_1$ state) using the bent geometry orbital terminology. If the energy difference between the frontier orbitals (σ

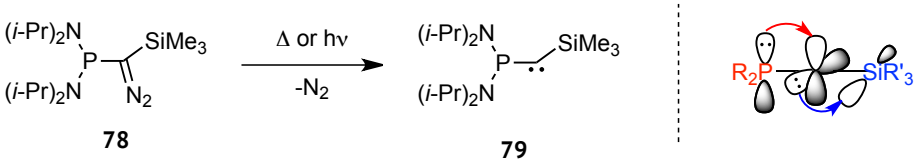
and p_π) is increased, such as with increasing bent geometry, the singlet carbene is preferred, with an electronic configuration of $\sigma^2 p_\pi^0$ ($^1A_1$ state) – see Figure 39.[93] This is exemplified by the comparison of diadamantylcarbene (large carbene bond angle of 152°) which has a triplet ground state, with cyclopentylidene which is constrained into a bent geometry and has a singlet ground state.[92]

As singlet carbenes possess a filled and a vacant orbital, their reactivity is ambiphilic. This can be compared to triplet carbenes which, due to their two unpaired electrons, may be treated more as (di)radical in nature.

4.1.2 Stabilised Singlet Carbenes

Although the use of reactive carbene intermediates became more prevalent in the years following the first hypotheses predicting their existence,[94,95] it was not until the late 1980s that the first stable carbene was synthesised by Bertrand,[96] closely followed by the synthesis and isolation of "A Stable Crystalline Carbene"[97] in 1991 by Arduengo which brought together many underlying ideas from the previous decades – notably from the works of Wanzlick,[98,99] Öfele[100] and Lappert[101,102] on the preparation of NHCs and their complexation to metals.

4.1.2.1 Bertrand's Phosphinosilyl Carbene



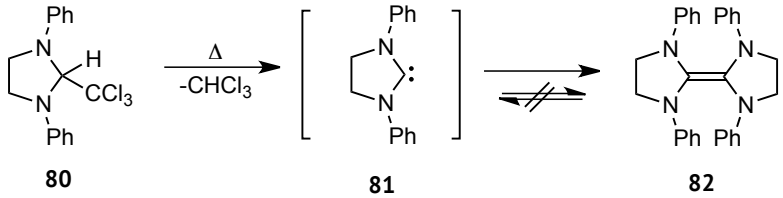
78 **79**

Scheme 23. Preparation of Bertrand's carbene and stabilisation effects.

The Bertrand phosphinosilylcarbene **79** was prepared *via* thermolysis or photolysis of the preceding diazo precursor **78** (Scheme 23),[92,96] a technique that had been well established for the generation of transient carbene compounds e.g. methylene (the simplest carbene – CH_2) from diazomethane. It was found that this resultant phosphinosilylcarbene was stable for weeks at room temperature in benzene and could be purified at 75–80 °C by distillation at reduced pressure. This 'quasi-linear' singlet carbene is stabilised electronically by the push-pull effect of the combined substituents simultaneously raising the energy of the empty p orbital through π-donation of the phosphine whilst stabilising the filled p orbital by negative hyperconjugation through π-withdrawal into vacant σ* orbitals of the silicon.[103] These interactions increase the σ–p_π gap and therefore favour the singlet state. This conceptually

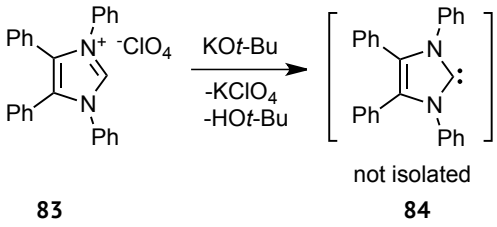
defines the notion of stabilisation through preservation of carbene electroneutrality, proposed by Pauling.[104]

4.1.2.2 Wanzlick's N-Heterocyclic Carbenes



Scheme 24. Wanzlick's NHC and the proposed "Wanzlck equilibrium".

Wanzlick proposed that 1,3-diphenylimidazolidine derived dihydroimidazol-2-ylidene **81** could be produced through the extrusion of chloroform from the 2-trichloromethyl substituted precursor **80**.[98] This was found to spontaneously dimerise to the tetraaminoethylene product **82**, which Wanzlick proposed would exist in equilibrium with its free carbene 'halves'.[105] This "Wanzlick equilibrium" hypothesis was initially disproven in the case of the molecules shown above, although may exist for carefully tuned substrates (Scheme 24).[106–112] It should also be noted that this dimerisation may require electrophilic catalysis to proceed as calculations have indicated that the energy barriers for the uncatalysed dimerisation may be prohibitively high.[113]

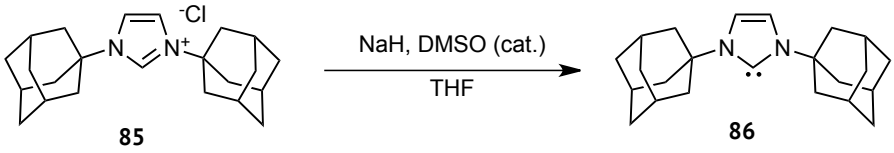


Scheme 25. Wanzlick's imidazolin-2-ylidene NHC formation.

In an attempt to electronically stabilise the carbene species, Wanzlick introduced unsaturation into the heterocyclic backbone to increase π-delocalisation resulting in the tetraphenylimidazolin-2-ylidine **84**. This was formed *via* deprotonation of the imidazolium precursor **83** to yield the carbene which again could only be identified by its reactions with water or metal salts.[114]

4.1.2.3 Arduengo's Stable N-Heterocyclic Carbene

In the groundbreaking work of Arduengo, the first isolated form of a free N-heterocyclic carbene was generated by the deprotonation of 1,3-di-1-adamantylimidazolium chloride **85** with *in situ* generated sodium dimsyl in THF (Scheme 26).[97]



Scheme 26. Arduengo's synthesis of a stable free carbene.

This carbene **86** was found to be stable in the absence of oxygen and moisture, could be recrystallised from toluene and had a melting point of 240–241 °C without decomposition. This structure also contained the *N*-adamantyl substituents which were proposed to provide kinetic stabilisation to help prevent this system from undergoing dimerisation, which are also employed to produce a saturated stable diaminocarbene which lacked cyclic 6π electron delocalisation.[115]

4.1.3 Electronic Stabilisation of NHCs

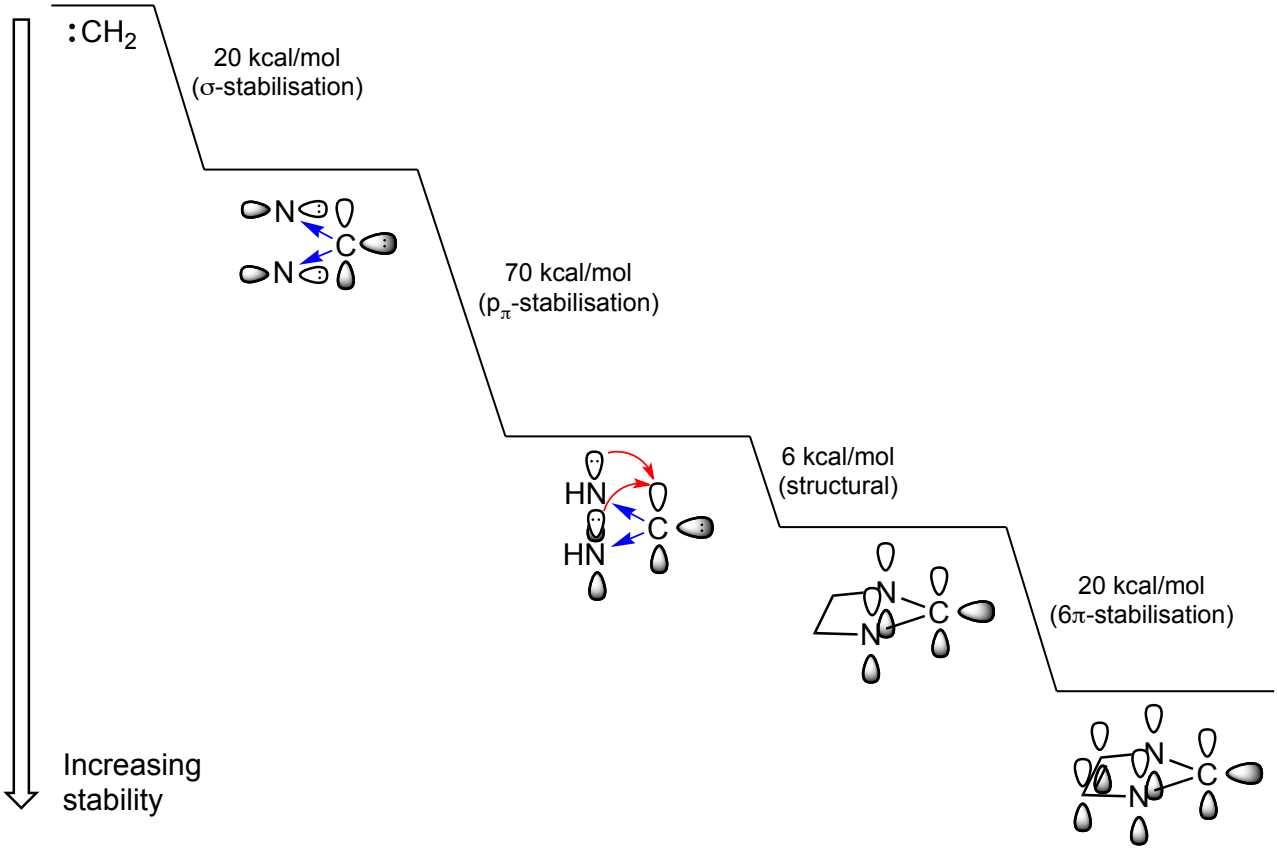


Figure 40. Calculated energy contributions of structural features to stabilisation of NHC (adapted from Herrmann & Köcher).[116]

As mentioned previously (see **4.1.2.1**), singlet carbenes can be stabilised through electron withdrawing interactions with the filled σ orbital and π-donation raising the energy of the p_π orbital thus increasing the σ–p_π gap.[92,103] To understand the contributions of the structural and electronic features of NHCs to the stabilisation of the carbene itself, Heinemann *et al.* performed *ab initio* calculations on a series of structures that described the different interactions within the N-heterocyclic carbene.[117] In the imidazol-2-ylidine example shown previously in the work of Wanzlick and Arduengo, the two flanking nitrogen atoms provide ~20 kcal/mol inductive stabilisation through σ-withdrawing interactions (shown by the perpendicular orientation of the *N*-lone pair orbitals), with the mesomeric 4π-electron donation of the nitrogen lone pairs into the empty p_π orbital calculated to provide an extra ~70 kcal/mol stabilisation. The cyclic form of the diaminocarbene is stabilised by ~6 kcal/mol proposed to be a result of the structural constraint enhancing the bent geometry at the carbene or aligning the nitrogen lone pairs with the carbene empty p orbital. The unsaturated backbone brings about a further ~20 kcal/mol increase in stabilisation energy through additional delocalisation of the electrons in the cyclic system (Figure 40) – there is ambiguity as to what extent this cyclic electron conjugation constitutes aromaticity as the delocalisation seen in the unsaturated carbenes is significant, but the aromatic character of these imidazolin-2-ylidenes is still smaller than that of their protonated or ionised forms.[117–119]

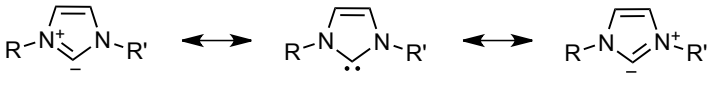


87 **88**

Figure 41. Electronically stabilised, sterically unhindered carbenes.

It was later discovered by Arduengo that electronic stabilisation of the carbene could be achieved to an extent that steric protection of the carbene was not a requirement with unhindered carbenes 1,3,4,5-tetramethylimidazolin-2-ylidine (**87**) being a stable crystalline solid and 1,3-dimethylimidazolin-2-ylidine (**88**) stable in solution for days.[120]

4.1.4 Carbene vs. Ylide Representation



Scheme 27. Representative interconversion of carbene and ylide tautomers.

Initially proposed as ylide forms by Breslow when considering the deprotonated thiamine but represented as carbenes in Wanzlick's early work,[98,121] the degree to which each form is the "correct" representation of these species has been the subject of much investigation (Scheme 27). This was spurred on in the years following Arduengo's breakthroughs in the isolation of these compounds, as a result of the ability to experimentally analyse the structures in question. Studies by Arduengo indicated that the ylidic form represented a minimal contribution to the overall structure of the imidazolin-2-ylidenes.[120,122,123] Electron distribution mapping 0.7 Å above the plane of the NHC revealed strong evidence of localised p_π electrons corresponding to the lone pairs of the nitrogen atoms with little indication of p_π–p_π delocalisation.[122] In addition, the C–N bonds of the carbenes were lengthened in comparison to their corresponding imidazolium precursors.[97,115]

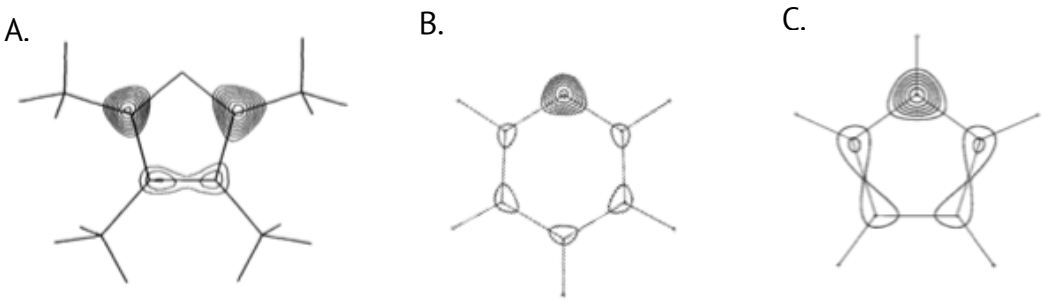


Figure 42. Electron density mapping at 0.7Å above the plane of the heterocycle: A) NHC **87** (experimental); B) pyridine (calculated); C) pyrrole (calculated). In all cases a lack of delocalisation is seen.

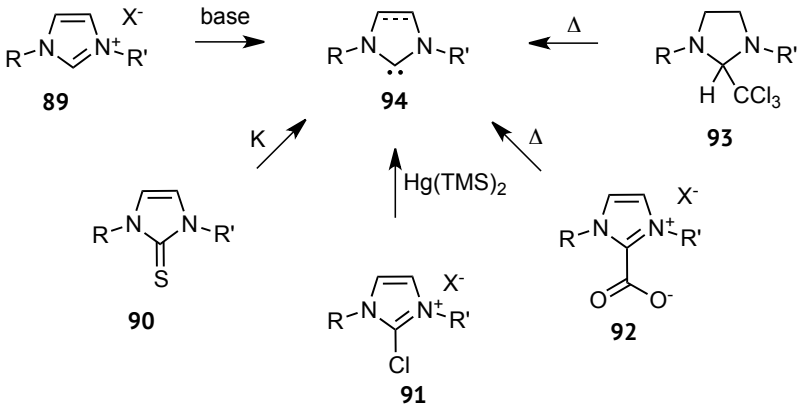
Boehme and Frenking chose to reinvestigate this issue on the grounds that similar electron distribution mapping, when applied to known aromatic compounds pyrrole and pyridine, showed similar localisation of electron density above the nitrogen heteroatoms and lack of delocalisation between the nitrogen atoms and their corresponding cyclic π-systems (Figure 42).[124] *In silico* calculations from these authors, Heinmann *et al.*,[117] Tafipolski *et al.*[119] and Sauers[118] all indicated that p_π–p_π interactions were in fact important in the stabilisation of these imidazolinylidines as well as in the saturated imidazolidinylidenes. The overall agreement was that although the carbene resonance form is still the dominant structural feature, the ylidic form plays an important contribution into the stabilisation of the molecule. It is common practice nowadays to portray the ylide contribution as a curve between the nitrogen atoms (Figure 43),[90] especially when the NHC is coordinated to metals; however, for clarity and simplicity in the mechanistic schemes to follow, NHCs in this work are represented as their pure carbene form.



Figure 43. Representation of NHC with ylidic resonance contribution.

4.1.5 Generation of N-Heterocyclic Carbenes

Free NHCs may be generated in a number of ways (Scheme 28),[93,125] of which the most prevalent by far is deprotonation of their corresponding (typically azolium) salt.[126] This method is favourable due to the ready availability and stability of the carbene precursors **89**.[127] Additionally, the reductive desulfurisation of thiocarbonyls **90** (e.g. thioureas) with potassium can be employed – this method can produce the free carbene in decent purity after a simple filtration as the potassium sulfide byproduct is largely insoluble in THF.[128] The de-chlorination of chloroimidazolium species **91** using bis(trimethylsilyl)mercury is another method which provides relatively facile removal of by-products (elemental mercury and TMSCl).[129] It is also possible to form NHCs from their covalent adducts with small molecules such as alcohols, carbon dioxide (e.g. **92**) or chloroform (e.g. **93**) *via* thermolysis.[130,131]



Scheme 28. Generation of carbene from precursors.

This list is by no means exhaustive and the method chosen often will depend on the purpose for which the NHC is required; for instance, when preparing NHCs to be used as ligands on metals the top priority may be the isolation of the free carbene cleanly in large quantities.[125] Alternatively in NHC organocatalysis, the carbene is often generated *in situ* which requires compatibility of the reaction conditions with carbene generation,[132] which may preclude the use of elemental potassium, metal bases that may produce metal–carbene complexes or high temperatures for thermolysis.

4.1.6 NHCs as Nucleophilic Carbenes

Singlet carbenes are historically known to show ambiphilic reactivity.[92,93] As a result of the stabilising effects of the nitrogen lone pairs on the carbene p_π orbital, the electrophilicity of NHCs is suppressed whilst the lone pair in the plane of the heterocyclic ring remains largely unaffected by the flanking nitrogens. N-Heterocyclic carbenes are therefore atypically nucleophilic in their reactivity,[98,125] providing opportunities for chemical synthesis that will be discussed in further detail in the following sections.

4.2 Synthetic Applications of *N*-Heterocyclic Carbenes

Amongst the diverse applications of NHCs in synthetic chemistry there are three main contributing areas: coordination to metals; coordination to *p*-block elements; and as organocatalysts (Figure 44).[91]

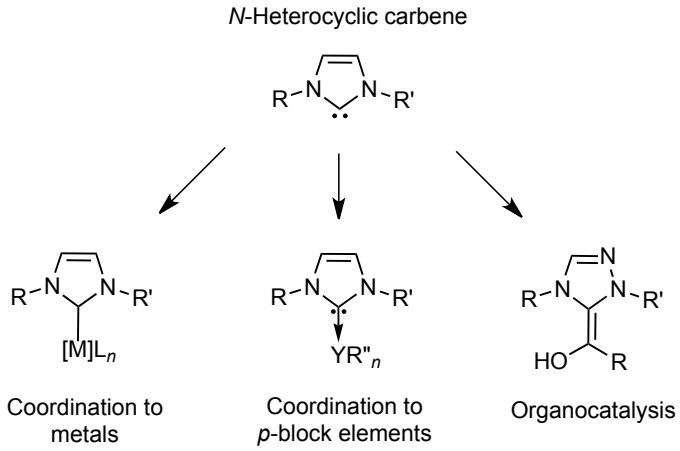


Figure 44. Applications of NHCs in synthesis.

4.2.1 NHC Coordination to Transition Metals

The formation of NHC–metal complexes initially provided a means of accessing and stabilising the heterocyclic carbenes.[99,100] Following the preparation of stable free carbenes, the potential use of NHCs as tunable ligands on metals became viable and this area rapidly expanded – within a few decades, complexes of NHCs with all of the transition metals and a reasonable proportion of the *s*- and *f*-block elements had been reported.[116] N-Heterocyclic carbene ligands are characterised by their strong σ-donating ability combined with a small π-backbonding contribution into the empty carbene p_π orbital; as such they were treated as phosphine-ligand mimetics.[133] It was soon found however, that the NHCs provided additional appealing features as ligands such as greater potential for tuning of the steric and electronic effects (and importantly orthogonal tuning of each of these parameters) than the phosphine

ligand class.[134] Further to this, the stronger metal–ligand interactions (larger energy of dissociation) of NHCs compared to phosphines renders NHC–metal complexes more oxidatively and thermally stable.[135]

The steric properties of these carbenes are remarkable with an umbrella-shaped steric field, directed towards the metal centre, contrasted with the cone-shaped phosphine ligands where the steric bulk faces away from the metal (Figure 45).[136]

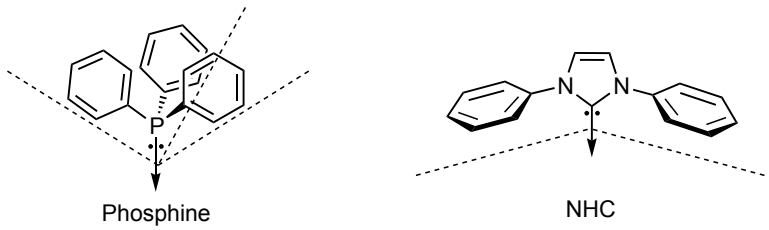


Figure 45. Steric influence: cone shaped phosphine ligand *vs.* umbrella shaped NHC ligand.

In addition, the ability to introduce chirality into the NHC through incorporation of a chiral *N*-substituent is another area of potential tunability for NHCs. The desirable features of NHC ligands has seen them introduced as ancillary ligands in some of the best known metal-catalysed reactions used in modern synthetic chemistry;[135,137] notable examples include the replacement of phosphine ligands for NHCs in the Grubbs II (**96**) and Hoveyda–Grubbs II (**97**) catalysts used for olefin metathesis and Organ's Pd-PEPPSI-NHC precatalyst systems (e.g. **98**) used in palladium cross-coupling reactions such as Suzuki–Miyaura, Negishi and Buchwald–Hartwig reactions (Figure 46).[134,138–142]

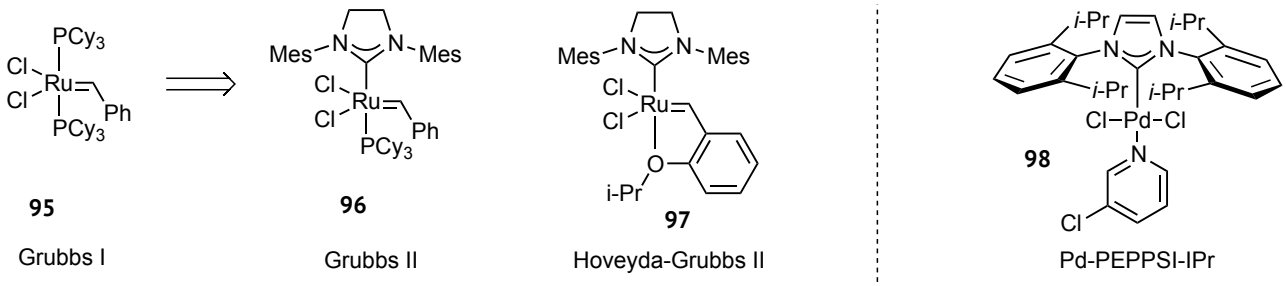
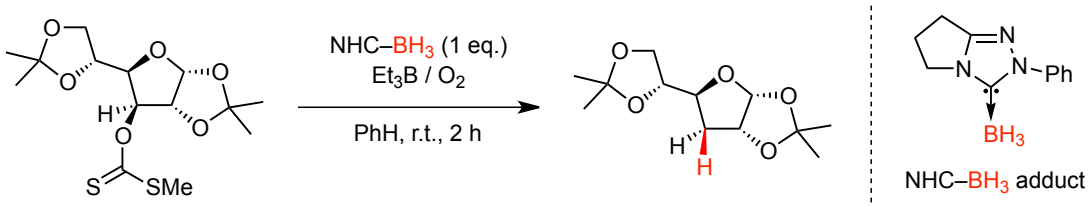


Figure 46. Phosphine ligand replacement in: A) ruthenium based olefin metathesis and B) palladium cross-coupling systems. PEPPSI is pyridine enhanced precatalyst preparation stabilisation and initiation.

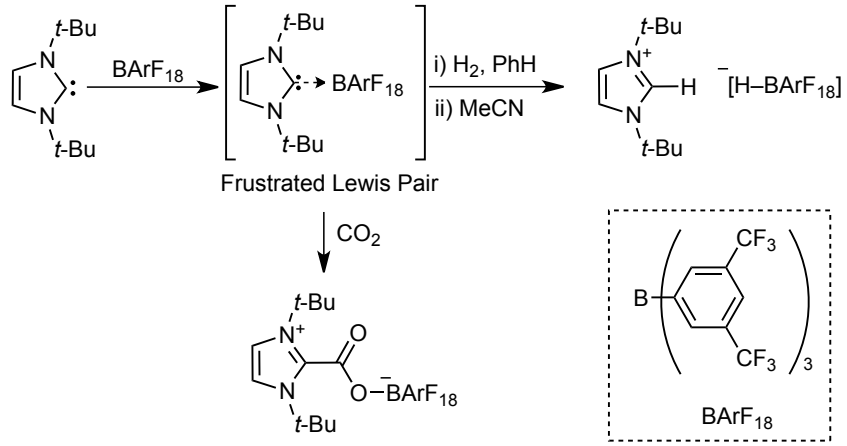
4.2.2 NHC–Non-Metallic Element Adducts

In addition to coordination to transition metals, NHCs have been shown to form intriguing adducts with *p*-block derived species including boron-,[143] phosphorus-[144] and silicon-containing compounds.[145–147]



Scheme 29. Barton–McCombie deoxygenation using NHC–BH_3 adduct as hydrogen radical source.

Synthetically NHC–borane adducts have provided the most interesting applications. These adducts have been utilised as tin-free radical hydrogen atom donors in reactions such as the Barton–McCombie deoxygenation (Scheme 29).[148] With sterically bulky boranes such as $B(C_6F_5)_3$ or $BArF_{18}$, NHCs form a frustrated Lewis pair (FLP) rather than a formal covalent adduct. These FLPs, with unstabilised reactive moieties, are capable of activation of small molecules such as CO_2 and hydrogen (Scheme 30).[149]



Scheme 30. FLP activation of small molecules using NHCs.

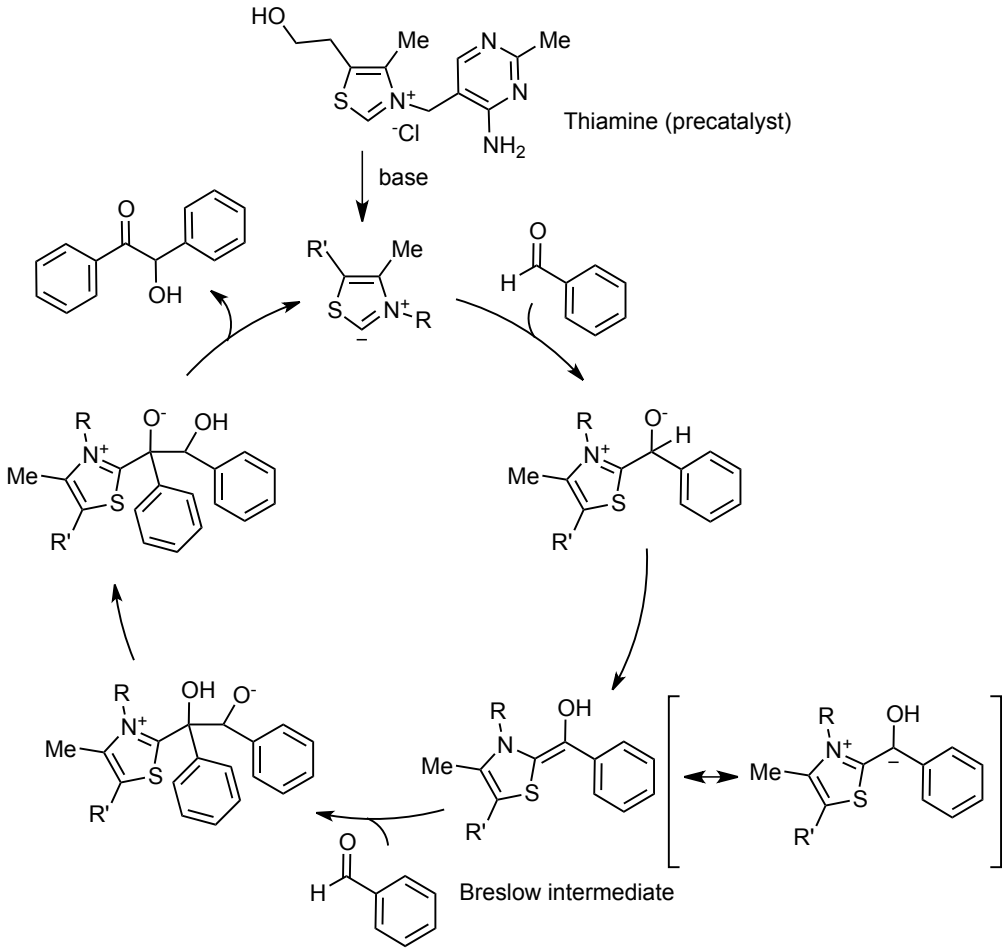
There are also numerous examples of the use of NHCs in synthetic transformation of silicon containing molecules, however, the degree to which a formal NHC–Si interaction is involved in these reactions is less well established.[150]

4.3 Organocatalysis with NHCs

A major area of synthetic utility provided by the NHCs is within organocatalysis.[151] The reaction of these stabilised nucleophilic carbenes with carbon-based electrophiles, and in particular carbonyl compounds, has led to the accessibility of a wide array of novel intermediates and the discovery of interesting reactivity.[152]

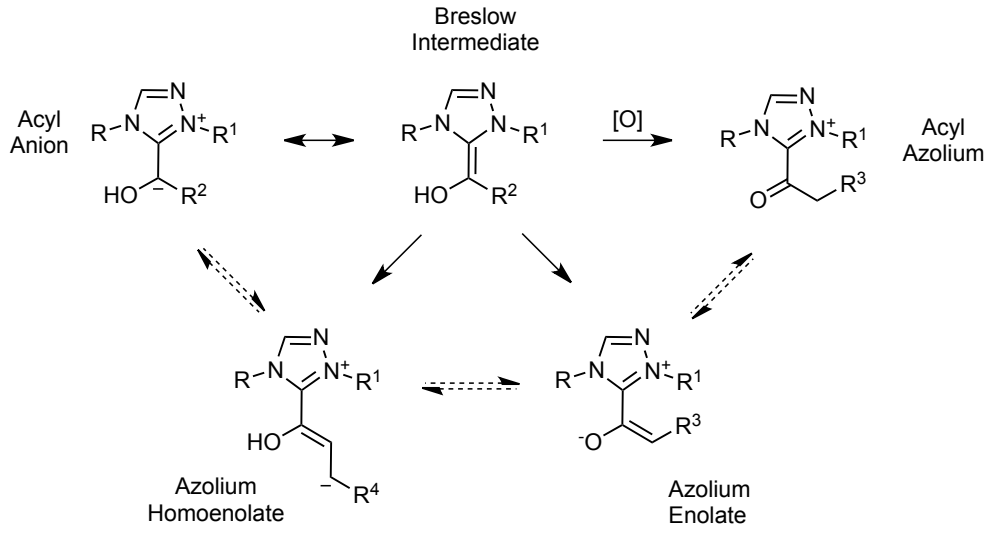
The use of NHCs in organocatalysis was reported as early as the 1940s by Ukai, who used thiazolium salts to catalyse benzoin reactions.[153] Breslow later expanded on the mechanism of this reaction (through comparison with Lapworth's mechanism for the classical benzoin

reaction)[154] and invoked an ambiphilic species (represented as an ylide structure by Breslow) formed from the deprotonation of the azolium precatalyst (Scheme 31).[121] A further important contribution from Breslow was the proposal of a key mechanistic intermediate structure that has come to be referred to as the "Breslow intermediate".[155] The Breslow intermediate, formed from the addition of the NHC to an aldehyde with a formal 1,2-proton shift, can be viewed formally as an acyl anion equivalent (umpolung reactivity) used in the formation of the benzoin product.



Scheme 31. Breslow's proposed mechanism for thiamine catalysed benzoin reaction (N.B. ylide representation of catalyst is as in original literature).

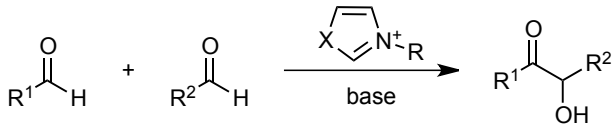
4.3.1 Reactive Species Formed from the Breslow Intermediate



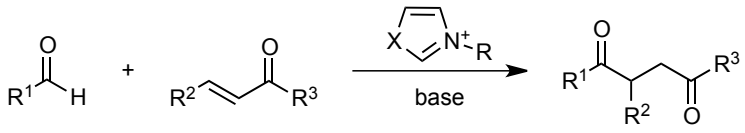
Scheme 32. Key intermediates in NHC organocatalysis.

From the Breslow intermediate, a number of chemical reactivities are accessible depending on the substitution and functionalisation of the initial electrophilic substrate (Scheme 32): the previously mentioned acyl anion chemistry; azolium enolate equivalents; azolium homoenolate equivalents (also known as conjugate umpolung); and acyl azolium species (cf. active esters).[91,156–159]

4.3.1.1 Acyl anion



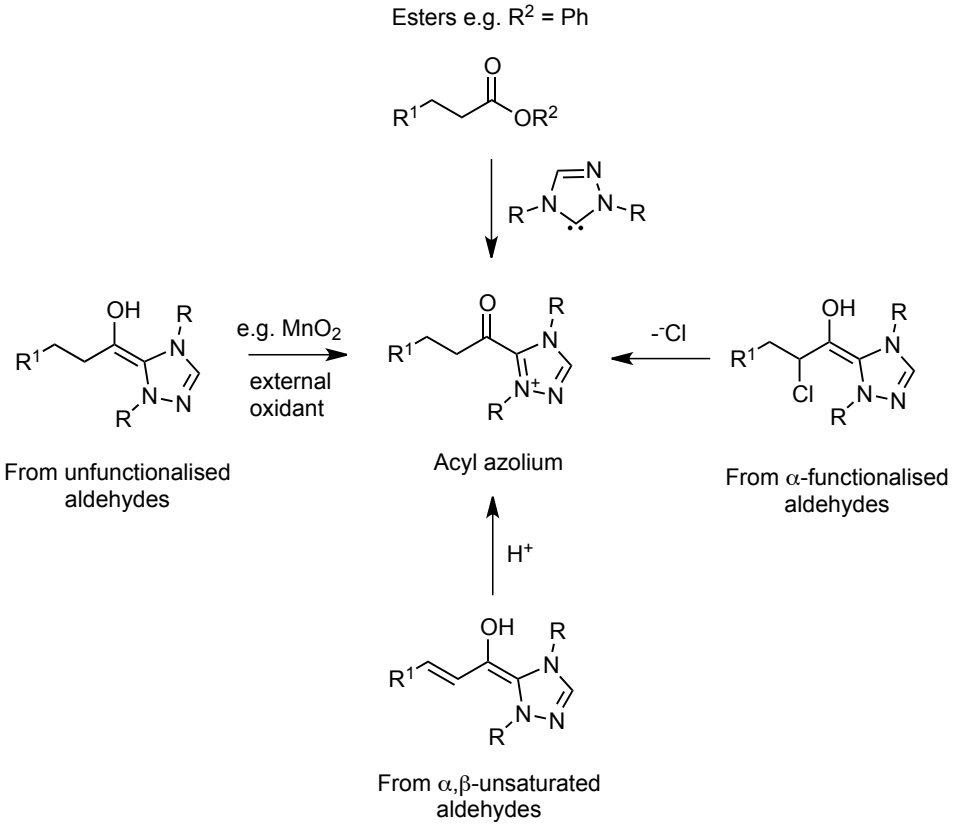
Scheme 33. Benzoin reaction. Crossed benzoin reactions ($R^1 \neq R^2$) and asymmetric variants also known.



Scheme 34. Stetter reaction. Asymmetric variants pubished as well as reactions with other electron withdrawn olefins.

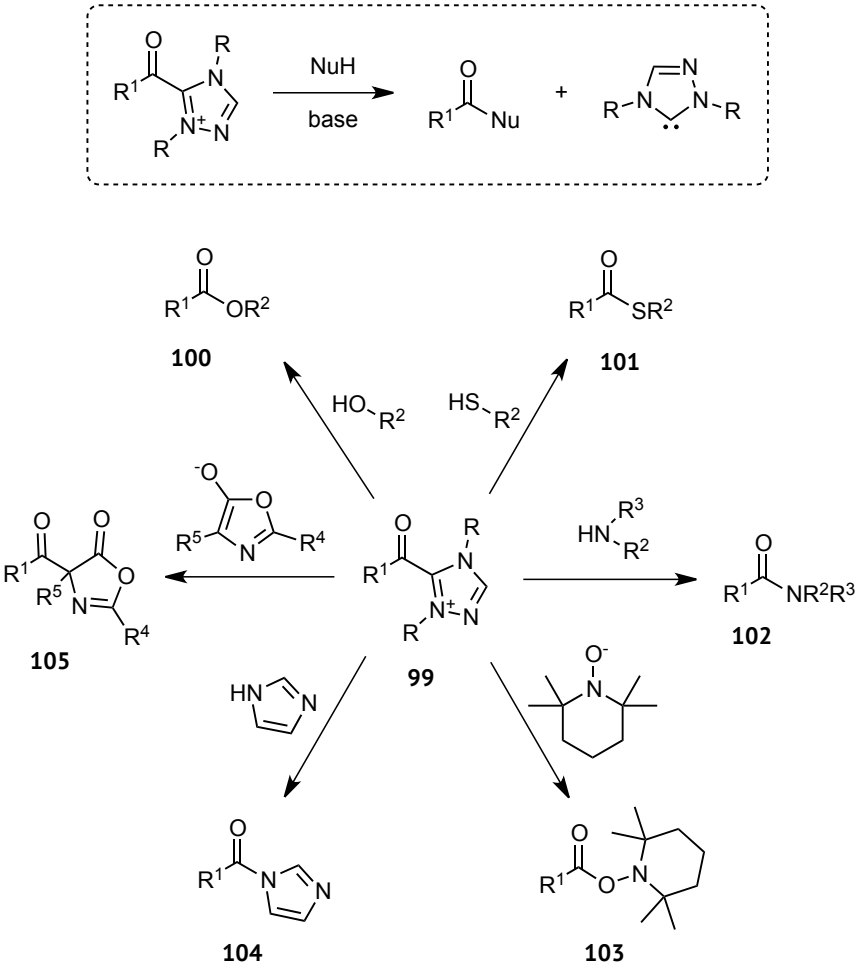
The acyl anion reactivity of the Breslow intermediate is exemplified in some of the earliest work in NHC organocatalysis namely the benzoin (Scheme 33)[160–163] and Stetter (Scheme 34)[164,165] reactions.[152] These reactions were originally catalysed using cyanide anions to form the umpolung intermediate meaning that the discovery of the analogous reactivity shown by NHC catalysts not only improved the practical safety of this reaction, but also enabled the reaction to be performed asymmetrically to yield stereoenriched products.[156]

4.3.1.2 Acyl Azolium



Scheme 35. Generation of acyl azolium species from differently functionalised aldehyde substrates.

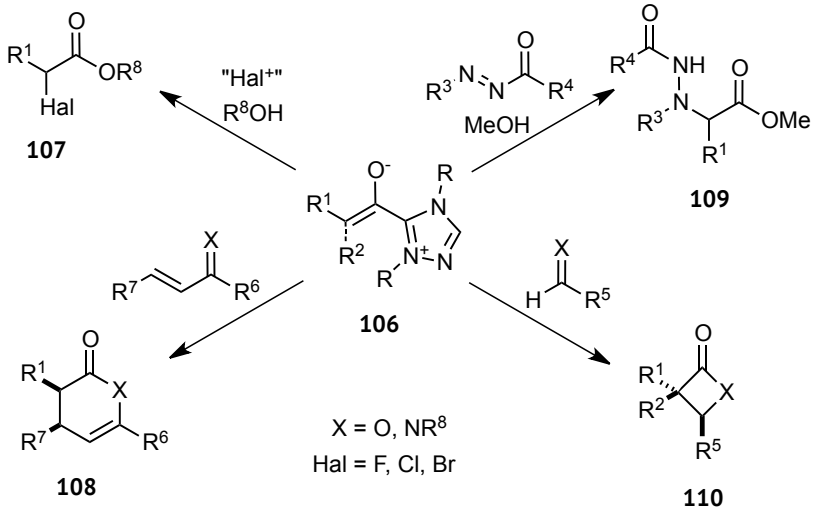
The acyl azolium is formed from the Breslow intermediate *via* an oxidation step (Scheme 35).[166] This is achieved by either using an external oxidant or intramolecularly through the expulsion of a reducible group included in the aldehyde substrate.[167–169] Another variation of this latter method is the protonation or electrophilic activation of Breslow intermediates derived from α,β-unsaturated aldehydes.[89,170] Alternatively the acyl azolium is directly accessed by an addition / elimination reaction of the NHC with a carbon electrophile in the carboxylic acid oxidation state (e.g. ester substrates).[171–173]



Scheme 36. Generic nucleophile acylation reaction with acyl azolium & representative examples of nucleophiles and their corresponding products.

Acyl azolium intermediates **99** have analogous reactivity to active esters (i.e. the acylation of nucleophiles) and are one of the intermediates that typically precede turnover of the catalyst.[168] As shown above (Scheme 36) they are effective acylating agents and have been shown to react with a wide range of nucleophiles to form esters **100**,[174] thioesters **101**,[175] amides **102**,[176] *C*–carboxylated products (e.g. **103**, R^1 = OMe)[177] and species such as imidazole[178] and TEMPO anion[179] to give more stable acylating compounds (e.g. **103** & **104**) – these are typically used when the catalytic reaction conditions are not compatible with the desired nucleophile (e.g. amines with aldehydes).

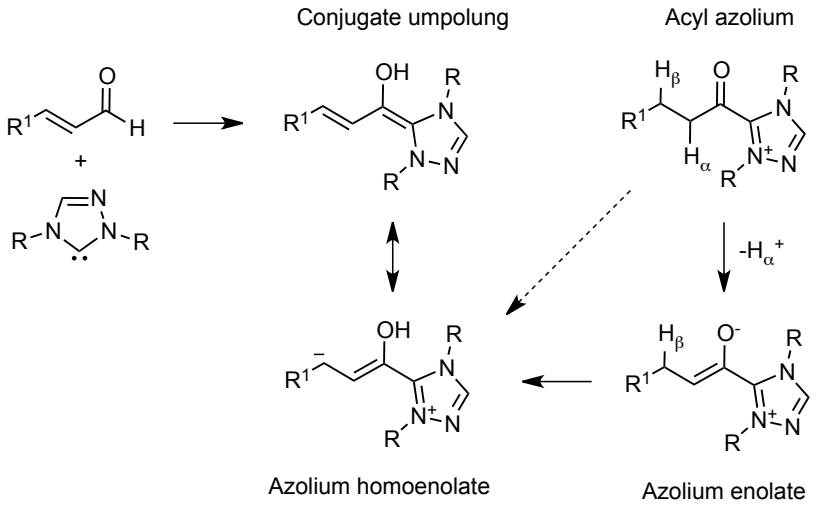
4.3.1.3 Azolium Enolate



Scheme 37. Reactions of azolium enolates.

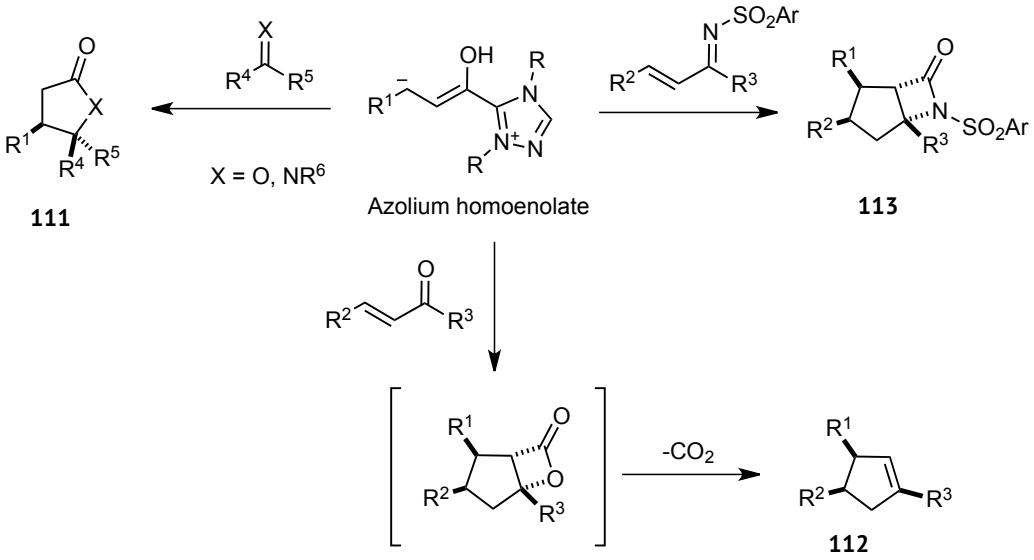
The azolium enolate intermediate **106** is a deprotonated tautomeric form of the acyl azolium and is nucleophilic as typical for generic enolate species. Some key reactions with these intermediates are α-functionalisation (e.g. halogenation) of carbonyls to give α-haloesters **107**,[180,181] hetero-Diels–Alder reactions with enones and α,β-unsaturated imines to give dihydropyrones and dihydropyridones **108**,[171,182–184] [4+2] reactions with azo compounds to give α-aminated products **109** upon solvolysis,[185] and formal [2+2] reactions of the enolate species with imines, ketones and other π-electophiles to form four-membered cyclised products **110** (Scheme 37).[186,187] Again the use of chiral NHCs has led to the production of enantioenriched products, with high levels of diastereoselectivity achievable in the hetero-Diels–Alder reactions and the formal [2+2] reactions.[188]

4.3.1.4 Azolium Homoenolate



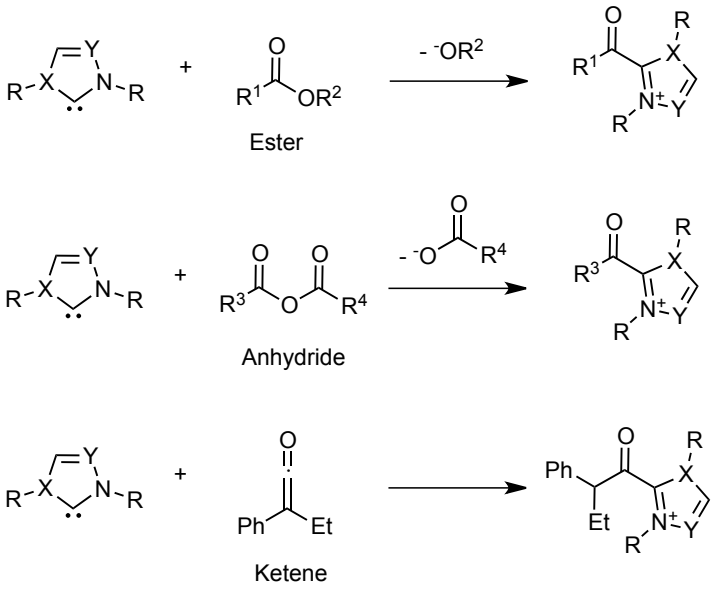
Scheme 38. Generation of azolium homoenolate and conjugate umpolung tautomer.

The conjugate umpolung or homoenolate system is formed from NHC addition to enones or through β-deprotonation of the acyl azolium / azolium enolate intermediate (Scheme 38).[91,189] These intermediates undergo formal [3+2] reactions with ketones and imines to give γ-lactones and lactams **111**,[190] with α,β-unsaturated ketones to give cyclopentenes **112** with expulsion of CO_2,[173] and with α,β-unsaturated imines to give fused [3.2.0] bicyclic β-lactams **113** (Scheme 39).[191]



Scheme 39. Reactions involving azolium homoenolates.

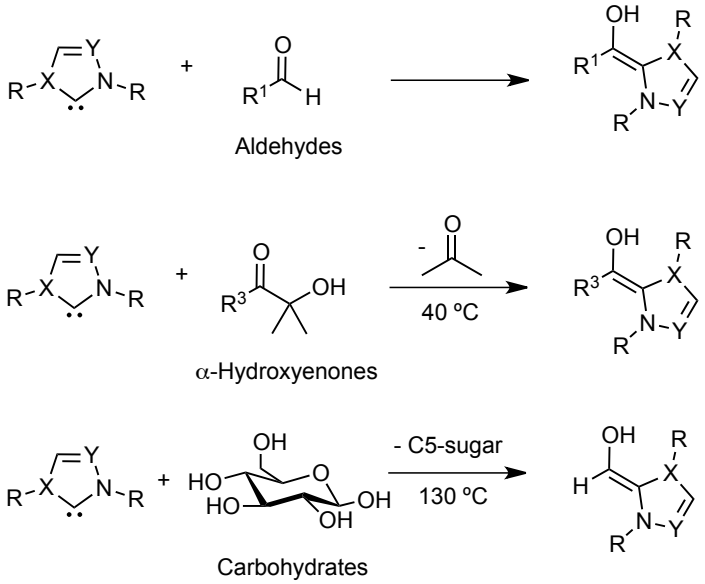
4.3.2 Carbonyl Containing Electrophilic Substrates



Scheme 40. NHC activation of substrates at carboxylic acid oxidation level.

The reactive intermediates above can be accessed from a varity of substrates. At the carboxylic acid oxidation state: esters, anhydrides and ketenes have been employed to

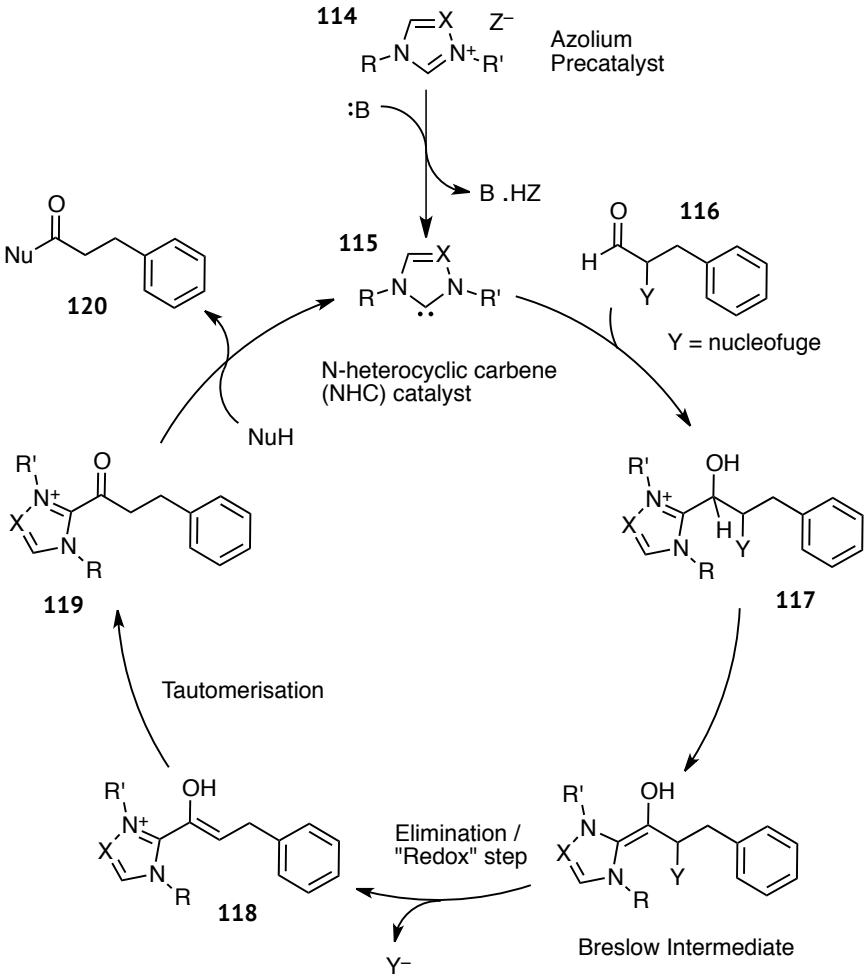
directly generate acyl azolium species without involvement of the Breslow intermediate (Scheme 40).[192–194]



Scheme 41. NHC activation of substrates at ketone oxidation level.

At the ketone oxidation state: aldehydes (including α-functionalised aldehydes and bisulfite adducts), enals, α'-hydroxyenones and hemiacetals were shown to access the Breslow intermediate (Scheme 41).[159,166,195,196] Interestingly in the latter two examples (in the cases where the hemiacetal contains an α-hydroxy group) the Breslow intermediate is obtained following a retro-benzoin reaction e.g. with the expulsion of formaldehyde or acetone.

4.4 Redox Acylation



Scheme 42. Representation of redox acylation catalytic cycle.

As exemplified by the groups of Rovis and Bode in the last decade, the NHC-catalysed intramolecular-redox formation of acyl azolium intermediates from α-functionalised aldehydes is a powerful method for the formation of acyling agents and corresponding carboxylate derivatives.[197,198] The general mechanism of this reaction (Scheme 42) comprises individual steps that have all been outlined previously (see **4.3.1**).[199] Upon deprotonation of the azolium precatalyst **114**, the free NHC **115** is generated which reacts with the aldehyde substrate **116** to form the Breslow intermediate *via* the initial adduct **117**. The leaving group is displaced in the formal "redox" step to access the enolate intermediate **118**, which upon tautomerisation yields the acyl azolium **119**. Attack of a nucleophile onto this final intermediate yields the acylated product **120** and releases the free carbene to undergo further catalytic cycles.

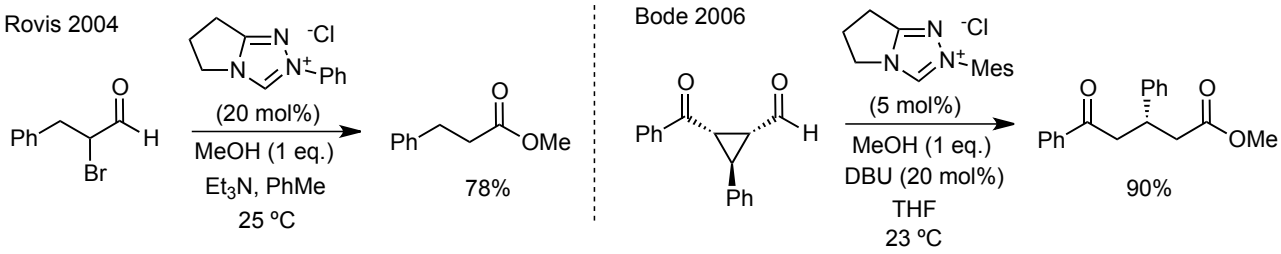
4.5 Project Aims

The aim of this project was to use the redox acylation strategy in the formation of amide bonds, and with carbohydrate substrates as masked aldehydes for oxidative esterification / lactonisation. The former of these reactions has been investigated by a number of groups including Rovis and Bode; however, there are interesting concepts left unexplored in this area and potential room for improvement for the practical procedure. The use of hemiacetals such as carbohydrate motifs as masked aldehyde substrates has limited known examples, the most prevalent of which being from Chi where unfunctionalised sugars were used to produce formyl anion equivalents for Stetter reactions, through sequential degradative retro-benzoin reactions.[196] This was the first example of activation of carbohydrates with NHC catalysts. These reactivities will be expanded upon further in their respective sections below (see **5** & **6**).

5 NHC-Catalysed Redox Amidation

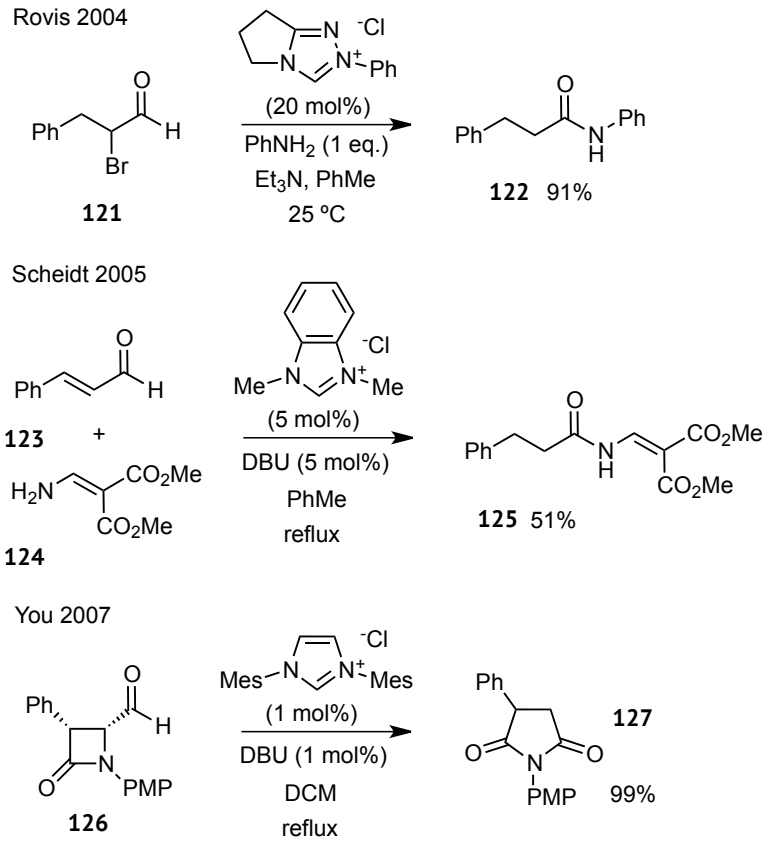
5.1 Background

Redox amidation is the formation of amide bonds *via* the redox acylation protocol described above (**4.4**) starting from aldehydes or ketones and amines with the aid of an NHC.[199] In comparison to redox esterification (e.g. Scheme 43), which is well precedented and explored in literature,[169,197,198,200–203] the equivalent amidation reaction is less thoroughly reported.



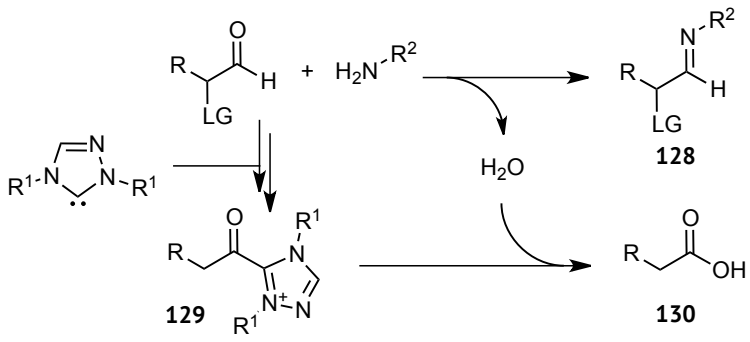
Scheme 43. Early examples of redox esterifications.

If the reaction is further defined as amide bond formation as a result of the attack of a nitrogen nucleophile on an intramolecular redox generated acyl azolium species, the number of reported examples is markedly smaller and typically involve electron withdrawn amines and / or cyclic systems (Scheme 44).[170,197,204–206]



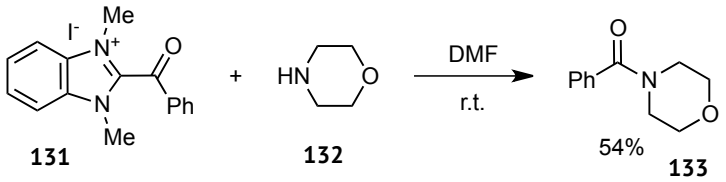
Scheme 44. Previous examples of redox amidations using electron deficient nitrogen nucleophiles.

These examples include the use of aniline with bromoaldehyde **121** by Rovis to form anilide **122**, an electron poor enamine **124** with enone **123** by Scheidt and an intramolecular amide nucleophile generated from a formyl β-lactam **126** by You to form succinimide **127**. There are a number of proposed reasons for the success of electron poor nitrogen nucleophiles in comparison to more electron rich alkyl amines; the most well accepted being the condensation side reaction between the electron rich amine nucleophiles and aldehyde substrates leading to unreactive imine species (e.g. **128**) and water (Scheme 45).[178,207] The formation of carboxylic acids (e.g. **130**) from the addition of a water nucleophile to acyl azolium intermediates (e.g. **129**) is known to be a facile reaction, and the consumption of the water generated upon imine formation leads to both a reduction in the reverse imine hydrolysis reaction and the conversion of the aldehyde starting material into an unwanted side-product (Scheme 45). The formation of these carboxylic acids may also lead to protonation of more basic NHCs, inhibiting the catalytic process.



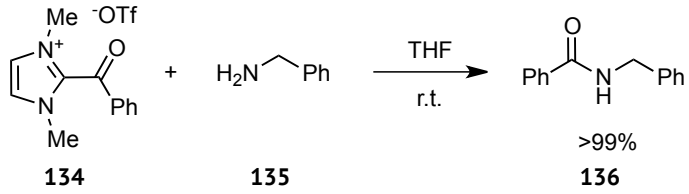
Scheme 45. Side reactions caused by substrate incompatibility; formation of imine and α-reduced carboxylic acid.

It has also been suggested that "amines do not react with the acyl azoliums to form amides directly and a co-catalyst is needed".[208,209] The studies referenced to support this hypothesis however, state that the acyl azolium "does not react with primary amines unless water is absent" referring only to the preferential reactivity of the *O*- based nucleophile compared to the *N*- based equivalent.[210] There have been several publications that investigate the outcome of alchohol *vs.* amine competition experiments with regards to their reactivity at the acyl azolium showing preferential esterification over amidation.[176,211] It should be noted however, that even as far back as the late 1990s there are examples of such amidations occurring.[212]



Scheme 46. Miyashita - stoichiometric amidation from acyl azolium **113** and morpholine.

Treatment of stoichiometric acyl azolium species **131** with morpholine (**132**) at room temperature gave the amide product in 54% yield (Scheme 46). Subsequently Studer reported the acylation of benzylamine (**135**) by a stoichiometric acyl azolium **134** proceeding in quantitative yield to give amide **136** at room temperature (Scheme 47).[176]



Scheme 47. Studer – stoichiometric amidation from acyl azolium **134** and benzylamine.

Interestingly Studer found that benzyl alcohol would not react with the benzoyl azolium unless activated by additional free carbene and Miyashita had previously observed in his stoichiometric studies that alcohols required high temperatures or deprotonation for benzoylation to occur.[176,212] It would seem from these results, that amines are comparatively better nucleophiles at the acyl azolium than alcohols, as would be expected; however, it is apparent from these studies and numerous others, that the alcohol nucleophiles are easier to activate through the use of additional free carbene or base (both present in typical NHC acylation processes) which explains the well established *O- vs. N-* chemoselectivity.[211]

5.2 Current Redox Amidation Approaches

The optimisation of redox amidation protocols have focused on favouring the amidation reaction through suppression of imine formation and improving the rate of amine acylation.

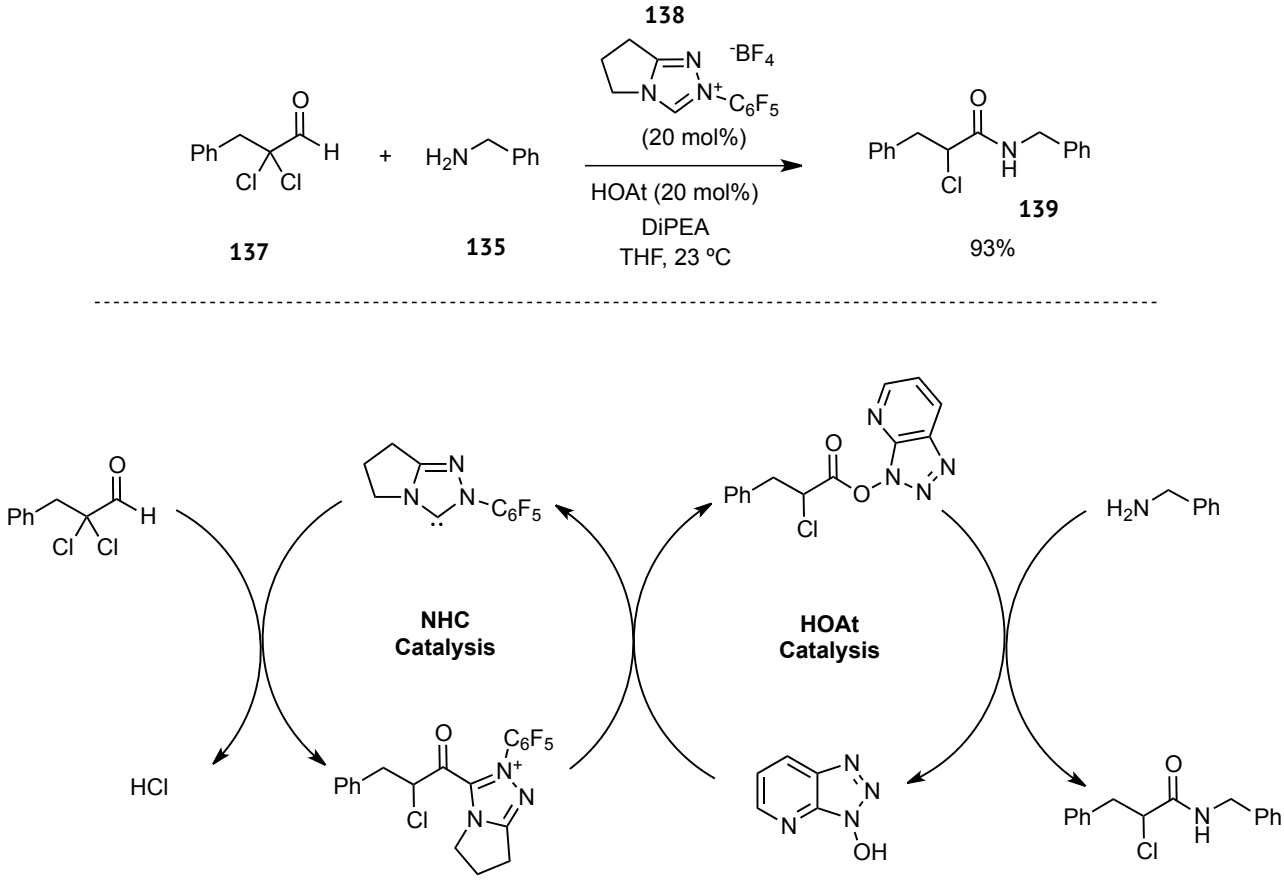
5.2.1 Co-catalyst Relay Redox Amidations

The prevailing approach towards NHC-catalysed redox amidation employs a co-catalytic additive. There are a number of compounds suitable for this purpose, the most common of these being HOAt,[207] hydroxamic acids,[209] HFIP (hexafluoroisopropanol),[174] phenol,[201] imidazole,[178,208] and 1,2,4-triazole.[213] The reactions proceed *via* initial acylation of the co-

catalytic species (e.g. HOAt) by the *in situ* generated acyl azolium, then subsequent acyl transfer to the amine, regenerating the co-catalyst.

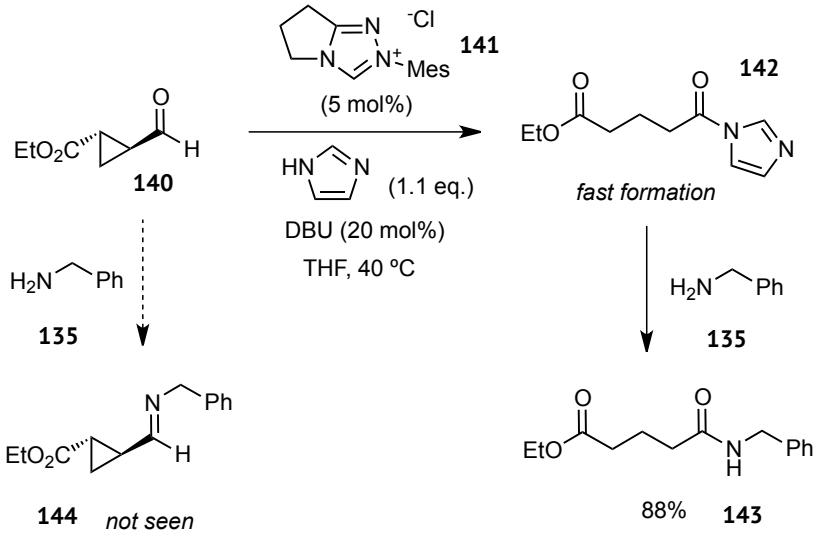
5.2.1.1 Use of Functionalised Aldehydes as NHC-Catalysed Redox Active Substrates

In the initial redox acylation work by Rovis, it was shown that aniline could undergo acylation with an α-bromohydrocinnamaldehyde derived acyl azolium (Scheme 44).[197] Following this, attempts to use other alkyl amines on similar systems such as α,α-dichlorohydrocinnamaldehyde (**137**), without the use of a co-catalyst, led to imine formation and the corresponding α-reduced carboxylic acid.[207] To prevent high reaction concentrations of the amine and aldehyde together, slow addition of one to the other was always required and the use of a co-catalyst proved to be essential. HOAt was found to give the best results although HOBt, DMAP, pentafluorophenol and imidazole were also shown to work to a similar extent at catalyst and co-catalyst loadings of 20 mol%. Under optimised conditions, the reaction between aldehyde **137** and benzylamine (**135**) with triazolium precatalyst **138** (20 mol%) and HOAt (20 mol%) produces the *N*-benzyl amide product **139** in very good yield (93%) (Scheme 48).



Scheme 48. Rovis – HOAt co-catalysed redox amidation protocol.

In a similar fashion, Bode showed that when using formyl cyclopropanes as the α-reducible aldehyde, stoichiometric imidazole could be employed to suppress imine formation without the need for slow addition of either the amine or aldehyde to produce the amide product.[178]

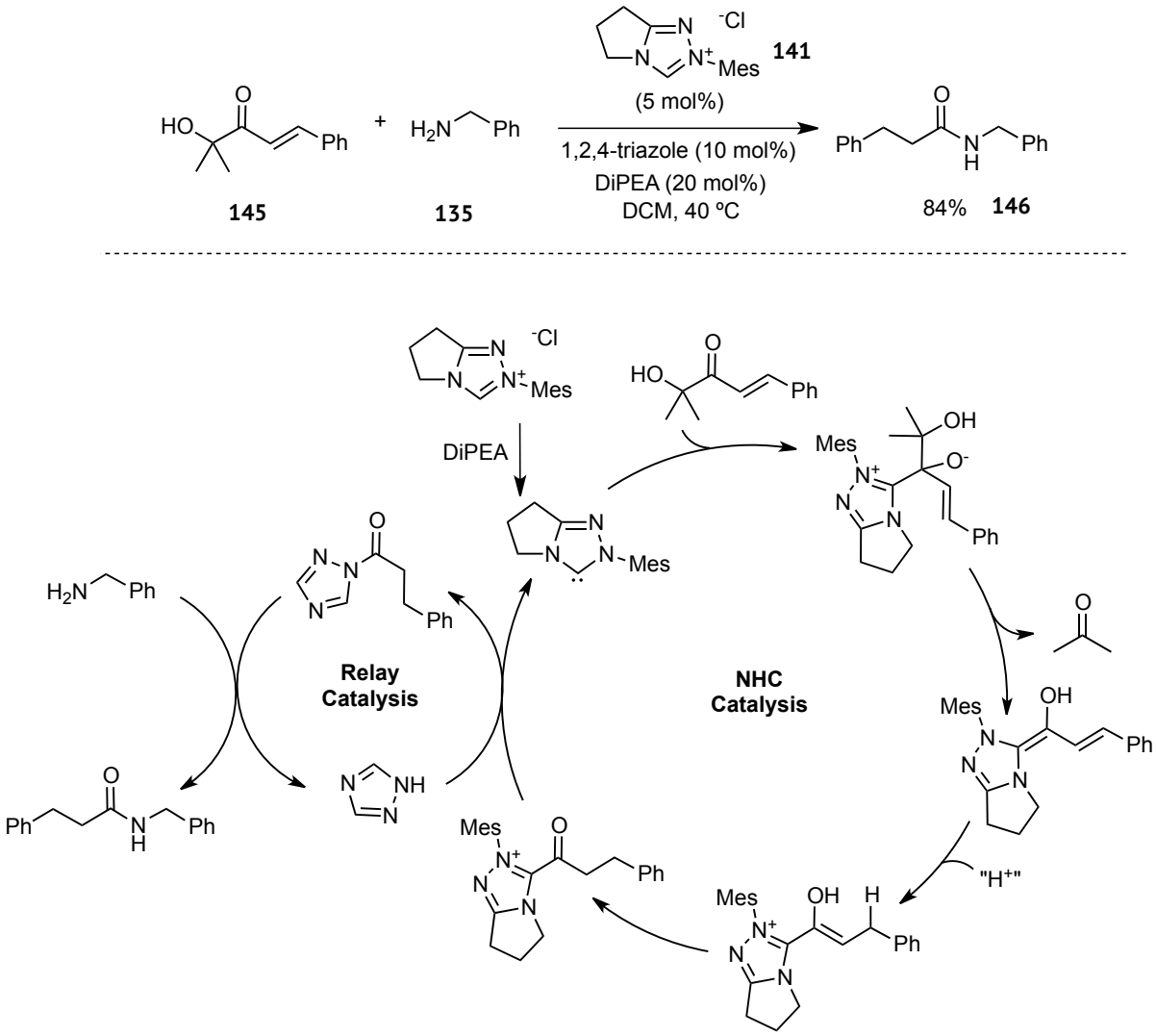


Scheme 49. Bode – redox amidation *via* acyl imidazole intermediate.

In this case the NHC generated from N-Mes triazolium precatalyst **141** (5 mol%) with imidazole (1 eq.) rapidly converts aldehyde **140** into acyl imidazole **142**, which reacts with the amine to form amide **143**. The formation of imine **144** is out-competed by consumption of the aldehyde substrate in forming the acyl imidazole and is no longer a significant by-product (Scheme 49).

5.2.1.2 Use of α'-Hydroxyenones as Substrates

Another interesting solution to the problem of imine formation proposed by Bode was the use of α'-hydroxyenones as α,β-unsaturated aldehyde surrogates.[213] These substrates (dimethylcarbinolyl enones) have been shown to form the same conjugate umpolung intermediates as their corresponding enals by a retro-benzoin reaction with ejection of acetone (Scheme 50). It was found that by using these α'-hydroxyenone substrates, the use of a stoichimetric additive was no longer required although in the absence of co-catalyst a reduced yield was observed. Using these conditions α'-hydroxyenone **145** and benzylamine (**135**) were converted to the corresponding *N*-benzyl amide **146** by triazolium precatalyst **141** (5 mol%) and 1,2,4-triazole (10 mol%).

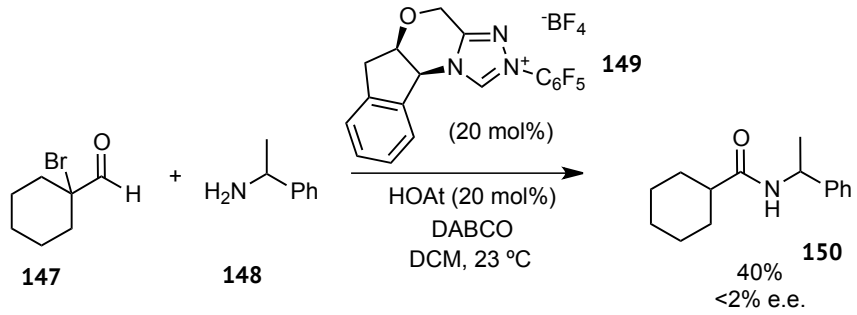


Scheme 50. Bode – redox amidation using 1,2,4-triazole co-catalyst relay and α'-hydroxyenone substrate.

5.2.2 Kinetic Resolution of Amines

The stereoselective acylation of amines is a highly desirable reaction both in terms of producing more complex amide products, and also for the potential stereoenrichment of the amine substrates themselves. Within NHC-catalysed redox amidation, with regards to introducing chirality into the amine portion of the amide product by means of a kinetic resolution, the use of a co-catalyst negates the potential for any stereoinduction to be achieved from the NHC due to the fact that the acylating species no longer contains the NHC structure.

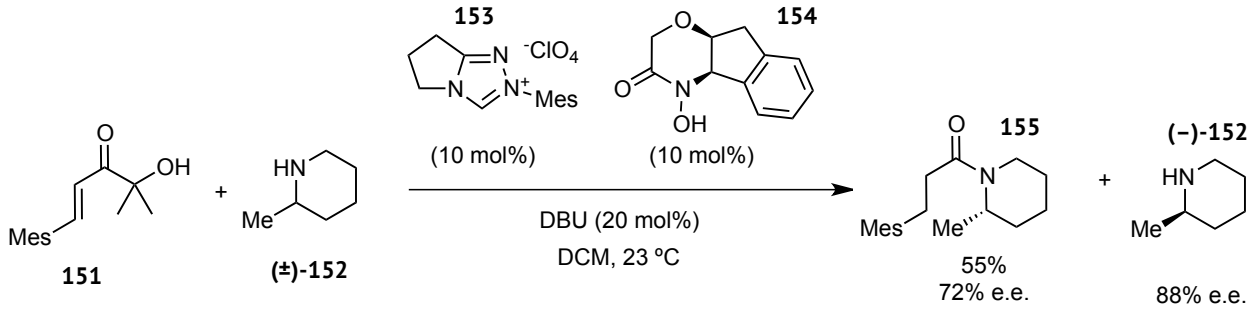
5.2.2.1 Chiral NHC with Achiral Co-catalyst



Scheme 51. HOAt relay catalysis results in a lack of enantiomeric excess in product.

In Rovis' NHC–HOAt relay reaction it was found that the use of **149**-derived chiral NHC and HOAt with bromoaldehyde **147** for the kinetic resolution of racemic α-methyl benzylamine (**148**) through formation of enantioenriched amide **150** led to negligible enantiomeric excess (Scheme 51).[207] This was seen to be confirmation of the co-catalytic role of the HOAt in the relay-catalytic system.

5.2.2.2 Achiral NHC with Chiral Co-catalyst



Scheme 52. Chiral hydroxamic acid relay catalysis for the kinetic resolution of amines.

Bode approached this chemistry through the use of a chiral hydroxamic acid co-catalyst **154** combined with an achiral NHC **153** (Scheme 52).[209] As the acyl group is first transferred to the hydroxamic acid before being intercepted by the amine, it is this latter species that affects the selectivity of the kinetic resolution and selectivities of *s* = ca. 20–74 were reported.

5.3 Proposed Direct Redox Amidation Approach

The work proposed for this project was towards performing the redox amidation directly from the acyl azolium without the use of a co-catalyst. The ability to perform this reaction without the need for a co-catalyst was desirable to examine the extent to which amines can be acylated by acyl azolium species or whether they are truly an inactive combination. It was

also intended that the reaction should be operationally simple; for example, the reagents should not require slow additions, stoichiometric reagents should be kept to a minimum and the dual catalytic system should be reduced to the need for only a singular catalyst. It was hoped that such simplification of conditions could help to provide insight into the subtle roles that each additional reagent can play in the reaction scheme that may not be inherently obvious, notably the effects that these reagents can play in proton transfer during the catalytic cycle which will be discussed in further detail below. A further desire for this work was that it could provide the groundwork towards enabling the use of chiral NHCs to directly perform the kinetic resolution of amine nucleophiles, reactivity that has been greatly exploited for alcoholic nucleophiles and would only be achievable in the absence of the co-catalyst.[197,214,215] The use of aldehydes in this chemistry was also a priority as there is a plethora of such substrates reported for NHC-catalysed redox acylation strategies that currently are not compatible with known conditions, thus tuning the reactivity to allow these reagents to be used would be highly desirable.

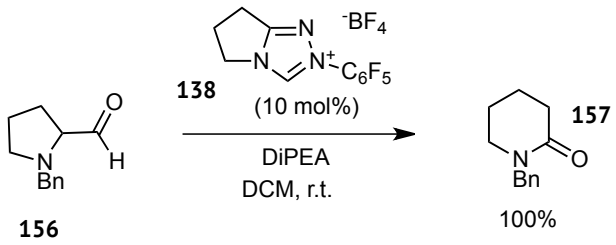
5.3.1 Masked Nucleophile Hypothesis

Assessment of the known literature for redox amidations suggested strongly that the issue of imine formation was by far the biggest obstacle to the success of these reactions. As such, it is very important to prevent the aldehyde and amine substrates from being exposed to one another in significant concentrations or for prolonged time periods – as exemplified in the above approaches. Instead of a physical approach towards this goal such as using slow addition of the substrate over a number of hours, which could potentially have issues with substrate specific variations in reactivity, it was considered that a chemical approach may be more advantageous in terms of generality and practical simplicity. The approach in mind was to have the amine present in the reaction as a masked nucleophile (i.e. suppressed nucleophilic reactivity) with the release of the latent nucleophile being chemically induced by the reaction conditions in a controlled manner.

5.4 Results and Discussion – NHC-catalysed Redox Amidation

5.4.1 Assessment of α-*O*-Carbamoyl Aldehyde Substrates

The reactivity that was conceptually most similar to what was desired in this project was the intramolecular lactamisation described by Gravel – one of the few reported reactions that could truly be described as an NHC-catalysed redox amidation (Scheme 53).[204]

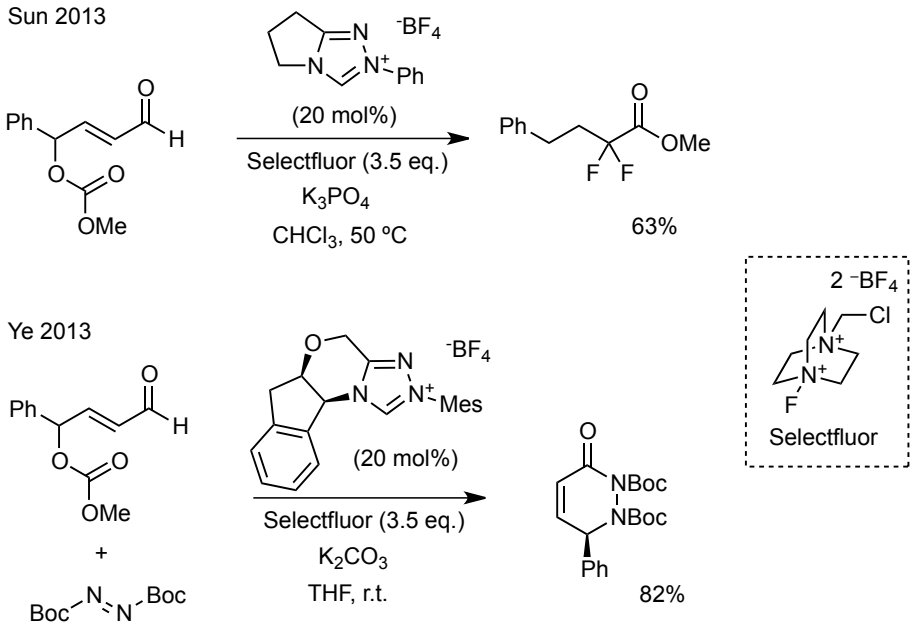


Scheme 53. Gravel – NHC-catalysed ring-expansion reaction; intramolecular redox amidation.

In the reaction, 1-benzyl-2-formylpyrrolidine (**156**) is converted to lactam **157** using **138** and DiPEA.

One of the outstanding features of this chemistry was the fact that the amine acts as the leaving group and nucleophile, therefore the nucleophile is only released during the catalytic cycle and that the catalytic cycle may only continue once the nucleophile is consumed. This idea was to be key in the development of the work undertaken in this project.

To extend this work past the intramolecular / cyclic systems, alternative substrates were required that still contained the amine nucleophile as part of the leaving group. Carbamate groups (e.g. Boc, Fmoc, alloc, Cbz, etc.) comprise some of the most prevalent protecting groups for amines, with the potential to sterically and electronically alter their nucleophilicity.[216,217] Along with the equivalent alcohol derived carbonate groups, carbamates are known to act as leaving groups in S_N2'-type reactions such as in Tsuji–Trost allylations and S_N2' displacements using organocuprates – reactivity which can be related to the displacement of the leaving group within the NHC redox acylation cycle.[218–222] Once displaced, protonation of the carbamic anion leads to rapid decomposition to give the amine nucleophile with loss of CO_2. These features of carbamate functionality imply that they should be ideal for use in the NHC redox amidation chemistry.

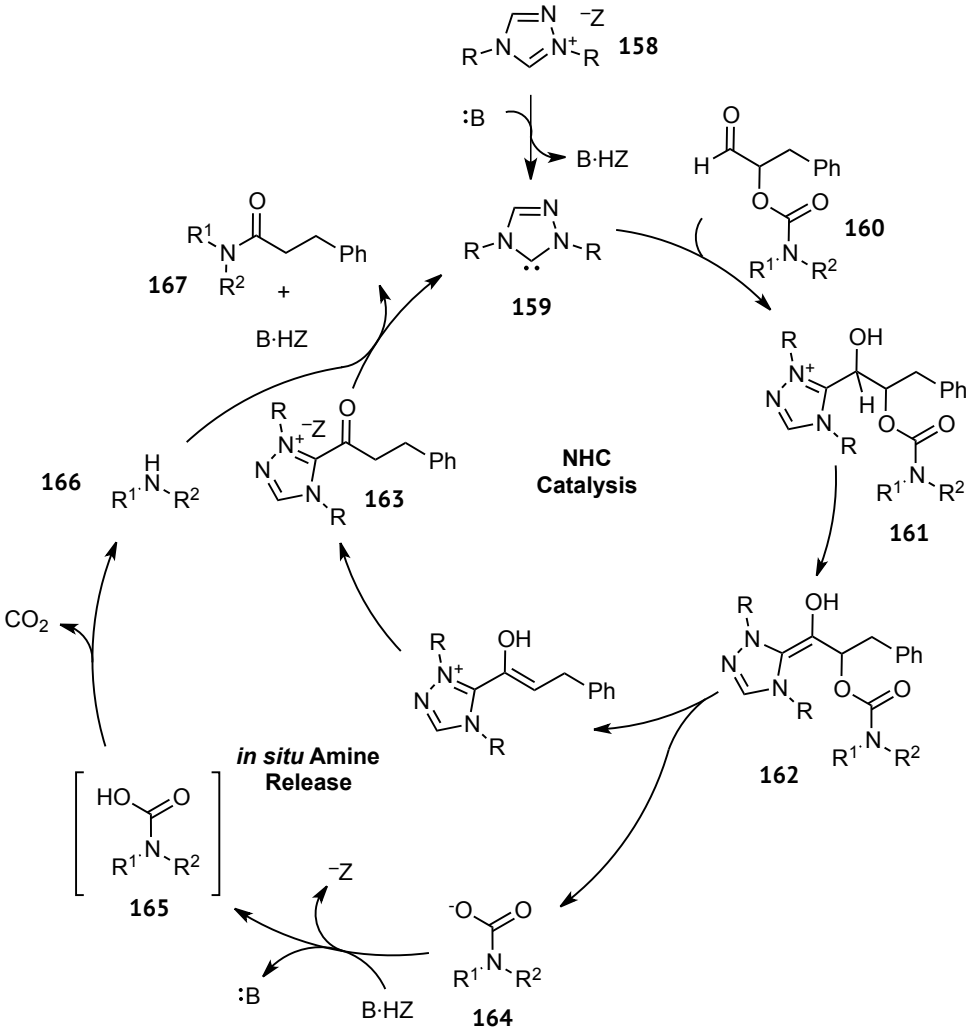


Scheme 54. NHC-catalysed redox reactions with γ-carbonate leaving groups.

With this in mind, it was an unexpected finding that these dual-function leaving groups are virtually unreported in NHC redox acylation chemistry – at the start of this work there was a single report of γ-carbonates being used as leaving groups (although additional alcohol nucleophile was required for the final esterification),[180] with two follow up publications in 2013 and 2014 from the same group and one from Ye in 2013 that uses the same substrate class (Scheme 54).[223–225]

At time of writing, α-carbonate, α-carbamate and γ-carbamate leaving groups are unreported.

5.4.1.1 Proposed Catalytic Cycle with α-*O*-Carbamoyl Aldehyde Substrates

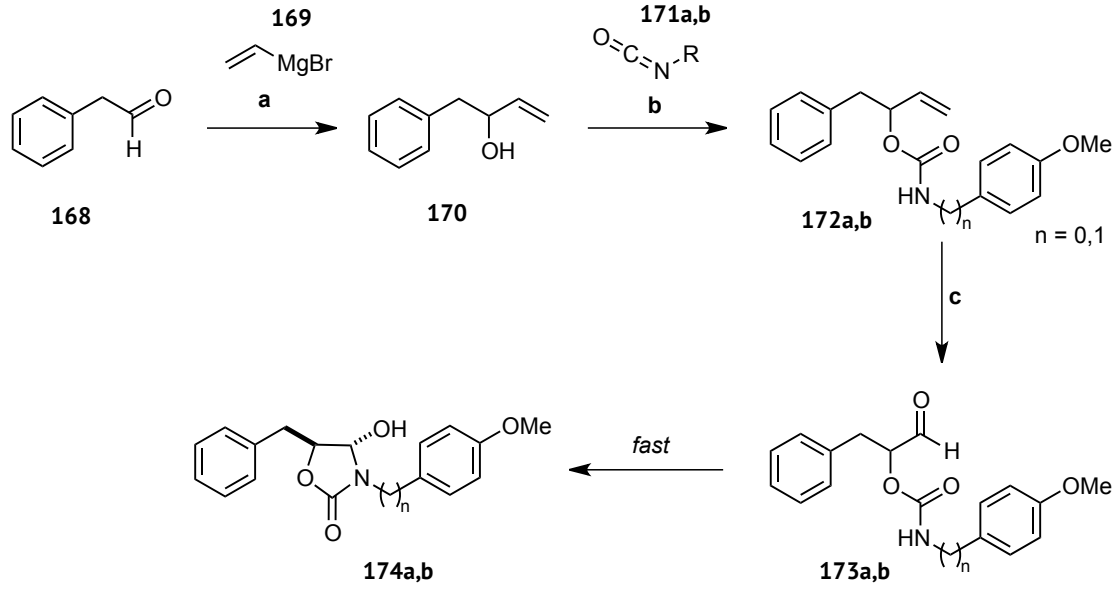


Scheme 55. NHC-catalysed redox amidation cycle with *in situ* release of amine nucleophile through decarboxylation of carbamate leaving group.

The catalytic cycle starts with the *N*-heterocyclic carbene **159**, generated *in situ* by deprotonation of the corresponding triazolium salt **158**, also generating the conjugate acid species B·HZ. The NHC then forms the classical adduct **161** with the aldehyde substrate **160**, resulting in the Breslow intermediate **162**. Expulsion of the leaving group and tautomerisation leads to the acyl azolium intermediate **163**. Consequently, the displaced leaving group **164** undergoes decarboxylation upon protonation by conjugate acidic species B·HZ (*via* carbamic acid **165**) to release the amine nucleophile **166**. Reaction between acyl azolium **163** and amine nucleophile **166** leads to the desired amide product **167** (in this turnover step B·HZ is regenerated).

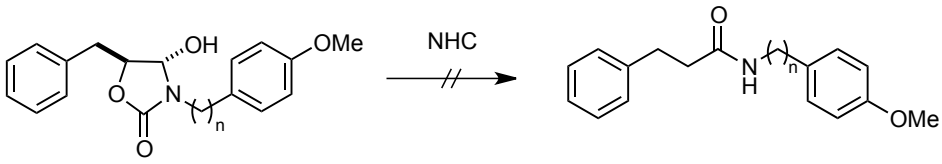
5.4.1.2 Preparation of 2° α-*O*-Carbamoyl Aldehyde Substrates

The substrates initially prepared for investigation were mono-*N*-substituted carbamates (Scheme 56). The synthesis started, similar to the preparation of α-aroyloxyaldehydes,[201] with the addition of vinylmagnesium bromide (**169**) to phenylacetaldehyde (**168**) to give the corresponding allylic alcohol **170**. The carbamates **172a** & **172b** were formed by addition of this alcohol to isocyanates **171a** & **171b** before the olefin was cleaved to give the corresponding aldehydes **173a** & **173b** under Lemieux–Johnson oxidative cleavage conditions.[226,227] This method of olefin cleavage was preferred to ozonolysis, which tended to result in more impure products.



Scheme 56. Synthesis of 2° α-*O*-carbamoylaldehyde substrates and cyclisation to hemiaminal. Reagents and conditions: (a) vinylmagnesium bromide, THF, -78 °C – r.t., 87%; (b) **171a** (R = PMP) or **171b** (R = PMB), DCM, r.t., 80%-quant.; (c) $K_2OsO_4{\cdot}2H_2O$ (3 mol%), $NaIO_4$ (2.5 eq.), 2,6-lutidine (4 eq.), 1,4-dioxane:H_2O (3:1), r.t., 44-83%. Cyclisation fast and quantitative (**174a** *trans*:*cis* ratio 9:1; **174b** *trans*:*cis* ratio >19:1).

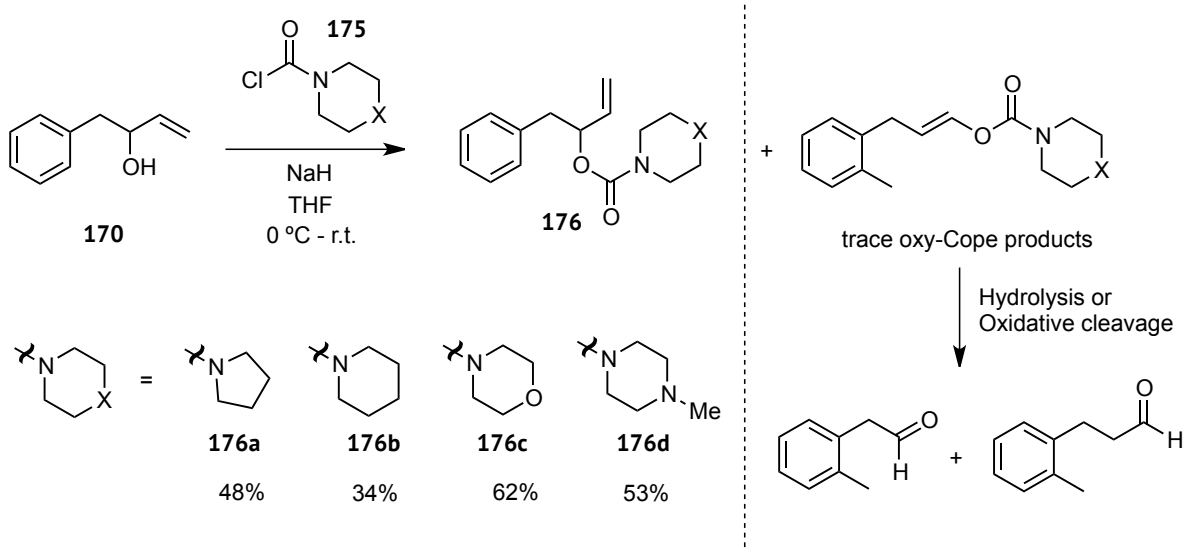
It was found that due to the free N–H of the carbamate **173a,b**, these substrates would rapidly cyclise to give 5-membered hemiaminals **174a,b** with major diastereomers assigned as *trans* through NOE correlations. These latter compounds were found to be very stable under the attempted NHC catalysis reaction conditions using electron rich (mesityl) and electron poor (C_6F_5) NHC *N*-aryl groups, with bases including KOAc, Et_3N, DBU and Cs_2CO_3. Under all reaction conditions surveyed, only starting material was recovered (Scheme 57).



Scheme 57. Unsuccessful reaction of hemiaminal substrates.

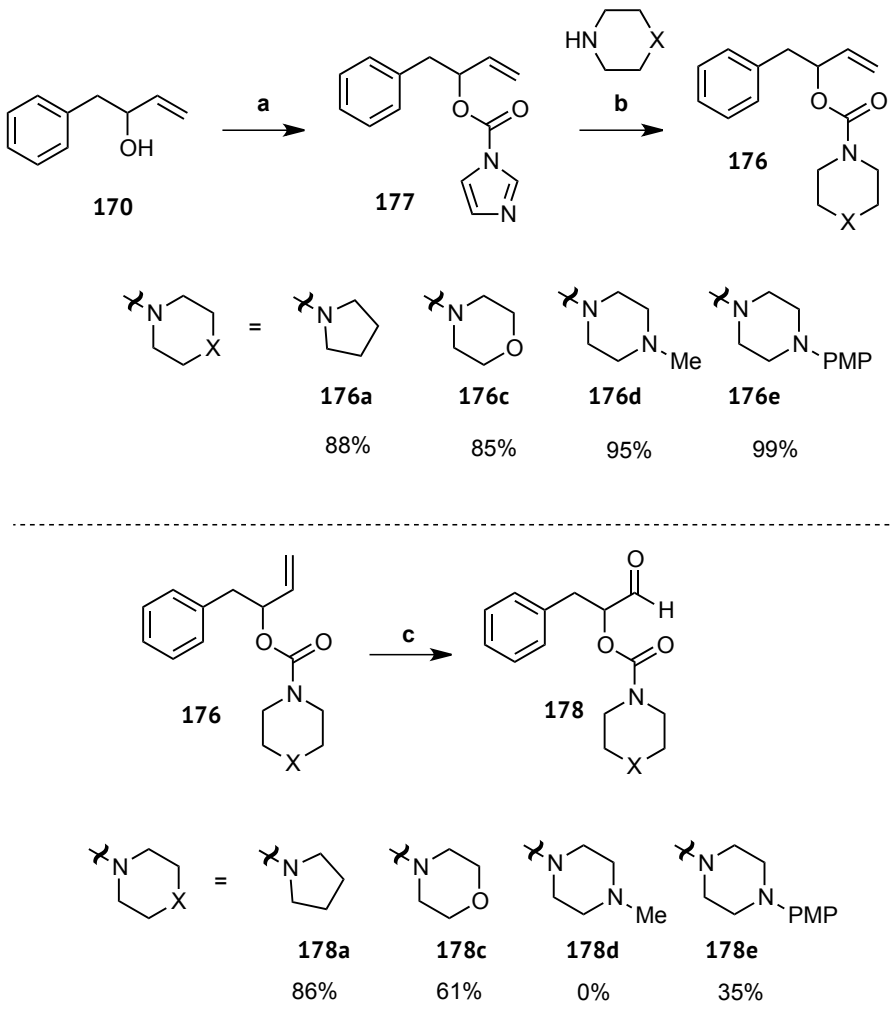
5.4.1.3 Preparation of 3° α-*O*-Carbamoyl Aldehyde Substrates

To prevent the cyclic hemiacetal formation, di-*N*-alkylated carbamates were synthesised. Originally these were prepared from the allylic alcohol **170** described previously and carbamoyl chlorides **175** in the place of the isocyanates (Scheme 58). It was necessary to deprotonate the alcohol to enable its reaction with the carbamoyl chloride; however, it was found that this led to the production of inseparable impurities in small quantities during the reaction. These impurities were tentatively assigned as the oxy-Cope products shown (Scheme 58) due to the observation of additional aldehyde ^{1}H NMR spectrum signals upon alkene cleavage that did not correspond to the desired α-*O*-carbamoylaldehyde products.

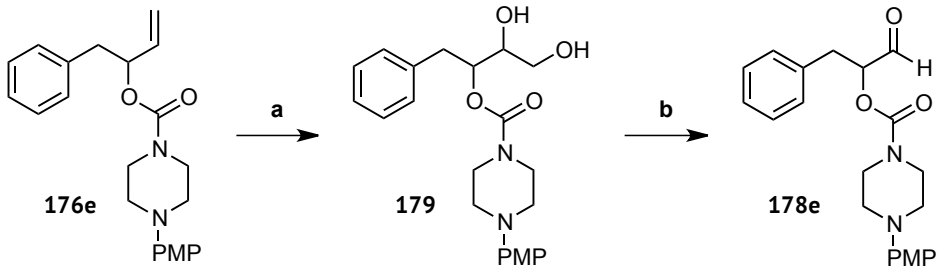


Scheme 58. Initial synthetic route to *O*-allylic carbamates. Possible by-products shown.

As the previous method (Scheme 58) typically resulted in only moderate yields as well as difficulty in purification of the final substrates, a new route to the carbamate substrates was required and so the allylic alcohol **170** was converted using *N*,*N*'-carbonyldiimidazole to its carboxyl imidazole derivative **177** which was to be used as the common intermediate for subsequent synthesis of carbamate analogues. After screening a number of solvents (DCM, THF, neat) and temperatures (r.t. to 100 °C) for the amine addition, it was soon discovered that the reaction proceeded cleanly and in high yield by combining **177** with the amines neat at 80 °C for 3–5h. The resulting *O*-allylic carbamates **176a,c,d,e** were then subjected to the Lemieux–Johnson cleavage conditions seen previously to give the α-*O*-carbamoylaldehyde substrates **178a,c,d,e** (Scheme 59).



Scheme 59. Preparation of α-*O*-carbamoylaldehyde substrates **178**. Reagents and conditions: (a) CDI, DCM, r.t., 98%; (b) amines, neat, 80 °C, 88–99%; (c) $K_2OsO_4{\cdot}2H_2O$ (1 mol%), $NaIO_4$ (2.5 eq.), 2,6-lutidine (4 eq.), 1,4-dioxane:H_2O (3:1), r.t., 35-86%.



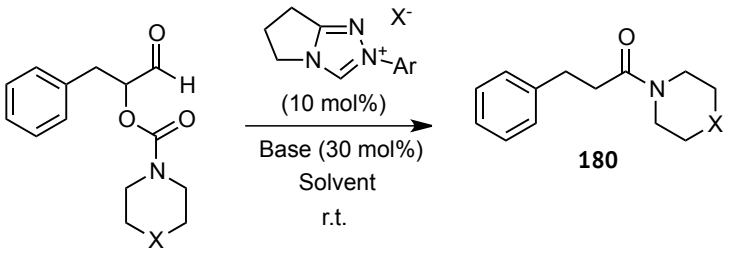
Scheme 60. Two stage oxidative cleavage. Reagents and conditions: (a) AD-mix α:β (1:1), *t*-BuOH, H_2O, r.t.; (b) $NaIO_4$, acetone, H_2O, r.t., 75% (2 steps).

It was found that when the carbamate moiety had additional basic nitrogens (such as those shown **176d,e**), the standard oxidative cleavage conditions resulted in poor yields especially on larger scale. This was due to over-oxidation of the substrates to form *N*-oxides. This reactivity could be reduced by greatly increasing the loading of osmium catalyst (to ~20 mol%); however, it was preferable to separate this step into its componant dihydroxylation and subsequent cleavage steps in an attempt to minimise the over-exposure of the substrates to oxidants. As a result the dihydroxylation conditions chosen for the allylic carbamates

(which were racemic) used a 1:1 ratio of the Sharpless asymmetric dihydroxylation mixtures α and β, due to the known ligand accelerating effects of $(DHQ)_2PHAL$ and $(DHQD)_2PHAL$.[228] The cleavage of the resulting diol could then be carried out with a much smaller quantity of $NaIO_4$ than was used in the one-pot oxidative cleavage procedure and the relative concentrations of diol to oxidant were much closer than in the catalytic system resulting in less opportunity for the over-oxidation of the substrate. With this method (*p*-methoxyphenylpiperazinyl)carbamyl aldehyde substrate **178e** was formed in an improved isolated yield of 75% from the allylic carbamate on multi-gram scale (Scheme 60).

5.4.2 NHC-Catalysed Reactivity of α-*O*-Carbamoyl Aldehyde Substrates

5.4.2.1 Base and Triazolium Compatibility



Scheme 61. General reaction screening conditions.

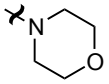
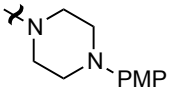
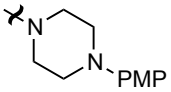
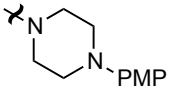
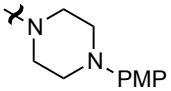
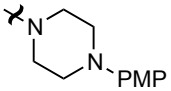
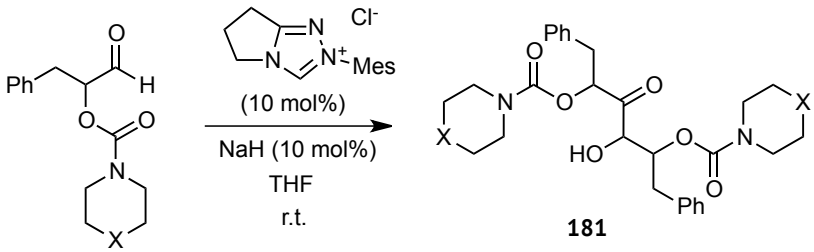
Entry	Substrate	Ar =	X⁻	Base	Solvent	Result
1.		Mes	⁻Cl	DBU	THF	No amide observed, acyloin products seen
2.		Mes	⁻Cl	NaH	THF	No amide observed, acyloin products seen
3.		C_6F_5	$^-BF_4$	DiPEA	THF	Slow conversion, no amide, acyloin products seen
4.		C_6F_5	$^-BF_4$	DiPEA	THF	Slow conversion, no amide, acyloin products seen
5.		Mes	⁻Cl	DBU	MeCN	<10% amide product, 10% acyloin product
6.		C_6F_5	$^-BF_4$	Et_3N	MeCN	Slow conversion to amide and acyloin products
7.		C_6F_5	$^-BF_4$	Et_3N	THF	Slow conversion to amide and acyloin products
8.		C_6F_5	$^-BF_4$	KOAc	MeCN	Slow conversion, distribution of products including amide, acyloin not observed.
9.		Mes	⁻Cl	Et_3N	MeCN	25% amide product isolated

Table 3. Initial screening conditions for formally intramolecular NHC-catalysed redox amidation. Where isolated yields are not given, products could not be isolated individually or in accurately measurable quantities.

With several substrates in hand, the NHC-catalysed redox amidation could be attempted. The initial reactivity of substrates **178a,c,e** with *N*-aryl triazolinylidene NHCs **138** (Ar = C_6F_5) and

141 (Ar = Mes) gave inseparable mixtures of products with a selection of bases and solvents (Table 3: entries 1-5). The main components of the isolated mixtures appeared to be acyloin compounds (e.g. **181**) implying that the carbamate group was not being effectively displaced for these substrates (Scheme 62). It was rationalised that for the electron poor NHC **138** (Ar = C_6F_5) the *N*-heterocycle was simply too electron deficient to provide the driving force required to eliminate the carbamate moiety. The same should not be true for the *N*-mesityl triazolinylidene **141**, which may explain why a small amount of amide was observed in entry 5 (Table 3); however, it had been observed in Gravel's NHC lactamisation chemistry that the conjugate acid of the base used to deprotonate the triazolium precursor plays an important role in activation of the leaving group *via* hydrogen bonding.[204] This led to investigations into the effects of base strength on NHC-catalysed redox amidation reactivity.



Scheme 62. Formation of acyloin products in conditions where leaving group displacement is not favoured.

The use of weaker bases Et_3N and KOAc to generate the NHCs led to a reduction in the acyloin products and indications of the desired redox amidation product in both systems (although it was still a minor product) leading to a slight revision of the initial conjecture that the combination of the electron poor NHC and carbamate substrates could not lead to acyl azolium species. This result reinforced the idea that hydrogen bonding activation of the leaving group by the conjugate carboxylic acid of the base could aid displacement even by the electron withdrawn NHC. The combination of carboxylate bases with the *N*-mesityl triazolium **141** was unsuccessful – attributed to insufficient deprotonation of the precatalyst in the reaction mixture.

The most promising results were obtained with Et_3N and the *N*-mesityl precatalyst **141** (Table 3: entry 9). Although the yields were still low, the acyloin side reactions were eliminated and the reaction proceeded seemingly cleanly to the amide product **180** (25% yield) and what appeared to be a hydrolysis product (i.e. hydrocinnamic acid). It should be noted that condensation products of amines and aldehydes were not observed in any of the reactions described so far.

5.4.2.2 Synthesis of Alternative Triazolium Precatalysts

With the information learnt from the initial experiments it was established that it was important to balance selection of the steric and electronic properties of the carbene with the resulting pK_a of its triazolium precursor – an area of study that has fast become prevalent in NHC catalysis.[229,230] The *N*-aryl group of the triazolium precatalysts shown (Figure 47) provides tunable steric and electronic influence over the carbene; however, as the aryl group is varied, the pK_a of the triazolium is affected. As indicated previously, the choice of base should be appropriate for the triazolium precatalyst being used, with stronger bases needed to bias the deprotonation equilibrium towards the free carbene. In the case of the present NHC-catalysed reaction, another variable is added as the conjugate acid (formed from the base upon deprotonation of the precatalyst) also plays an additional role in assisting the leaving group displacement. This meant that, for the desired reaction there should be a 'pK_a window' in which the dual roles of the base would be complementary. It was apparent that non-commercial NHC precursors may be required to provide intermediate reactivity between the very different properties of the *N*-mesityl (electron rich, sterically bulky) and *N*-C_6F_5 triazolium (electron poor, less sterically bulky) precatalysts.

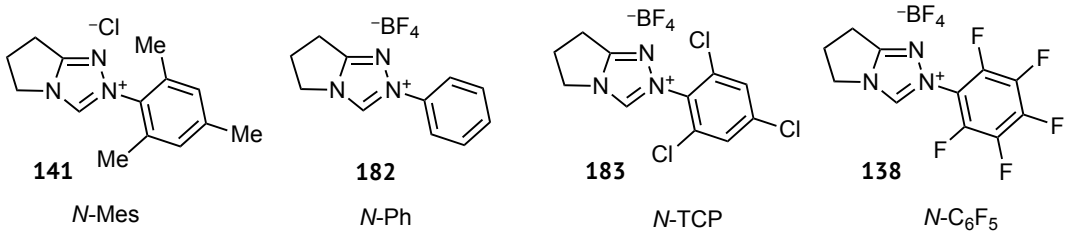
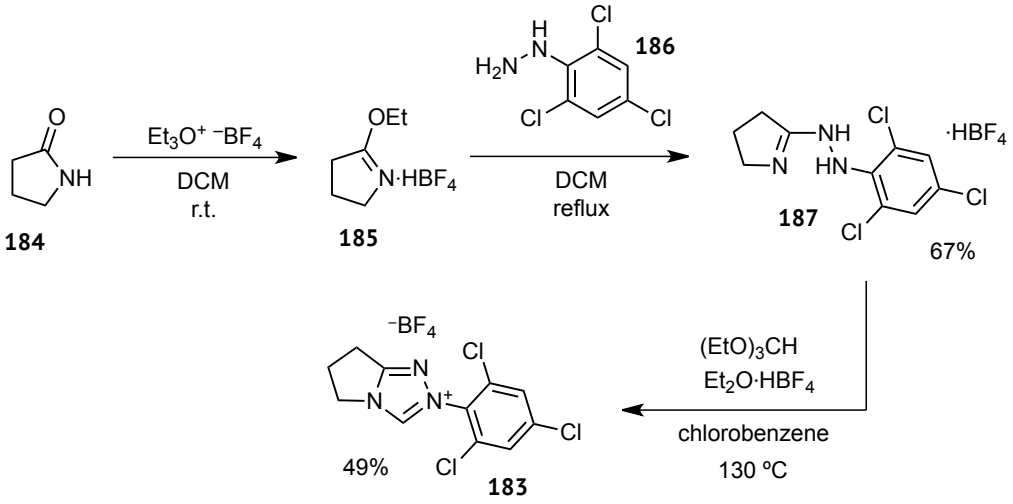


Figure 47. Triazolium precatalysts.

The precatalyst hypothesised to present the optimal combination of properties was the *N*-2,4,6-trichlorophenyl (*N*-TCP) triazolium **183** due to the fact that its electron withdrawing nature would aid the acylation step and lower its pK_a compared to the *N*-mesityl triazolium **141**, which would allow weaker bases to still provide sufficient equilibrium concentrations of deprotonated carbene.[231] These weaker bases are needed for their conjugate acid assistance in the leaving group displacement step. It was also possible that the extra steric bulk of the *o,o'*-substituents would aid the formation of the Breslow intermediate and displacement of the α leaving group. The *N*-TCP triazolium **183** was synthesised with two small modifications to the literature known procedure.[229,232] First, triethyloxonium tetrafluoroborate was used for the initial alkylation to give **185**. This was due to the greater stability (of the commercial

preparations) and lower cost of this Meerwein salt compared to the trimethyloxonium tetrafluoroborate. Subsequent treatment of the protonated imidate **185** with 2,4,6-trichlorophenylhydrazine (**186**) gave the pre-cyclised hydrazinium tetrafluoroborate **187**. The second modification to the literature procedure was the addition of $HBF_4{\cdot}Et_2O$ to the cyclisation step with triethylorthoformate in chlorobenzene. This additional acid provided greater reproducibility in the cyclisation of this sterically hindered molecule.



Scheme 63. Synthesis of *N*-TCP triazolium **183** NHC precursor.

To provide a benchmark of intermediate properties, the *N*-Ph triazolium **182** was also synthesised – in this case the literature procedures were satisfactory.[232]

5.4.2.3 Optimisation of Formal Intramolecular NHC-catalysed Redox Amidation

The reaction was then attempted on model substrate **178e** with the four precatalysts and a number of bases shown – again continuing the trend of decreasing basicity.

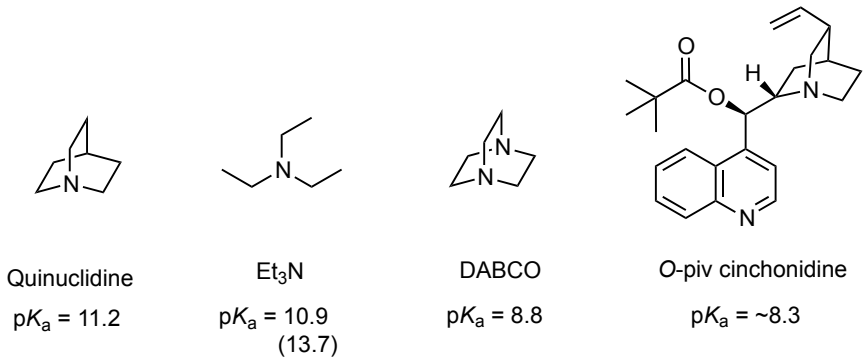
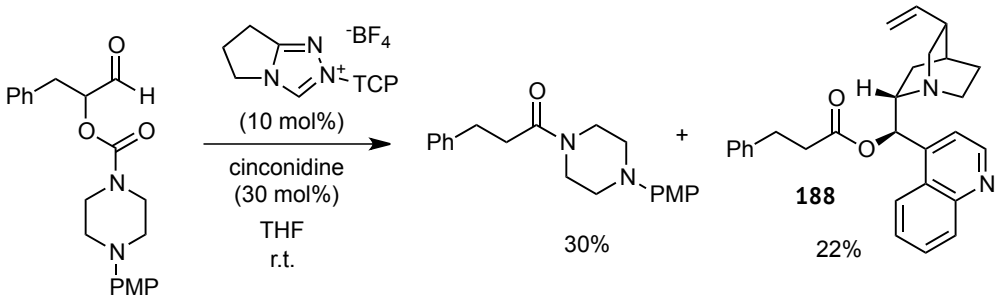


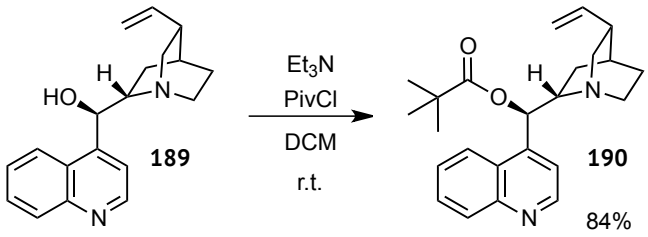
Figure 48. Bases for reaction optimisation - pK_a values for protonated species determined in H_2O (value in parentheses determined in THF).[233–235]

It was also thought that the constrained structure of the bicyclic tertiary amine bases would enable greater accessibility of the proton to aid the elimination step. For this purpose, quinuclidine was potentially too basic but the related DABCO and cinchonidine were appropriate choices.



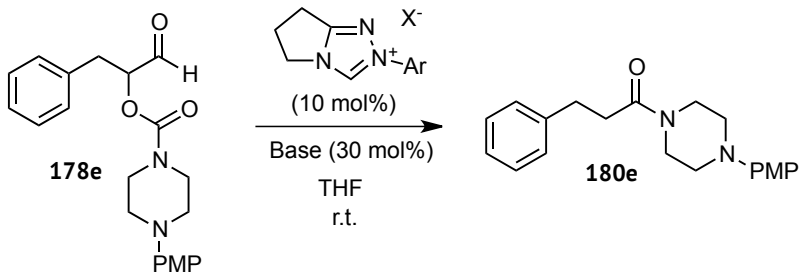
Scheme 64. Formation of cinchonidine ester by-product **188** when using unprotected cinchonidine as base.

Initially when unprotected cinchonidine (**189**) was used, a redox esterification occurred to give *O*-hydrocinnamoyl cinchonidine **188** (Scheme 64). Thus the free hydroxyl was protected as the pivalate **190** (Scheme 65).



Scheme 65. Synthesis of *O*-piv cinchonidine.

Pleasingly it was found that the *N*-TCP triazolium precatalyst **183** was the most successful in all reaction conditions (Scheme 66, Table 4: column 3). In comparison, it was found that the *N*-C_6F_5 triazolium precatalyst system produced the amide **180e** but showed incomplete conversion after 18 h, the *N*-mesityl precatalyst led to slow conversion as well as the most side products, and the *N*-Ph precatalyst gave the best conversion in combination with the base DABCO (23% yield). The main side products recovered from the below reactions were hydrocinnamic acid and the decarboxylated amine.

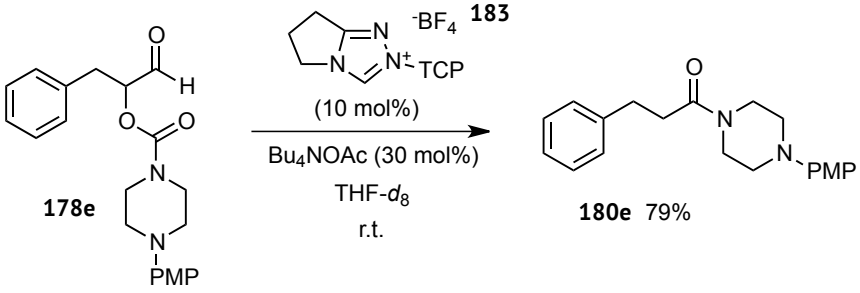


Scheme 66. General scheme for conditions screening using model substrate **178e**.

Base	*N*-Mes	*N*-Ph	*N*-TCP	*N*-C_6F_5
Quinuclidine	No product	No product	No product	No product
Et_3N	15% amide	No product	34% amide	<5% amide
DABCO	<5% amide	23% amide	25% amide	<5% amide
O-piv cinchonidine	11% amide	No product	61% amide	<5% amide

Table 4. Base and triazolium precatalyst compatibility screening for the formation of amide **180e**.

The best result for this chemistry was obtained in an ^{1}H NMR spectroscopy experiment when using tetrabutylammonium acetate (*n*-Bu_4NOAc) (30 mol%) as base with the *N*-TCP triazolium (10 mol%) in THF-d_8 which gave clean conversion in the ^{1}H NMR and ^{13}C NMR spectra with no signals corresponding to the acid by-product, in addition a respectable isolated yield of 79% was obtained (Scheme 67); however, upon scaling up the reaction from 0.05 mmol to 1 mmol of substrate, the carboxylic acid became a substantial by-product.



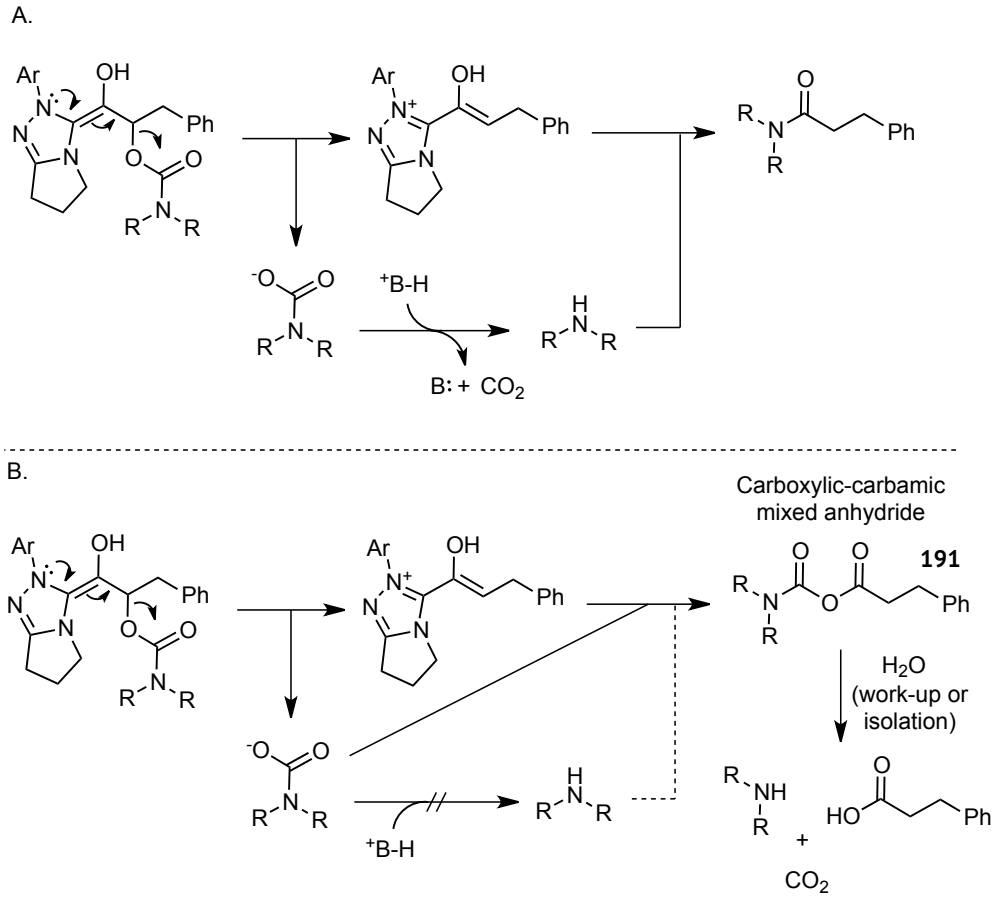
Scheme 67. 1H NMR spectroscopy experiment on 0.05 mmol scale to give amide **180e**.

5.4.2.4 Formation of Hydrolysis Products

It was initially assumed that the formation of the carboxylic acid and corresponding amine was due to trace amounts of water being present in the reagents. This would mean that the

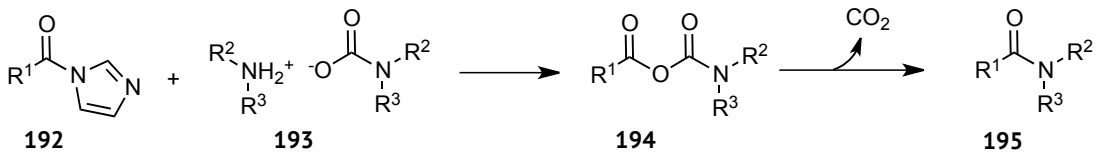
water could out-compete the amine at the acylation step producing the acid by-product and unacylated amine. This was indeed the most likely explanation for the extremely hygroscopic bases such as DABCO and *n*-Bu_4NOAc. The latter of these bears close resemblance to known phase transfer catalysts and in addition was not particularly soluble in a number of organic solvents used for these reactions meaning that pre-drying of a stock solution of this compound over molecular sieves was not particularly successful.

In some situations however, even though rigorous care was taken to exclude moisture, the same carboxylic acid and amine products were formed to a degree that was unlikely to be due to trace amounts of water. It was also noted that the reactions that were suspected to contain larger amounts of water (e.g. DABCO base) led to a much faster conversion of the aldehyde substrates (<1.5 h) than reactions with bases such as Et_3N that gave the same "hydrolysis" by-products as the major isolated species but still contained traces of aldehyde starting material after 12 h. This could potentially be explained in that the displacement of the leaving group assisted to a greater extent by DABCO–H^+ than Et_3N^+H, but an alternative explanation may also be proposed.



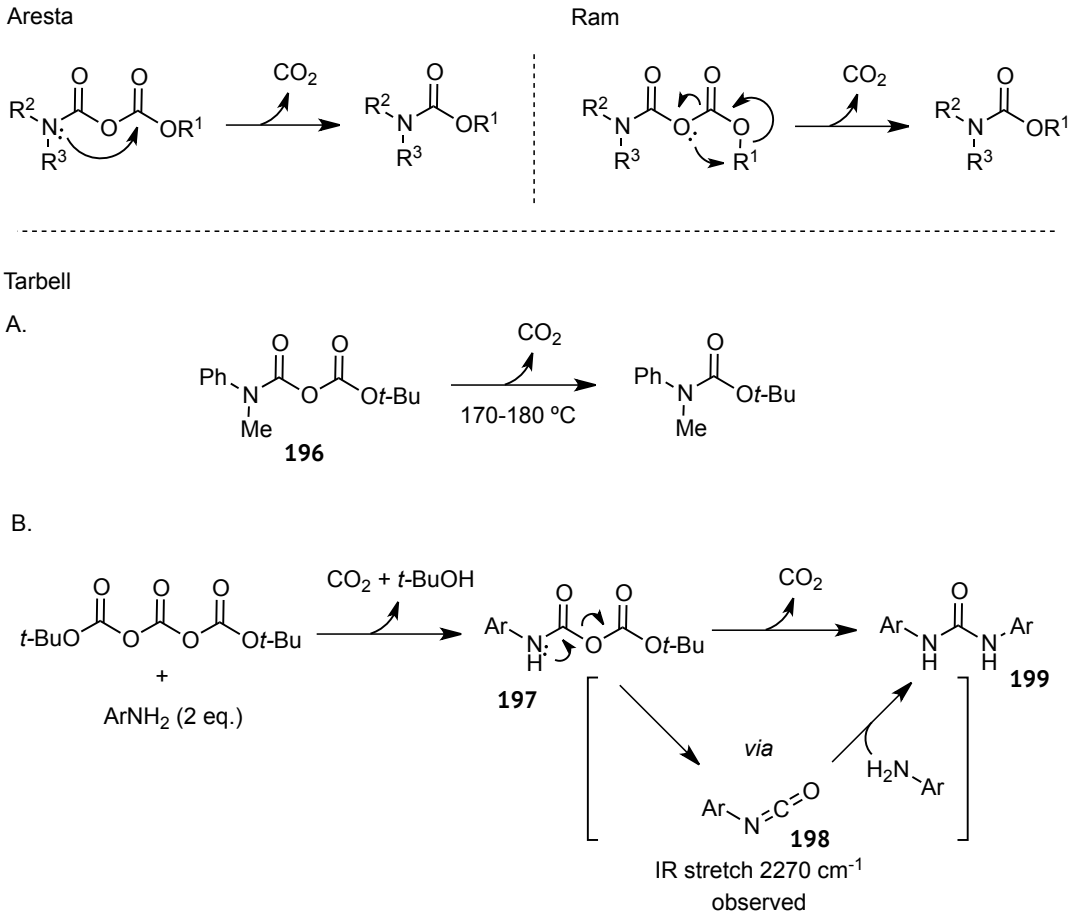
Scheme 68. A) Proposed decarboxylative amide formation; B) Formation of hydrolysis products resulting from insufficient protonation of carbamate anion.

Although carbamic acids readily decompose to release the parent amine and CO_2, carbamate anions are relatively stable. These anions have been implicated as nucleophiles in alkylation and acylation reactions.[236,237] If the conjugate acid species in the reaction is insufficiently capable of protonating the carbamate anion to form the amine, formation of a carboxylic–carbamic mixed anhydride **191** in the acylation step of the catalytic cycle is plausible (Scheme 68). This intermediate **191** undergoes hydrolytic cleavage (upon isolation) to give the acid and amine by-products. There have been transformations proposed by which a general mixed anhydride intermediate **194** may rearrange intramolecularly with decarboxylation to form the corresponding amide **195**, namely in the use of CO_2 to accelerate amide bond formation when reacting amines with acyl imidazoles (Scheme 69);[237] however, the implied intramolecular mechanism seems questionable due to the 4-membered transition state requiring nucleophilic intramolecular attack from an electron deficient nitrogen (occasionally tri-substituted).



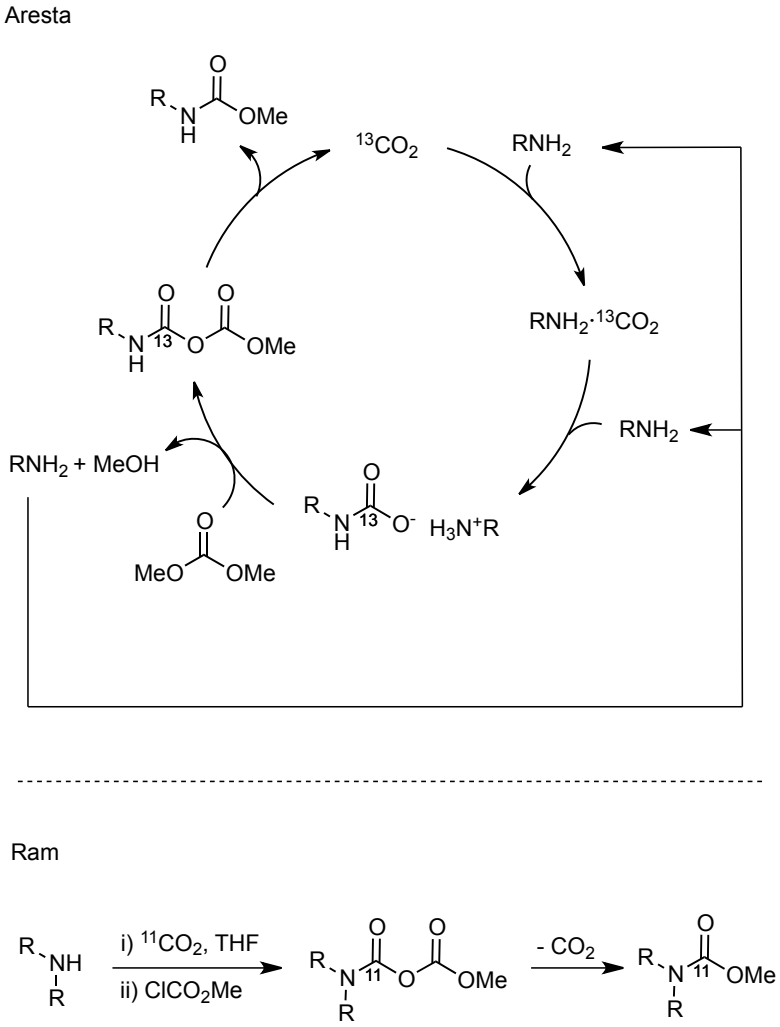
Scheme 69. Amidation from acyl imidazole - proposed direct transformation by Vaidyanathan *et al.* from carboxylic-carbamic mixed anhydride to amide.

The evidence in favour of the proposed mechanism usually concerns the formation of carbamates rather than amides from carbonic–carbamic mixed anhydrides.[238,239] In situations where excess equivalents of the nucleophiles may be taken into account, it could be proposed that it is these that react with the mixed anhydride intermediates to give the final products. There have, however, been examples of isolated carbonic–carbamic mixed anhydrides forming the carbamates directly (Scheme 70).[239–241]



Scheme 70. Proposed mechanisms for carbonic-carbamic mixed anhydride decarboxylative transformations.

In these cases there have been a number of proposed mechanisms including intramolecular rearrangements. It was observed by Tarbell that carbonic–carbamic mixed anhydrides derived from secondary amines (e.g. **196**) were relatively stable and would undergo thermolysis at 170–180 °C. Tarbell also noticed that in the cases of carbonic–carbamic mixed anhydrides derived from primary amines (e.g. **197**), it was possible to form ureas **199** *via* the readily formed isocyanate **198** – supported by the observation of an IR absorption at 2270 cm^{-1} during the reaction.[241] An equivalent fragmentation for the carboxylic-carbamic mixed anhydrides proposed for the present work and more appropriately the work below would likely not result in subsequent decarboxylation and would result in a recombination of the two unaltered parts. Interestingly, the above mechanistic proposals from Aresta and Ram are based on the results of isotopic labeling studies. These studies give different results for the origin of the carbamate carbonyl although proposing similar intermediates (Scheme 71). The differences between these conditions are that the Ram variant uses secondary amines compared to the primary amines used by Aresta and there is potential for excess amine nucleophile to be present in the conditions outlined by Aresta as the CO_2 is proposed to be used catalytically.[238,239,242]



Scheme 71. Isotopic labeling studies from Aresta and Ram to form methyl carbamate derivatives showing similar intermediates. Catalytic cycle from Aresta reproduced as in publication.

Considering the alternative mechanistic explanations for these transformations that do not involve direct intramolecular rearrangement, it is plausible that the mixed anhydride would not spontaneously rearrange to give the amide and that it may have been the alternative source for what appear to be direct hydrolysis products (Scheme 68). The most likely explanations for the rate enhancement observed for the acyl imidazole amidations (Scheme 69) would either be the mild acidic promotion of the acylation step, as seen in related work using imidazole·HCl to promote the same amidation reaction,[243] or if proceeding via the carboxylic–carbamic mixed anhydride, addition of an *in situ* released second amine equivalent that has been deprotonated by the displaced imidazolide leaving group (a similar mechanism could be proposed for Aresta's above mentioned formation of carbamates from dimethylcarbonate which may explain the discrepancy in carbon isotopic labeling results). From this it can be seen that for the NHC-catalysed redox amidation of α-*O*-carbamoyl aldehydes, protonation of the carbamate leaving group is an important step in this

mechanism and the base is not only used to generate the free carbene in the reaction but also plays an important proton shuttling role.

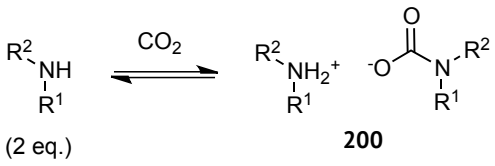
5.4.2.5 Summary

The reactivity outlined above in this formal decarboxylative intramolecular rearrangement of α-*O*-carbamoyl aldehydes to amides has not yet been fully optimised, but from the work undertaken it was evident that NHC-catalysed redox amidation can proceed without the use of a co-catalyst and without the need for sequential or slow reagent additions. Further to this, it was learnt that *O*-carbamates could act as suitable leaving groups in NHC-catalysed redox acylation chemistry. It was also pleasing to see the *in situ* decarboxylative amine nucleophile generation was a feasible approach to solving the problem of slow addition. This generation of the nucleophile from the leaving group also means that the only stoichiometric by-product of this reaction is a single equivalent of CO_2. As has been previously reported, the balance of the pK_as between reagents plays very important subtle roles in this chemistry,[170,244] shown here in shifting the reactivity from undesired benzoin chemistry to the desired redox acylation chemistry and dictating whether or not the carbamate will undergo decarboxylation to reveal the amine nucleophile. The optimisation of this reaction will likely be achieved by further reducing the basicity of the added base and ensuring strictly anhydrous conditions.

5.4.3 Intermolecular NHC-Catalysed Redox Amidation

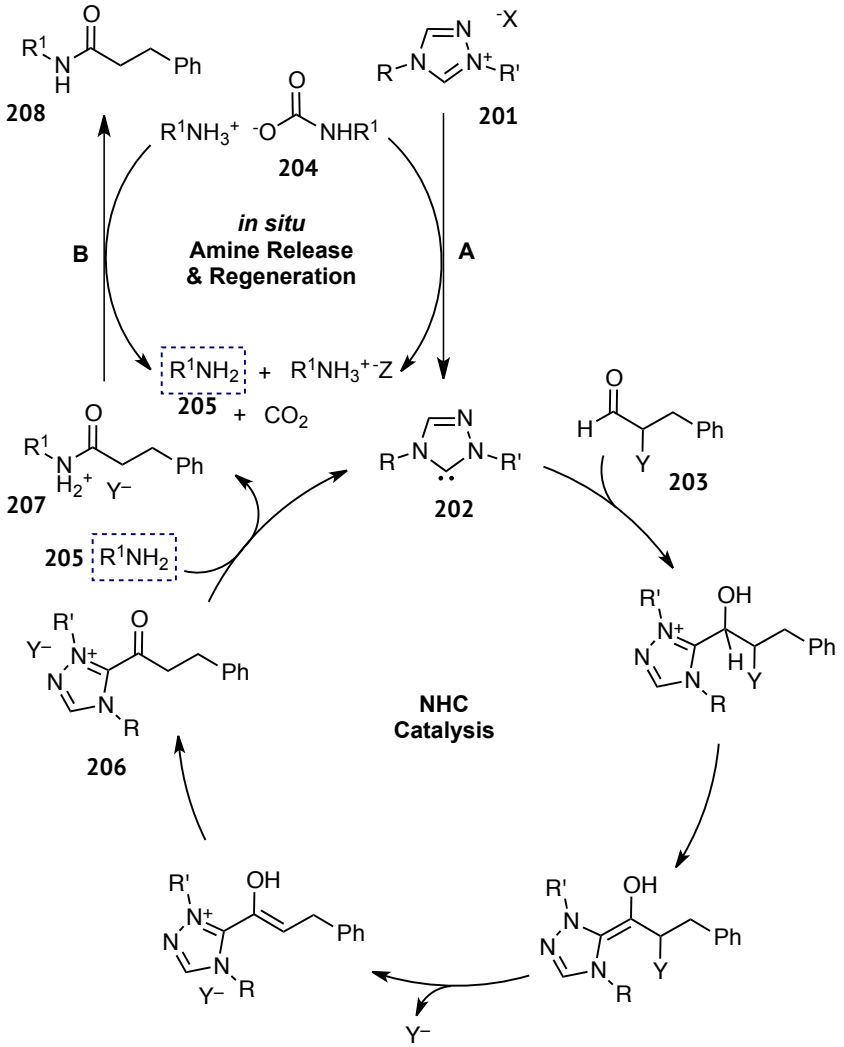
The above chemistry showed good progress towards what could be considered a true NHC-catalysed redox amidation, but there were some requirements for this reactivity that limit its applicability: first, the α-*O*-carbamoyl aldehyde substrates contain quite specific functionality that may restrict their general synthetic application; second, due to the hemiaminal formation seen in section **5.4.1.2**, these reactions are limited to accessing the amide products from 2° amines and prohibit those from 1° amines.

In order to access broader substrate scope, it was hypothesised that an intermolecular variation, that takes advantage of similar reactivity, would be worth studying.



Scheme 72. Reversible formation of alkylammonium alkylcarbamates from amines and CO_2.

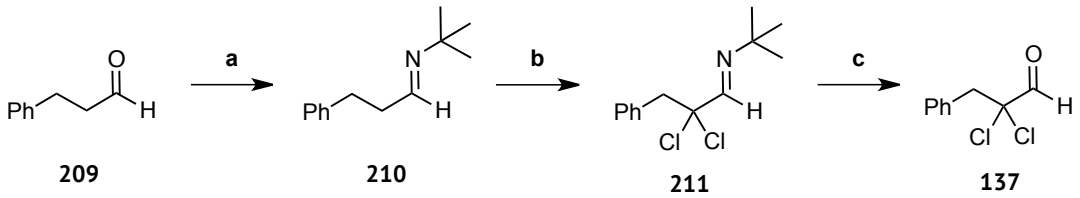
The treatment of amines with CO_2 is well known to produce ammonium carbamate salt pairs (e.g. **200**) (Scheme 72).[245–250] These species are again of suppressed nucleophilicity. In the context of the redox amidation, the triazolium precatalyst **201** needs to be deprotonated to produce the free NHC. If this deprotonation is made by the carbamate anion of **204**, the unstable carbamic acid is produced along with the NHC catalyst **202**, and the former degrades to give the amine nucleophile **205** and CO_2. The NHC will undergo the typical redox transfer chemistry with aldehyde **203** to produce the acyl azolium **206**, which is then intercepted by the amine. The desired amide **208** is produced upon deprotonation of its transient protonated intermediate **207** by another carbamic anion **204**. In this way, the new decarboxylated amine species is only produced after the previous amine has been consumed, thus reducing the chance of imine formation.



Scheme 73. Proposed NHC-catalysed redox amidation using alkylammonium alkylcarbamate. Amine release upon NHC generation (A) and subsequently regenerated in the turnover amidation step (B). Ammonium counterion Z^- either from triazolium precatalyst (X^-) or displaced leaving group (Y^-).

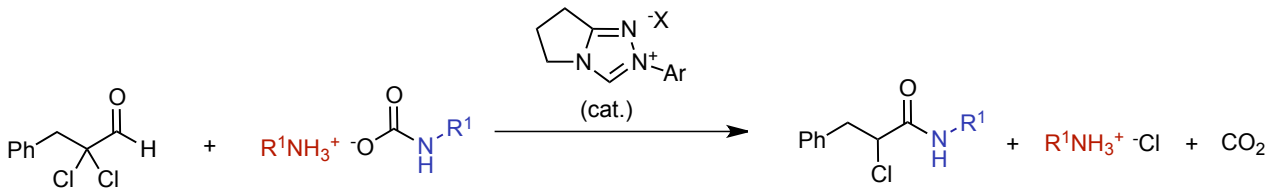
5.4.3.1 Redox amidation reactions using α,α-Dichlorohydrocinnamaldehyde (137)

In order to directly compare this reaction to literature reported results, the aldehyde substrate chosen for initial work was α,α-dichlorohydrocinnamaldehyde (**137**) seen previously in the redox amidation work by Rovis (see **5.2.1.1**, Scheme 48).[207] This was synthesised by double chlorination of the *tert*-butyl imine intermediate **210** derived from hydrocinnamaldehyde (**209**) using *N*-chlorosuccinimide (NCS) to give the dichloroimine **211**, followed by acidic hydrolysis to yield the desired aldehyde **137** (Scheme 74).



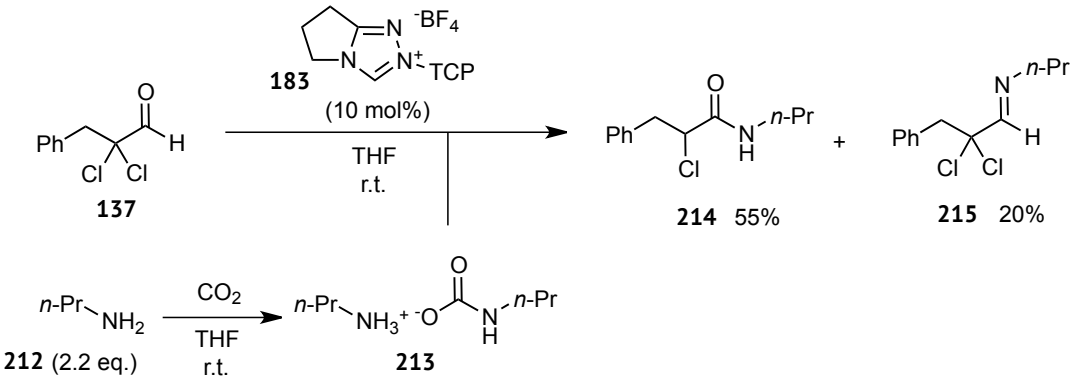
Scheme 74. Synthesis of α,α-dichlorohydrocinnamaldehyde substrate. Reagents and conditions: (a) *t*-BuNH$_2$, MgSO$_4$, r.t.; (b) NCS (3 eq.), DCM, r.t., 57% (2 steps); (c) 3M HCl$_{(aq)}$, r.t., 98%. (further purification by distillation gives 80% recovery).

This substrate is stable for months as a colourless oil at room temperature under argon if purified effectively. In the NHC-catalysed redox amidation reaction with this substrate, one equivalent of chloride is also produced – this ends up taking the place of the carbamic anion in the ammonium salt species leading to overall a surprisingly economical transformation as no additional base is required (Scheme 75).



Scheme 75. Overall equation for intermolecular NHC-catalysed redox amidation.

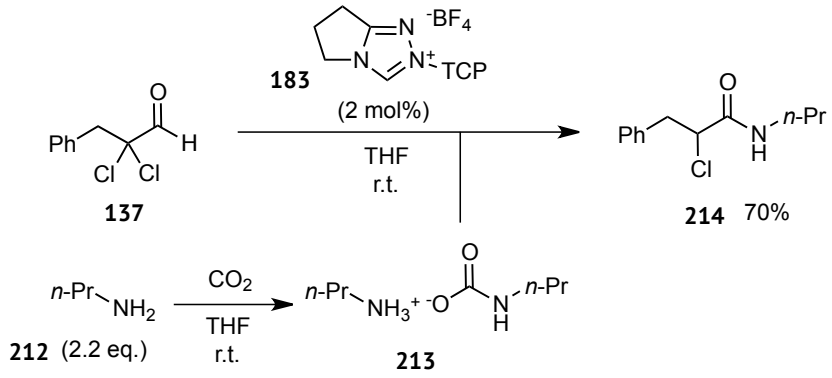
The reaction was first attempted with *n*-propylamine (**212**) at 10 mol% loading of *N*-TCP triazolium precatalyst **183** (Scheme 76). The alkyl ammonium carbamate **213** was formed using sublimed CO_2 from dry ice, bubbled through a solution of the amine in THF. The CO_2 source was removed prior to addition of the precatalyst and aldehyde as NHCs are known to form adducts with CO_2,[131,251] and any additional CO_2 may regenerate the ammonium carbamate pair from the released amine, preventing it from reacting as a nucleophile. These scenarios would both be detrimental to the reaction proceeding.



Scheme 76. Initial reaction of α,α-dichlorohydrocinnamaldehyde (**137**) with alkylammonium alkylcarbamate **213** under NHC-catalysed redox amidation conditions.

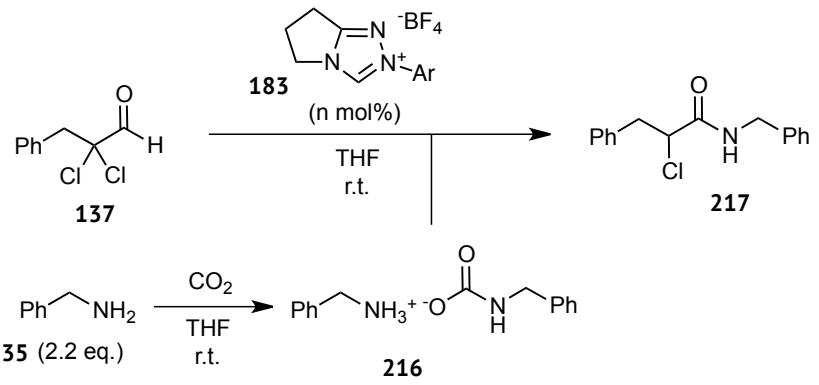
It was observed that upon addition of the aldehyde **137** to a solution of the *n*-propylammonium *N*-*n*-propylcarbamate **213** and triazolium precatalyst **183**, the solution changed colour from colourless to yellow, effervescence was observed and after 10 minutes a white precipitate of the ammonium chloride side-product was formed. Upon completion of the reaction, the solution once again became colourless. The desired amide product **214** was isolated in 55% yield with 20% imine **215** formed (Scheme 76).

As the alkylammonium alkylcarbamates are sensitive to decomposition in the presence of water, it was considered important to attempt to make the reactions as close to anhydrous as possible. To achieve this, the reagents were all distilled prior to use and the CO_2 source was switched to a vapour bottle instead of dry ice.



Scheme 77. Reaction at 2 mol% precatalyst loading, reaction time <45 min. Imine formed in <10% yield.

Due to the rapid conversion seen at 10 mol% precatalyst loading, the use of lower loadings was attempted. It was found that decreasing the precatalyst loading to 2 mol% still resulted in short reaction times, high yield (70%) of **214** and low imine formation (<10%) (Scheme 77).

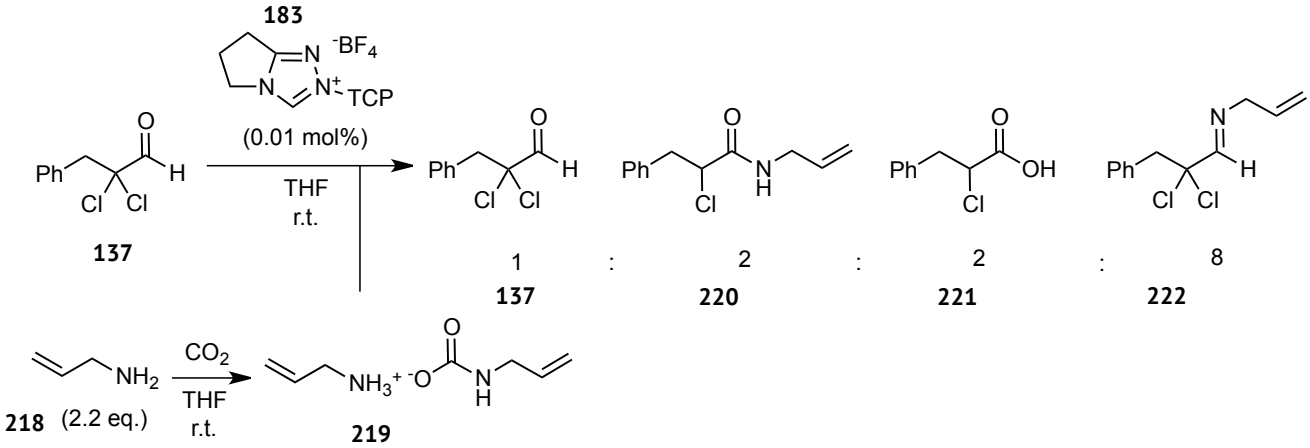


Scheme 78. Reactions with benzylammonium benzylcarbamate (**216**) at 2 mol% and 0.25 mol% with *N*-TCP triazolium precatalyst and at 2 mol% with *N*-C_6F_5 triazolium precatalyst.

Entry	Triazolium Ar =	Precatalyst Loading n = (mol %)	Time (h)	Yield of Amide (%)
1	*N*-TCP	2	0.5	48
2	*N*-TCP	0.25	2	51
3	*N*-C_6F_5	2	0.5	37

Table 5. Effect of low precatalyst loading and *N*-Ar variation.

Using benzylamine derived substrate **216**, it was found that the loading could in fact be decreased as low as 0.25 mol% without detriment to the yield of the reaction and that the *N*-TCP precatalyst **183** was slightly preferable to the *N*-C_6F_5 triazolium **138**. Amide **217** was formed in moderate yield (51%) and, as with the propylamine substrate, the formation of the benzyl imine was pleasingly low (10–15% yield).



Scheme 79. Product distribution at extreme low (0.01 mol%) precatalyst loading.

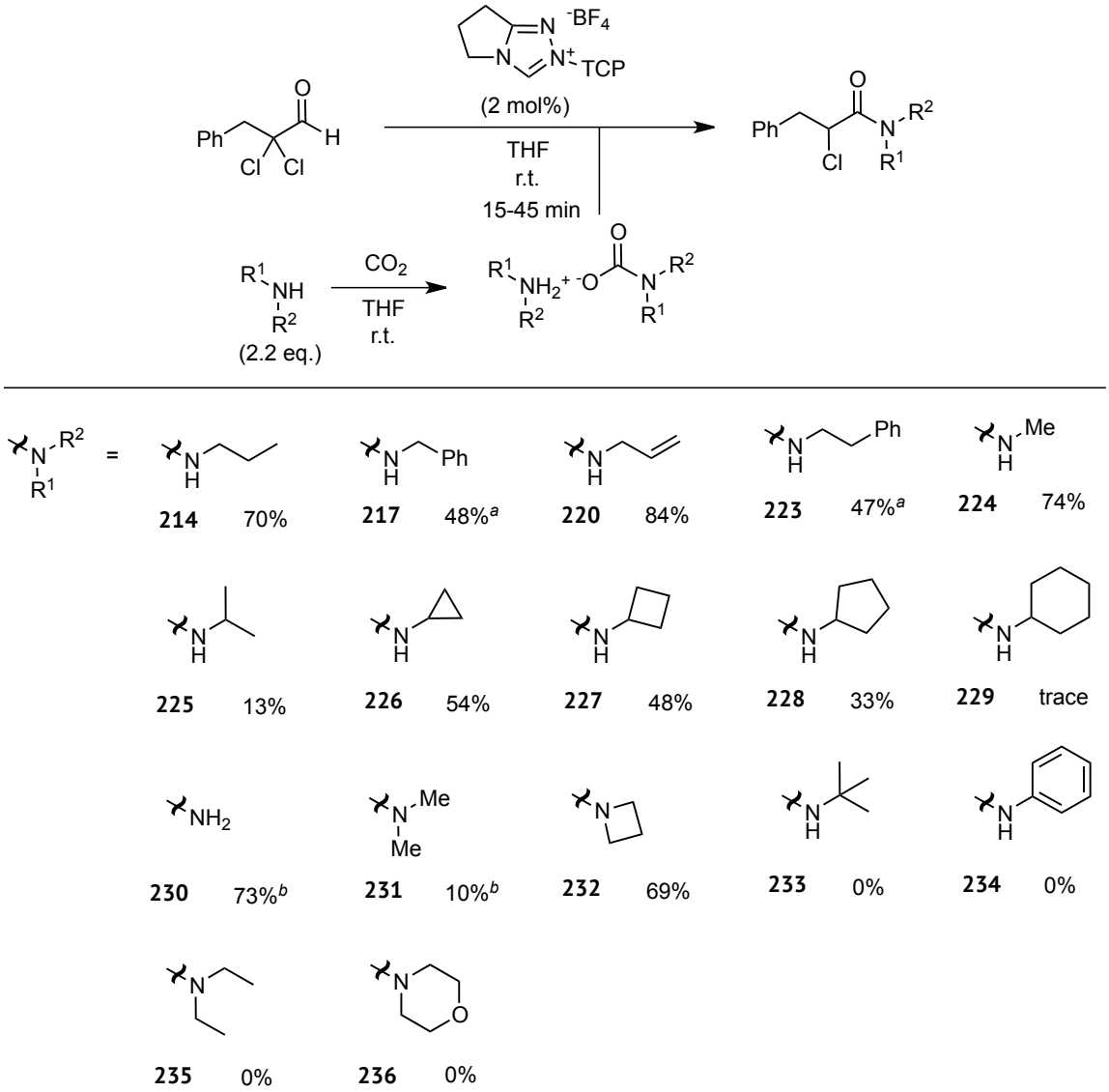
At 0.01 mol% loading of precatalyst **183** using alkylammonium alkylcarbamate **219** from allylamine (**218**), after one hour there was a distribution of starting aldehyde **137**: amide **220**:

carboxylic acid **221**: imine **222** (1:2:2:8), which still represents an approximate 15% conversion to the desired product.

From these initial results it was seen that the *N*-TCP triazolium precatalyst was able to perform this transformation at pleasingly low loadings and in short reaction times.

5.4.3.2 Amine Substrate Scope

To investigate the substrate tolerance of this reaction, a precatalyst loading of 2 mol% was chosen – this was the lowest amount that could be used in the reaction, which still provided observable indications of reaction progression (e.g. colour changes and effervescence). A number of amines were chosen for this reaction summarised below (Scheme 80).



Scheme 80. Substrate scope for NHC-catalysed redox amidation reactions with alkylammonium alkylcarbamate substrates. [a] Amine not distilled prior to use. [b] Alkylammonium alkylcarbamate from commercial sources, not generated *in situ* - 1.1 eq. used.

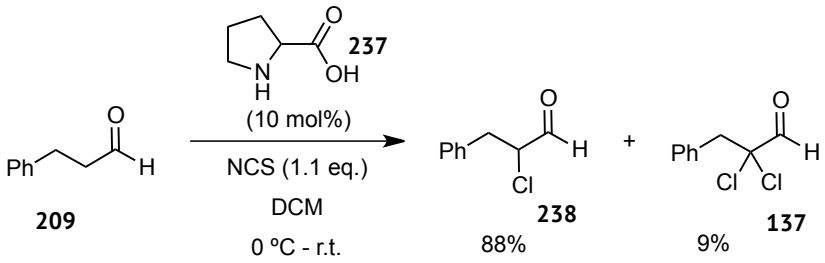
It was found that reactions with primary carbinamines (i.e. H_2NCH_2R) proceeded smoothly - Scheme 80, top row (**214**, **217**, **220**, **223**, **224**). The use of more sterically hindered primary amines such as *iso*-propylamine and its derivatives led to a large decrease in yield e.g. *N-iso*-propyl amide **213** (13%). To examine the effect of the second α-substituent on the amine, a series of cyclic amines (*c*-Pr, *c*-Bu, *c*-Pent, *c*-Hex) were investigated that showed a strong trend of decreasing yield upon increasing steric bulk (% yield **226**>**227**>**228**>**229**). In addition, secondary amines also fared poorly under these conditions such as dimethylamine giving a poor yield – diethylamine, morphiline, pyrrolidine and piperidine (amides **235**, **236** – latter two not shown) were unproductive in this reaction. It was therefore pleasing to see through the use of azetidine that secondary amines could in fact be successfully employed in this redox acylation reaction, with the desired amide product **232** isolated in a good yield of 69%. The use of *t*-$BuNH_2$ resulted in imine and carboxylic acid byproduct formation. The use of aniline was also found to be unfavourable presumably due to its electron poor nature – as this reagent has been used successfully by Rovis in redox acylations with and without a co-catalyst, it was thought that the issue in this case would most likely be the lack of generation of the carbene due to the insufficient basicity of aniline. Another welcome result in this substrate screen was the conversion of ammonium carbamate ($H_2NCOONH_4$) into the corresponding primary amide **230** (70%). Ammonium carbamate is a commercially available, bench stable solid and in this reaction, a desirable source of ammonia.

Also noteworthy in these reactions was the rate at which the product forms compared to both the known redox amidation procedures as well as the redox esterification procedures i.e. <1 h for this reaction compared to 3–24 h commonly needed for previously reported NHC catalysed redox acylation reactions. There are a few possible explanations for this but the most likely are: there is a reduction in hemiacetal / hemiaminal formation between the aldehyde and nucleophilic substrates which may retard formation of the initial NHC–aldehyde adduct and reduce the concentration of available nucleophile for acylation; neutral amines are immediately reactive at the acyl azolium without the need for activation with another carbene or by deprotonation as required by alcohol substrates (in agreement with the findings of Studer but contrary to those of Bode); in combination with the previous statement, the acyl azolium may be a more proficient acylating agent than the species resulting from the co-catalytic relay chemistries and thus would react faster with the amine nucleophiles.

In the less successful reactions, the main by-product was the α-reduced carboxylic acid. In these reactions the carboxylic acid was formed disproportionately compared to the imine, which implied that the water formed upon imine condensation could not account for the formation of all of the carboxylic acid. In addition, the reagents were pre-dried to the same extent as in the successful reactions meaning that it was also unlikely that trace water was playing a large role in this reaction. Finally, it was observed that in these reactions there was limited to no effervescence seen, which in combination with the other data suggests that the sterically hindered amines are being outcompeted by the less nucleophilic but less sterically hindered carbamate anions that are present in much greater concentration especially at the start of the reaction. The products of this reactivity would be carboxylic–carbamic mixed anhydrides, analogous to those seen previously (section **5.4.2.4**), and would undergo the same hydrolytic decomposition to give the carboxylic acid and amine.

5.4.3.3 Synthesis and Reactions of α-Chloroaldehyde Substrate 238

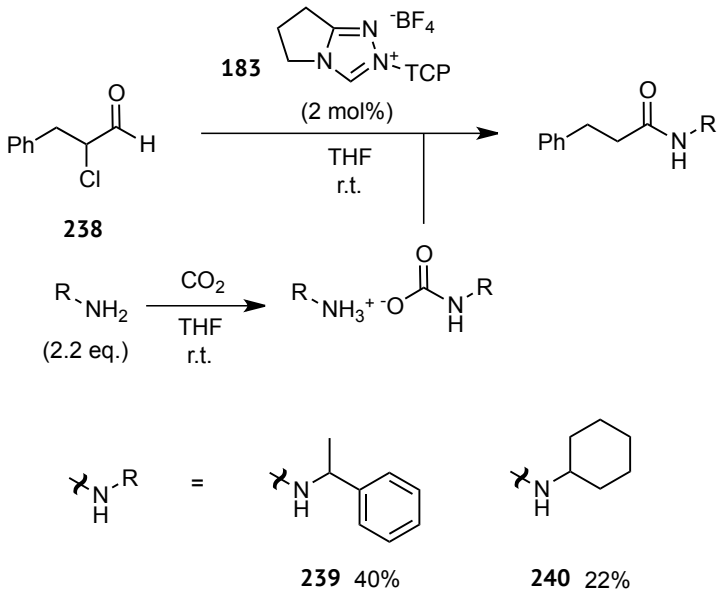
The main obstacle to this intermolecular NHC-catalysed redox amidation reaction was the steric incompatibility of the more bulky amine nucleophiles with the α-chloro acyl azolium intermediate. Given the successes seen previously with 6-membered cyclic secondary amines being acylated by the less hindered acyl azolium species (section 5.4.2), it was thought that by using an equivalent α-monosubstituted aldehyde substrate, the same acyl azolium intermediate should be obtained and this would be more accessible to more sterically hindered amines.



Scheme 81. Synthesis of mono-α-chloroaldehyde **238**.

For this purpose α-chloroaldehyde **238** was synthesised from hydrocinnamaldehyde (**209**) using proline (**237**) and NCS (Scheme 81).[252] When this substrate was used in combination with alkylammonium alkylcarbamates derived from α-methylbenzylamine and cyclohexylamine, the corresponding amide products **239** & **240** were formed in 40% and 22% isolated yields respectively. These were pleasing yields for preliminary results, especially as

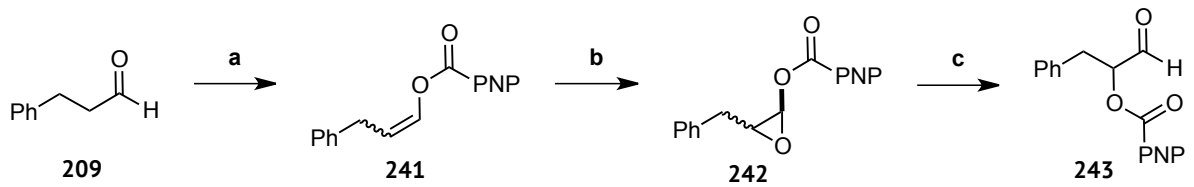
the aldehyde starting material was contaminated with some of the over-chlorinated α,α-dichloroaldehyde **137**.



Scheme 82. Reactions of monochloroaldehyde substrate **238** with hindered amines.

5.4.3.4 Synthesis of α-Aroyloxyaldehyde Substrate 243

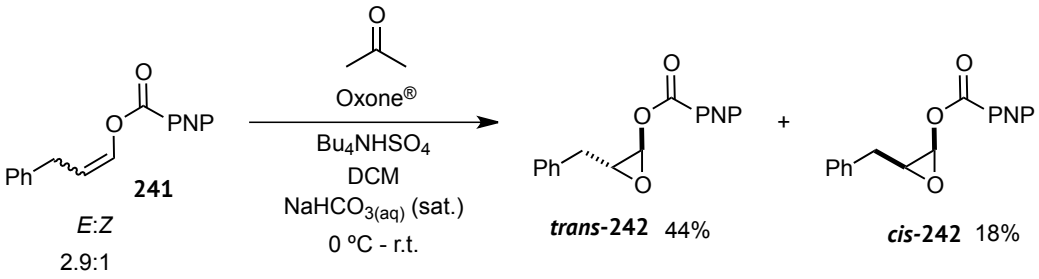
It was proposed that the preparation of α-aroyloxyaldehydes would give control over the monosubstitution of the aldehyde. Although there are known routes to these compounds,[201,253] it was considered intellectually interesting to investigate an approach to the synthesis through a Hassner–Rubottom-type oxidation with the final step as a thermally activated rearrangement of an enol ester epoxide with carboxyl migration.[254–256] This transformation has good literature precedent,[257,258] notably from Shi who performed the transformation stereoselectively through the use of a chiral dioxirane to produce enantioenriched chiral α-acyloxy ketones.[259] The most appealing feature of this chemistry was that in the thermal rearrangement step, no additional reagents are required and the transformation is typically very clean so the substrate can potentially be obtained in high purity.



Scheme 83. Synthesis of aldehyde **243**. Reagents and conditions: (a) 4-nitrobenzoyl chloride, Et_3N, DCM, r.t., 64% (*E*:*Z* ratio 1:2); (b) *m*CPBA, DCM, 0 °C – r.t., 20% (*trans*:*cis* ratio 1.4:1); (c) 165-190 °C, quant. conversion (not isolated pure). PNP = *para*-nitrophenyl.

The enol ester **241** was formed from hydrocinnamaldehyde using 4-nitrobenzoyl chloride and Et_3N as a mixture of stereoisomers. Epoxidation of this mixure with *m*CPBA gave reasonable conversion to the enol ester epoxide **242** (as a mixture of diastereomeric enantiomers) but was found to be difficult to purify although these epoxides are stable to purification using silica – the main impurity being surplus *m*CPBA. The thermal rearrangement was then attempted at 165 °C for 5 min and it was observed that the *trans*-substituted epoxides could rearrange to the desired aldehyde **243**, but the *cis*-diastereomers would not. The mixture was then heated at 180 °C for a further 10 min whereupon it was seen that the *cis*-diastereomers would undergo the thermal rearrangement. A further 10 min heating at 190 °C led to almost complete conversion of the starting material; however, it was found that a small impurity had started to form. Unfortunately purification of the final material by flash column chromatography led to the introduction of further impurities.

In an attempt to form the epoxide in greater purity, alternative epoxidation conditions were required. It was found that the enol ester *E* & *Z* diastereomers could be enriched as the *E*-form is crystalline and the *Z*-form is an oil. As the *trans*-enolester epoxide is more desirable for the thermal rearrangement, the reaction was pursued with the *E*-enriched enol ester. Using acetone and Oxone® under biphasic conditions, it was possible to perform the epoxidation of **241** with *in situ* generated DMDO (dimethyldioxirane).[260–262]



Scheme 84. Synthesis of enol ester epoxides using Oxone® and acetone to generate DMDO *in situ*. Oxone® (6 eq.) added in 3 portions.

Although this reaction did not go to completion, the crude material was a lot easier to purify, giving the enol ester epoxide **242** in moderate yield (Scheme 84) as diastereomeric enantiomers (*trans*:*cis* ratio 2.4:1). Time constraints meant that the thermal rearrangement of this new material was not attempted and optimisation of the temperature and duration of this reaction will be required.

5.4.3.5 Summary of Intermolecular NHC-catalysed Redox Amidation

The intermolecular varient of this redox amidation protocol saw some of the highest yields achieved. These yields compared favourably with literature reported yields for one-pot conditions, with the reactions proceeding at room temperature and in a fraction of the time (<45 min). These reactions are also procedurally very simple, only requiring the aldehyde and amine substrates, the triazolium precatalyst and CO_2. Even at 2 mol% precatalyst loading this is one of the lowest reported loadings for NHC-catalysed redox amidations and, as seen above (**5.4.3.1**, Table 5, entry 2), there is potential for the loading to be reduced further. Once again, it can be seen that the direct nucleophilic attack of an amine nucleophile without the need for a co-catalyst is in fact possible and it is hoped that if the α-aroyloxyaldehyde substrates are compatible with more sterically bulky amines in these conditions, direct kinetic resolutions of amines using chiral NHCs will be achievable.

6 Activation of Carbohydrates for NHC-catalysed Redox Acylation

Carbohydrates comprise the most abundant group of natural products.[263] As a result, outside the conventional carbohydrate chemistry of forming higher order oligosaccharides, monosaccharides (the simplest carbohydrate units) have been found to play an important role in chemical synthesis as chiral pool molecules.[264–267] This includes in the synthesis of highly functionalised building blocks as well as being the source of chiral information in the construction of natural product molecules and pharmaceuticals.[268–271] For this reason, the investigation into synthetically useful transformations of monosaccharides especially in the context of the production of high value functionalised intermediates.

6.1 Carbohydrate Lactols as Masked Aldehydes

Monosaccharides unprotected at the anomeric position equilibrate between a number of forms in solution of which the open chain form **244** is typically present far below 10% of the total distribution.[272]

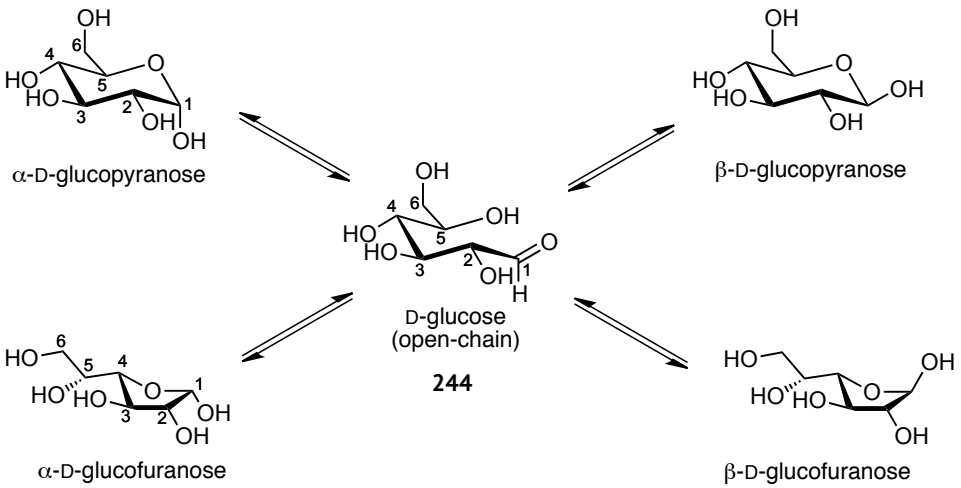


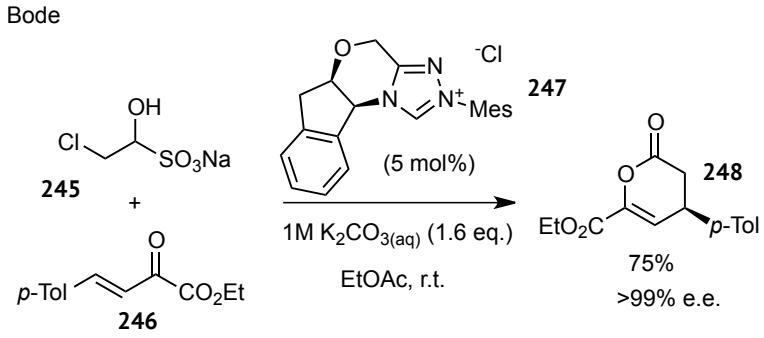
Figure 49. Structures and numbering of D-glucose forms.

Despite this, the electrophilic reactivity of the open-chain form allows carbohydrates to undergo many reactions typical of carbonyl functionality. These reactions depleting the open form of the sugars end up driving the equilibrium towards the ring-opened form of the monosaccharides resulting in high conversions to the carbonyl derived products.[273] Some of the reactions that best exemplify this are C–1 imine (e.g. Amadori rearrangement)[274–276] and oxime formations,[277–279] Wittig olefinations of open-form carbohydrate lactols,[280–284] and the

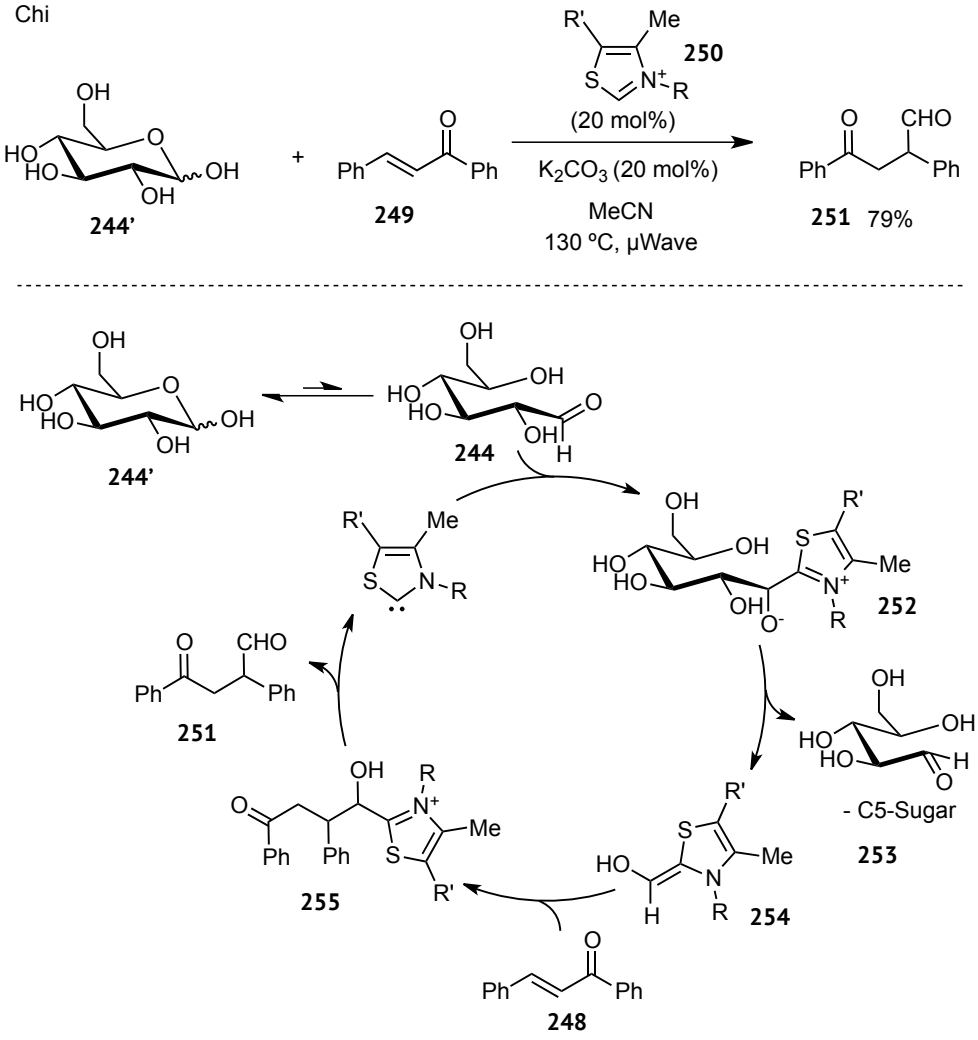
nucleophilic addition of organometallics to the anomeric position carbonyl of these same species.[285]

6.2 Reactions of NHCs with Masked Aldehydes

There are limited examples of N-heterocyclic carbenes forming adducts with aldehydes derived from latent carbonyl functionality.



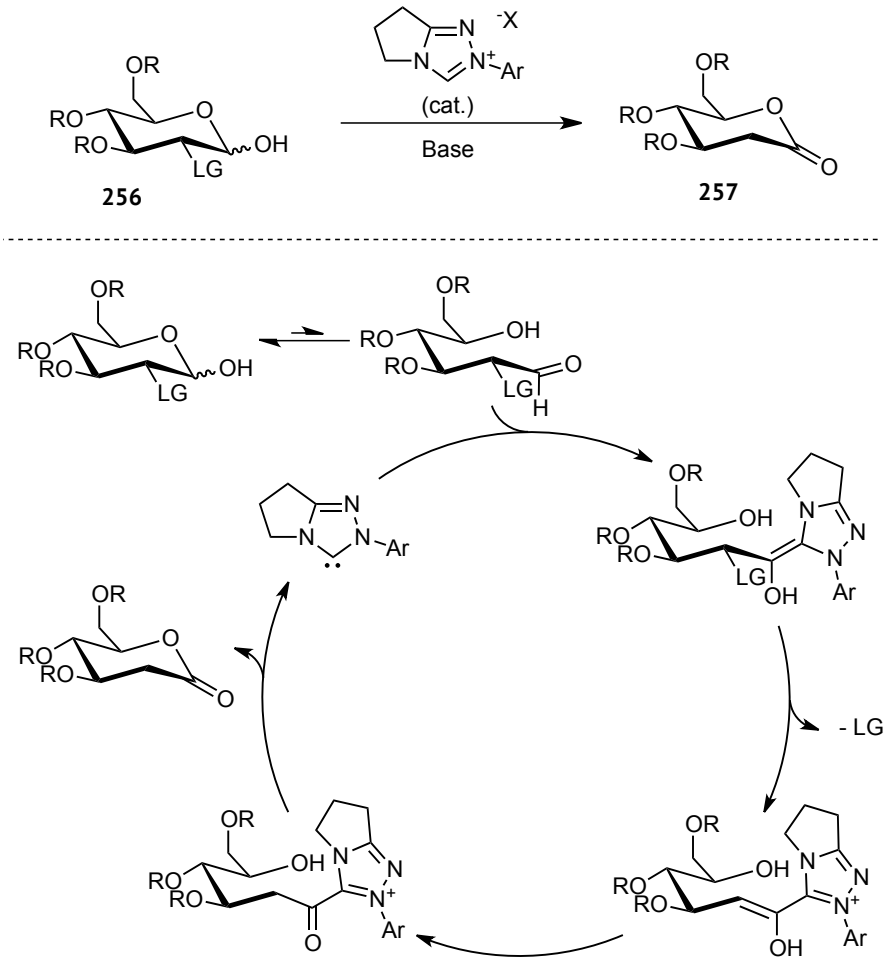
Scheme 85. Bode - NHC-catalysed reaction of bisulfite adduct with oxodiene.



Scheme 86. Chi – Carbohydrate activation for use in Stetter reaction with proposed catalytic cycle.

The main two examples of this concept (shown above) are the use of bisulfite adducts to stabilise α-chloroaldehydes for use in hetero-Diels–Alder reactions with oxodienes (Scheme 85),[286] and the degredative formation of formyl anions from carbohydrates for use in Stetter reactions (Scheme 86).[196] In the former example, the bisulfite adduct **245** is decomposed *in situ* to form aldehyde substrates that would otherwise exhibit poor stability if stored as the aldehydes. The resulting aldehyde reacts with **247** derived NHC and α,β-unsaturated ketoester **236** to form the hetero-Diels–Alder product **248**. The latter example from Chi, makes use of the equilibrating forms of the carbohydrate, reacting with the open-chain aldehyde form **244** to give initial adduct **252**, which generates the Breslow intermediate **254** through a retro-Benzoin reaction with the expulsion of C–1 degraded sugar **253** (cf. α'-hydroxyenone substrates, Scheme 50). This formyl anion equivalent **254** then undergoes Stetter chemistry with chalcone **248** to give 1,4-dicarbonyl product **251**.

6.3 Redox Esterification of Carbohydrate Monosaccharide Lactols using NHCs

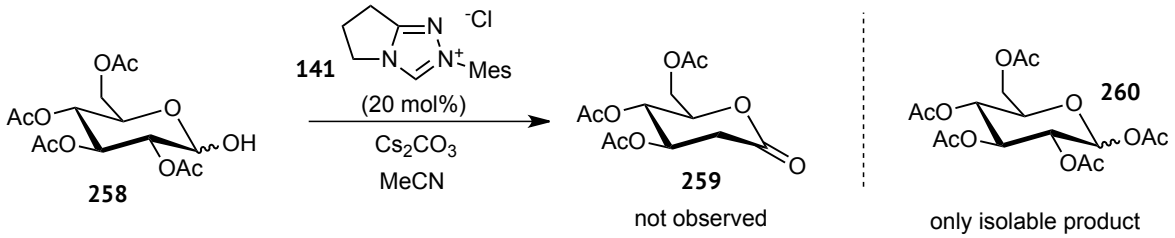


Scheme 87. Proposed NHC-catalysed intramolecular redox lactonisation of carbohydrate derived hemiacetal substrates. LG = leaving group.

The idea of this project was to use NHCs to activate monosaccharides in their open-chain form and through careful selection of the C–2 protecting group (e.g. **256**), perform the typical internal redox rearrangement seen in redox acylation chemistry leading to an acyl azolium intermediate, followed by lactonisation from the C–5 hydroxyl (originally displaced from the hemiacetal). The products of such reactions would be 2-deoxysugar derivatives **257** (oxidised at C–1), which are a prevalent but often synthetically challenging subclass of carbohydrates to produce.[287]

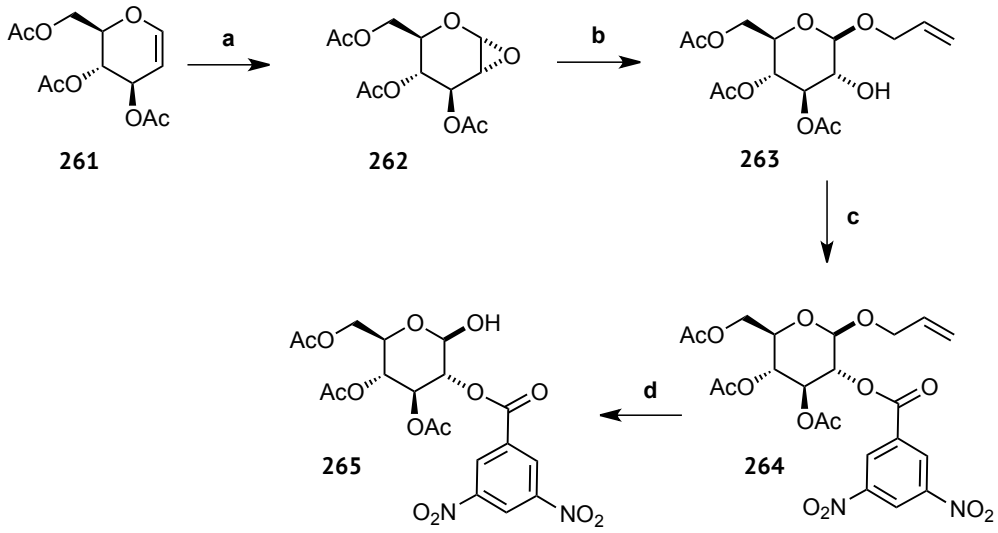
6.3.1 Attempted Reactions with 2,3,4,6-tetra-*O*-Substituted Glucose derivatives

As acyl groups are commonly employed as protecting groups for sugars and are also known to act as leaving groups in NHC-catalysed redox acylation chemistry, the reactions first attempted were with 2,3,4,6-tetra-*O*-acetyl-D-glucopyranose (**258**) with 2-deoxy-3,4,6-tri-*O*-acetyl-D-gluconolactone (**259**) as the intended product.



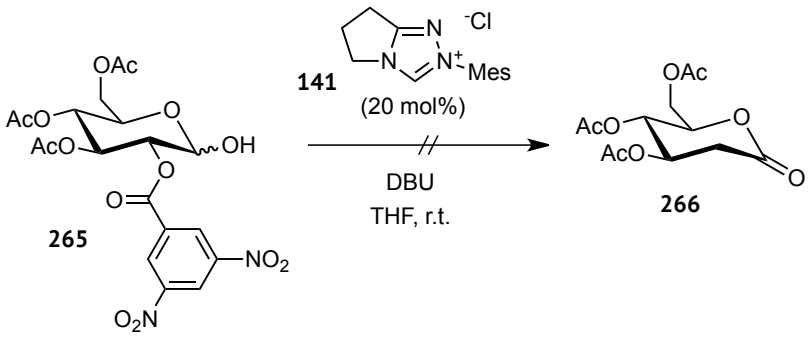
Scheme 88. Attempted NHC-catalysed activation / lactonisation of 2,3,4,6-tetra-*O*-acetyl-D-glucopyranose.

When the reaction was attempted with the *N*-Mes triazolium precatalyst **141** (20 mol%) in acetonitrile with Cs_2CO_3 (Scheme 88), although the starting material was consumed, the only product recoverable was a trace amount of per-acetylated glucose (**260**) (<10% isolated), the remainder of the mass balance was not recoverable. Other bases such as NaH, Et_3N and DBU as well as the *N*-C_6F_5 triazolium precatalyst gave similar results. It was thought that the acetate group might not be sufficient to act as a leaving group in this chemistry so the C–2 group was changed to a 3,5-dinitrobenzoate.



Scheme 89. Synthesis of 3,4,6-tri-*O*-acetyl-2-*O*-(3,5-dinitrobenzoyl)-D-glucose **265**. Reagents and conditions: (a) *m*CPBA (2.5 eq.), KF (5 eq.), DCM, r.t.; (b) allyl alcohol (5 eq.), $ZnCl_2$ 1.0 M in THF (1 eq.), THF, 0 °C – r.t., 48% (2 steps); (c) 3,5-dinitrobenzoyl chloride, Et_3N, DCM, r.t., 80%; (d) $PdCl_2$ (10 mol%), DCM:MeOH (1:1), 47%.

Lactol **265** was synthesised starting from the tri-acetylated glucal **261**. Epoxidation of the glucal was performed using *m*CPBA with KF to precipitate the *m*-chlorobenzoate side-product – previously the *m*-chlorobenzoic acid formed had facilitated ring opening of the epoxide and added into the anomeric position through trapping of the resulting oxocarbenium ion. To install an orthogonally protected hydroxyl at the anomeric position, the epoxide was treated with allyl alcohol with $ZnCl_2$ Lewis acid to give **263**.[288] The remaining unprotected hydroxyl group of **263** was then acylated with 3,5-dinitrobenzoyl chloride and the resulting **264** deprotected at the anomeric position with $PdCl_2$ in 1:1 DCM:MeOH to give the desired **265** (Scheme 89).



Scheme 90. Attempted NHC-catalysed lactonisation with **265**.

When the NHC redox esterification was attempted with **265**, upon combination of the carbene and the carbohydrate substrate, a red precipitate rapidly formed with degradation of the substrate (Scheme 90). The most likely explanation for this and the previous result with the per-acetylated product is that the NHC, if not able to react with the aldehyde form of the

sugars, will perform acyl transfer reactions of the protecting groups *via* acyl azolium intermediates (e.g. Figure 50), leading to scrambling of the acyl groups and a large distribution of possible products.

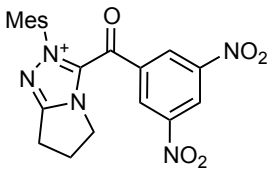
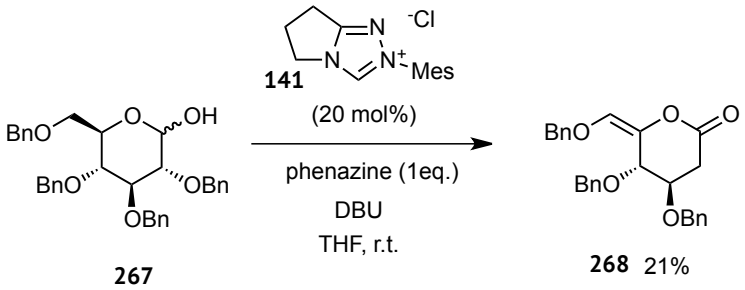


Figure 50. Proposed acyl azolium biproduct.

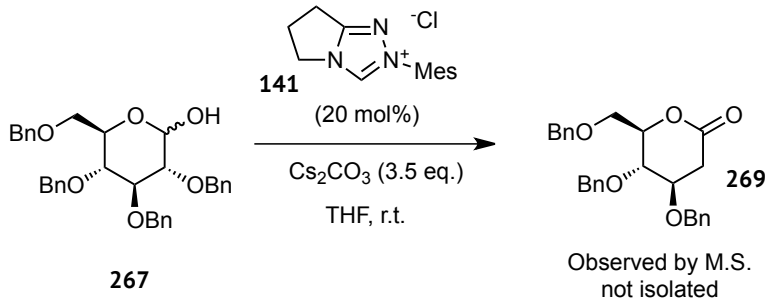
Although it has been shown by Chi that it is possible for NHCs to react with the open-chain carbohydate form, this was under particularly harsh thermal conditions (superheating MeCN to 130 °C).[196] To investigate whether or not it was possible for the NHC to interact with the ring-opened form of the carbohydrate under conditions less likely to degrade the starting material or products, 2,3,4,6-tetra-*O*-benzyl-D-glucopyranose (**267**) was chosen as the next substrate as it lacked the potential for NHC reactivity at the protecting groups. It was expected that this substrate should require the use of an external oxidant to perform the oxidation to the acyl azolium, due to the poor leaving ability of the benzyloxy group, and the expected product in this case was the oxidised form of the sugar, 2,3,4,6-tetra-*O*-benzyl-D-gluconolactone. The initial reaction used phenazine as an external oxidant. With the *N*-C_6F_5 triazolin-2-ylidene, no reaction was observed; however, with the *N*-mesityl triazolin-2-ylidene, it was found unexpectedly that displacement of the C–2 benzyloxy group had occurred, although it was observed that extra oxidation had occurred at the C–5 position resulting in the formation of enol ester **268** upon ring closing (Scheme 91).



Scheme 91. NHC-catalysed reaction of 2,3,4,6-tetra-*O*-benzyl-D-glucose under oxidative conditions.

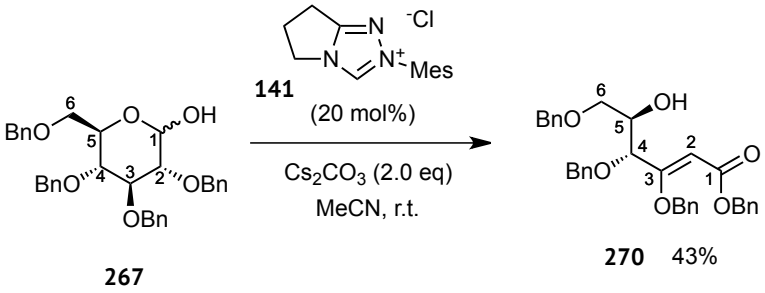
To further investigate this reactivity, the external oxidant was removed to prevent over-oxidation of the product and deliver the originally intended reactivity. It was found that the major product of the reaction did change upon removal of the external oxidant and upon

changing the base to Cs_2CO_3, the desired saturated lactone product **269** was observed by mass spectroscopy but could not be isolated (Scheme 92).



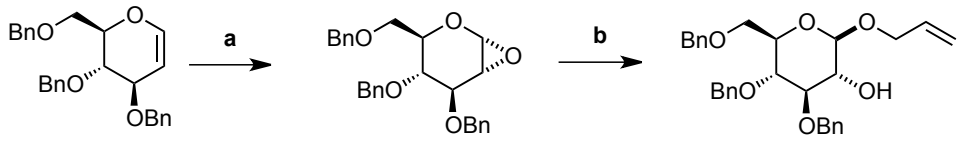
Scheme 92. Reaction of 2,3,4,6-tetra-*O*-benzyl-D-glucose without external oxidant.

Interestingly when the solvent was changed to MeCN, instead of the desired lactone product, the open chain **270** was formed, which intriguingly contained extra, unexpected unsaturation (Scheme 93).



Scheme 93. Formation of ring opened α,β-unsaturated ester product.

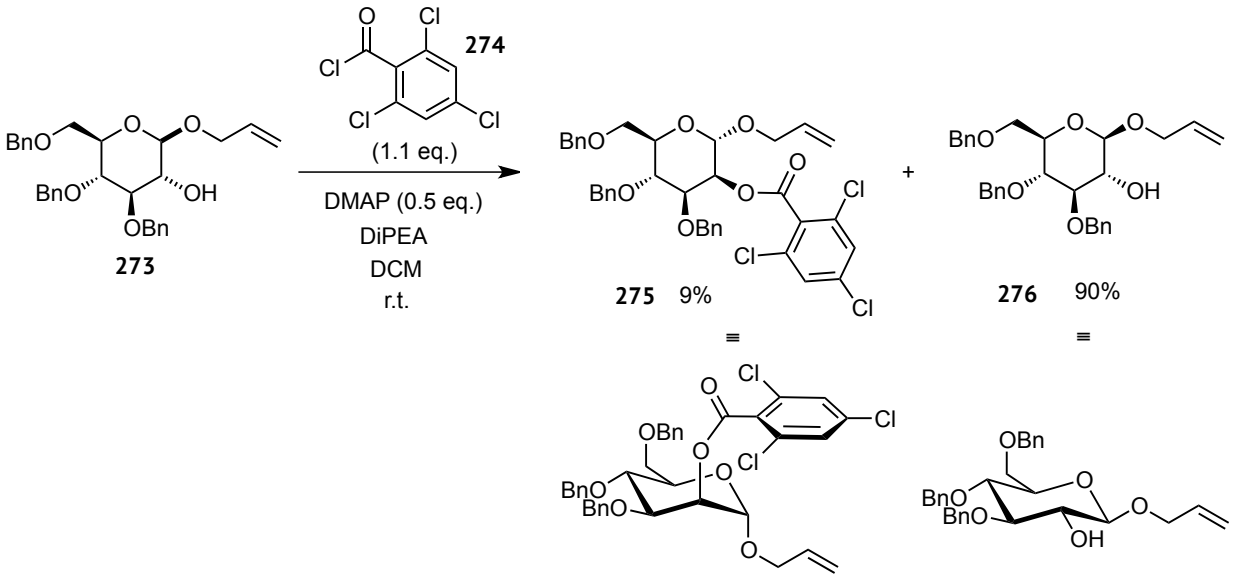
Whilst it was difficult to rationalise the extra oxidative step for this system, which persisted even after precautions to exclude molecular oxygen and other external oxidants were taken, it was proposed that the ring-opening reactivity could be suppressed. Although it was not known whether the lactone was forming initially and then being opened by the displaced benzyloxy group or if the external nucleophile was outcompeting the internal at the acyl azolium intermediate, the solution to overcome this reactivity would be to displace a less nucleophilic leaving group. In the context of internal redox chemistry this would also have been favourable for the elimination step. As most acyl groups were not fit for this purpose, the sterically hindered 2,4,6-trichlorobenzoyl group was chosen to try and prevent nucleophilic attack of the NHC. The synthesis towards this compound was similar to that described above, starting from the tri-*O*-benzyl glucal **271**. After epoxidation and ring opening with allyl alcohol, **273** was obtained as a 9:1 mixture of diastereomers (Scheme 94).



271 272 273

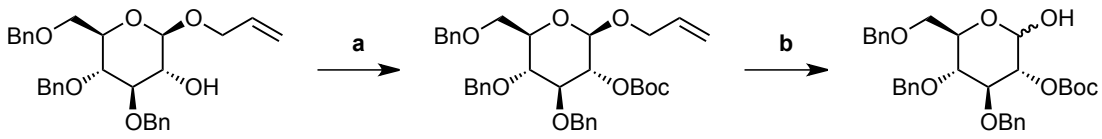
Scheme 94. Epoxidation and ring opening of 3,4,6-tri-*O*-benzyl-D-glucal. Reagents and conditions: (a) *m*CPBA (2.5 eq.), KF (5 eq.), DCM, r.t.; (b) allyl alcohol (5 eq.), $ZnCl_2$ 1.0 M in THF (1 eq.), THF, 0 °C – r.t., 68% (d.r. 9:1, major diastereomer shown) (2 steps).

The acylation of **273** was attempted with 2,4,6-trichlorobenzoyl chloride (**274**) which resulted in the rapid acylation of the minor diastereomer to give **275** with only slight acylation of the major meaning that insufficient product was obtained to be synthetically useful, although this meant it was possible to recover the unreacted diastereomer **276** as essentially a single isomer (Scheme 95).

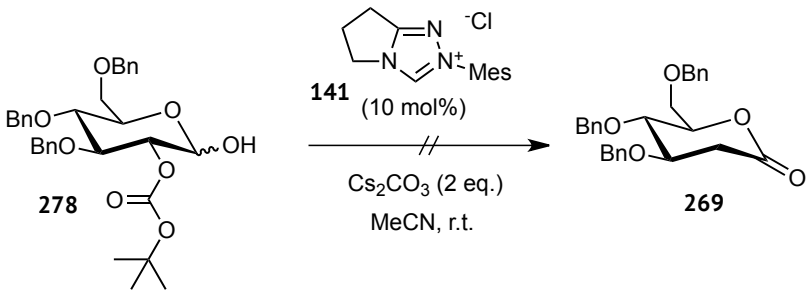


Scheme 95. Attempted acylation of **273** with 2,4,6-trichlorobenzoyl chloride (**274**).

An alternative leaving group investigated was the *tert*-butyloxycarbonyl (Boc) group, installed by treatment of **276** with Boc anhydride followed by the palladium catalysed de-allylation of **277** at the anomeric position, as seen previously (Scheme 89), to give **278** (Scheme 96). When the NHC catalysis reaction was attempted on this substrate only degradation was seen with no indication of the desired product (Scheme 97). This could possibly be the result of using the same harsh conditions required to displace the benzyloxy group, when they may no longer have been required.



Scheme 96. Synthesis of Boc-protected substrate **278**. Reagents and conditions: (a) Boc_2O (1.5 eq.), DMAP (10 mol%), DCM, 96%; (b) $PdCl_2$ (10 mol%), DCM:MeOH (1:1), 42%.



Scheme 97. Attempted reaction of **278** to form lactone **269**.

6.4 Summary of NHC-catalysed Reactions with Carbohydrate Lactol Substrates

This brief investigation of monosaccharide substrates for NHC-catalysed redox chemistry showed some interesting and promising initial results. Due to the subtleties involved in the pK_a balancing for both NHC chemistry and the ring-open–ring-closed equilibria of such carbohydrates, it is very possible that this reaction is viable and should be further explored. With this in mind, it would also be worth screening milder conditions, less prone to substrate degradation, and higher catalyst loadings to increase the probability of the transient open-chain form of the sugar being intercepted by the NHC before ring closure.

7 Conclusions and Future Work (Chapter II)

In this chapter, the use of NHC catalysis with previously unreported substrates has been investigated. It was discovered that, despite previous reports, direct redox amidation is possible using NHCs – it is hoped that this step will open up the possibility to perform kinetic resolution of amines using chiral NHCs. For the formally intramolecular variant of this reactivity it was also found that under the correct conditions, carbamates are suitable leaving groups for NHC-catalysed redox acylation chemistry. Both of these reactions (formally intramolecular and intermolecular) are operationally simple, require minimal reagents (i.e. no additional co-catalyst) and generate low amounts of waste. It was also found that the intermolecular variant proceeded rapidly and at low catalyst loadings (**5.4.3**). Studies will be undertaken to verify the implicated involvement of a carboxylic-carbamic mixed anhydride intermediate in possible side reactions in this chemistry.

The application of this type of chemistry to carbohydrate lactols did show indications of promising reactivity such as the displacement of the C–2 group, oxidation of the C–1 position and formation of esters; however, it was quickly identified that if insufficient aldehyde form of the monosaccharides was available, the NHC reactivity would favour transesterification.

8 Experimental

8.1 General Comments

Reagents obtained from commercial sources and used as received unless otherwise indicated. Reactions requiring anhydrous conditions were conducted in oven-dried glassware and under dried N_2 (Drierite®) or Ar atmosphere, using anhydrous solvents, with solvent and liquid reagent transfers performed under Ar atmosphere using purged needles and syringes. Specified solvents were dried by distillation from CaH_2 (Et_3N), Mg (DCM, MeOH) or Na (PhMe, THF – benzophenone indicator) and stored under dried N_2 atmosphere. Commercially obtained anhydrous solvents were supplied by Sigma Aldrich (EtOH) or Merck (MeCN, DMF) as anhydrous or SeccoSolv® quality respectively and used as received.

Microwave reactions were performed in a CEM Discover® SP single-mode microwave reactor with dynamic control mode.

Melting points were obtained on a Reichert-Thermovar melting point apparatus and are uncorrected.

Infrared spectra were recorded on a Perkin Elmer (Spectrum Express Version 1.03.00) spectrometer with automated background substraction. Reported absorption are strong (s) or medium (m) strength unless stated as weak (w) and given in wavenumbers (cm^{-1}).

^1H NMR spectra were recorded on a Bruker DRX-400 spectrometer operating at 400 MHz. ^{13}C NMR spectra were recorded on a Bruker DRX-400 spectrometer operating at 100 MHz. Chemical shifts (δ) are quoted in units of parts per million (ppm) downfield from tetramethylsilane and are referenced to a residual solvent peak: $CDCl_3$ (δ_H: 7.26, δ_C: 77.2), DMSO-d_6 (δ_H: 2.50, δ_C: 39.5), acetone-d_6 (δ_H: 2.05, δ_C: 206.3, 29.8).[289] Coupling constants (*J*) are quoted in units of Hertz (Hz). The following abbreviations are used to designate multiplicity within ^1H NMR analysis: s = singlet, d = doublet, t = triplet, q = quartet, sext = sextet, sept = septet, m = multiplet, br. = broad signal, app. = apparent (denotes incomplete evidence for stated multiplicity). Unless otherwise stated, NMR spectra were obtained at ambient temperature (293–299 K).

Low and high resolution mass spectrometry (EI, CI, ESI) were recorded by the Imperial College London Department of Chemistry Mass Spectrometry Service using a Micromass Platform II

and Micromass AutoSpec-Q spectrometer. Reported *m/z* values correspond to major ion peak, isotopic ion peaks are included where relevant.

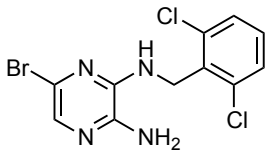
Specific rotation $[\alpha]_D^T$ was recorded on a Perkin-Elmer 241 polarimeter at 589 nm (Na D-line) with a path length of 0.5 dm. Concentrations (c) are quoted in g/100 mL and specific rotations are quoted in units of $deg.dm^{-1}cm^3g^{-1}$ at the indicated temperature (in °C)

All flash column chromatography was carried out on Merck silica gel 60, particle size 0.040–0.063 mm unless otherwise stated. Petroleum ether (PE) used for chromatography refers to the fractions boiling between 40–60 °C. Methanolic ammonia solution (NH_3/MeOH) used for chromatography refers to a 10-fold dilution (MeOH) of a saturated solution prepared by passing gaseous ammonia through ice cold MeOH.

Thin layer chromatography (TLC) was performed on pre-coated glass backed plates (Merck Kieselgel 60 F_{254}), and visualised with ultraviolet light (254 nm). Visualisation using anisaldehyde, ethanolic H_2SO_4, ninhydrin, phosphomolybdic acid (PMA), potassium permanganate ($KMnO_4$) or vanillin stains was performed where deemed appropriate.

8.2 Experimental Procedures – Chapter I

5-Bromo-*N*^{3}-(2,6-dichlorobenzyl)pyrazine-2,3-diamine (5a)[45]



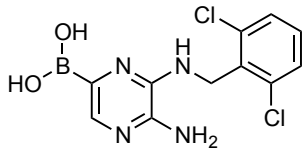
Following the above referenced literature procedure.

2-Amino-3,5-dibromopyrazine (**8**) (500 mg, 0.20 mmol) and 2,6-dichlorobenzylamine (**9**) (380 mg, 0.22 mmol) were placed in a 35 mL microwave vial with EtOH (10 mL) and Hünig's base (380 µL, 0.22 mmol). The reaction mixture was heated by microwave irradiation to 150 °C for 6 h with stirring. The solvent was evaporated and the residue purified *via* flash column chromatography (10% EtOAc in DCM) to yield 360 mg (52%) **5a** as a yellow solid.

R_f 0.15 (EtOAc:DCM, 1:9); IR (neat) 3432, 3348, 3221, 1632, 1504, 1147 cm^{-1}; ^1H NMR (400MHz, $CDCl_3$): δ_H 7.50 (s, 1H, Ar*H*), 7.37 (d, *J* = 8.0 Hz, 2H, Ar*H*), 7.23 (t, *J* = 8.0 Hz, 1H, Ar*H*), 4.89 (d, *J* = 5.4 Hz, 2H, CH_2), 4.53 (t, *J* = 5.4 Hz, 1H, CH_2NH), 4.22 (br. s, 2H, NH_2); ^{13}C NMR (100MHz, $CDCl_3$): δ_C 144.0, 142.1, 136.4, 133.6, 130.7, 129.7, 128.5, 126.4, 41.6; MS (ESI) *m/z*

347 $[M+H]^+$, isotopic *m/z* peaks 347, 349, 351, 353 – splitting corresponds to $^{79/81}Br$ and 2x $^{35/37}Cl$ isotope combinations

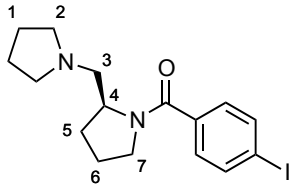
5-Amino-6-(2,6-dichlorobenzylamino)pyrazin-2-ylboronic acid (5b)



5-bromo-*N*^{3}-(2,6-dichlorobenzyl)pyrazine-2,3-diamine (**5a**) (80 mg, 0.23 mmol) was dissolved in 1,4-dioxane (1 mL) in a microwave vial and bis(pinacolato)diboron (60 mg, 0.23 mmol), KOAc (80 mg, 0.8 mmol) and Pd(dppf)Cl_2·DCM (10 mg, 0.01 mmol) were added. The mixture was sparged with N_2 for 10 min then heated by microwave irradiation at 100 °C for 1 h with stirring. The resulting mixture was passed through Celite® with EtOAc (15 mL) as eluant and the organic phase washed was with water (2x 10 mL), then brine (10 mL). The organic layer was dried over $MgSO_4$ and concentrated *in vacuo*. The resultant solid was purified *via* flash column chromatography (10% MeOH in EtOAc) to yield 56 mg (80%) **5b** as a pale brown solid.

R_f 0.2 (MeOH:EtOAc, 1:9); ^1H NMR (400MHz, DMSO-d_6): δ_H 7.66 (s, 1H, Ar*H*), 7.53 (d, *J* = 7.8 Hz, 1H, Ar*H*), 7.52 (br. s, 2H, B(O*H*)$_2$), 7.40 (t, *J* = 7.8 Hz, 1H, Ar*H*), 6.28 (br. s, 2H, N*H*$_2$), 6.13 (t, *J* = 4.1 Hz, 1H, CH_2N*H*), 4.76 (d, *J* = 4.1 Hz, 2H, C*H*$_2$); ^{13}C NMR (100MHz, DMSO-d_6): δ_C 150.9, 145.7, 142.4, 136.8, 136.3, 134.8, 130.6, 129.1, 41.8; MS (ESI) *m/z* 313 $[M+H]^+$, isotopic *m/z* peaks 312, 313, 314, 315, 316, 317 – splitting corresponds to $^{10/11}B$ and 2x $^{35/37}Cl$ isotope combinations.

(*S*)-(4-iodophenyl)(2-(pyrrolidin-1-ylmethyl)pyrrolidin-1-yl)methanone (4a)

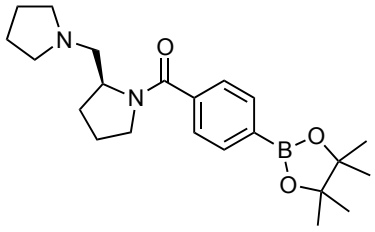


(*S*)-2-(pyrrolidin-1-ylmethyl)pyrrolidine **6** (250 mg, 1.6 mmol) and *p*-iodobenzoyl chloride **7** (432 mg, 1.6 mmol) were dissolved in DCM (8 mL). Et_3N (248 µL, 1.8 mmol) was added and the reaction mixture was stirred at room temperature for 4 h. Et_3N·HCl precipitated as a white solid and was filtered off. The filtrate was diluted with DCM (10 mL) and washed with water (2x 20 mL) and brine (1x 20 mL). The organic layer was concentrated *in vacuo* and loaded

onto silica for purification via flash column chromatography (5% NH_3/MeOH in DCM) to yield 530 mg (86%) **4a** as a colourless oil.

R_f 0.2 (NH_3/MeOH:DCM, 1:19); $[\alpha]_D^{25}$ −74.6 (*c* 1.00, $CHCl_3$); IR (neat) 2969, 2877, 2791, 1618, 1586, 1409 cm^{-1}; ^1H NMR (400MHz, DMSO-d_6, 373 K): δ_H 7.78 (d, *J* = 8.0 Hz, 2H, Ar*H*), 7.24 (d, *J* = 8.0 Hz, 2H, Ar*H*), 4.13 (br. s, 1H, C*H*–4), 3.41 (m, 2H, CH_2–7), 2.50 (m, 4H, 2x CH_2–2), 2.38 (br. s, 2H, CH_2–3), 2.05–1.69 (m, 4H, CH_2–5 & CH_2–6), 1.63 (m, 4H, 2x CH_2–1); ^{13}C NMR (100MHz, DMSO-d_6, 373K): δ_C 167.3, 136.8, 136.5, 128.3, 94.8, 57.6, 56.3, 53.5, 47.2, 28.2, 22.9, 22.7; MS (ESI) *m/z* 385 $[M+H]^+$.

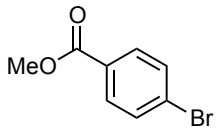
(*S*)-(2-(pyrrolidin-1-ylmethyl)pyrrolidin-1-yl)(4-(4,4,5,5-tetramethyl-1,3,2-dioxaborolan-2-yl)phenyl)methanone (4b)



(*S*)-(4-iodophenyl)(2-(pyrrolidin-1-ylmethyl)pyrrolidin-1-yl)methanone (**4a**) (515 mg, 1.34 mmol) was dissolved in 1,4-dioxane (5 mL) in a microwave vial and bis(pinacolato)diboron (340 mg, 1.34 mmol), KOAc (461 mg, 4.7 mmol) and Pd(dppf)Cl_2·DCM (55 mg, 0.07 mmol) were added. The mixture was sparged with N_2 for 10 min then heated by microwave irradiation at 120 °C for 1 h with stirring. The resulting mixture was passed through Celite® with EtOAc (70 mL) as eluant. The organic phase washed with water (2x 50 mL), then brine (2x 50 mL). The organic layer was dried over $MgSO_4$ and concentrated by rotary evaporation to yield 440 mg (86%) **4b** as a pale brown solid, which was used without further purification.

^1H NMR (400 MHz, $CDCl_3$) δ_H 7.84 (d, *J* = 7.6 Hz, 2H, Ar*H*), 7.49 (d, *J* = 7.6 Hz, 2H, Ar*H*), 4.43 (s, 1H, C*H*NC=O), 3.72–3.20 (m, 2H, CH_2NC=O), 3.12–2.74 (m, 6H, pyrrolidin. CH_2N), 2.54–1.55 (m, 8H, pyrrolidin. CH_2), 1.36 (s, 12H, 2x C(CH_3)$_2$); MS (ESI) *m/z* 385 $[M+H]^+$, ^{10}B isotope peak *m/z* 384.

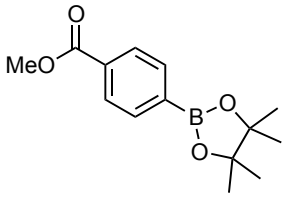
Methyl 4-bromobenzoate (12)[290]



4-Bromobenzoic acid (**11**) (800 mg, 3.98 mmol) was dissolved in PhMe:MeOH 1:1 (18 mL and 2.0 M $TMSCHN_2$ in *n*-hexane (2.0 mL, 4.0 mmol) was added. The mixture was stirred at r.t. for 12 h. The resulting mixture was quenched with AcOH dropwise until no yellow colour remained. The solvent was removed *in vacuo* and the residue dissolved in Et_2O (70 mL). The organic solution was washed with water (2x 50 mL) and brine (50 mL), dried over $MgSO_4$ and concentrated *in vacuo* to yield 730 mg (85%) **12** as a white solid.

^1H NMR (400 MHz, $CDCl_3$) δ_H 7.93 (d, *J* = 8.6 Hz, 2H, Ar*H*), 7.61 (d, *J* = 8.6 Hz, 2H, Ar*H*), 3.94 (s, 3H, OCH_3); MS (EI) *m/z* 214 $[M]^+$, ^{81}Br isotope peak *m/z* 216.

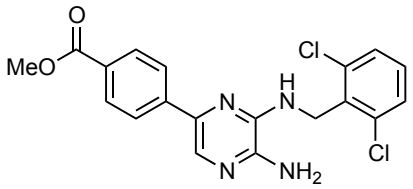
Methyl 4-(4,4,5,5-tetramethyl-1,3,2-dioxaborolan-2-yl)benzoate (13)[291]



Methyl 4-bromobenzoate (**12**) (580 mg, 2.7 mmol) was dissolved in 1,4-dioxane (7 mL) in a microwave vial and bis(pinacolato)diboron (750 mg, 3.0 mmol), KOAc (930 mg, 9.4 mmol) and Pd(dppf)Cl_2·DCM (110 mg, 0.13 mmol) were added. The mixture was sparged with N_2 for 10 min before being heated by microwave irradiation at 120 °C for 1 h with stirring. The resulting mixture was passed through Celite® with EtOAc (25 mL) as eluant. The organic phase washed with water (2x 20 mL), then brine (20 mL). The organic layer was dried over $MgSO_4$ and concentrated *in vacuo* to yield 520 mg (73%) of the crude product **13** as a tan solid.

^1H NMR (400MHz, $CDCl_3$): δ_H 8.05 (d, *J* = 7.9 Hz, 2H, Ar*H*), 7.90 (d, *J* = 7.8 Hz, 2H, Ar*H*), 3.95 (s, 2H, OCH_3), 1.39 (s, 12H, 2x C(CH_3)$_2$).

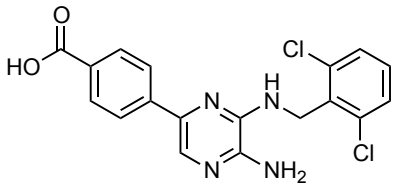
Methyl 4-(5-amino-6-(2,6-dichlorobenzylamino)pyrazin-2yl)benzoate (14)



Methyl 4-(4,4,5,5-tetramethyl-1,3,2-dioxaborolan-2-yl)benzoate (**13**) (260 mg, 0.99 mmol) and 5-bromo-N^3-(2,6-dichlorobenzyl)pyrazine-2,3-diamine (**5a**) (348 mg, 0.99 mmol) were dissolved in 1,4-dioxane (4 mL) and 2 M $Na_2CO_{3(aq)}$ (1.25 mL, 2.48 mmol), $Pd(OAc)_2$ (22 mg, 0.1 mmol) and PPh_3 (80 mg, 0.3 mmol) were added. The mixture was sparged with N_2 for 10 min before being heated in a sealed tube at 80 °C for 18 h with stirring. The resulting mixture was passed through Celite® with EtOAc (15 mL) as eluant. The organic phase washed with water (2x 10 mL), then brine (10 mL). The organic layer was dried over $MgSO_4$ and concentrated *in vacuo*, then purified *via* flash column chromatography (50% EtOAc in PE) to yield 240 mg (60%) **14** as a yellow brown solid.

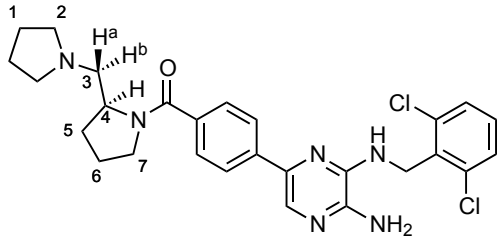
R_f 0.25 (EtOAc:PE, 1:1); ^{1}H NMR (400MHz, $CDCl_3$): δ_H 8.14 (d, *J* = 8.6 Hz, 2H, Ar*H*), 8.04 (d, *J* = 8.6 Hz, 2H Ar*H*), 8.01 (s, 1H, Ar*H*), 7.36 (d, *J* = 8.0 Hz, 2H, Ar*H*), 7.21 (t, *J* = 8.0 Hz, 1H, Ar*H*), 5.06 (d, *J* = 5.4 Hz, 1H, CH_2N), 4.59 (br. t, *J* = 5.4 Hz, 1H, CH_2N*H*), 4.45 (br. s, 2H, NH_2), 3.97 (s, 3H, OCH_3).

4-(5-Amino-6-((2,6-dichlorobenzyl)amino)pyrazin-2-yl)benzoic acid (10)



Methyl 4-(5-amino-6-(2,6-dichlorobenzylamino)pyrazin-2yl)benzoate (**14**) (110 mg, 0.27 mmol) was dissolved in THF:H_2O 1:1 (5 mL) and LiOH·:H_2O (60 mg, 1.37 mmol) was added. The reaction mixture was stirred for 14 h at r.t., then the pH of the solution was adjusted to pH <7 using 0.1 M $HCl_{(aq)}$. The reaction suspension was filtered under vacuum and the solid obtained was triturated with EtOAc. The white precipitate of **10** (100 mg) was isolated by vacuum filtration and used directly in the subsequent step.

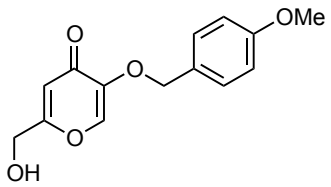
(*S*)-(4-(5-Amino-6-(2,6-dichlorobenzylamino)pyrazin-2-yl)phenyl)(2-(pyrrolidin-1-ylmethyl)pyrrolidin-1-yl)methanone (1)[43]



4-(5-Amino-6-(2,6-dichlorobenzylamino)pyrazin-2yl)benzoic acid (**10**) (100 mg, 0.26 mmol) was suspended in DCM (1 mL). Bispyrrolidine **6** (40 mg, 0.26 mmol) and EDCI (50 mg, 0.26mmol) were added and the mixture was stirred at r.t. for 12 h, by which time a homogeneous solution had formed. The resulting mixture was diluted with DCM (15 mL) and the organic phase washed with brine (3x 20 mL). The organic layer was dried over $MgSO_4$ and the solvent removed *in vacuo*. The resulting residue was purified *via* flash column chromatography (10% NH_3/MeOH in EtOAc) to yield 60 mg (44%) **1** as an off-white foam.

R_f 0.2 (NH_3/MeOH:EtOAc, 1:9); ^{1}H NMR (400MHz, $CDCl_3$): δ_H 8.02 (d, *J* = 8.3 Hz, 2H, Ar*H*), 7.93 (s, 1H, Ar*H*), 7.57 (br. m, 2H, Ar*H*), 7.34 (d, *J* = 8.0 Hz, 2H, Ar*H*), 7.19 (t, *J* = 8.0 Hz, 1H, Ar*H*), 5.04 (d, *J* = 5.3 Hz, 2H, CH_2N), 4.90 (br. t, *J* = 5.3 Hz, 1H, CH_2N*H*), 4.65 (br. s, 2H, NH_2), 4.45 (br. s, 1H, C*H*–4), 3.54 (br. s, 2H, CH_2–7), 2.96 (br. s, *J* = 11.7 Hz, 1H, C*H*–3b), 2.72 (br. m, 5H, 2x CH_2–2 & C*H*–3a), 2.20–1.95 (br. m, 2H, CH_2–5), 1.90–1.50 (br. m, 6H, 2x CH_2–1 & CH_2–6); ^{13}C NMR (100MHz, $CDCl_3$): δ_C 170.1, 143.2, 143.1, 139.7, 136.4, 134.5, 129.5, 128.5, 127.7, 127.1, 125.4, 58.7, 56.7, 54.7, 50.3, 41.3, 29.5, 23.6, 22.6; HRMS (ESI) calcd. for $C_{27}H_{31}{}^{35}Cl_2N_6O$ $[M+H]^+$: 525.1936; found *m/z*: 525.1914.

2-(Hydroxymethyl)-5-(4-methoxybenzyloxy)-4*H*-pyran-4-one (16)[292]



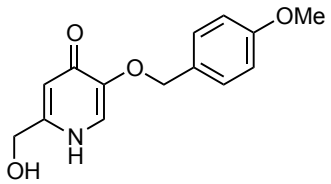
Following the above referenced literature procedure.

Kojic acid (**15**) (500 mg, 3.5 mmol) and 4-methoxybenzyl chloride (525 µL, 3.9 mmol) were dissolved in DMF (3 mL) and K_2CO_3 (970 mg, 7 mmol) was added. The reaction mixture was stirred at 80 °C for 1.5 h. The mixture was cooled to r.t. and water (30 mL) added. The

aqueous phase was extracted with DCM (3x 20 mL). The organics were combined and dried over $MgSO_4$ and the solvent removed *in vacuo*. The dark brown residue was cooled to 0 °C and $CHCl_3$ (20 mL) added to precipitate a light yellow solid, which was collected *via* vacuum filtration. The solid was then washed with cold $CHCl_3$ and further dried *in vacuo* to yield 700 mg (76%) 2-(hydroxymethyl)-5-(4-methoxybenzyloxy)-4*H*-pyran-4-one **16** as a yellow powder.

^{1}H NMR (400MHz, DMSO-d_6): δ_H 8.16 (s, 1H, Ar*H*), 7.35 (d, *J* = 8.6 Hz, 2H, Ar*H*), 6.95 (d, *J* = 8.6 Hz, 2H, Ar*H*), 6.33 (s, 1H, Ar*H*), 5.71 (t, *J* = 6.1 Hz, 1H, CH_2O*H*), 4.87 (s, 2H, OCH_2), 4.31 (d, *J* = 6.1 Hz, 2H, CH_2OH), 3.77 (s, 3H, OCH_3); ^{13}C NMR (100MHz, DMSO-d_6): δ_C 173.7, 168.5, 159.7, 147.0, 141.6, 130.5, 128.5, 114.3, 111.6, 70.7, 59.8, 55.6; MS (ESI) *m/z* 326 $[M+MeCN+Na]^+$.

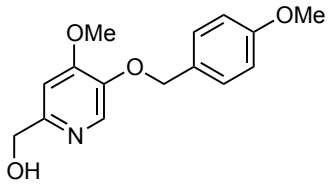
2-(Hydroxymethyl)-5-((4-methoxybenzyl)oxy)-4(1*H*)-pyridone (17)[51]



Pyranone **16** (650 mg, 2.5 mmol) was dissolved in EtOH (1.5 mL) and conc. $NH_4OH_{(aq)}$ (4.6 mL) was added. The reaction mixture was heated to 100 °C in a sealed tube for 6 h, during which time the product formed a grey precipitate. The solid was collected via vacuum filtration, washed with cold water then cold EtOH before being further dried *in vacuo* to yield 460 mg (70%) **17** as a grey powder.

IR (neat) 3149, 2846, 1615, 1517 cm^{-1}; ^{1}H NMR (400MHz, DMSO-d_6): δ_H 11.1 (s, 1H, N*H*), 7.35 (br. s, 1H, Ar*H*) 7.33 (d, *J* = 8.6 Hz, 2H, Ar*H*), 6.93 (d, *J* = 8.6 Hz, 2H, Ar*H*), 6.18 (br. s, 1H, Ar*H*), 5.56 (br. s, 1H, CH_2O*H*), 4.93 (s, 2H, OCH_2), 4.34 (s, 2H, CH_2OH), 3.76 (s, 3H, OCH_3); MS (ESI) *m/z* 262 $[M+H]^+$.

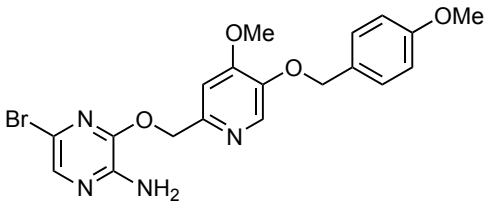
(4-Methoxy-5-(4-methoxybenzyloxy)pyridin-2-yl)methanol (18)[43]



Pyridone **17** (600 mg, 2.3 mmol) was suspended in 1:1 MeOH:PhMe (9 mL) and 2.0 M $TMSCHN_2$ in *n*-hexane (1.15 mL, 2.3 mmol) was added. The mixture was stirred at r.t. for 32 h, then quenched with AcOH. The unreacted starting material **17** was removed by filtration and the filtrate was concentrated *in vacuo*. The residue was dissolved in EtOAc (30 mL) and washed with water (3x 20 mL). The organic layer was dried over $MgSO_4$ and the solvent removed *in vacuo*. The resulting residue was purified *via* flash column chromatography (100% EtOAc) to yield 240 mg (38%) **18** as a white solid.

R_f 0.2 (EtOAc); IR (neat) 3184, 1617 (w), 1596, 1515 cm^{-1}; ^1H NMR (400MHz, DMSO-d_6): δ_H 8.08 (s, 1H, Ar*H*), 7.36 (d, *J* = 8.6 Hz, 2H, Ar*H*), 7.08 (s, 1H, Ar*H*), 6.94 (d, *J* = 8.6 Hz, 2H, Ar*H*), 5.32 (t, *J* = 5.7 Hz, 1H, CH_2O*H*), 5.04 (s, 2H, OCH_2), 4.45 (d, *J* = 5.7 Hz, 2H, CH_2OH), 3.84 (s, 3H, OCH_3), 3.76 (s, 3H, OCH_3); ^{13}C NMR (100MHz, DMSO-d_6): δ_C 159.6, 157.0, 156.2, 143.4, 135.4, 130.2, 129.2, 114.2, 104.3, 71.1, 64.6, 55.8, 55.6; MS (ESI) *m/z* 276 $[M+H]^+$.

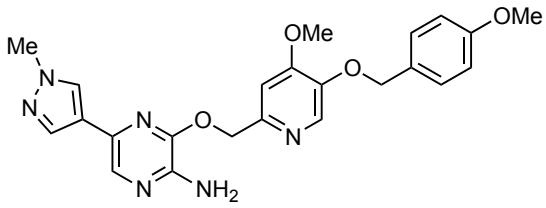
5-Bromo-3-(4-methoxy-5-(4-methoxybenzyloxy)pyridin-2-yl)methoxy)pyrazin-2-amine (19)[43]



2-Amino-3,5-dibromopyrazine (**8**) (172 mg, 0.63 mmol) and alcohol **18** (220 mg, 0.63 mmol) were dissolved in THF (2.5 mL). 2 M KO*t*Bu in THF (0.5 mL, 1.25 mmol) was added with stirring. The reaction mixture was heated to 60 °C for 12 h with stirring, then returned to room temperature, diluted with EtOAc (50 mL) and washed with water (3x 20 mL). The organic layer was dried over $MgSO_4$ and concentrated *in vacuo*. The residue was purified *via* flash column chromatography (50% EtOAc in DCM) to yield 195 mg (69%) **19** as an amorphous yellow solid.

R_f 0.25 (EtOAc:DCM, 1:1); ^{1}H NMR (400MHz, $CDCl_3$): δ_H 8.18 (s, 1H, Ar*H*), 7.68 (s, 1H, Ar*H*), 7.38 (d, *J* = 8.6 Hz, 2H, Ar*H*), 7.12 (s, 1H, Ar*H*), 6.92 (d, *J* = 8.6 Hz, 2H, Ar*H*), 5.43 (s, 2H, OCH_2), 5.14 (s, 2H, OCH_2), 4.92 (br. s, 2H, NH_2), 3.96 (s, 3H, OCH_3), 3.83 (s, 3H, OCH_3); ^{13}C NMR (100MHz, $CDCl_3$): δ_C 159.7, 156.1, 149.7, 146.7, 144.5, 144.2, 135.7, 134.9, 129.4, 128.2, 120.6, 114.1, 107.4, 71.7, 69.7, 55.9, 55.3; MS (ESI) *m/z* 447 $[M+H]^+$, ^{81}Br isotope peak *m/z* 449; HRMS (ESI) calcd. for $C_{19}H_{20}{}^{79}BrN_4O_4$ $[M+H]^+$: 447.0668; found *m/z*: 447.0660.

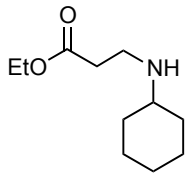
3-((4-Methoxy-5-(4-methoxybenzyloxy)pyridin-2-yl)methoxy)-5-(1-methyl-1*H*-pyrazol-4-yl)pyrazin-2-amine (2)[43]



Bromopyrazine **19** (150 mg, 0.34 mmol) and 1-methylpyrazole-4-boronic acid pinacol ester (**20**) (77 mg, 0.37 mmol) were dissolved in DME (1.5 mL). $Pd(PPh_3)_2Cl_2$ (24 mg, 0.03 mmol) and 2 M $Na_2CO_{3\,(aq)}$ (335 µL, 0.67 mmol) were added and the reaction mixture was sparged with N_2 for 10 min before being heated at 80 °C for 48 h. The mixture was cooled to r.t., passed through Celite® with EtOAc (15 mL) as eluant. The organic phase washed with brine (3x 10 mL). The organic layer was dried over $MgSO_4$, concentrated *in vacuo* and purified *via* flash column chromatography (50% acetone in EtOAc) to yield 5.4 mg (4%) of **2** as a yellow film.

R_f 0.25 (Acetone:EtOAc, 1:1); IR (neat) 3335, 3190, 1515 cm^{-1}; ^{1}H NMR (400MHz, $CDCl_3$): δ_H 8.17 (s, 1H, Ar*H*), 7.86 (s, 1H, Ar*H*), 7.82 (s, 1H, Ar*H*), 7.73 (s, 1H, Ar*H*), 7.40 (d, *J* = 8.6 Hz, 2H, Ar*H*), 7.05 (s, 1H, Ar*H*), 6.92 (d, *J* = 8.6 Hz, 2H, Ar*H*), 5.51 (s, 2H, CH_2O), 5.14 (s, 2H, CH_2O), 4.81 (br. d, 2H, NH_2), 3.95 (s, 3H, CH_3), 3.91 (s, 3H, CH_3), 3.83 (s, 3H, CH_3); ^{13}C NMR (100MHz, $CDCl_3$): δ_C 159.7, 156.3, 151.2, 147.5, 144.3, 143.2, 136.4, 135.8, 134.9, 133.3, 129.4, 129.2, 128.3, 127.3, 114.1, 105.8, 71.7, 68.7, 55.8, 55.3, 39.1; MS (ESI) *m/z* 449 $[M+H]^+$.

Ethyl 3-(cyclohexylamino)propanoate (21)[293]

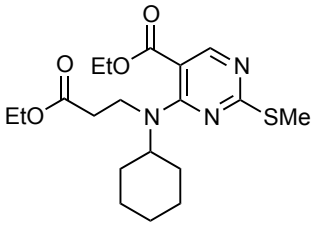


Following the above referenced literature procedure.

β-Alanine ethyl ester hydrochloride (6 g, 39 mmol) and cyclohexanone (4.1 mL, 39 mmol) were dissolved in a 3:2 mixture of DCM:MeOH (75 mL) and NaOH (780 mg, 20 mmol) and $NaB(OAc)_3H$ (9.3 g, 45 mmol) were added. The mixture was stirred at r.t. for 6 h before sat. $NaHCO_{3(aq)}$ (75 mL) was added. The resulting mixture was extracted with EtOAc (3x 50 mL) and the combined organic phases were dried over $MgSO_4$, concentrated *in vacuo*, then purified *via* flash column chromatography (50% EtOAc in PE) to yield 7.3 g (94%) **21**.

R_f 0.2 (EtOAc:PE, 1:1); ^{1}H NMR (400MHz, $CDCl_3$): δ_H 4.17 (q, *J* = 7.1 Hz, 2H, CH_3CH_2O), 3.47 (tt, *J* = 10.4, 3.8 Hz, 1H NCH_{ax}), 2.93 (t, *J* = 6.6 Hz, 2H, EtO_2CCH_2), 2.54 (t, *J* = 6.6 Hz, 2H, CH_2CH_2N), 1.91 (m, 2H, CH_{eq}), 1.75 (m, 2H, CH_{eq}), 1.70 (br. s, 1H, N*H*), 1.64 (m, 1H, CH_{eq}), 1.33 (t, *J* = 7.1 Hz, 3H, CH_3CH_2O), 1.36–1.20 (m, 2H, CH_{ax}), 1.19 (app. tt, *J* = 12.0, 3.0 Hz, 1H, CH_{ax}), 1.15–0.98 (m, 2H, CH_{ax}).

Ethyl 4-(cyclohexyl(3-ethoxy-3-oxopropyl)amino)-2-(methylthio)pyrimidine-5-carboxylate (23)[294]



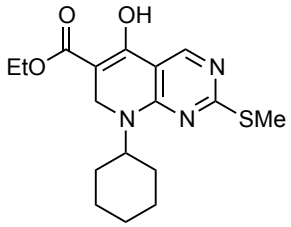
Following the above referenced literature procedure.

Ethyl 4-chloro-2-(methylthio)pyrimidine-5-carboxylate (**22**) (7.3 g, 31 mmol) and ethyl 3-(cyclohexylamino)propanoate (**21**) (6.2 g, 31 mmol) were dissolved in DCM (90 mL) and Hünig's base (5.5 mL, 31 mmol) was added. The reaction mixture was stirred at r.t. for 16 h then partitioned with the addition of 100 mL water. The organic layer was further washed with water (2x 50 mL) and brine (50 mL) then dried over Mg_2SO_4. The solvent was removed *in*

vacuo and the residue purified *via* flash column chromatography (100% DCM) to yield 12.0 g (95%) **23** as a pale yellow oil.

R_f 0.35 (DCM); ^{1}H NMR (400MHz, $CDCl_3$): δ_H 8.43 (s, 1H, Ar*H*), 4.34 (q, *J* = 7.1 Hz, 2H, CH_3CH_2O), 4.17 (q, *J* = 7.1 Hz, 2H, CH_3CH_2O), 3.81 (t, *J* = 7.8 Hz, 2H, EtO_2CCH_2), 3.48 (m, 1H, cyclohex. NC*H*), 2.70 (t, *J* = 7.8 Hz, 2H, CH_2CH_2N), 2.52 (s, 3H, SCH_3), 1.86 (m, 4H, cyclohex. C*H*), 1.67 (m, 1H, cyclohex. C*H*), 1.56 (m, 2H, cyclohex. C*H*), 1.39 (t, *J* = 7.1 Hz, 3H, CH_3CH_2O), 1.28 (t, *J* = 7.1 Hz, 3H, CH_3CH_2O), 1.34–1.05 (m, 3H cyclohex. C*H*). HRMS (ESI) calcd. for $C_{19}H_{30}N_3O_4S$ $[M+H]^+$: 396.1957; found *m/z*: 396.1955.

Ethyl 8-cyclohexyl-5-hydroxy-2-(methylthio)-7,8-dihydropyrido[2,3-*d*]pyrimidine-6-carboxylate (24)[294]

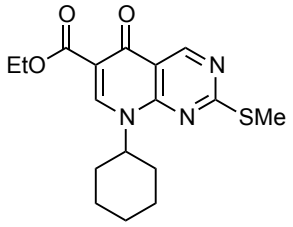


Following the above referenced literature procedure.

Ethyl 4-(cyclohexyl(3-ethoxy-3-oxopropyl)amino)-2-(methylthio)pyrimidine-5-carboxylate (**23**) (5.0 g, 12.6 mmol) was dissolved in toluene (50 mL) and 1.0 M KO*t*-Bu in THF (15 mL) was added, then the reaction mixture was heated 90 °C for 0.5 h. The reaction mixture was then cooled to room temperature and a yellow precipate formed which was isolated by vacuum filtration to yield 2.0 g (45%) **24** as a yellow powder.

^{1}H NMR (400MHz, $CDCl_3$): δ_H 11.82 (s, 1H, O*H*), 8.11 (s, 1H, Ar*H*), 4.70 (m, 1H, cyclohex. NC*H*), 4.47 (s, 2H, CH_2N), 4.33 (q, *J* = 7.1 Hz, 2H, CH_3CH_2O), 2.65 (s, 3H, SCH_3), 2.06–1.88 (m, 2H, cyclohex. C*H*), 1.86–1.73 (m, 3H, cyclohex. C*H*), 1.62 (m, 2H, cyclohex. C*H*), 1.47–1.32 (m, 2H, cyclohex. C*H*), 1.36 (t, *J* = 7.1 Hz, 3H, CH_3CH_2O), 1.29–1.12 (m, 1H, cyclohex. C*H*). HRMS (ESI) calcd. for $C_{17}H_{24}N_3O_3S$ $[M+H]^+$: 350.1538; found *m/z*: 350.1546.

Ethyl 8-cyclohexyl-2-(methylthio)-5-oxo-5,8-dihydropyrido[2,3-*d*]pyrimidine-6-carboxylate (25)[294]

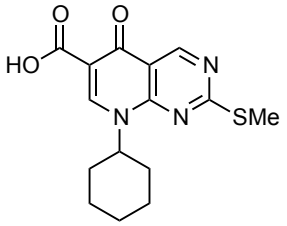


Following the above referenced literature procedure.

8-Cyclohexyl-5-hydroxy-2-(methylthio)-7,8-dihydropyrido[2,3-*d*]pyrimidine-6-carboxylic acid ethyl ester (**24**) (2 g, 5.7 mmol) was dissolved in DCM (60 mL) and Br_2 (0.3 mL, 5.8 mmol) was added. The reaction mixture was stirred at r.t. for 0.5 h. The reaction mixture was then concentrated and re-dissolved in DCM (60 mL) before Hünig's base (1.2 mL, 7 mmol) was added and the solution stirred at r.t. for 15 h. The organic layer was partitioned with water (50 mL) and then washed with brine (2x 50 mL). The organic layer was dried over $MgSO_4$, the solvent removed *in vacuo* and the crude off-white solid obtained was purified by flash column chromatography (25–50% EtOAc in pentane) to yield 1.2 g (60%) **25** as a white solid.

R_f 0.4 (EtOAc:Pentane, 1:1); ^{1}H NMR (400MHz, $CDCl_3$): δ_H 9.43 (s, 1H, Ar*H*), 8.63 (s, 1H, Ar*H*), 5.25 (m, 1H, cyclohex. NC*H*), 4.43 (q, *J* = 7.2 Hz, 2H, CH_3CH_2O), 2.67 (s, 3H, SCH_3), 2.06 (m, 4H, cyclohex. C*H*), 1.86 (m, 1H, cyclohex. C*H*), 1.74 (m, 2H, cyclohex. C*H*), 1.57 (m, 2H, cyclohex. C*H*), 1.42 (t, *J* = 7.2 Hz, 3H, CH_3CH_2O), 1.37 (m, 1H, cyclohex. C*H*); HRMS (ESI) calcd. for $C_{17}H_{22}N_3O_3S$ $[M+H]^+$: 348.1382; found *m/z*: 348.1398.

8-cyclohexyl-2-(methylthio)-5-oxo-5,8-dihydropyrido[2,3-*d*]pyrimidine-6-carboxylic acid (26)

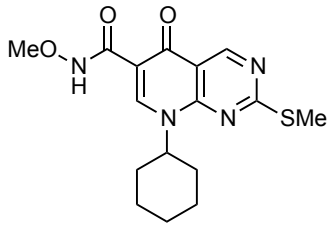


Ethyl 8-cyclohexyl-2-(methylthio)-5-oxo-5,8-dihydropyrido[2,3-*d*]pyrimidine-6-carboxylate (**25**) (1.2 g, 3.5 mmol) was dissolved in 1,4-dioxane (15 mL) and 1 M $HCl_{(aq)}$ (12 mL) was added. The mixture was heated to 105 °C by microwave irradiation for 4 h with stirring. The mixture was returned to r.t. and the product started to crystallise. The mixture was then

further cooled to 0 °C, filtered and washed with cold water to yield 850 mg (72%) **26** as tan crystals.

^{1}H NMR (400MHz, DMSO-d_6): δ_H 14.28 (s, 1H, CO_2H), 9.40 (s, 1H, Ar*H*), 8.93 (s, 1H, Ar*H*), 5.23 (m, 1H, cyclohex. NC*H*), 2.67 (s, 3H, SCH_3), 1.98 (m, 2H, cyclohex. C*H*), 1.91 (m, 4H, cyclohex. C*H*), 1.68 (m, 1H, cyclohex. C*H*), 1.56–1.39 (m, 2H, cyclohex. C*H*), 1.31 (m, 1H, cyclohex. C*H*); HRMS (ESI) calcd. for $C_{15}H_{18}N_3O_3S$ $[M+H]^+$: 320.1069; found *m/z*: 320.1072.

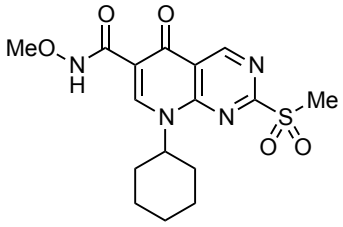
8-cyclohexyl-*N*-methoxy-2-(methylthio)-5-oxo-5,8-dihydropyrido[2,3-*d*]pyrimidine-6-carboxamide (27)[44]



8-Cyclohexyl-2-(methylthio)-5-oxo-5,8-dihydropyrido[2,3-*d*]pyrimidine-6-carboxylic acid (**26**) (500 mg, 1.6 mmol) was suspended in DCM (20 mL). Oxalyl chloride (150 µL, 1.7 mmol), Et_3N (750 µL, 5.5 mmol) and cat. DMF (10 µL) were added and the reaction mixture stirred at r.t. for 1 h. $MeONH_2$·HCl (160 mg, 1.88 mmol) was added and the reaction mixture stirred at r.t. for 2 h. DCM (30 mL) was added and the organic phase was washed with 1 M $HCl_{(aq)}$ (50 mL), water (50 mL) and brine (50 mL). The solvent was removed *in vacuo* to give 530 mg (97%) **27** as a yellow solid.

^{1}H NMR (400MHz, DMSO-d_6): δ_H 11.81 (s, 1H, MeONH), 9.30 (s, 1H, Ar*H*), 8.81 (s, 1H, Ar*H*), 5.16 (m, 1H, cyclohex. NC*H*), 3.75 (s, 3H, CH_3ON), 2.66 (s, 3H, SCH_3), 2.07–1.74 (m, 6H, cyclohex. C*H*), 1.76–1.59 (m, 1H, cyclohex. C*H*), 1.58–1.41 (m, 2H, cyclohex. C*H*), 1.40–1.26 (m, 1H, cyclohex. C*H*); HRMS (ESI) calcd. for $C_{16}H_{21}N_4O_3S$ $[M+H]^+$: 349.1334; found *m/z*: 349.1350.

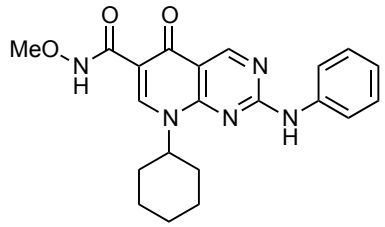
8-cyclohexyl-*N*-methoxy-2-(methylsulfonyl)-5-oxo-5,8-dihydropyrido[2,3-*d*]pyrimidine-6-carboxamide (28)[44]



8-Cyclohexyl-*N*-methoxy-2-(methylthio)-5-oxo-5,8-dihydropyrido[2,3-*d*]pyrimidine-6-carboxamide (**27**) (250 mg, 0.72 mmol) was dissolved in DCM (15 mL). *m*CPBA (≤77% purity, 400 mg, 1.8 mmol) was added at 0 °C and the reaction mixture stirred for 1 h before being warmed to r.t. and stirred for a further 4 h. 10% $NaHSO_{3(aq)}$ (30 mL) was added and the biphasic solution stirred at r.t. for 0.5 h. DCM (30 mL) was added and the phases were separated. The organic layer was washed with water (50 mL) and brine (50 mL). The solvent was removed *in vacuo* to give 260 mg (95%) **28** as a white solid.

^{1}H NMR (400MHz, DMSO-d_6): δ_H 11.69 (s, 1H, MeONH), 9.73 (s, 1H, ArH), 8.96 (s, 1H, ArH), 5.15 (m, 1H, cyclohex. NCH), 3.75 (s, 3H, CH_3ON), 3.55 (s, 3H, SO_2CH_3), 2.09–1.77 (m, 6H, cyclohex. CH), 1.70 (m, 1H, cyclohex. CH), 1.61–1.42 (m, 2H, cyclohex. CH), 1.42–1.30 (m, 1H, cyclohex. CH); ^{13}C NMR (100MHz, DMSO-d_6): δ_C 174.4, 166.2, 161.4, 160.9, 154.2, 147.2, 120.2, 116.5, 64.2, 59.0, 55.4, 31.4, 25.8, 24.9; HRMS (ESI) calcd. for $C_{16}H_{21}N_4O_5S$ $[M+H]^+$: 381.1233; found *m/z*: 381.1253.

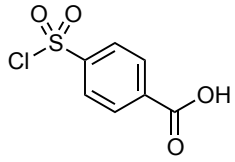
8-Cyclohexyl-*N*-methoxy-5-oxo-2-(phenylamino)-5,8-dihydropyrido[2,3-*d*]pyrimidine-6-carboxamide (3)



8-Cyclohexyl-*N*-methoxy-2-(methylthio)-5-oxo-5,8-dihydropyrido[2,3-*d*]pyrimidine-6-carboxamide (**28**) (150 mg, 0.39 mmol) was dissolved in *i*-PrOH (2mL) and aniline (100 µL, 1.1 mmol) was added. The mixture was cooled to r.t. and the solvent evaporated *in vacuo*. The resulting residue was purified *via* flash column chromatography (10% NH_3/MeOH in DCM) to yield 70 mg (46%) **3** as an off-white solid.

m.p. 238–240 °C; R_f 0.2 (NH_3/MeOH:DCM 19:1); IR (neat) 3280, 2923, 1674, 1595 cm cm^{-1}; ^{1}H NMR (400MHz, DMSO-d_6): δ_H 11.93 (s, 1H, MeON*H*), 10.56 (br. s, 1H, ArN*H*), 9.23 (s, 1H, Ar*H*), 8.69 (s, 1H, Ar*H*), 7.80 (d, *J* = 8.0 Hz, 2H, Ar*H*), 7.39 (t, *J* = 8.0 Hz, 2H, Ar*H*), 7.11 (t, *J* = 7.3 Hz, 1H, Ar*H*), 5.04 (br. s, 1H, cyclohex. NC*H*), 3.74 (s, 3H, CH_3ON), 2.07–1.90 (m, 4H, cyclohex. C*H*), 1.88–1.66 (m, 3H, cyclohex. C*H*), 1.54–1.25 (m, 3H, cyclohex. C*H*); ^{13}C NMR (100MHz, DMSO-d_6): δ_C 174.3, 162.0, 160.8. 160.2, 155.2, 144.7, 139.4, 129.1, 123.8, 120.6, 114.3, 113.9, 111.7, 64.3, 31.6, 26.2, 25.0; HRMS (ESI) calcd. for $C_{21}H_{24}N_5O_3$ $[M+H]^+$: 394.1879; found *m/z*: 394.1880.

4-(Chlorosulfonyl)benzoic acid (31)[65]

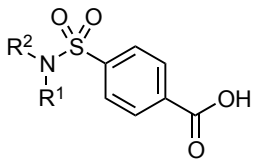


Following the above referenced literature procedure.

Potassium 4-carboxybenzenesulfonate (**32**) (12 g, 50 mmol) was added portion-wise to stirring chlorosulfonic acid (40 mL, 250 mmol) at 0 °C. The reaction mixture stirred for 14 h at r.t. before being stirred into crushed ice and the white precipitate collected *via* vacuum filtration and washed with cold water. The white solid was dried by high vacuum and isolated to yield 10 g (90%) **31**.

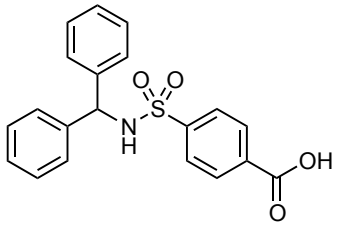
HRMS (CI) calcd. for $C_7H_6O_4S^{35}Cl$ $[M+H]^+$: 220.9675; found *m/z*: 220.9681.

General procedure for the preparation of 4-sulfamoylbenzoic acids 32a-c



Secondary amine (7.9 mmol, 3.5 eq.) and 4-(chlorosulfonyl)benzoic acid (**31**) (500 mg, 2.3 mmol, 1 eq.) were stirred in DCM (10 mL) at r.t. for 18 h. The resulting off-white slurry was diluted with 1M $HCl_{(aq)}$ (50 mL) extracted with EtOAc (3x 40 mL). The combined organic layers were concentrated *in vacuo* to give a white solid, which was triturated with DCM to remove any remaining amine. The white solid was isolated *via* vacuum filtration to yield the desired product **32a-c**.

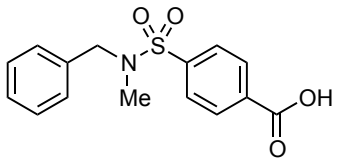
4-(*N*-Benzhydrylsulfamoyl)benzoic acid (32a)



Yield **32a** 87% (720 mg) as a white solid.

m.p. 190–192 °C; IR (neat) 3294, 2556, 1693, 1427, 1336, 1165 cm^{-1}; ^1H NMR (400MHz, DMSO-d_6): δ_H 13.33 (br. s, 1H, CO_2H), 9.01 (d, *J* = 9.6 Hz, 1H, SO_2NH), 7.86 (d, *J* = 8.3 Hz, 2H, Ar*H*), 7.70 (d, *J* = 8.4 Hz, 2H, Ar*H*), 7.27–7.09 (m, 10H, Ar*H*), 5.61 (d, *J* = 9.6 Hz, 1H, Ph_2CHN); HRMS (ESI) calcd. for $C_{20}H_{16}NO_4S$ $[M\text{-}H^+]^-$: 366.0800; found *m/z*: 366.0799.

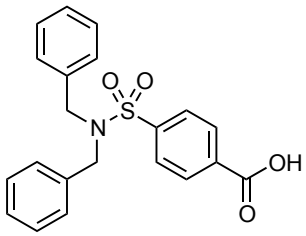
4-(*N*-Benzyl-*N*-methylsulfamoyl)benzoic acid (32b)



Yield **32b** 94% (650 mg) as a white solid.

m.p. 201–204 °C; IR (neat) 2544, 1690, 1432, 1362, 1345, 1288, 1163 cm^{-1}; ^1H NMR (400MHz, DMSO-d6): δ_H 13.51 (br. s, 1H, CO_2H), 8.18 (d, *J* = 8.2 Hz, 2H, Ar*H*), 7.97 (d, *J* = 8.5 Hz, 2H), 7.45–7.22 (m, 5H, Ar*H*), 4.17 (s, 2H, NCH_2), 2.57 (s, 3H, NCH_3); HRMS (ESI) calcd. for $C_{15}H_{14}NO_4S$ $[M\text{-}H^+]^-$: 304.0644; found *m/z*: 304.0648.

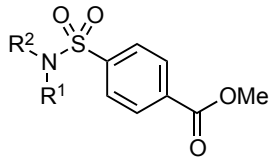
4-(*N,N*-Dibenzylsulfamoyl)benzoic acid (32c)[295]



Yield **32c** 93% (810 mg) as a white solid.

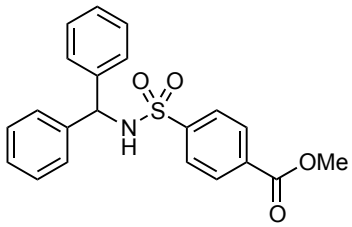
m.p. 175–177 °C; ^1H NMR (400MHz, DMSO-d6): δ_H 13.46 (s, 1H, CO_2H), 8.12 (d, *J* = 8.3 Hz, 2H, Ar*H*), 7.99 (d, *J* = 8.4 Hz, 2H, Ar*H*), 7.21 (m, 6H, Ar*H*), 7.14–6.97 (m, 4H, Ar*H*), 4.34 (s, 4H, $PhCH_2$); HRMS (ESI) calcd. for $C_{21}H_{20}NO_4S$ $[M+H]^+$: 382.1113; found *m/z*: 382.1118.

General Procedure for Preparation of Methyl 4-Sulfamoylbenzoates 33a-c



To 4-sulfamoylbenzoic acid **32a-c** (125 mg, 0.33 mmol) in 1:1 MeOH:PhMe (2mL) was added 2.0 M $TMSCHN_2$ in *n*-heptane (0.17 mL, 0.34 mmol) and the reaction stirred for 4 h. The reaction was quenched with AcOH (50 μL), diluted with EtOAc (20 mL) and washed with H_2O (2x 20 mL) and brine (20 mL). The organic layer was concentrated *in vacuo* and the resulting residue recrystallised (EtOAc / pentane) to give the desired compound **33a-c**.

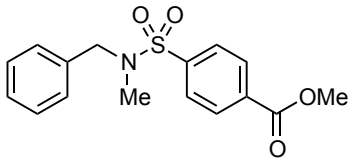
Methyl 4-(*N*-benzhydrylsulfamoyl)benzoate (33a)



Yield **33a** 44% (55 mg) as a white solid.

m.p. 162–164 °C; IR (neat) 3282, 1703, 1449, 1434, 1347, 1283, 1159, 1088 cm^{-1}; ^1H NMR (400MHz, acetone-d_6): δ_H 7.98 (d, *J* = 8.6 Hz, 2H, Ar*H*), 7.82 (d, *J* = 8.6 Hz, 2H, Ar*H*), 7.71 (d, *J* = 9.1 Hz, 1H, SO_2NH), 7.29–7.16 (m, 10H, Ar*H*), 5.76 (d, *J* = 9.1 Hz, 1H, Ph_2CHN), 3.94 (s, 3H, OCH_3); ^{13}C NMR (100MHz, acetone-d_6): δ_C 166.3, 145.8, 141.2, 133.0, 129.6, 128.3, 127.4, 127.2, 127.0, 61.4, 51.9; HRMS (ESI) calcd. for $C_{21}H_{20}NO_4S$ $[M+H]^+$: 382.1113; found *m/z*: 382.0388.

Methyl 4-(*N*-Benzyl-*N*-methylsulfamoyl)benzoate (33b)

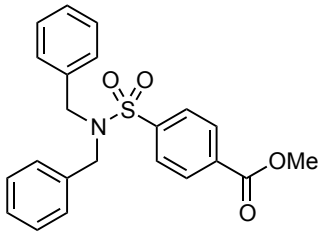


Yield **33b** 57% (60 mg) as a white solid.

m.p. 94–96 °C; IR (neat) 1717, 1453, 1434, 1370, 1337, 1277, 1160, 1110 cm^{-1}; ^1H NMR (400MHz, acetone-d_6): δ_H 8.28 (d, *J* = 8.5 Hz, 2H, Ar*H*), 8.05 (d, *J* = 8.5 Hz, 2H, Ar*H*), 7.39–7.30 (m, 5H, Ar*H*), 4.26 (s, 2H, CH_2N), 3.99 (s, 3H, OCH_3), 2.67 (s, 3H, NCH_3); ^{13}C NMR (100MHz,

acetone-d_6): δ_C 165.3, 141.8, 136.1, 133.9, 130.2, 128.6, 128.3, 127.8, 127.7, 53.7, 52.1, 34.0; HRMS (ESI) calcd. for $C_{16}H_{18}NO_4S$ $[M+H]^+$: 320.0957; found *m/z*: 320.0956.

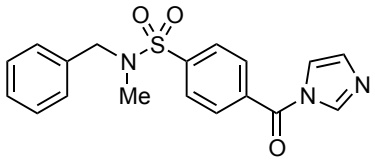
Methyl 4-(*N,N*-dibenzylsulfamoyl)benzoate 33c



Yield **33c** 69% (90 mg) as a white solid.

m.p. 103–105 °C; IR (neat) 1722, 1454, 1377, 1340, 1277, 1156, 1095 cm^{-1}; ^1H NMR (400MHz, acetone-d_6): δ_H 8.21 (d, *J* = 8.6 Hz, 2H, Ar*H*), 8.04 (d, *J* = 8.6 Hz, 2H, Ar*H*), 7.24 (m, 6H, Ar*H*), 7.16 (m, 4H, Ar*H*), 4.43 (s, 4H, PhCH_2N), 3.98 (s, 3H, OCH_3); ^{13}C NMR (100MHz, acetone-d_6): δ_C 166.7, 145.5, 136.0, 133.9, 130.1, 128.5, 128.3, 127.5, 127.4, 52.0, 51.1; HRMS (ESI) calcd. for $C_{22}H_{22}NO_4S$ $[M+H]^+$: 396.1270; found *m/z*: 396.1268.

***N*-Benzyl-4-(1*H*-imidazole-1-carbonyl)-*N*-methylbenzenesulfonamide (34c)**

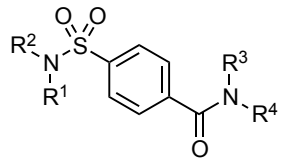


To 4-(*N*-Benzyl-*N*-methylsulfamoyl)benzoic acid (500 mg, 1.6 mmol) in DCM (3 mL) was added CDI (292 mg, 1.8 mmol) and the reaction stirred for 0.5 h until $CO_{2(g)}$ evolution ended. The reaction mixture diluted with DCM (30 mL) and washed with H_2O (3x 10 mL). The organic phase was dried over $MgSO_4$ and the solvent removed *in vacuo* to yield 530 mg (93%) **34c** as a white solid.

m.p. 104–106 °C; IR (neat) 1710, 1531, 1475, 1380, 1252, 1160 cm^{-1}; ^1H NMR (400MHz, $CDCl_3$): δ_H 8.11 (m, 1H, imid. Ar*H*), 8.06 (d, *J* = 8.8 Hz, 1H, Ar*H*), 8.00 (d, *J* = 8.5 Hz, 2H, Ar*H*), 7.57 (m, 1H, imid. Ar*H*), 7.43–7.31 (m, 5H, Ar*H*), 7.26 (m, *J* = 1.4 Hz, 1H, imid. Ar*H*), 4.28 (s, 2H, CH_2N), 2.74 (s, 3H, NCH_3); ^{13}C NMR (100MHz, $CDCl_3$): δ_C 164.8, 142.5, 137.9, 135.6, 135.0, 131.6, 130.3, 128.8, 128.4, 128.2, 127.9, 117.9, 54.1, 34.4; HRMS (ESI) calcd. for $C_{18}H_{18}N_3O_3S$ $[M+H]^+$: 356.1073; found *m/z*: 396.1069.

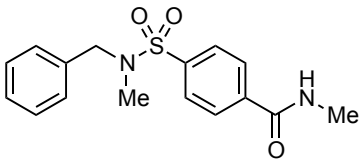
The previous preparation was a representative procedure, in subsequent reactions the desired product was used in solution (DCM) without isolation. Acyl imidazoles **34a-c** were prepared as above, then diluted with DCM (13 mL) to obtain a 0.1 M concentration stock solution.

General procedure for amidation of acyl imidazoles 34a-c



To acyl imidazole (0.25 mmol, 1 eq.) in DCM (2.5 mL) was added the corresponding amine (0.3 mmol, 1.4 eq.) and the reaction stirred under N_2 for 6 h. The reactions were then diluted with DCM (10 mL) and washed with 1 M HCl (10 mL), H_2O (10 mL) and brine (10 mL) before being concentrated *in vacuo*. The off-white residues were recrystallised (EtOAc / pentane) to yield the desired products **36-42**.

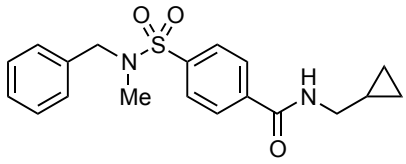
4-(*N*-Benzyl-*N*-methylsulfamoyl)-*N*-methylbenzamide (36)



Yield **36** 41% (33 mg) as a white solid.

m.p. 139–140 °C; IR (neat) 3364, 1631, 1548, 1344, 1163 cm^{-1}; ^1H NMR (400MHz, acetone-d_6): δ_H 8.14 (d, *J* = 8.3 Hz, 2H, Ar*H*), 7.99 (br. s, 1H, CON*H*), 7.98 (d, *J* = 8.3 Hz, 2H, Ar*H*), 7.41–7.24 (m, 5H, Ar*H*), 4.23 (s, 2H, CH_2N), 2.97 (d, *J* = 4.5 Hz, 3H, NHCH_3), 2.65 (s, 3H, NCH_3); ^{13}C NMR (100MHz, acetone-d_6): δ_C 165.6, 139.9, 138.9, 136.2, 128.6, 128.3, 128.0, 127.8, 127.5, 53.8, 34.0, 26.0; HRMS (ESI) calcd. for $C_{16}H_{19}N_2O_3S$ $[M+H]^+$: 319.1116; found *m/z*: 319.1129.

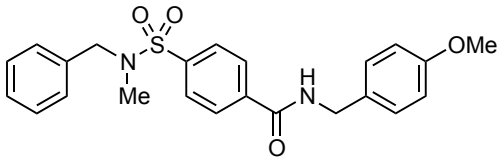
4-(*N*-Benzyl-*N*-methylsulfamoyl)-*N*-(cyclopropylmethyl)benzamide (37)



Yield **37** 59% (53 mg) as a white solid.

m.p. 141–143 °C; IR (neat) 3323, 1642, 1536, 1455, 1342, 1165, 737 cm^{-1}; ^{1}H NMR (400MHz, acetone-d_6): δ_H 8.16 (d, *J* = 8.3 Hz, 2H, Ar*H*), 8.14 (br. s, 1H, CON*H*), 7.98 (d, *J* = 8.3 Hz, 2H, Ar*H*), 7.47–7.26 (m, 5H, Ar*H*), 4.23 (s, 2H, CH_2N), 3.33 (dd, *J*=7.0, 5.6Hz, 2H, NHCH_2), 2.65 (s, 3H, NCH_3), 1.15 (m, 1H, cyclopr. C*H*), 0.51 (m, 2H, cyclopr. C*H*), 0.32 (m, 2H, cyclopr. C*H*); HRMS (ESI) calcd. for $C_{19}H_{23}N_2O_3S$ $[M+H]^+$: 359.1429; found *m/z*: 359.1425.

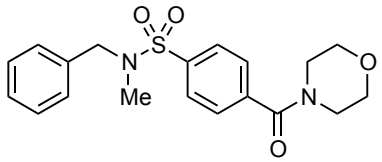
4-(*N*-Benzyl-*N*-methylsulfamoyl)-*N*-(4-methoxybenzyl)benzamide (38)



Yield **38** 65% (69 mg) as a white solid.

m.p. 143–144 °C; IR (neat) 3397, 1655, 1534, 1509, 1456, 1342, 1166 cm^{-1}; ^{1}H NMR (400MHz, acetone-d_6): δ_H 8.45 (br. t, *J* = 5.8 Hz, 1H, CON*H*), 8.19 (d, *J* = 8.3 Hz, 2H, Ar*H*), 7.98 (d, *J* = 8.3 Hz, 2H, Ar*H*), 7.41–7.28 (m, 5H, Ar*H*), 7.35 (d, *J* = 8.6 Hz, 2H, Ar*H*), 6.92 (d, *J* = 8.6 Hz, 2H, Ar*H*), 4.59 (d, *J* = 5.8 Hz, 2H, NHCH_2), 4.22 (s, 2H CH_2N), 3.80 (s, 3H, OCH_3), 2.64 (s, 3H, NCH_3); ^{13}C NMR (100MHz, acetone-d_6): δ_C 165.0, 159.0, 140.0, 138.8, 136.2, 129.0, 128.6, 128.3, 128.2, 127.8, 127.5, 127.0, 113.7, 54.6, 53.8, 42.8, 34.0; HRMS (ESI) calcd. for $C_{23}H_{25}N_2O_4S$ $[M+H]^+$: 425.1535; found *m/z*: 425.1538.

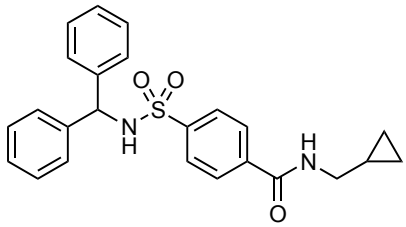
_N_-Benzyl-_N_-methyl-4-(morpholine-4-carbonyl)benzenesulfonamide (39)



Yield **39** 58% (54 mg) as a white solid.

m.p. 116–117 °C; IR (neat) 1614, 1493, 1453, 1436, 1338, 1279, 1166 cm^{-1}; ^{1}H NMR (400MHz, acetone-d_6): δ_H 7.97 (d, J = 8.2 Hz, 2H, Ar*H*), 7.72 (d, J = 8.2 Hz, 2H, Ar*H*), 7.45–7.31 (m, 5H, Ar*H*), 4.25 (s, 2H, CH_2N), 3.70 (m, 6H, morpholin. C*H*), 3.46 (m, 2H, morpholin. C*H*), 2.67 (s, 3H, NCH_3); ^{13}C NMR (100MHz, acetone-d_6): δ_C 168.0, 140.4, 138.6, 136.2, 128.6, 128.4, 128.0, 127.8, 127.6, 78.3, 66.4, 53.8, 34.0; HRMS (ESI) calcd. for $C_{19}H_{23}N_2O_4S$ $[M+H]^+$: 375.1379; found *m/z*: 375.1378.

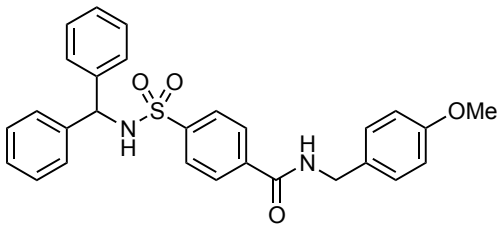
4-(_N_-Benzhydrylsulfamoyl)-_N_-(cyclopropylmethyl)benzamide (40)



Yield **40** 46% (48 mg) as a white solid.

m.p. 164–165 °C; IR (neat) 3390, 3117, 1647, 1546, 1459, 1321, 1164 cm^{-1}; ^{1}H NMR (400MHz, acetone-d_6): δ_H 7.98 (br. s, 1H, CON*H*), 7.89 (d, J = 8.3 Hz, 2H, Ar*H*), 7.77 (d, J = 8.3 Hz, 2H, Ar*H*), 7.62 (br. d, J = 4.7 Hz 1H, SO_2N*H*), 7.28–7.15 (m, 10H, Ar*H*), 5.73 (br. d, J = 4.7 Hz, 1H, Ph_2C*H*N), 3.30 (dd, J = 6.9, 5.7 Hz, 2H, NCH_2), 1.11 (m, 1H, cyclopr. C*H*), 0.50 (m, 2H, cyclopr. C*H*), 0.30 (m, 2H, cyclopr. C*H*); ^{13}C NMR (100MHz, acetone-d_6): δ_C 165.1, 143.8, 141.4, 138.2, 128.3, 127.5, 127.4, 127.2, 126.8, 61.33, 44.3, 10.8, 2.9; HRMS (ESI) calcd. for $C_{24}H_{25}N_2O_3S$ $[M+H]^+$: 421.1586; found *m/z*: 421.1571.

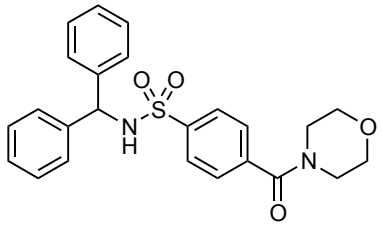
4-(*N*-Benzhydrylsulfamoyl)-*N*-(4-methoxybenzyl)benzamide (41)



Yield **41** 45% (55 mg) as a white solid.

m.p. 166–167 °C; IR (neat) 3326, 3273, 1646, 1540, 1513, 1441, 1348, 1244, 1161, 1146 cm^{-1}; ^{1}H NMR (400MHz, acetone-d_6): δ_H 8.28 (br. t, *J* = 5.8 Hz, 1H, CON*H*), 7.91 (d, *J* = 8.6 Hz, 2H, Ar*H*), 7.77 (d, *J* = 8.6 Hz, 2H, Ar*H*), 7.61 (br. d, *J* = 6.8 Hz, 1H, SO_2N*H*), 7.33 (d, *J* = 8.6 Hz, 2H, Ar*H*), 7.28–7.11 (m, 10H, Ar*H*), 6.92 (d, *J* = 8.6 Hz, 2H, Ar*H*), 5.72 (br. d, *J* = 6.8 Hz, 1H, Ph2C*H*N), 4.56 (d, *J* = 5.8 Hz, 2H, NHCH_2), 3.80 (s, 3H, OCH_3); ^{13}C NMR (100MHz, acetone-d_6): δ_C 165.0, 159.0, 144.0, 141.4, 138.0, 131.4, 129.0, 128.3, 127.5, 127.4, 127.2, 126.9, 113.7, 61.3, 54.6, 42.7; HRMS (ESI) calcd. for $C_{28}H_{27}N_2O_4S$ $[M+H]^+$: 487.1692; found *m/z*: 487.1682.

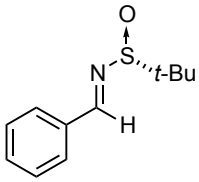
***N*-Benzhydryl-4-(morpholine-4-carbonyl)benzenesulfonamide (42)**



Yield **42** 52% (57 mg) as a white solid.

m.p. 158–160 °C; IR (neat) 3224, 1618, 1496, 1439, 1340, 1331, 1168, 1155 cm^{-1}; ^{1}H NMR (400MHz, acetone-d_6): δ_H 7.75 (d, *J* = 8.3 Hz, 2H, Ar*H*), 7.66 (d, *J* = 9.4 Hz, 1H, SO_2N*H*), 7.40 (d, *J* = 8.3Hz, 2H, Ar*H*), 7.32–7.14 (m, 10H, Ar*H*), 5.75 (d, *J* = 9.4 Hz, 1H, Ph_2C*H*N), 3.69 (br. s, 6H, morpholin. C*H*), 3.30 (br. s, 2H, morpholin. C*H*); HRMS (ESI) calcd. for $C_{22}H_{22}NO_4S$ $[M+H]^+$: 437.1535; found *m/z*: 437.1521.

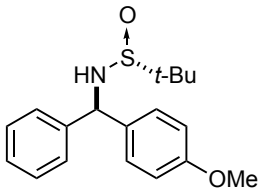
_N_-Benzylidene-2-methylpropane-2-sulfinamide (47)



To *tert*-butyl sulfinamide (590 mg, 4.9 mmol) and benzaldehyde (610 μL, 5.8 mmol) in DCM (15 mL) was added Cs_2CO_3 (2 g, 5.8 mmol). The reaction was stirred and heated at reflux for 18 h. The reaction was then cooled to r.t., filtered through celite and the solvent evaporated to yield 930 mg (91%) of the desired compound **47** as a pale yellow oil that solidified on standing.

^{1}H NMR (400MHz, $CDCl_3$): δ_H 8.63 (s, 1H, N=C*H*), 7.92–7.84 (m, 2H, Ar*H*), 7.59–7.47 (m, 3H, Ar*H*), 1.30 (s, 9H, C(CH_3)$_3$); ^{13}C NMR (100MHz, $CDCl_3$): δ_C 162.8, 134.1, 132.4, 129.4, 129.0, 57.8, 22.6.

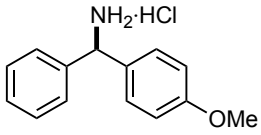
_N_-(4-Methoxyphenyl)phenylmethyl-2-methylpropane-2-sulfinamide (48)



To *N*-benzylidene-2-methylpropane-2-sulfinamide (100 mg, 0.48 mmol) in PhMe (2 mL) at -40 °C was added 4-methoxyphenylmagnesium bromide (1.0 M in THF, 960 μL, 0.96mmol) and the reaction mixture stirred for 4 h. Saturated $NH_4Cl_{(aq)}$ (2 mL) was added and the reaction mixture warmed to r.t. for 1 h. The biphasic mixture was diluted with EtOAc (10 mL) and H_2O (10 mL). The organic layer was separated, washed with brine (10 mL), concentrated *in vacuo* before and the residue purified *via* flash chromatography (10% EtOAc in pentane) to yield 110 mg (73%) **48** as a colourless oil (>19:1 d.r.).

R_f 0.2 (EtOAc:pentane, 1:9); ^{1}H NMR (400MHz, $CDCl_3$): δ_H 7.46–7.41 (m, 2H, Ar*H*), 7.39–7.26 (m, 3H, Ar*H*), 7.31 (d, *J* = 8.7 Hz, 2H, Ar*H*), 6.87 (d, *J* = 8.7 Hz, 1H, Ar*H*), 5.63 (d, *J* = 2.6 Hz, 1H, C*H*N), 3.80 (s, 3H, OCH_3), 3.68 (d, *J* = 2.8 Hz, 1H, SON*H*), 1.28 (s, 9H, C(CH_3)$_3$).

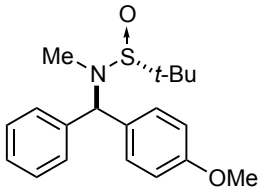
(4-Methoxyphenyl)(phenyl)methanamine hydrochloride (49)[296]



To *N*-(4-methoxyphenyl)phenylmethyl-2-methylpropane-2-sulfinamide (630 mg, 2 mmol) in Et_2O (5 mL) was added 4.0 M HCl in dioxane (1 mL, 4 mmol) and the reaction mixture stirred for 1 h. The white precipitate that formed was isolated *via* vacuum filtration, washed with Et_2O and dried under high-vacuum to yield 450 mg (90%) **49** as a white solid.

^{1}H NMR (400MHz, DMSO-d_6): δ_H 9.07 (s, 3H, NH_3), 7.54–7.49 (m, 2H, Ar*H*), 7.44 (d, *J* = 8.7 Hz, 2H, Ar*H*), 7.44–7.38 (m, 2H, Ar*H*), 7.38–7.32 (m, 1H, Ar*H*), 6.98 (d, *J* = 8.7 Hz, 2H, Ar*H*), 5.57 (s, 1H, NC*H*), 3.75 (s, 3H, OCH_3); HRMS (CI) calcd. for $C_{14}H_{15}NO$ $[M+H]^+$: 213.1143; found *m/z*: 213.1163.

***N*-((4-Methoxyphenyl)(phenyl)methyl)-*N*,2-dimethylpropane-2-sulfinamide (50)**

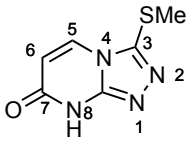


To *N*-benzylidene-2-methylpropane-2-sulfinamide (**47**) (1.0 g, 4.7 mmol) in PhMe (10 mL) at −45 °C, was added 4-methoxyphenylmagnesium bromide (1.0 M in THF, 5.0 mL, 5.0 mmol) and the reaction stirred for 5 h. Once all starting material was consumed, CuI (540 mg, 2.8 mmol) and THF (5 mL) were added and the reaction warmed to 0 °C. After 0.5 h, DMSO (5 mL) was added, followed by MeI (350 μL, 5.6 mmol). The reaction was then warmed to r.t. and stirred for 12 h. The reaction was quenched with sat. $NH_4Cl_{(aq)}$ (30 mL), the aqueous layer extracted with Et_2O (2x 20 mL) and the combined organics washed with H_2O (2x 30 mL) and brine (30 mL). The organic layer was concentrated *in vacuo* and the resulting oil purified *via* flash column chromatography (10% EtOAc in DCM) to give 970 mg (62%) **50** as a pale yellow oil, separated from 260 mg (20%) un-methylated product **48**.

R_f 0.4 (EtOAc:DCM, 1:9); IR (neat) 1610, 1509, 1453, 1360, 1247, 1176, 1067, 1031 cm^{-1}; ^{1}H NMR (400MHz, $CDCl_3$): δ_H 7.36–7.24 (m, 5H, Ar*H*), 7.19 (d, *J* = 8.6 Hz, 2H, Ar*H*), 6.86 (d, *J* = 8.6 Hz, 2H, Ar*H*), 5.73 (s, 1H, NC*H*), 3.80 (s, 3H, OCH_3), 2.54 (s, 3H NCH_3), 1.16 (s, 9H, C(CH_3)$_3$); ^{13}C

NMR (100MHz, $CDCl_3$): δ_C 158.9, 140.3, 132.0, 130.7, 129.9, 129.1, 128.4, 127.4, 113.7, 58.8, 55.3, 29.7, 23.7.; HRMS (ESI) calcd. for $C_{19}H_{26}NO_2S$ $[M+H]^+$: 332.1684; found *m/z*: 332.1688.

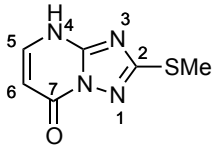
3-(Methylthio)-[1,2,4]triazolo[4,3-*a*]pyrimidin-7(8*H*)-one (62)



To methyl propiolate (0.2 mL, 2.2 mmol) in EtOH (6.0 mL) was added 5-methylthio-3-amino-1,2,4-triazole (260 mg, 2.0 mmol) and hydroquinone (4.0 mg, cat.). The reaction stirred and heated to 90 °C by microwave irradiation for 2 h during which time an off-white solid precipitated. The solid was isolated *via* vacuum filtration washing with EtOH and dried under high vacuum to yield 160 mg (44%) **62** as an off-white solid.

IR (neat) 2719, 1687, 1663, 1569, 1493, 1267 cm^{-1}; ^1H NMR (500MHz, DMSO-d_6): δ_H 12.77 (br. s, 1H, N*H*–8), 8.19 (d, *J* = 7.8 Hz, 1H, C*H*–5), 6.09 (d, *J* = 7.8 Hz, 1H, C*H*–6), 2.56 (s, 3H, SCH_3); ^{13}C NMR (100MHz, DMSO-d_6): δ_C 160.8, 150.2, 142.1, 133.0, 110.0, 16.7; HRMS (ESI) calcd. for $C_6H_7N_4OS$ $[M+H]^+$: 183.0341; found *m/z*: 183.0349. ^1H NMR NOE correlation observed between signals at δ_H 8.19 (C*H*–5) & 2.56 (SCH_3), no observable NOE correlations from N*H*-8 (δ_H 12.77).

2-(Methylthio)-[1,2,4]triazolo[1,5-*a*]pyrimidin-7(4*H*)-one (66)[298]

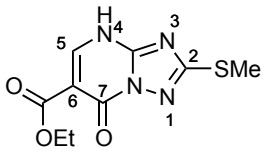


To methyl 3,3-dimethoxypropionate (285 μL, 2.0 mmol) in AcOH (5.0 mL) was added 5-methylthio-3-amino-1,2,4-triazole (260 mg, 2.0 mmol). The reaction was heated to 130 °C by microwave irradiation for 1.5 h with stirring, during which time a white solid precipitated. The solid was isolated *via* vacuum filtration, washing with MeCN, and dried under high vacuum to yield 220 mg (61%) **66** as a white solid.

IR (neat) 3084, 2963, 1678, 1627, 1580, 1402, 1274 cm^{-1}; ^1H NMR (500MHz, DMSO-d_6): δ_H 13.23 (br. s, 1H, N*H*–4), 7.90 (d, *J* = 7.6 Hz, 1H, C*H*–5), 5.90 (d, *J* = 7.6 Hz, 1H, C*H*–6), 2.58 (s, 3H, SCH_3); ^{13}C NMR (100MHz, DMSO-d_6): δ_C 163.7, 155.8, 151.8, 140.0, 100.0, 13.9; HRMS (ESI) calcd. for $C_6H_7N_4OS$ $[M+H]^+$: 183.0341; found *m/z*: 183.0343. ^1H NMR NOE correlation

observed between signals at δ_H 13.23 (N*H*–4) & 7.90 (C*H*–5), no observable NOE correlations from methyl group (δ_H 2.58).

Ethyl 2-(methylthio)-7-oxo-4,7-dihydro-[1,2,4]triazolo[1,5-*a*]pyrimidine-6-carboxylate (74)[299]

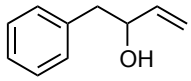


To 5-methylthio-3-amino-1,2,4-triazole (1.0 g, 7.7 mmol) in xylenes (20 mL) at 140 °C was added diethyl (ethoxymethylene)malonate (2.0 mL, 9.9 mmol). The reaction was heated at this temperature for 12 h with stirring, during which time a white solid precipitated. The solid was isolated *via* vacuum filtration, washing with EtOH, and dried under high vacuum to yield 1.1 g (58%) **74** as a white solid.

IR (neat) 3376, 1682, 1666, 1536, 1302, 1282, 1238, 1168 cm^{-1}; ^1H NMR (500MHz, DMSO-d_6): δ_H 8.58 (s, 1H, C*H*–5), 4.25 (q, *J* = 7.1 Hz, 2H, CH_3CH_2O), 2.61 (s, 3H, SCH_3), 1.29 (t, *J* = 7.0 Hz, 3H, CH_3CH_2O); ^{13}C NMR (100MHz, DMSO-d_6): δ_C 164.1, 163.4, 153.4, 151.3, 146.4, 103.2, 60.8, 14.7, 14.0; MS (CI) *m/z* 255 $[M+H]^+$. No observable ^1H NMR NOE correlations from the methyl or ethyl groups (δ_H 2.61 & 1.29 respectively).

8.3 Experimental Procedures – Chapter II

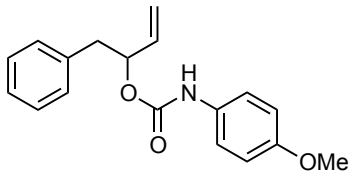
1-Phenylbut-3-en-2-ol (170)[300]



Reaction performed in a 3 L Morton flask. To a vigourously stirred solution of vinylmagnesium bromide (0.7 M in THF, 1.6 L, 1.1 mol) at 0 °C was added phenylacetaldehyde (117 mL, 1.0 mol) in THF (100 mL) dropwise. The reaction mixture was warmed to r.t. and stirred for 6 h then returned to 0 °C and quenched with sat. $NH_4Cl_{(aq)}$ (500 mL). The biphasic mixture was transferred to a 5 L separatory funnel and water (1 L) was added. The layers were separated and the aqueous layer extracted with Et_2O (3x 500 mL). The combined organics were dried over $MgSO_4$ and the solvent removed portionwise (1 L) *in vacuo* to give a pale yellow oil. The oil was redissolved in Et_2O (500 mL) and 40% $NaHSO_{3(aq)}$ (250 mL) was added. The biphasic mixture was stirred for 4 h during which time a white precipitate formed (bisulfite adduct of phenylacetaldehyde). The solid was removed by vacuum filtration and the solvent from the filtrate removed *in vacuo* to give **170** as a pale yellow oil (120 g). The product was further purified by distillation under reduced pressure (108–110 °C, 20 mbar) to yield 105 g (63%) **170** as a colourless oil.

R_f 0.15 (DCM); IR (neat) 3368, 1645, 1603, 1455, 1117, 1077, 1030, 991, 697 cm^{-1}; ^1H NMR (400MHz, $CDCl_3$): δ_H 7.36 (m, 2H, Ar*H*), 7.28 (m, 3H, Ar*H*), 5.98 (ddd, *J* = 16.7, 10.5, 5.8 Hz, 1H, C*H*=CH_2), 5.29 (d, *J* = 17.2 Hz, 1H, CH=CH_2), 5.17 (d, *J* = 10.3 Hz, 1H, CH=CH_2), 4.39 (m, 1H, C*H*OH), 2.92 (dd, *J* = 13.5, 5.0 Hz, 1H, C*H*), 2.83 (dd, *J* = 13.6, 8.0 Hz, 1H, C*H*), 1.65 (d, *J* = 4.0 Hz, 1H, O*H*); ^{13}C NMR (100MHz, $CDCl_3$): δ_C 140.1, 137.7, 129.6, 128.5, 126.6, 115.0, 73.7, 43.8; HRMS (CI) calcd. for $C_{10}H_{16}NO$ $[M+NH_4]^+$: 166.1232; found *m/z*: 166.1236.

1-Phenylbut-3-en-2-yl (4-methoxyphenyl)carbamate (172a)

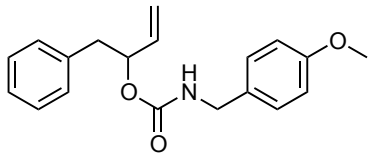


To allylic alcohol **170** (500 mg, 3.4 mmol) in DCM (14 mL) was added 4-methoxyphenyl isocyanate (0.44 mL, 3.4 mmol) and the reaction mixture was stirred at r.t. for 3 h. The solvent was removed *in vacuo* and the residue purified *via* flash column chromatography (50% DCM in

pentane) to yield 800 mg (80%) **172a** as a colourless oil that solidified into an amorphous white solid.

R_f 0.25 (DCM); ^{1}H NMR (400MHz, $CDCl_3$): δ_H 7.42–7.17 (m, 7H, Ar*H*), 6.96–6.71 (m, 2H, Ar*H*), 6.47 (br. s, 1H, N*H*), 5.88 (ddd, *J* = 17.1, 10.6, 6.3 Hz, 1H, C*H*=CH_2), 5.49 (m, 1H, C*H*), 5.29 (d, *J* = 17.0 Hz, 1H, CH=CH_2), 5.21 (d, *J* = 10.3 Hz, 1H, CH=CH_2), 3.81 (s, 3H, OCH_3), 3.06 (dd, *J* = 13.8, 7.0 Hz, 1H, C*H*), 2.96 (dd, *J* = 13.8, 6.4 Hz, 1H, C*H*); HRMS (CI) calcd. for $C_{18}H_{23}N_2O_3$ $[M+NH_4]^+$: 315.1709; found *m/z*: 315.1698.

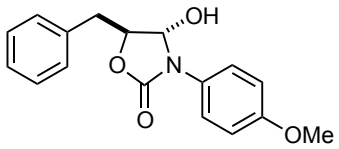
1-Phenylbut-3-en-2-yl (4-methoxybenzyl)carbamate (172b)



To allylic alcohol **170** (1.0 g, 6.7 mmol) in DCM (25 mL) was added 4-methoxybenzyl isocyanate (0.96 mL, 6.7 mmol) and the reaction mixture was stirred at r.t. for 3 h. The solvent was removed *in vacuo* and the residue purified *via* flash column chromatography (50% DCM in pentane) to yield 2.1 g (quant.) **172b** as a pale yellow oil that solidified into an amorphous pale yellow solid.

R_f 0.25 (DCM); IR (neat) 3317, 1683, 1612, 1513, 1454, 1244, 1178, 1038, 698 cm^{-1}; ^{1}H NMR (400MHz, $CDCl_3$): δ_H 7.35–7.13 (m, 7H, Ar*H*), 6.87 (d, *J* = 8.7 Hz, 2H, Ar*H*), 5.85 (ddd, *J* = 17.0, 10.6, 6.1 Hz, 1H, C*H*=CH_2), 5.45 (m, 1H, C*H*), 5.24 (d, *J* = 17.1 Hz, 1H, CH=CH_2), 5.17 (d, *J* = 10.6 Hz, 1H, CH=CH_2), 4.96 (br. s, 1H, N*H*), 4.28 (d, *J* = 5.9 Hz, 2H, CH_2), 3.82 (s, 3H, OCH_3) 3.00 (dd, *J* = 13.7, 7.1 Hz, 1H, C*H*), 2.92 (dd, *J* = 13.8, 6.3 Hz, 1H, C*H*); ^{13}C NMR (100MHz, $CDCl_3$): δ_C 159.0, 155.8, 137.0, 136.4, 130.6, 129.6, 128.8, 128.3, 126.5, 116.5, 114.1, 75.5, 55.3, 44.5, 44.1; HRMS (ESI) calcd. for $C_{19}H_{22}NO_3$ $[M+H]^+$: 312.1600; found *m/z*: 312.1593.

5-Benzyl-4-hydroxy-3-(4-methoxyphenyl)oxazolidin-2-one (174a)

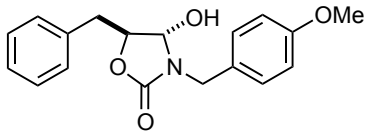


To allylic carbamate **172a** (700 mg, 2.35 mmol) in 1,4-dioxane:H_2O (3:1, 32 mL) was added 2,6-lutidine (1.1 mL, 9.4 mmol), $K_2OsO_4 \cdot 2H_2O$ (26 mg, 0.07 mmol) and $NaIO_4$ (1.25 g, 5.88

mmol). The reaction mixture was stirred at r.t. for 3 days then partitioned with DCM (20 mL) and water (20 mL). The layers were separated and the aqueous phase extracted with DCM (3x 50mL). The combined organic phases were washed sequentially with 1 M $HCl_{(aq)}$ (50 mL), 1 M $NaOH_{(aq)}$ (50 mL), water (50 mL) and brine (50 mL). The organic layer was then dried over $MgSO_4$ and the solvent was removed *in vacuo* to yield 310 mg (44%) **174a** as a brown crystalline solid (major diastereomer *trans*; 9:1 d.r.).

m.p. 143–145 °C; IR (neat) 3361, 1735, 1607, 1511, 1432, 1249, 1136, 702 cm^{-1}; ^1H NMR (400MHz, $CDCl_3$): δ_H 7.38–7.25 (m, 5H, Ar*H*), 7.08 (d, *J* = 8.9 Hz, 2H, Ar*H*), 6.81 (d, *J* = 8.9 Hz, 2H, Ar*H*), 5.18 (dd, *J* = 9.3, 1.7 Hz, 1H, C*H*OH), 4.61 (ddd, *J* = 5.8, 5.7, 1.8 Hz, 1H, C*H*), 4.14 (d, *J* = 9.3 Hz, 1H, CHO*H*), 3.80 (s, 3H, OCH_3), 3.08 (dd, *J* = 14.5, 5.7 Hz, 1H, C*H*), 3.02 (dd, *J* = 14.5, 5.8 Hz, 1H, C*H*); ^{13}C NMR (100MHz, $CDCl_3$): δ_C 158.2, 155.6, 134.3, 129.5, 128.8, 128.4, 127.4, 125.5, 114.3, 85.3, 81.8, 55.5, 38.7; HRMS (ESI) calcd. for $C_{17}H_{18}NO_4$ $[M+H]^+$: 300.1236; found *m/z*: 300.1238.

5-Benzyl-4-hydroxy-3-(4-methoxybenzyl)oxazolidin-2-one (174b)

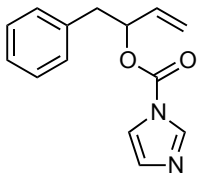


To allylic carbamate **172b** (400 mg, 1.3 mmol) in 1,4-dioxane:H_2O (3:1, 16 mL) was added 2,6-lutidine (0.6 mL, 5.2 mmol), $K_2OsO_4 \cdot 2H_2O$ (14 mg, 0.04 mmol) and $NaIO_4$ (550 g, 2.6 mmol). The reaction mixture was stirred at r.t. for 3 days then partitioned with DCM (20 mL) and water (20 mL). The layers were separated and the aqueous phase extracted with DCM (3x 50mL). The combined organic phases were washed sequentially with 1 M $HCl_{(aq)}$ (50 mL), 1 M $NaOH_{(aq)}$ (50 mL), water (50 mL) and brine (50 mL). The organic layer was then dried over $MgSO_4$ and the solvent was removed *in vacuo* to yield 340 mg (83%) **174b** as a brown crystalline solid (major diastereomer *trans*; >19:1 d.r.).

m.p. 137–138 °C; IR (neat) 3261, 1731, 1712, 1615, 1510, 1458, 1251, 1118, 1087, 710 cm^{-1}; ^1H NMR (400MHz, $CDCl_3$): δ_H 7.33–7.25 (m, 3H, Ar*H*), 7.19–7.11 (m, 2H, Ar*H*), 7.00 (d, *J* = 8.5 Hz, 2H, Ar*H*), 6.84 (d, *J* = 8.6 Hz, 2H, Ar*H*), 4.76 (dd, *J* = 8.8, 2.2 Hz, 1H, C*H*OH), 4.58 (d, *J* = 15.0 Hz, 1H, NCH_2), 4.53 (td, *J* = 5.9, 2.2 Hz, 1H, C*H*), 4.15 (d, *J* = 14.9 Hz, 1H, NCH_2), 3.84 (s, 3H, OCH_3), 3.83 (d, *J* = 9.1 Hz, 1H, CHO*H*), 2.93 (d, *J* = 5.9 Hz, 2H, CH_2); ^{13}C NMR (100MHz, $CDCl_3$): δ_C 159.3,

156.7, 134.4, 129.5, 129.4, 128.8, 127.3, 127.2, 114.2, 82.2, 82.0, 55.3, 44.1, 38.5; HRMS (ESI) calcd. for $C_{18}H_{20}NO_4$ $[M+H]^+$: 314.1392; found *m/z*: 314.1404.

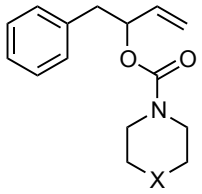
1-Phenylbut-3-en-2-yl 1*H*-imidazole-1-carboxylate (175)



To allylic alcohol **170** (6.0 g, 6.7 mmol) in DCM (120 mL) was added 1,1'-carbonyldiimidazole (10.0 g, 60.7 mmol) and the reaction mixture was stirred at r.t. for 12 h. The reaction mixture was diluted with DCM (100 mL), partitioned with water (100 mL) washed with further portions of water (2x 100 mL) and brine (100 mL). The organic layer was dried over $MgSO_4$, then the solvent was removed *in vacuo* to yield 9.6 g (98%) **175** as a pale yellow oil.

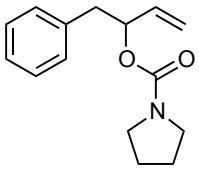
R_f 0.15 ($CHCl_3$); IR (neat) 1754, 1648, 1604, 1526, 1471, 1387, 1278, 1237, 1171, 999, 699 cm^{-1}; ^1H NMR (400MHz, $CDCl_3$): δ_H 8.11 (s, 1H, imid. Ar*H*), 7.40 (m, 1H, imid. Ar*H*), 7.35–7.20 (m, 5H, Ar*H*), 7.07 (m, 1H, imid. Ar*H*), 5.93 (ddd, *J* = 17.1, 10.5, 6.7 Hz, 1H, C*H*=CH_2), 5.63 (app. q, *J* = 6.7 Hz, 1H, C*H*), 5.38 (d, *J* = 17.5 Hz, 1H, CH=CH_2), 5.32 (d, *J* = 10.5 Hz, 1H, CH=CH_2), 3.11 (m, 2H, CH_2); ^{13}C NMR (100MHz, $CDCl_3$): δ_C 147.9, 137.0, 135.7, 134.2, 130.6, 129.5, 128.6, 127.1, 119.1, 117.0, 79.8, 40.7; MS (CI) *m/z* 243 $[M+H]^+$.

General procedure for the addition of 2° amines to carboxyl imidazole 175



To 1-phenylbut-3-en-2-yl 1*H*-imidazole-1-carboxylate (**175**) (2.0 g, 8.0 mmol) was added secondary amine (8.0 mmol) and the reaction mixture was heated to 80 °C for 3 h with stirring. The reaction mixture was cooled to r.t. and purified directly *via* flash column chromatography to yield the desired products **176a** & **176c-e**.

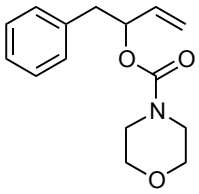
1-Phenylbut-3-en-2-yl pyrrolidine-1-carboxylate (176a)



Yield **176a** 88% (1.75 g) as a colourless oil.

IR (neat) 1697, 1646, 1604, 1497, 1407, 1177, 1094, 699 cm^{-1}; ^{1}H NMR (400MHz, $CDCl_3$): δ_H 7.35–7.18 (m, 5H, Ar*H*), 5.86 (ddd, *J* = 17.0, 10.6, 6.0 Hz, 1H, C*H*=CH_2), 5.41 (app. q, *J* = 6.5 Hz, 1H, C*H*), 5.23 (d, *J* = 17.0 Hz, 1H, CH=CH_2), 5.15 (d, *J* = 10.8 Hz, 1H, CH=CH_2), 3.35 (m, 4H, CH_2NCH_2), 3.02 (dd, *J* = 13.7, 6.9 Hz, 1H, CH_2), 2.92 (dd, *J* = 13.7, 6.4 Hz, 1H, CH_2), 1.86 (m, 4H, CH_2CH_2); ^{13}C NMR (100MHz, $CDCl_3$): δ_C 154.3, 137.3, 136.8, 129.7, 128.2, 126.4, 116.1, 75.4, 46.1, 45.6, 41.3, 25.7, 24.9; HRMS (ESI) calcd. for $C_{15}H_{19}NO_2Na$ $[M+Na]^+$: 268.1313; found *m/z*: 268.1316.

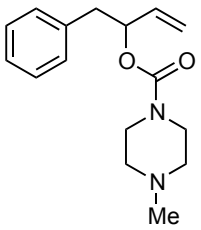
1-Phenylbut-3-en-2-yl morpholine-4-carboxylate (176c)



Yield **176c** 85% (2.2 g) as a colourless oil. (Reaction performed on 10 mmol scale)

IR (neat) 1697, 1647, 1604, 1497, 1456, 1420, 1237, 1114, 700 cm^{-1}; ^{1}H NMR (400MHz, $CDCl_3$): δ_H 7.36–7.17 (m, 5H, Ar*H*), 5.86 (ddd, *J* = 16.9, 10.5, 6.0 Hz, 1H, C*H*=CH_2), 5.44 (m, 1H, C*H*), 5.23 (d, *J* = 16.7 Hz, 1H, CH=CH_2), 5.17 (d, *J* = 10.5 Hz, 1H, CH=CH_2), 3.63 (m, 4H, CH_2NCH_2), 3.45 (m, 4H, CH_2OCH_2), 2.98 (m, 2H, CH_2); ^{13}C NMR (100MHz, $CDCl_3$): δ_C 154.6, 137.0, 136.4, 129.6, 128.2, 126.5, 116.5, 76.1, 66.6, 44.1, 41.1; HRMS (ESI) calcd. for $C_{15}H_{20}NO_3$ $[M+H]^+$: 262.1443; found *m/z*: 262.1449.

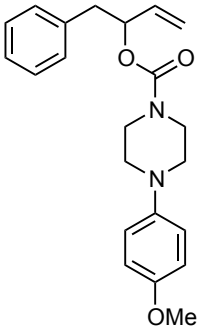
1-Phenylbut-3-en-2-yl 4-methylpiperazine-1-carboxylate (176d)



Yield **176d** 95% (2.1 g) as a pale yellow oil.

^{1}H NMR (400MHz, $CDCl_3$): δ_H 7.33–7.26 (m, 2H), 7.26–7.17 (m, 3H), 5.85 (ddd, *J* = 17.1, 10.8, 6.0 Hz, 1H, C*H*=CH_2), 5.41 (m, 1H, C*H*), 5.21 (dt, *J* = 17.1, 1.5 Hz, 1H, CH=CH_2), 5.16 (dt, *J* = 10.8, 1.4 Hz, 1H, CH=CH_2), 3.48 (m, 4H, CH_2NCH_2), 2.99 (dd, *J* = 13.8, 7.3 Hz, 1H, CH_2), 2.93 (dd, *J* = 13.8, 6.3 Hz, 1H, CH_2), 2.33 (br. s, 4H, MeN(CH_2)$_2$), 2.30 (s, 3H, NCH_3); ^{13}C NMR (100MHz, $CDCl_3$): δ_C 154.6, 137.1, 136.5, 129.6, 128.4, 126.5, 116.2, 75.9, 54.7, 46.2, 43.6, 41.1.

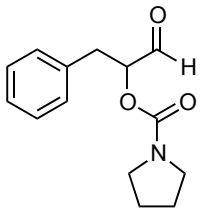
1-Phenylbut-3-en-2-yl 4-(4-methoxyphenyl)piperazine-1-carboxylate (176e)



Yield **176e** 99% (3.0 g) as a yellow oil.

IR (neat) 1697, 1646, 1604, 1509, 1455, 1428, 1239, 1225, 1119, 1033, 700 cm^{-1}; ^{1}H NMR (400MHz, $CDCl_3$): δ_H 7.34–7.27 (m, 2H, Ar*H*), 7.27–7.21 (m, 3H, Ar*H*), 6.92 (d, *J* = 9.2 Hz, 2H, Ar*H*), 6.87 (d, *J* = 9.0 Hz, 2H, Ar*H*), 5.88 (ddd, *J* = 17.0, 10.8, 6.0 Hz, 1H, C*H*=CH_2), 5.45 (m, 1H, C*H*), 5.25 (dt, *J* = 17.0, 1.4 Hz, 1H, CH=CH_2), 5.19 (dt, *J* = 10.8, 1.5 Hz, 1H, CH=CH_2), 3.80 (s, 3H, OCH_3), 3.62 (br. s, 4H, CH_2NCH_2), 2.99 (m, 6H, CH_2N(PMP)CH_2 & CH_2); ^{13}C NMR (100MHz, $CDCl_3$): δ_C 154.6, 154.3, 145.6, 137.1, 136.5, 129.7, 128.3, 126.5, 119.0, 116.4, 114.5, 76.0, 55.6, 50.9, 43.9, 41.2; HRMS (ESI) calcd. for $C_{22}H_{27}N_2O_3$ $[M+H]^+$: 367.2022; found *m/z*: 367.2021.

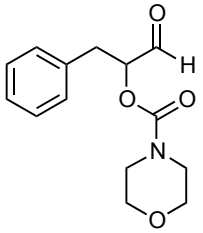
1-Oxo-3-phenylpropan-2-yl pyrrolidine-1-carboxylate (178a)



To 1-phenylbut-3-en-2-yl pyrrolidine-1-carboxylate (**176a**) (4.0 g, 16 mmol) in 1,4-dioxane:H_2O (3:1, 360 mL) was added 2,6-lutidine (7.4 mL, 64 mmol), $K_2OsO_4 \cdot 2H_2O$ (60 mg, 0.16 mmol) and $NaIO_4$ (8.6 g, 40 mmol). The reaction mixture was stirred at r.t. for 3 days then partitioned with DCM (200 mL) and water (200 mL). The layers were separated and the aqueous phase extracted with DCM (3x 250mL). The combined organic phases were washed sequentially with 1 M $HCl_{(aq)}$ (200 mL), 1 M $NaOH_{(aq)}$ (200 mL), water (200 mL) and brine (200 mL). The organic layer was then dried over $MgSO_4$ and the solvent was removed *in vacuo* to yield 3.4 g (86%) **178a** as a yellow oil.

IR (neat) 1731, 1694, 1415, 1096, 700 cm^{-1}; ^1H NMR (400MHz, $CDCl_3$): δ_H 9.62 (s, 1H, C*H*O), 7.34–7.21 (m, 5H, Ar*H*), 5.06 (dd, *J* = 8.5, 4.5 Hz, 1H, C*H*), 3.47–3.24 (m, 4H, CH_2NCH_2), 3.16 (dd, *J* = 14.3, 4.6 Hz, 1H, CH_2), 3.04 (dd, *J* = 14.3, 8.5 Hz, 1H, CH_2), 2.00–1.76 (m, 2H, CH_2CH_2); ^{13}C NMR (100MHz, $CDCl_3$): δ_C 199.6, 154.0, 136.0, 129.5, 128.4, 126.9, 79.2, 46.3, 45.8, 35.5, 25.7, 24.9; HRMS (ESI) calcd. for $C_{14}H_{18}NO_3$ $[M+H]^+$: 248.1287; found *m/z*: 248.1290.

1-Oxo-3-phenylpropan-2-yl morpholine-4-carboxylate (178c)

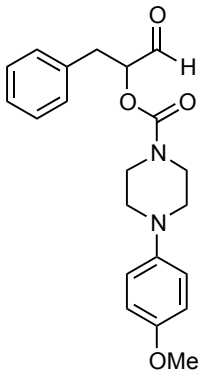


To 1-phenylbut-3-en-2-yl morpholine-4-carboxylate (**176c**) (1.8 g, 6.9 mmol) in 1,4-dioxane:H_2O (3:1, 160 mL) was added 2,6-lutidine (3.2 mL, 27.5 mmol), $K_2OsO_4 \cdot 2H_2O$ (25 mg, 0.07 mmol) and $NaIO_4$ (3.7 g, 17.2 mmol). The reaction mixture was stirred at r.t. for 3 days then partitioned with DCM (100 mL) and water 100 mL). The layers were separated and the aqueous phase extracted with DCM (3x 100mL). The combined organic phases were washed sequentially with 1 M $HCl_{(aq)}$ (100 mL), 1 M $NaOH_{(aq)}$ (100 mL), water (100 mL) and brine (100

mL). The organic layer was then dried over $MgSO_4$ and the solvent was removed *in vacuo* to yield 1.1 g (61%) **178c** as a pale yellow oil.

IR (neat) 1736, 1698, 1429, 1241, 1113, 701 cm^{-1}; ^1H NMR (400MHz, $CDCl_3$): δ_H 9.63 (s, 1H, C*H*O), 7.38–7.17 (m, 5H, Ar*H*), 5.15 (dd, *J* = 8.6, 4.7 Hz, 1H, C*H*), 3.77–3.52 (m, 4H, CH_2NCH_2), 3.47 (br. s, 4H, CH_2OCH_2), 3.20 (dd, *J* = 14.3, 4.8 Hz, 1H, CH_2), 3.06 (dd, *J* = 14.4, 8.6 Hz, 1H, CH_2); ^{13}C NMR (100MHz, $CDCl_3$): δ_C 198.8, 154.4, 135.6, 129.4, 128.6, 127.1, 79.56, 66.5, 66.3, 44.4, 44.1, 35.4; HRMS (ESI) calcd. for $C_{14}H_{18}NO_4$ $[M+H]^+$: 264.1236; found *m/z*: 264.1237.

1-Oxo-3-phenylpropan-2-yl 4-(4-methoxyphenyl)piperazine-1-carboxylate (178e)

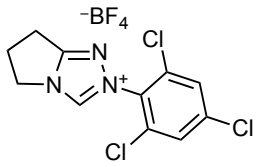


To 1-phenylbut-3-en-2-yl 4-(4-methoxyphenyl)piperazine-1-carboxylate **(176e)** (4.5 g, 12.3 mmol) in *t*-BuOH:H_2O (1:1, 140 mL) was added AD-mix (α:β - 1:1, 20 g, 14 mmol of $K_2OsO_4 \cdot 2H_2O$). The reaction mixture was stirred at r.t. for 6 h then $Na_2SO_{3(s)}$ (20 g) was added. The mixture was stirred for a further 1 h then extracted with EtOAc (3x 100 mL). The combined organic phases were dried over $MgSO_4$, the solvent was removed *in vacuo* and the resulting oil purified using a short silica plug (EtOAc). The solvent was again removed and the residue dissolved in acetone:H_2O (1.5:1, 250 mL). $NaIO_4$ (3.2 g, 15 mmol) was added in 4 portions (800 mg each) over 1 h and the reaction mixture was stirred at r.t. for 12 h. The reaction mixure was diluted with water (200 mL) and extracted with EtOAc (3x 100 mL). The combined organic phases were dried over $MgSO_4$ and the solvent removed *in vacuo* to yield 3.4 g (75%) **178e** as a yellow oil.

R_f 0.35 (Et_2O); IR (neat) 1739, 1692, 1509, 1436, 1241, 1032, 749, 700 cm^{-1}; ^1H NMR (400MHz, $CDCl_3$): δ_H 9.65 (s, 1H, C*H*O), 7.39–7.19 (m, 5H, Ar*H*), 6.96–6.82 (m, 4H, Ar*H*), 5.15 (dd, *J* = 8.6, 4.7 Hz, 1H, C*H*), 3.80 (s, 3H, OCH_3), 3.67–3.47 (m, 4H, CH_2NCH_2), 3.22 (dd, *J* = 14.5, 4.8 Hz, 1H, CH_2), 3.08 (dd, *J* = 14.4, 8.6 Hz, 1H, CH_2), 3.05–2.87 (m, 4H, $CH_2N(PMP)CH_2$); ^{13}C NMR (100MHz,

$CDCl_3$): δ_C 199.0, 154.4, 154.3, 145.4, 135.7, 129.4, 128.6, 127.1, 119.0, 114.5, 79.6, 55.6, 50.8, 44.2, 35.4; HRMS (ESI) calcd. for $C_{21}H_{25}N_2O_4$ $[M+H]^+$: 369.1814; found *m/z*: 369.1822.

2-(2,4,6-Trichlorophenyl)-6,7-dihydro-5H-pyrrolo[2,1-c][1,2,4]triazol-2-ium tetrafluoroborate (183)[229]

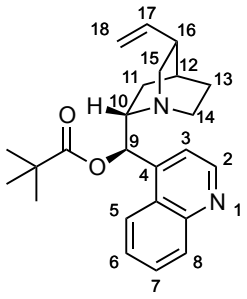


Procedure modified from literature preparation.[229]

To 2-pyrrolidinone (2.5 mL, 33 mmol) in DCM (125 mL) was added triethyloxonium tetrafluoroborate 6.3 g, 33 mmol). The reaction mixture was stirred at r.t. for 16 h then 2,4,6-trichlorophenylhydrazine (7 g, 33 mmol) was added. The mixture was heated to 50 °C and stirred for a further 1 h during which time a white precipitate formed. The reaction mixture was returned to r.t. and the precipitate isolated by vacuum filtration. The white powder was suspended in a mixture of chlorobenzene (30 mL) and triethylorthoformate (120 ml, 710 mmol), $Et_2O{\cdot}HBF_4$ (1 mL, 7.1 mmol) was added, and the reaction heated to 120 °C for 12 h. Upon cooling an off-white precipitate formed which was isolated by vacuum filtration. The precipitate was recrystallised from EtOH to yield 6.5 g (32%) **183** as a crystalline white solid.

^{1}H NMR (400MHz, acetone-d_6): δ_H 10.31 (s, 1H, N=C*H*N), 7.97 (s, 2H, Ar*H*), 4.86–4.78 (m, 2H, CH_2), 3.50–3.43 (m, 2H, CH_2), 3.11–2.98 (m, 2H, CH_2).

***O*-Pivaloyl cinchonidine: (*R*)-quinolin-4-yl((1*S*,2*S*,4*S*,5*R*)-5-vinylquinuclidin-2-yl)methyl pivalate (190)**

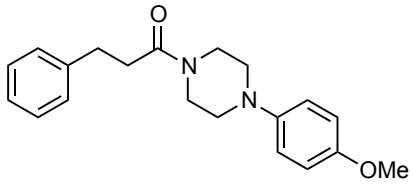


To cinchonidine (3.0 g, 10 mmol) in DCM (50 mL) was added pivaloyl chloride (1.6 mL, 13 mmol) and Et_3N (2.1 g, 15 mmol). The reaction was stirred at r.t. for 12 h. The reaction mixture was then diluted with DCM (50 mL) and the organic phase washed with water

(50 mL) and brine (50 mL). The organic layer was dried over $MgSO_4$ and the solvent removed *in vacuo*. The resulting residue was purified *via* flash column chromatography (100 % EtOAc) to yield 3.2 g (84%) of the desired compound **190** as a pale yellow oil that solidified on standing.

R_f 0.3 (EtOAc); ^{1}H NMR (400MHz, $CDCl_3$): δ_H 8.90 (d, *J* = 4.4 Hz, 1H, Ar*H*–2), 8.25 (d, *J* = 8.5 Hz, 1H, Ar*H*–8), 8.14 (d, *J* = 8.5 Hz, 1H, Ar*H*–5), 7.73 (m, 1H, Ar*H*–7), 7.61 (m, 1H, Ar*H*–6), 7.39 (d, *J* = 4.5 Hz, 1H, Ar*H*–3), 6.48 (d, *J* = 7.4 Hz, 1H, C*H*–9), 5.86 (ddd, *J* = 17.5, 10.6, 7.8 Hz, 1H, CH_2=C*H*–17), 5.03 (m, 2H, CH=CH_2–18), 3.39 (m, 1H, C*H*–10), 3.17 (m, 1H, C*H*–14$_a$), 3.04 (m, 1H, C*H*–15$_a$), 2.66 (m, 1H, C*H*–14$_b$), 2.58 (m, 1H, C*H*–15$_b$), 2.28 (m, 1H, C*H*–16), 1.95 (m, 1H, C*H*–11$_a$), 1.88 (m, 1H, C*H*–12), 1.74 (m, 1H, C*H*–13$_a$), 1.62–1.48 (m, 2H, C*H*–13$_b$ & C*H*–11$_b$), 1.24 (s, 9H, C(CH_3)$_3$); ^{13}C NMR (100MHz, $CDCl_3$): δ_C 177.4, 149.9, 148.7, 145.8, 141.8, 130.5, 129.2, 126.7, 126.0, 123.4, 118.6, 114.5, 74.1, 60.0, 56.7, 42.3, 39.8, 38.9, 27.8, 27.6, 27.1, 24.8.

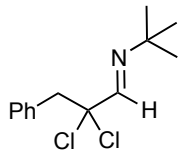
1-(4-(4-Methoxyphenyl)piperazin-1-yl)-3-phenylpropan-1-one (180e)



To α-*O*-carbamoyl aldehyde **178e** (100 mg, 0.27 mmol) in THF (1 mL) was added *N*-TCP triazolium **183** (10 mg, 0.027 mmol) and *O*-pivaloyl cinchonidine **190** (24 mg, 0.08 mmol) in THF (0.4 mL). The reaction mixture was stirred at r.t. for 24 h then the solvent was removed *in vacuo* and the resulting residue purified *via* flash column chromatography (100% Et_2O) to yield 53 mg (61%) **180e** as an amorphous yellow solid.

R_f 0.2 (Et_2O); IR (neat) 1626, 1510, 1440, 1224, 1059, 819, 697 cm^{-1}; ^{1}H NMR (400MHz, $CDCl_3$): δ_H 7.37–7.19 (m, 5H, Ar*H*), 6.94–6.83 (m, 4H, Ar*H*), 3.81 (m, 2H, CH_2), 3.80 (s, 3H, OCH_3) 3.55 (m, 2H, CH_2), 3.03 (m, 4H, PhCH_2 & CH_2), 2.93 (m, 2H, CH_2), 2.70 (m, 2H, CH_2C=O); ^{13}C NMR (100MHz, $CDCl_3$): δ_C 170.7, 154.4, 145.3, 128.6, 128.5, 126.2, 118.9, 114.5, 55.6, 51.1, 50.9, 45.7, 41.7, 35.0, 31.6; HRMS (ESI) calcd. for $C_{20}H_{25}N_2O_2$ [M+H]$^+$: 325.1916; found *m/z*: 325.1920

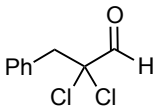
_N_-(2,2-Dichloro-3-phenylpropylidene)-2-methylpropan-2-amine (211)[301]



To hydrocinnamaldehyde (**209**) (20 mL, 150 mmol) was added *t*-$BuNH_2$ (16 mL, 150 mmol) and the reaction mixture was stirred at r.t. for 5 min. $MgSO_4$ was added to form a slurry and the reaction was stirred for another 30 min - the heat generated was dissipated through the use of and external water bath at ambient temperature. The slurry was poured into DCM (500 mL) to aid removal of $MgSO_4$ by gravity filtration. The filtrate was transferred to a foil covered round-bottomed flask, *N*-chlorosuccinimide (60 g 450 mmol) was added and the reaction mixture stirred rapidly for 12 h. The resulting suspension was filtered and the solids washed with DCM. The solvent of the filtrate was removed *in vacuo* and the resulting residue purified *via* flash column chromatography (1-5% Et_2O in pentane) to yield 22 g (57%) **211** as a white solid.

^1H NMR (400MHz, $CDCl_3$): δ_H 7.72 (s, 1H, imine C*H*), 7.43 (m, 2H, Ar*H*), 7.34 (m, 3H, Ar*H*), 3.76 (s, 2H, CH_2), 1.27 (s, 9H, C(CH_3)$_3$); ^{13}C NMR (100MHz, $CDCl_3$): δ_C 155.2, 134.5, 131.9, 127.8, 127.4, 88.8, 57.5, 48.9, 29.2.

2,2-Dichloro-3-phenylpropanal (137)[302]



N-(2,2-Dichloro-3-phenylpropylidene)-2-methylpropan-2-amine (**211**) (22 g, 85 mmol) was treated with 3 M $HCl_{(aq)}$ (250 mL) and the reaction mixture was stirred at r.t. for 5 h. The aqueous reaction mixture was extracted with Et_2O (3x 250 mL) and the combined organics were dried over $MgSO_4$ and the solvent evaporated *in vacuo* to yield the mono-hydrated (*gem*-diol) form of desired product **137** as an off white solid. The solid was dissolved in PhMe (500 mL) and the water removed from the mono-hydrate adduct by azeotropic distillation using Dean–Stark apparatus. The organic solvent was removed *in vacuo* to yield 17 g (98%) **137** as a pale yellow oil. Distillation of this oil from NaH under reduced pressure (101-105 °C, 2 mbar) gave a recovery of 14 g (82%) **137** as a colourless oil.

IR (neat) 1741, 1497, 1456, 1224, 1079, 752, 697 cm^{-1}; ^{1}H NMR (400MHz, $CDCl_3$): δ_H 9.35 (s, 1H, C*H*O), 7.37 (s, 5H, Ar*H*), 3.62 (s, 2H, CH_2); ^{13}C NMR (100MHz, $CDCl_3$): δ_C 185.3, 132.6, 131.4, 128.3, 128.0, 87.3, 46.2.

General procedure for the NHC-catalysed redox amidation of dichloroaldehyde 137:

Amines were purified *via* distillation from CaH_2 prior to use or following the relevant procedures outlined in *Purification of Laboratory Chemicals*.[303] The aldehyde **137** was used as purified in the above procedure.

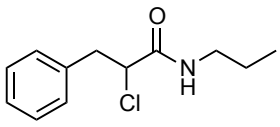
(A) From commercially available amines.

$CO_{2(g)}$ was passed through a solution of amine (2.2 mmol, 2.2 eq.) in THF (5.0 mL) for 10 min with stirring. To this solution was added *N*-TCP triazolium **183** (7.5 mg, 0.020 mmol, 2.0 mol%) followed by dichloroaldehyde **137** (200 mg, 1.0 mmol, 1.0 eq.) in THF (5.0 mL) dropwise at r.t. with stirring. Upon addition of the aldehyde reaction mixture solution turned yellow, accompanied by gas evolution. After 10 min a white precipitate formed and after a further 20 min the reaction mixture solution returned to colourless. The reaction mixture was stirred at r.t. for a further 15 min before SiO_2 (2.0 g) was added and the reaction evaporated *in vacuo* to dryness. The adsorbed compound on silica was dry loaded for purification *via* flash column chromatography (10–40% Et_2O in pentane) to yield the desired amide products.

(B) From commercially available alkylammonium alkylcarbamates.

The preparative procedure used for amidation using isolated alkylammonium alkylcarbamates was the same as above but using 1.1 mmol alkylammonium alkylcarbamate (2.2 mol eq. amine) without the use of additional $CO_{2(g)}$.

2-Chloro-3-phenyl-*N*-propylpropanamide (214)

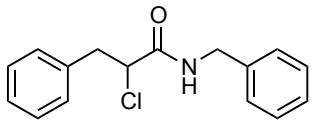


Using general procedure **A**: Yield **214** 70% (158 mg) as a white solid.

IR (neat) 3280, 1655, 1560, 1456, 1216, 979, 747, 695 cm^{-1}; ^{1}H NMR (400MHz, $CDCl_3$): δ_H 7.36–7.24 (m, 5H, Ar*H*), 6.50 (br. s, 1H, N*H*), 4.57 (dd, *J* = 7.7, 4.4 Hz, 1H, C*H*), 3.47 (dd, *J* = 14.4, 4.4 Hz, 1H, PhCH_2), 3.28–3.18 (m, 3H, PhCH_2 & NCH_2), 1.50 (sext, *J* = 7.0 Hz, 2H, $CH_2CH_2CH_3$),

0.89 (t, *J* = 7.5 Hz, 3H, $CH_2CH_2CH_3$); ^{13}C NMR (100MHz, $CDCl_3$): δ_C 168.0, 136.2, 129.7, 128.3, 127.2, 61.8, 41.6, 41.3, 22.5, 11.2; HRMS (ESI) calcd. for $C_{12}H_{17}NO^{35}Cl$ $[M+H]^+$: 226.0999; found *m/z*: 226.0991.

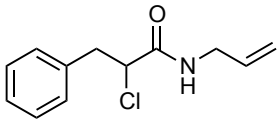
_N_-Benzyl-2-chloro-3-phenylpropanamide (217)[302]



Using general procedure **A**: Yield **217** 48% (130 mg) as a white solid.

IR (neat) 3277, 1681, 1662, 1553, 1493, 1454, 745, 694 cm^{-1}; ^1H NMR (400MHz, $CDCl_3$): δ_H 7.39–7.25 (m, 8H, Ar*H*), 7.18 (m, 2H, Ar*H*), 6.73 (br. s, 1H, N*H*), 4.64 (dd, *J* = 7.6, 4.4 Hz, 1H, C*H*), 4.47 (dd, *J* = 14.8, 5.8 Hz, 1H, NHCH_2), 4.45 (dd, *J* = 14.9, 5.6 Hz, 1H, NHCH_2), 3.50 (dd, *J* = 14.3, 4.5 Hz, 1H, CH_2), 3.29 (dd, *J* = 14.1, 7.5 Hz, 1H, CH_2); ^{13}C NMR (100MHz, $CDCl_3$): δ_C 168.0, 137.2, 136.0, 129.8, 128.8, 128.4, 127.1, 127.2, 61.5, 43.9, 41.3; HRMS (ESI) calcd. for $C_{16}H_{17}NO^{35}Cl$ $[M+H]^+$: 274.0999; found *m/z*: 274.1001.

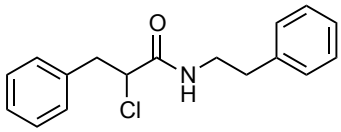
_N_-Allyl-2-chloro-3-phenylpropanamide (220)



Using general procedure **A**: Yield **220** 84% (187 mg) as a white solid.

IR (neat) 3254, 1665, 1644, 1553, 1509, 1261, 990, 927, 744, 693 cm^{-1}; ^1H NMR (400MHz, $CDCl_3$): δ_H 7.38–7.24 (m, 5H, Ar*H*), 6.59 (br. s, 1H, N*H*), 5.78 (ddt, *J* = 16.5, 11.0, 5.6 Hz, 1H, CH_2CH=CH_2), 5.14 (m, 2H, CH_2CH=CH_2), 4.59 (dd, *J* = 7.8, 4.4 Hz, 1H, C*H*), 3.90 (m, 2H, CH_2CH=CH_2), 3.48 (dd, *J* = 14.2, 4.4 Hz, 1H, CH_2), 3.24 (dd, *J* = 14.2, 7.8 Hz, 1H, CH_2); ^{13}C NMR (100MHz, $CDCl_3$): δ_C 168.0, 136.1, 133.3, 129.7, 128.4, 127.2, 116.8, 61.5, 42.2, 41.3; HRMS (ESI) calcd. for $C_{12}H_{15}NO^{35}Cl$ $[M+H]^+$: 224.0842; found *m/z*: 224.0845.

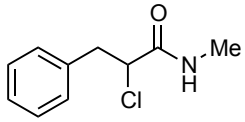
2-chloro-*N*-phenethyl-3-phenylpropanamide (223)



Using general procedure **A**: Yield **223** 47% (120 mg) as a white solid.

IR (neat) 3257, 1642, 1552, 1495, 1454, 739, 699 cm^{-1}; ^{1}H NMR (400MHz, $CDCl_3$): δ_H 7.41–7.19 (m, 8H, Ar*H*), 7.11 (m, 2H, Ar*H*), 6.45 (br. s, 1H, N*H*), 4.54 (dd, *J* = 7.7, 4.4 Hz, 1H, C*H*), 3.63–3.44 (m, 2H, CH_2), 3.45 (dd, *J* = 14.5, 4.3 Hz, 1H, CH_2), 3.22 (dd, *J* = 14.2, 7.7 Hz, 1H, CH_2), 2.84–2.70 (m, 2H, CH_2); ^{13}C NMR (100MHz, $CDCl_3$): δ_C 168.0, 138.4, 136.1, 129.8, 128.8, 128.7, 128.4, 127.2, 126.7, 61.6, 41.3, 41.1, 35.5; HRMS (ESI) calcd. for $C_{17}H_{19}NO^{35}Cl$ $[M+H]^+$: 288.1155; found *m/z*: 288.1150.

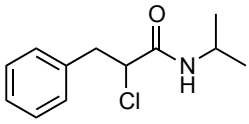
2-Chloro-*N*-methyl-3-phenylpropanamide (224)[304]



Using general procedure **A**: Yield **224** 74% (146 mg) as a white solid.

IR (neat) 3255, 3090, 1652, 1571, 1454, 1215, 747, 697, 680 cm^{-1}; ^{1}H NMR (400MHz, $CDCl_3$): δ_H 7.36–7.22 (m, 5H, Ar*H*), 6.50 (br. s, 1H, N*H*), 4.57 (dd, *J* = 7.9, 4.2 Hz, 1H, C*H*), 3.48 (dd, *J* = 14.2, 4.3 Hz, 1H, CH_2), 3.22 (dd, *J* = 14.3, 8.0 Hz, 1H, CH_2), 2.84 (d, *J* = 4.9 Hz, 3H, NCH_3); ^{13}C NMR (100MHz, $CDCl_3$): δ_C 168.7, 136.2, 129.7, 128.3, 127.2, 61.7, 41.4, 26.6; HRMS (ESI) calcd. for $C_{10}H_{13}NO^{35}Cl$ $[M+H]^+$: 198.0686; found *m/z*: 198.0695.

2-chloro-*N*-isopropyl-3-phenylpropanamide (225)

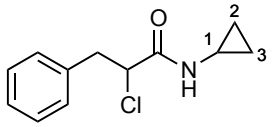


Using general procedure **A**: Yield **225** 13% (30 mg) as a white solid.

IR (neat) 3247, 1671, 1644, 1560, 1494, 1455, 1216, 745, 695 cm^{-1}; ^{1}H NMR (400MHz, $CDCl_3$): δ_H 7.40–7.22 (m, 5H, Ar*H*), 6.21 (br. s, 1H, N*H*), 4.54 (dd, *J* = 7.6, 4.4 Hz, 1H, C*H*), 4.06 (dsept, *J* = 7.9, 6.6 Hz, 1H, NHC*H*(CH_3)$_2$)), 3.45 (dd, *J* = 14.3, 4.4 Hz, 1H, CH_2), 3.25 (dd, *J* = 14.2, 7.6 Hz, 1H,

CH_2), 1.15 (d, *J* = 6.5 Hz, 3H, CH(CH_3)$_2$)), 1.10 (d, *J* = 6.6 Hz, 3H, CH(CH_3)$_2$)); ^{13}C NMR (100MHz, $CDCl_3$): δ_C 167.1, 136.1, 129.8, 128.3, 128.0, 127.2, 61.6, 42.0, 22.4; HRMS (ESI) calcd. for $C_{12}H_{17}NO^{35}Cl$ $[M+H]^+$: 226.0999; found *m/z*: 226.0993.

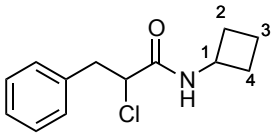
2-chloro-*N*-cyclopropyl-3-phenylpropanamide (226)



Using general procedure **A**: Yield **226** 54% (120 mg) as a white solid.

IR (neat) 3253, 1687, 1655, 1556, 1493, 1456, 1361, 742, 697 cm^{-1}; ^{1}H NMR (400MHz, $CDCl_3$): δ_H 7.37–7.23 (m, 5H, Ar*H*), 6.45 (s, 1H, N*H*), 4.54 (dd, *J* = 7.5, 4.4 Hz, 1H, C*H*), 3.45 (dd, *J* = 14.3, 4.3 Hz, 1H, CH_2), 3.24 (dd, *J* = 14.3, 7.6 Hz, 1H, CH_2), 2.71 (m, 1H, C*H*–1), 0.79 (m, 2H, C*H*–2_a & C*H*–3_a), 0.47 (m, 2H, C*H*–2_b & C*H*–3_b); ^{13}C NMR (100MHz, $CDCl_3$): δ_C 169.4, 136.0, 129.8, 128.3, 127.2, 61.3, 41.3, 22.8, 6.5, 6.4; HRMS (ESI) calcd. for $C_{12}H_{15}NO^{35}Cl$ $[M+H]^+$: 224.0842; found *m/z*: 224.0848.

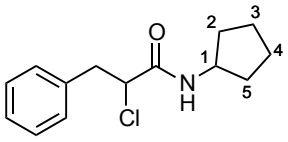
2-chloro-*N*-cyclobutyl-3-phenylpropanamide (227)



Using general procedure **A**: Yield **227** 48% (114 mg) as a white solid.

IR (neat) 3252, 1681, 1647, 1557, 1492, 1455, 1308, 742, 697 cm^{-1}; ^{1}H NMR (400MHz, $CDCl_3$): δ_H 7.37–7.22 (m, 5H, Ar*H*), 6.50 (br. s, 1H, N*H*), 4.53 (dd, *J* = 7.7, 4.2 Hz, 1H, C*H*), 4.37 (m, 1H, C*H*–1), 3.45 (dd, *J* = 14.3, 4.3 Hz, 1H, CH_2), 3.23 (dd, *J* = 14.2, 7.7 Hz, 1H, CH_2), 2.34 (m, 2H, C*H*–2_a & C*H*–4_a), 1.93 – 1.67 (m, 4H, C*H*–2_b, C*H*–3_a, C*H*–3_b & C*H*–4_b); ^{13}C NMR (100MHz, $CDCl_3$): δ_C 167.0, 136.1, 129.8, 128.3, 127.2, 61.5, 45.0, 41.3, 30.9, 30.8, 15.1; HRMS (ESI) calcd. for $C_{13}H_{17}NO^{35}Cl$ $[M+H]^+$: 238.0999; found *m/z*: 238.0999.

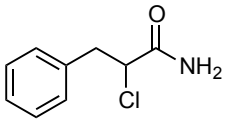
2-chloro-*N*-cyclopentyl-3-phenylpropanamide (228)



Using general procedure **A**: Yield **228** 33% (83 mg) as a white solid.

IR (neat) 3256, 2955, 1649, 1561, 1497, 1452, 1227, 947, 703, 679 cm^{-1}; ^{1}H NMR (400MHz, $CDCl_3$): δ_H 7.47–7.12 (m, 5H, Ar*H*), 6.32 (br. d, *J* = 7.8 Hz, 1H, N*H*), 4.55 (dd, *J* = 7.6, 4.4 Hz, 1H, C*H*), 4.18 (m, 1H, C*H*–1), 3.44 (dd, *J* = 14.2, 4.4 Hz, 1H, CH_2), 3.25 (dd, *J* = 14.3, 7.5 Hz, 1H, CH_2), 2.96 (m, 2H, C*H*–2_a & C*H*–5_a), 1.61 (m, 4H, CH_2–3 & CH_2–4), 1.44–1.21 (m, 2H, C*H*–2_b & C*H*–5_b); ^{13}C NMR (100MHz, $CDCl_3$): δ_C 167.5, 136.1, 129.8, 128.3, 127.1, 61.6, 51.6, 41.3, 32.8, 23.6; HRMS (ESI) calcd. for $C_{14}H_{19}NO^{35}Cl$ $[M+H]^+$: 252.1155; found *m/z*: 252.1155.

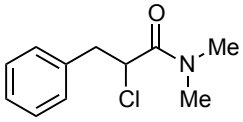
2-Chloro-3-phenylpropanamide (230)[305]



Using general procedure **B**: Yield **230** 73% (136 mg) as a white solid.

IR (neat) 3391, 3187, 1651, 1606, 1498, 1453, 1432, 1260, 744, 694 cm^{-1}; ^{1}H NMR (400MHz, $CDCl_3$): δ_H 7.40–7.22 (m, 5H, Ar*H*), 6.41 (br. s, 1H, NH_2), 5.86 (br. s, 1H, NH_2), 4.55 (dd, *J* = 8.1, 4.4 Hz, 1H, C*H*), 3.50 (dd, *J* = 14.3, 4.4 Hz, 1H, CH_2), 3.23 (dd, *J* = 14.2, 8.2 Hz, 1H, CH_2); ^{13}C NMR (100MHz, $CDCl_3$): δ_C 170.9, 136.1, 129.7, 128.4, 127.3, 60.6, 41.2; HRMS (ESI) calcd. for $C_9H_{11}NO^{35}Cl$ $[M+H]^+$: 184.0529; found *m/z*: 184.0532.

2-Chloro-*N*,*N*-dimethyl-3-phenylpropanamide (231)[306]

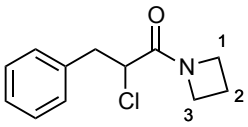


Using general procedure **B**: Yield **231** 10% (21 mg) as a pale yellow oil.

IR (neat) 1650, 1495, 1454, 1400, 1136, 746, 699 cm^{-1}; ^{1}H NMR (400MHz, $CDCl_3$): δ_H 7.33–7.22 (m, 5H, Ar*H*), 4.65 (dd, *J* = 7.3, 7.2 Hz, 1H, C*H*), 3.49 (dd, *J* = 13.9, 7.5 Hz, 1H, CH_2), 3.19 (dd, *J* = 13.9, 7.0 Hz, 1H, CH_2), 2.98 (s, 3H, NCH_3), 2.97 (s, 3H, NCH_3); ^{13}C NMR (100MHz, $CDCl_3$): δ_C

168.1, 137.0, 129.5, 128.5, 127.1, 54.2, 40.8, 37.2, 36.2; HRMS (ESI) calcd. for $C_{11}H_{15}NO^{35}Cl$ $[M+H]^+$: 212.0842; found *m/z*: 212.0848.

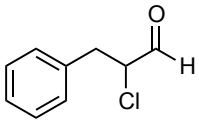
1-(Azetidin-1-yl)-2-chloro-3-phenylpropan-1-one (232)



Using general procedure **A**: Yield **232** 69% (154 mg) as a colourless oil.

IR (neat) 1654, 1498, 1454, 1437, 745, 698 cm^{-1}; ^1H NMR (400MHz, $CDCl_3$): δ_H 7.38–7.23 (m, 5H, Ar*H*), 4.28 (dd, *J* = 8.2, 6.5 Hz, 1H, C*H*), 4.15 (td, *J* = 8.7, 6.1 Hz, 1H, C*H*–3_a), 4.07 (td, *J* = 9.7, 6.1 Hz, 1H, C*H*–1_a), 3.97 (td, *J* = 9.7, 6.2 Hz, 1H, C*H*–1_b), 3.80 (td, *J* = 8.7, 5.9 Hz, 1H, C*H*–3_b), 3.41 (dd, *J* = 13.8, 8.2 Hz, 1H, CH_2), 3.16 (dd, *J* = 13.6, 6.7 Hz, 1H, CH_2), 2.24 (m, 1H, C*H*–2_a), 2.14 (m, 1H, C*H*–2_b); ^{13}C NMR (100MHz, $CDCl_3$): δ_C 167.5, 136.6, 129.5, 128.6, 127.2, 53.8, 50.5, 48.3, 40.6, 15.3; HRMS (ESI) calcd. for $C_{12}H_{15}NO^{35}Cl$ $[M+H]^+$: 224.0842; found *m/z*: 224.0840.

2-Chloro-3-phenylpropanal (238)[307]



To hydrocinnamaldehyde (**209**) (10 mL, 76 mmol) in DCM (150 mL) was added DL-proline (875 mg, 7.6 mmol) and *N*-chlorosuccinimide (10.7 g 80 mmol). The reaction mixture was stirred at r.t. for 12 h then the solids filtered off and the solvent removed *in vacuo* to yield 12.5 g (97%) **238** as a colourless oil (comprises ~10% wt. dichloroaldehyde **137**).

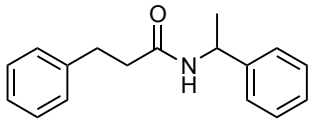
^1H NMR (400MHz, $CDCl_3$): δ_H 9.57 (d, *J* = 2.2 Hz, 1H), 7.39–7.23 (m, 5H, Ar*H*), 4.41 (ddd, *J* = 8.1, 5.7, 2.2 Hz, 1H, C*H*), 3.41 (dd, *J* = 14.4, 5.7 Hz, 1H, CH_2), 3.11 (dd, *J* = 14.4, 8.1 Hz, 1H, CH_2); ^{13}C NMR (100MHz, $CDCl_3$): δ_C 194.4, 135.4, 129.4, 128.7, 127.4, 63.9, 38.3.

General procedure for the NHC-catalysed redox amidation of chloroaldehyde 238:

$CO_{2(g)}$ was passed through a solution of amine (2.2 mmol) in THF (5 mL) for 10 min with stirring. To this solution was added *N*-TCP triazolium **183** (7.5 mg, 0.02 mmol) followed by 2-chloro-3-phenylpropanal **238** (~90% purity 190 mg, 1.0 mmol) in THF (5 mL) dropwise at r.t. with stirring. The reaction mixture was stirred at r.t. for 45 min before SiO_2 (2 g) was added

and the reaction evaporated *in vacuo* to dryness. The adsorbed compound on silica was dry loaded for purification *via* flash column chromatography (10-40% Et_2O in pentane) to yield the desired products **239** & **240**.

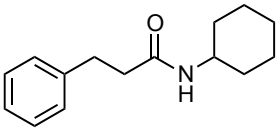
3-phenyl-*N*-(1-phenylethyl)propanamide (239)[308]



Yield **239** 40% (102 mg) as a yellow oil.

^{1}H NMR (400MHz, $CDCl_3$): δ_H 7.40–7.13 (m, 10H, Ar*H*), 5.61 (br. d, *J* = 7.7 Hz, 1H, N*H*), 5.12 (dq, *J* = 7.2, 7.2 Hz, 1H, NHC*H*CH_3), 2.99 (t, *J* = 7.5 Hz, 2H, CH_2), 2.50 (m, 2H, CH_2), 1.43 (d, *J* = 6.8 Hz, 3H, CHCH_3).

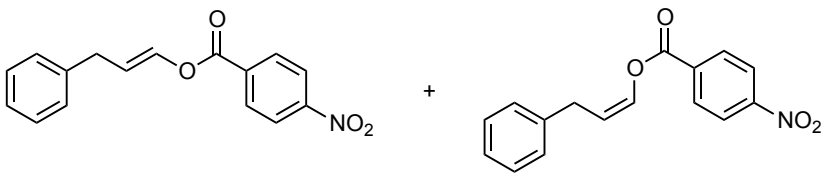
***N*-Cyclohexyl-3-phenylpropanamide (240)**[309]



Yield **240** 22% (51 mg) as a yellow oil.

^{1}H NMR (400MHz, $CDCl_3$): δ_H 7.35–7.17 (m, 5H, Ar*H*), 5.17 (br. d, *J* = 5.1 Hz, 1H, N*H*), 3.75 (m, 1H, C*H*), 2.98 (t, *J* = 7.6 Hz, 2H, CH_2), 2.45 (t, *J* = 7.5 Hz, 2H, CH_2), 1.85 (m, 2H, CH_{eq}), 1.71–1.57 (m, 3H, CH_{eq}), 1.42–1.29 (m, 2H, CH_{ax}), 1.19–1.09 (m, 1H, CH_{ax}), 1.08–0.97 (m, 2H, CH_{ax}); ^{13}C NMR (100MHz, $CDCl_3$): δ_C 171.0, 140.9, 128.5, 128.4, 126.2, 48.0, 38.8, 33.1, 31.9, 25.5, 24.8.

(*E*)- & (*Z*)-3-phenylprop-1-en-1-yl 4-nitrobenzoate (241)



To hydrocinnamaldehyde (**209**) (40 mL, 300 mmol) in DCM (600 mL) was added Et_3N (63 mL, 450 mmol) and 4-nitrobenzoyl chloride (74 g, 450 mmol) the reaction mixture was stirred at r.t. for 15 h. The reaction was no longer progressing so 20% $NaHSO_{3(aq)}$ (300 mL) was added and the reaction stirred vigourously at r.t. for 4 h. The solid bisulfite adduct of the starting

aldehyde was removed by vacuum filtration and the biphasic filtrate layers separated. The organic layer was washed with water (3x 500 mL) and brine (500 mL). The organic layer was then dried over $MgSO_4$ and the solvent removed *in vacuo* to give an oily suspension of **241** (*E*:*Z* ratio, 1:2). The mixture was dissolved in cyclohexane (600 mL) with warming. Upon slow cooling, a separable precipitate was formed which was isolated by vacuum filtration to give 18 g (21%) **241** (*E*:*Z* ratio, 2.9:1) as a pale yellow solid. The cyclohexane was removed from the filtrate to yield 37 g (44%) **241** (*E*:*Z* ratio, 1:4.4) as a yellow oil.

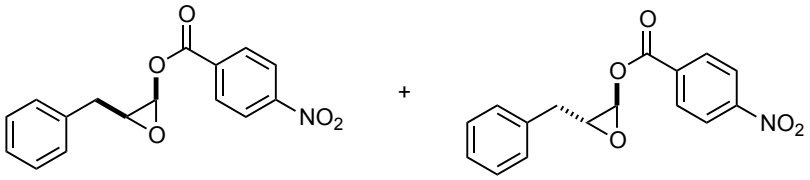
IR (neat) of (*E*)-**241** & (*Z*)-**241** mixture (*E*:*Z* ratio, 2.9:1): 1724, 1671, 1607, 1523, 1304, 1202, 1128, 1104, 942, 841, 712, 700 cm^{-1}.

(*E*)-**241**: ^{1}H NMR (400MHz, $CDCl_3$): δ_H 8.36–8.21 (m, 4H, Ar*H*), 7.47 (m, 1H, CH_2CH=C*H*), 7.39–7.34 (m, 2H, Ar*H*), 7.33–7.25 (m, 3H, Ar*H*), 5.91 (dt, *J* = 12.3, 7.5 Hz, 1H, CH_2CH=CH), 3.48 (d, *J* = 7.8 Hz, 2H, CH_2CH=CH); ^{13}C NMR (100MHz, $CDCl_3$): δ_C 161.9, 150.8, 139.3, 136.2, 134.5, 131.0, 128.6, 128.4, 126.5, 123.7, 115.8, 33.7.

(*Z*)-**241**: ^{1}H NMR (400MHz, $CDCl_3$): δ_H 8.40–8.23 (m, 4H, Ar*H*), 7.44 (m, 1H, CH_2CH=C*H*), 7.39–7.32 (m, 2H, Ar*H*), 7.32–7.23 (m, 3H, Ar*H*), 5.36 (m, 1H, CH_2CH=CH), 3.69 (d, *J* = 7.4 Hz, 2H, CH_2CH=CH); ^{13}C NMR (100MHz, $CDCl_3$): δ_C 161.7, 150.9, 139.5, 136.2, 134.7, 131.1, 128.7, 128.3, 126.4, 123.7, 114.2, 31.0.

HRMS (CI) calcd. for $C_{16}H_{17}N_2O_4$ $[M+NH_4]^+$: 301.1188; found *m/z*: 301.1191. Performed on (*E*)-**241** & (*Z*)-**241** mixture (*E*:*Z* ratio, 2.9:1).

***cis*- & *trans*- 3-Benzyloxiran-2-yl 4-nitrobenzoate (242)**



To a mixture of (*E*)- & (*Z*)-**241** (*E*:*Z* ratio, 2.9:1, 8.0 g, 28 mmol) in DCM (120 mL) was added acetone (12 mL) and Bu_4NHSO_4 (420 mg 1.2 mmol). To this mixture, with vigourous stirring was added concurrently Oxone® (34 g, 56 mmol) in H_2O (140 mL) and sat. $NaHCO_{3(aq)}$ (200 mL) dropwise. the reaction mixture was stirred at r.t. for 12 h. The orgnanic layer was separated and treated with the same conditions a further two times equaling a total of 6 eq. Oxone®. The organic layer was separated and washed with water (2x 100 mL) and brine

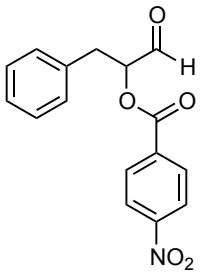
(100 mL) then dried over $MgSO_4$. The solvent was removed *in vacuo* and the residue was purified *via* flash column chromatography (20% EtOAc in pentane) to give 5.6 g (62%) **242** (*cis*:*trans* ratio, 1:2.4) as a colourless oil that slowly solidified into a white solid.

IR (neat) of *cis*-**242** & *trans*-**242** mixture (*cis*:*trans* ratio, 1:2.4): 1736, 1609, 1524, 1494, 1345, 1261, 1126, 1098, 946, 837, 699 cm^{-1}.

cis-**242**: ^{1}H NMR (400MHz, $CDCl_3$): δ_H 8.36 (d, *J* = 8.7 Hz, 2H, Ar*H*), 8.27 (d, *J* = 9.2 Hz, 2H, Ar*H*), 7.41–7.29 (m, 5H, Ar*H*), 5.94 (d, *J* = 2.6 Hz, 1H, C*H*), 3.40 (td, *J* = 6.3, 2.5 Hz, 1H, C*H*), 3.21 (dd, *J* = 14.8, 6.1 Hz, 1H, CH_2), 3.12 (dd, *J* = 14.8, 6.1 Hz, 1H, CH_2); ^{13}C NMR (100MHz, $CDCl_3$): δ_C 164.3, 151.1, 136.3, 134.2, 131.0, 128.9, 128.8, 127.1, 123.8, 76.9, 56.7, 33.7.

trans-**242**: ^{1}H NMR (400MHz, $CDCl_3$): δ_H 8.31 (d, *J* = 8.8 Hz, 2H, Ar*H*), 8.22 (d, *J* = 8.7 Hz, 2H, Ar*H*), 7.41–7.29 (m, 5H, Ar*H*), 5.67 (d, *J* = 0.7 Hz, 1H, C*H*), 3.56 (m, 1H, C*H*), 3.08–2.96 (m, 2H, CH_2); ^{13}C NMR (100MHz, $CDCl_3$): δ_C 164.3, 151.0, 135.4, 132.3, 131.0, 129.1, 128.8, 127.2, 123.7, 77.5, 57.5, 36.0.

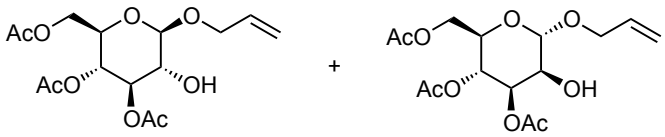
1-Oxo-3-phenylpropan-2-yl 4-nitrobenzoate (243)[201]



cis- & *trans*-**242** (*cis*:*trans* ratio, 1:2.4, 5.6 g, 19 mmol) were heated for 5 min at 165 °C with stirring. Unreacted starting material remained so the reaction mixture was heated to 180 °C for 10 min, then 190 °C for 10 min, monitored by ^{1}H NMR spectroscopy. Conversion was achieved to give aldehyde **243**, with no loss of mass; however, the desired product could not be isolated from its trace impurities.

^{1}H NMR (400MHz, $CDCl_3$): δ_H 9.71 (s, 1H, C*H*O), 8.33 (d, *J* = 8.8 Hz, 2H, Ar*H*), 8.22 (d, *J* = 8.8 Hz, 2H, Ar*H*), 7.39–7.33 (m, 2H, Ar*H*), 7.33–7.27 (m, 3H, Ar*H*), 5.55 (dd, *J* = 8.4, 4.9 Hz, 1H, C*H*), 3.38 (dd, *J* = 14.6, 5.0 Hz, 1H, CH_2), 3.25 (dd, *J* = 14.6, 8.5 Hz, 1H, CH_2).

Allyl 3,4,6-tri-*O*-acetyl-β-D-glucopyranoside (263)[310]



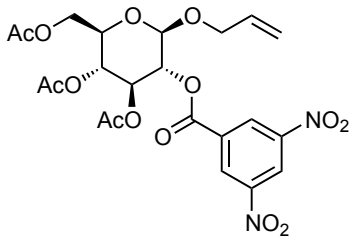
major trace

Synthesised following literature procedure for the preparation of allyl tri-*O*-benzyl-β-D-glucopyranoside (**273**).[288]

To *m*CPBA (⩽77% purity, 4.0 g, 18 mmol) in DCM (180 mL) was added KF (2.1 g, 36 mmol) and the suspension was stirred for 30 min. Tri-*O*-acetyl-D-glucal (**261**) (2.0 g, 7.3 mmol) in DCM (10 mL) was added dropwise and the reaction mixture stirred at r.t. for 24 h. The solids were removed by filtration and the solvent removed from the filtrate *in vacuo*. The resulting oil was dissolved in THF (10 mL) and the solution was cooled to 0 °C. Allyl alcohol (2.0 mL, 29 mmol) was added followed by 1.0 M $ZnCl_2$ in THF (7.0 mL, 7.0 mmol) and the reaction warmed to r.t. and stirred for a further 12 h. Brine (50 mL) was added and the aqueous layer extracted with EtOAc (3x 50 mL). The organic layer was dried over $MgSO_4$ and the solvent removed *in vacuo*. The viscous residue was purified *via* flash column chromatography (30–100% Et*2*O in pentane) to yield 1.2 g (48%) **263** as a viscous colourless oil (containing trace amounts of allyl 3,4,6-tri-*O*-acetyl-β-D-mannopyranoside).

^{1}H NMR (400MHz, $CDCl_3$): δ_H 5.93 (m, 1H), 5.33 (m, 1H), 5.25 (m, 1H), 5.12 (m, 1H), 5.03 (m, 1H), 4.42 (d, *J* = 7.8 Hz, 1H), 4.38 (m, 1H), 4.27 (dd, *J* = 12.3, 4.9 Hz, 1H), 4.16 (m, 1H), 4.12 (dd, *J* = 12.2, 2.5 Hz, 1H), 3.68 (ddd, *J* = 9.8, 4.8, 2.3 Hz, 1H), 3.61 (ddd, *J* = 9.3, 7.8, 2.9 Hz, 1H), 2.41 (d, *J* = 2.8 Hz, 1H), 2.09 (s, 3H), 2.08 (s, 3H), 2.03 (s, 3H).

Allyl 3,4,6-tri-*O*-acetyl-2-(3,5-dinitrobenzoyl)-β-D-glucopyranoside (264)

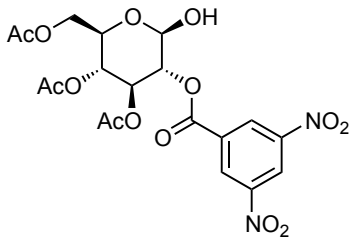


To allyl 3,4,6-tri-*O*-acetyl-β-D-glucopyranoside (**263**) (800 mg, 2.3 mmol) in DCM (10 mL) was added Et_3N (450 µL, 3.2 mmol) and 3,5-dinitrobenzoyl chloride (750 mg, 450 mmol). The reaction mixture was stirred at r.t. for 5 h. DCM (10 mL) was added and the organic solution

with water (2x 20 mL) and brine (20 mL). The organic layer was dried over $MgSO_4$ and the solvent removed *in vacuo*. The residue was purified *via* flash column chromatography (100% $CHCl_3$) to yield 1.0 g (80%) **264** as a white foam.

R_f 0.3 ($CHCl_3$); ^{1}H NMR (400MHz, $CDCl_3$): δ_H 9.25 (t, *J* = 2.2 Hz, 1H), 9.13 (d, *J* = 2.2 Hz, 2H), 5.79 (m, 1H), 5.44 (m, 1H), 5.34–5.16 (m, 3H), 4.81 (d, *J* = 7.9 Hz, 1H), 4.40–4.30 (m, 2H), 4.20 (dd, *J* = 12.2, 2.4 Hz, 1H), 4.13 (m, 1H), 3.81 (ddd, *J* = 10.3, 4.8, 2.5 Hz, 1H), 2.13 (s, 3H), 2.06 (s, 3H), 1.95 (s, 3H); ^{13}C NMR (100MHz, $CDCl_3$): δ_C 170.6, 170.2, 169.4, 161.3, 148.8, 134.0, 133.0, 129.6, 122.8, 118.4, 99.0, 73.6, 72.7, 72.0, 70.2, 68.2, 61.8, 20.7, 20.6 (2C).

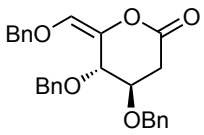
3,4,6-Tri-*O*-acetyl-2-(3,5-dinitrobenzoyl)-β-D-glucopyranose (265)



To allyl 3,4,6-tri-*O*-acetyl-2-(3,5-dinitrobenzoyl)-β-D-glucopyranoside (**264**) (1.0 g, 1.9 mmol) in MeOH:DCM (1:1, 40 mL) was added $PdCl_2$ (36 mg, 0.20 mmol). The reaction mixture was stirred at r.t. for 10 h. The reaction mixture was filtered through Celite® using DCM. The solvent was removed *in vacuo* and the residue was purified *via* flash column chromatography (50–100% Et_2O in pentane) to yield 450 mg (47%) **265** as a yellow foam.

R_f 0.45 (Et_2O); ^{1}H NMR (400MHz, $CDCl_3$): δ_H 9.26 (t, *J* = 2.1 Hz, 1H), 9.15 (d, *J* = 2.0 Hz, 2H), 5.77 (m, 1H), 5.69 (m, 1H), 5.22 (t, *J* = 9.8 Hz, 1H), 5.17 (m, 1H), 4.40–4.28 (m, 2H), 4.19 (dd, *J* = 12.2, 2.1 Hz, 1H), 3.26 (dd, *J* = 3.8, 1.5 Hz, 1H), 2.14 (s, 3H), 2.09 (s, 3H), 2.00 (s, 3H); ^{13}C NMR (100MHz, $CDCl_3$): δ_C 170.7, 170.1, 169.6, 161.8, 148.8, 132.8, 129.7, 122.9, 89.9, 73.5, 69.8, 68.1, 67.4, 61.8, 20.8, 20.7, 20.6.

(4*R*,5*S*)-4,5-bis(benzyloxy)-6-((benzyloxy)methylene)tetrahydro-2*H*-pyran-2-one (268)

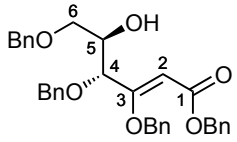


To 2,3,4,6-tetra-*O*-benzyl-2-β-D-glucopyranose (**267**) (270 mg, 0.50 mmol) in THF (2.0 mL) with 4 Å molecular sieves was added *N*-Mes triazolium chloride precatalyst **141** (13 mg,

0.05 mmol), phenazine (90 mg, 0.50 mmol) and DBU (85 µL, 0.55 mmol). The reaction mixture was stirred at r.t. for 12 h. The solvent was removed *in vacuo* and the residue was purified *via* flash column chromatography (20–40% EtOAc in pentane) to yield 45 mg (21%) **268** as a yellow oil.

R_f 0.4 (EtOAc:pentane, 3:2); ^{1}H NMR (400MHz, $CDCl_3$): δ_H 7.48–7.26 (m, 15H, Ar*H*), 5.69 (d, *J* = 4.0 Hz, 1H, C=C*H*), 4.93 (m, 2H, PhCH_2), 4.65–4.47 (m, 6H, 2x PhCH_2 & C*H*C*H*CH_2), 3.77 (dd, *J* = 10.6, 3.8 Hz, 1H, CH_2–a), 3.69 (dd, *J* = 10.6, 4.6 Hz, 1H, CH_2–b); ^{13}C NMR (100MHz, $CDCl_3$): δ_C 159.5, 144.1, 137.5, 137.4, 135.3, 128.7, 128.6, 128.5, 128.3, 128.2, 128.0, 127.9, 127.8, 127.5, 110.2, 79.8, 73.6, 71.2, 70.4, 69.4, 68.3; MS (ESI) *m/z* 453 $[M+Na]^+$.

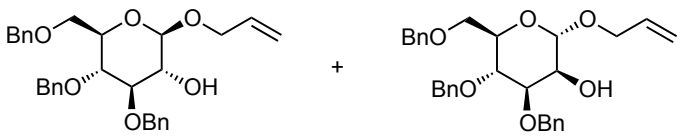
(4*R*,5*R*)-Benzyl 3,4,6-tris(benzyloxy)-5-hydroxyhex-2-enoate (270)



To 2,3,4,6-tetra-*O*-benzyl-2-β-D-glucopyranose (**267**) (270 mg, 0.50 mmol) in MeCN (10 mL) was added *N*-Mes triazolium chloride precatalyst **141** (13 mg, 0.05 mmol) and Cs_2CO_3 (320 mg, 1.0 mmol). The reaction mixture was stirred at r.t. for 12 h. The solvent was removed *in vacuo* and the residue was purified *via* flash column chromatography (20–40% EtOAc in pentane) to yield 115 mg (43%) **270** as a colourless oil.

R_f 0.45 (EtOAc:pentane, 3:2); ^{1}H NMR (400MHz, $CDCl_3$): δ_H 7.46–7.23 (m, 20H), 6.33 (d, *J* = 9.4 Hz, 1H, C*H*–2), 5.31 (m, 2H, PhCH_2), 4.93 (m, 2H, PhCH_2), 4.50 (s, 2H, PhCH_2), 4.45 (m, 1H, C*H*–3), 4.41 (d, *J* = 11.6 Hz, 1H, PhCH_2–a), 4.21 (d, *J* = 11.8 Hz, 1H, PhCH_2–b), 3.87 (m, 1H, C*H*–5), 3.52 (d, *J* = 5.0 Hz, 2H, CH_2–6), 2.34 (d, *J* = 5.4 Hz, 1H, O*H*) ; ^{13}C NMR (100MHz, $CDCl_3$): δ_C 163.0, 147.6, 138.0, 136.5, 135.5, 128.8, 128.7, 128.6, 128.5 (2C), 128.4, 128.3 (2C), 128.2, 127.9, 127.8, 127.7, 127.6, 125.1, 74.2, 73.6, 73.4, 72.2, 70.9, 67.1; HRMS (ESI) calcd. for $C_{34}H_{34}O_6Na$ $[M+Na]^+$: 561.2253; found *m/z*: 561.2228; Δ = −4.5 ppm.

Allyl 3,4,6-tri-*O*-benzyl-β-D-glucopyranoside (273)[288]



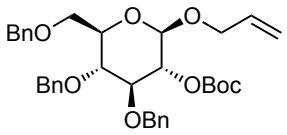
major minor

Following above referenced literature procedure.

To *m*CPBA (⩽77% purity, 7.0 g, 31 mmol) in DCM (360 mL) was added KF (3.5 g, 60 mmol) and the suspension was stirred for 30 min. Tri-*O*-benzyl-D-glucal (**271**) (5.0 g, 12 mmol) in DCM (20 mL) was added dropwise and the reaction mixture stirred at r.t. for 16 h. The solids were removed by filtration and the solvent removed from the filtrate *in vacuo*. The resulting oil was dissolved in THF (20 mL) and the solution was cooled to 0 °C. Allyl alcohol (4.0 mL, 58 mmol) was added followed by 1.0 M $ZnCl_2$ in THF (14 mL, 14 mmol) and the reaction warmed to r.t. and stirred for a further 12 h. Brine (100 mL) was added and the aqueous layer extracted with EtOAc (3x 100 mL). The organic layer was dried over $MgSO_4$ and the solvent removed *in vacuo*. The viscous residue was purified *via* flash column chromatography (30–100% Et_2O in pentane) to yield 4.0 g (68%) **273** as a viscous colourless oil (containing 10% minor stereoisomer allyl 3,4,6-tri-*O*-benzyl-α-D-mannopyranoside).

^{1}H NMR (400MHz, $CDCl_3$): δ_H 7.48–7.25 (m, 13H), 7.20 (m, 2H), 5.98 (ddt, *J* = 16.9, 11.1, 5.8 Hz, 1H), 5.35 (m, 1H), 5.24 (m, 1H), 4.96 (m, 1H), 4.87 (m, 2H), 4.65 (m, 1H), 4.57 (m, 2H), 4.43 (m, 1H), 4.34 (m, 1H), 4.15 (m, 1H), 3.83–3.70 (m, 2H), 3.69–3.55 (m, 3H), 3.51 (m, 1H); ^{13}C NMR (100MHz, $CDCl_3$): δ_C 138.6, 138.1 (2C), 133.9, 128.5, 128.4 (2C), 128.0, 127.8 (2C), 127.7, 117.9, 101.7, 84.6, 77.6, 75.2, 75.1, 75.0, 74.7, 73.5, 70.3, 68.9. ^{13}C spectrum missing two signals, expected in congested region 127.5-128.5, all other signals in good agreement with literature data.

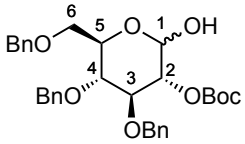
Allyl 3,4,6-tri-*O*-benzyl-2-*O*-(*tert*-butyloxycarbonyl)-β-D-glucopyranoside (278)



To allyl 3,4,6-tri-*O*-benzyl-β-D-glucopyranoside (**276**) (2.0 g, 4.0 mmol) in DCM (4 mL) was added Boc_2O (1.3 g, 6.0 mmol) and DMAP (22 mg, 0.20 mmol). The reaction mixture was stirred at r.t. for 3 h. DCM (10 mL) was added and the organic solution with water (2x 20 mL) and brine (20 mL). The organic layer was dried over $MgSO_4$ and the solvent removed *in vacuo* to yield 2.3 g (96%) **277** as a viscous colourless oil.

^{1}H NMR (400MHz, $CDCl_3$): δ_H 7.40–7.27 (m, 13H), 7.19 (m, 2H), 5.90 (m, 1H), 5.31 (m, 1H), 5.18 (m, 1H), 4.80 (m, 4H), 4.65 (m, 1H), 4.57 (m, 2H) 4.46 (d, *J* = 8.0 Hz, 1H), 4.43–4.36 (m, 1H), 4.09 (m, 1H), 3.78–3.65 (m, 4H), 3.50 (m, 1H), 1.51 (s, 9H).

3,4,6-Tri-*O*-benzyl-2-(*tert*-butyloxycarbonyl)-D-glucopyranose (278)



To allyl 3,4,6-tri-*O*-benzyl-2-*O*-(*tert*-butyloxycarbonyl)-β-D-glucopyranoside (**277**) (2.3 g, 3.9 mmol) in MeOH:DCM (1:1, 80 mL) was added $PdCl_2$ (36 mg, 0.20 mmol). The reaction mixture was stirred at r.t. for 12 h. The reaction mixture was filtered through Celite® using DCM. The solvent was removed *in vacuo* and the residue was purified *via* flash column chromatography (50–100% Et_2O in pentane) to yield 900 mg (42%) **278** as a viscous colourless oil (3:2 mixture of anomers).

Major isomer assigned, correlates well with assignments for 3,4,6-tri-*O*-benzyl-2-*O*-acetyl-α-D-glucopyranose.[311]

R_f 0.2 (Et_2O: pentane, 1:1); ^{1}H NMR (400MHz, $CDCl_3$): δ_H 7.39–7.15 (m, 15H, Ar*H*), 5.45 (m, 1H, C*H*–1), 4.85–4.76 (m, 4H, C*H*–2, 1.5x PhCH_2), 4.65–4.50 (m, 3H, 1.5x PhCH_2), 4.12–4.04 (m, 2H, C*H*–3 & C*H*–4), 3.77–3.63 (m, 2H, C*H*–5, C*H*–6a), 3.56–3.47 (m, 1H, C*H*–6b), 2.83 (m, 1H, O*H*), 1.49 (s, 9H, C(CH_3)$_3$).

References

(1) Burns, C. J.; Wilks, A. F. *Expert Opin. Ther. Pat.* **2011**, *21*, 147–165.

(2) Pixley, F. J.; Stanley, E. R. *Trends Cell Biol.* **2004**, *14*, 628–638.

(3) Sacca, R.; Stanley, E. R.; Sherr, C. J.; Rettenmier, C. W. *Proc. Natl. Acad. Sci. U. S. A.* **1986**, *83*, 3331–3335.

(4) Sapi, E. *Exp. Biol. Med.* **2004**, *229*, 1–11.

(5) Stanley, E. R.; Berg, K. L.; Einstein, D. B.; Lee, P. S.; Pixley, F. J.; Wang, Y.; Yeung, Y. G. *Mol. Reprod. Dev.* **1997**, *46*, 4–10.

(6) Walter, M.; Lucet, I. S.; Patel, O.; Broughton, S. E.; Bamert, R.; Williams, N. K.; Fantino, E.; Wilks, A. F.; Rossjohn, J. *J. Mol. Biol.* **2007**, *367*, 839–847.

(7) Bikker, J. A; Brooijmans, N.; Wissner, A.; Mansour, T. S. *J. Med. Chem.* **2009**, *52*, 1493–1509.

(8) Patch, R. J.; Brandt, B. M.; Asgari, D.; Baindur, N.; Chadha, N. K.; Georgiadis, T.; Cheung, W. S.; Petrounia, I. P.; Donatelli, R. R.; Chaikin, M. a; Player, M. R. *Bioorg. Med. Chem. Lett.* **2007**, *17*, 6070–6074.

(9) Mashkani, B.; Griffith, R.; Ashman, L. K. *Bioorg. Med. Chem.* **2010**, *18*, 1789–1797.

(10) Chitu, V.; Stanley, E. R. *Curr. Opin. Immunol.* **2006**, *18*, 39–48.

(11) Pollard, J. W. *Nat. Rev. Immunol.* **2009**, *9*, 259–270.

(12) Mantovani, A.; Sozzani, S.; Locati, M.; Allavena, P.; Sica, A. *Trends Immunol.* **2002**, *23*, 549–555.

(13) Brownlow, N.; Mol, C.; Hayford, C.; Ghaem-Maghami, S.; Dibb, N. J. *Leukemia* **2009**, *23*, 590–594.

(14) Pollard, J. W. *Nat. Rev. Cancer* **2004**, *4*, 71–78.

(15) Qian, B.-Z.; Pollard, J. W. *Cell* **2010**, *141*, 39–51.

(16) Bergers, G.; Benjamin, L. E. *Nat. Rev. Cancer* **2003**, *3*, 401–410.

(17) Hanahan, D.; Weinberg, R. A.; Francisco, S. *Cell* **2000**, *100*, 57–70.

(18) Hanahan, D.; Weinberg, R. A. *Cell* **2011**, *144*, 646–674.

(19) Xu, L. B.; Sun, W.; Liu, H. Y.; Wang, L. L.; Xiao, J. H.; Yang, X. H.; Li, S. *Chin. Chem. Lett.* **2010**, *21*, 1318–1321.

(20) Lin, E. Y.; Nguyen, a V; Russell, R. G.; Pollard, J. W. *J. Exp. Med.* **2001**, *193*, 727–740.

(21) Campbell, I. K.; Rich, M. J.; Bischof, R. J.; Hamilton, J. A. *J. Leukocyte Biol.* **2000**, *68*, 144–150

(22) Dewar, A. L.; Zannettino, A. C. W.; Lyons, A. B. *Cell Cycle* **2005**, 851–853.

(23) El Hajj Dib, I.; Gallet, M.; Mentaverri, R.; Sévenet, N.; Brazier, M.; Kamel, S. *Eur. J. Pharmacol.* **2006**, *551*, 27–33.

(24) Manning, G.; Whyte, D. B.; Martinez, R.; Hunter, T.; Sudarsanam, S. *Science* **2002**, *298*, 1912–1934.

(25) Zhang, J.; Yang, P. L.; Gray, N. S. *Nat. Rev. Cancer* **2009**, *9*, 28–39.

(26) Cowan-Jacob, S. W.; Möbitz, H.; Fabbro, D. *Curr. Opin. Cell Biol.* **2009**, *21*, 280–287.

(27) Peng, Y.-H.; Shiao, H.-Y.; Tu, C.-H.; Liu, P.-M.; Hsu, J. T.-A.; Amancha, P. K.; Wu, J.-S.; Coumar, M. S.; Chen, C.-H.; Wang, S.-Y.; Lin, W.-H.; Sun, H.-Y.; Chao, Y.-S.; Lyu, P.-C.; Hsieh, H.-P.; Wu, S. *J. Med. Chem.* **2013**, *56*, 3889–3903.

(28) Zuccotto, F.; Ardini, E.; Casale, E.; Angiolini, M. *J. Med. Chem.* **2010**, *53*, 2681–2694.

(29) Liu, Y.; Gray, N. S. *Nat. Chem. Biol.* **2006**, *2*, 358–364.

(30) Schubert, C.; Schalk-Hihi, C.; Struble, G. T.; Ma, H.-C.; Petrounia, I. P.; Brandt, B.; Deckman, I. C.; Patch, R. J.; Player, M. R.; Spurlino, J. C.; Springer, B. A. *J. Biol. Chem.* **2007**, *282*, 4094–4101.

(31) Head, M. S. In *Drug Design*; Merz, K. M.; Ringe, D.; Reynolds, C. H., Eds.; Cambridge University Press, **2010**; pp. 98–119.

(32) http://www.rcsb.org/pdb/.

(33) Höltje, H.-D.; Sippl, W.; Rognan, D.; Folkers, G. In *Molecular Modeling*; Wiley-VCH Verlag GmbH & Co., **2008**; pp. 181–216.

(34) Kitchen, D. B.; Decornez, H.; Furr, J. R.; Bajorath, J. *Nat. Rev. Drug Discov.* **2004**, *3*, 935–949.

(35) Friesner, R. a; Banks, J. L.; Murphy, R. B.; Halgren, T. a; Klicic, J. J.; Mainz, D. T.; Repasky, M. P.; Knoll, E. H.; Shelley, M.; Perry, J. K.; Shaw, D. E.; Francis, P.; Shenkin, P. S. *J. Med. Chem.* **2004**, *47*, 1739–1749.

(36) http://www.schrodinger.com/.

(37) Warren, G. L.; Andrews, C. W.; Capelli, A.-M.; Clarke, B.; LaLonde, J.; Lambert, M. H.; Lindvall, M.; Nevins, N.; Semus, S. F.; Senger, S.; Tedesco, G.; Wall, I. D.; Woolven, J. M.; Peishoff, C. E.; Head, M. S. *J. Med. Chem.* **2006**, *49*, 5912–5931.

(38) Tresadern, G.; Bemporad, D.; Howe, T. *J. Mol. Graph. Model.* **2009**, *27*, 860–870.

(39) Cheeseright, T. J.; Mackey, M. D.; Melville, J. L.; Vinter, J. G. *J. Chem. Inf. Model.* **2008**, *48*, 2108–2117.

(40) Cheeseright, T.; Mackey, M.; Rose, S.; Vinter, A. *J. Chem. Inf. Model.* **2006**, *46*, 665–676.

(41) Bellenie, B. R.; Barton, N. P.; Emmons, A. J.; Heer, J. P.; Salvagno, C. *Bioorg. Med. Chem. Lett.* **2009**, *19*, 990–994.

(42) Fernández, A.; Crespo, A.; Tiwari, A. *Drug Discov. Today* **2009**, *14*, 1–5.

(43) Meyers, M. J.; Pelc, M.; Kamtekar, S.; Day, J.; Poda, G. I.; Hall, M. K.; Michener, M. L.; Reitz, B. a; Mathis, K. J.; Pierce, B. S.; Parikh, M. D.; Mischke, D. a; Long, S. a; Parlow, J. J.; Anderson, D. R.; Thorarensen, A. *Bioorg. Med. Chem. Lett.* **2010**, *20*, 1543–1547.

(44) Huang, H.; Hutta, D. A.; Rinker, J. M.; Hu, H.; Parsons, W. H.; Schubert, C.; DesJarlais, R. L.; Crysler, C. S.; Chaikin, M. A.; Donatelli, R. R.; Chen, Y.; Cheng, D.; Zhou, Z.; Yurkow, E.; Manthey, C. L.; Player, M. R. *J. Med. Chem.* **2009**, *52*, 1081–1099.

(45) Harris, J.; Church, N.; Proud, A.; Kling, M.; Vickery, B. D. WO 2004/085409 A2, **2004**.

(46) Hashimoto, N.; Aoyama, T.; Shioiri, T. *Chem. Pharm. Bull.* **1981**, *29*, 1475–1478.

(47) Kühnel, E.; Laffan, D. D. P.; Lloyd-Jones, G. C.; Martínez Del Campo, T.; Shepperson, I. R.; Slaughter, J. L. *Angew. Chem. Int. Ed.* **2007**, *46*, 7075–7078.

(48) Basha, A.; Lipton, M.; Weinreb, S. M. *Tetrahedron Lett.* **1977**, *48*, 4171–4174.

(49) Novak, A.; Humphreys, L. D.; Walker, M. D.; Woodward, S. *Tetrahedron Lett.* **2006**, *47*, 5767–5769.

(50) Bassett, H. L.; Thomas, C. R. *J. Chem. Soc.* **1954**, 1188–1190.

(51) Miller, W. H.; Pendrak, I.; Seefeld, M. A. WO 2006/002047 A2, **2006**.

(52) Huang, H.; Hutta, D. a; Hu, H.; DesJarlais, R. L.; Schubert, C.; Petrounia, I. P.; Chaikin, M. a; Manthey, C. L.; Player, M. R. *Bioorg. Med. Chem. Lett.* **2008**, *18*, 2355–2361.

(53) Player, M. R.; Parsons, W. H.; Huang, H.; Hutta, D. A.; Hu, H.; Rinker, J. US 2008/114007 A1, **2008**.

(54) Hajduk, P. J.; Greer, J. *Nat. Rev. Drug Discov.* **2007**, *6*, 211–219.

(55) Hopkins, A. L.; Groom, C. R.; Alex, A. *Drug Discov. Today* **2004**, *9*, 430–431.

(56) Plant, N.; Abad-Zapatero, C.; Metz, J. T. *Drug Discov. Today* **2005**, *10*, 464–469.

(57) Reynolds, C. H.; Bembenek, S. D.; Tounge, B. A. *Bioorg. Med. Chem. Lett.* **2007**, *17*, 4258–4261.

(58) Williams, D. P.; Park, B. K. *Drug Discov. Today* **2003**, *8*, 1044–1050.

(59) Park, K.; Williams, D. P.; Naisbitt, D. J.; Kitteringham, N. R.; Pirmohamed, M. *Toxicol. Appl. Pharmacol.* **2005**, *207*, 425–434.

(60) Kazius, J.; McGuire, R.; Bursi, R. *J. Med. Chem.* **2005**, *48*, 312–320.

(61) Williams, D. P. *Toxicology* **2006**, *226*, 1–11.

(62) Hann, M. M. *Med. Chem. Commun.* **2011**, *2*, 349–355.

(63) Tarcsay, A.; Nyíri, K.; Keseru, G. M. *J. Med. Chem.* **2012**, *55*, 1252–1260.

(64) Lipinski, C. A.; Lombardo, F.; Dominy, B. W.; Feeney, P. J. *Adv. Drug Deliv. Rev.* **2001**, *46*, 3–26.

(65) Yan, L.; Müller, C. E. *J. Med. Chem.* **2004**, *47*, 1031–1043.

(66) Li, L.; Liu, J.; Zhu, L.; Cutler, S.; Hasegawa, H.; Shan, B.; Medina, J. C. *Bioorg. Med. Chem. Lett.* **2006**, *16*, 1638–1642.

(67) Staab, H. A. *Angew. Chemie Int. Ed.* **1962**, *1*, 351–367.

(68) Robak, M. T.; Herbage, M. A.; Ellman, J. A. *Chem. Rev.* **2010**, *110*, 3600–3740.

(69) Morton, D.; Stockman, R. A. *Tetrahedron* **2006**, *62*, 8869–8905.

(70) Naskar, D.; Roy, A.; Seibel, W. L.; Portlock, D. E. *Tetrahedron Lett.* **2003**, *44*, 8865–8868.

(71) Batey, R. A.; MacKay, D. B.; Santhakumar, V. *J. Am. Chem. Soc.* **1999**, *121*, 5075–5076.

(72) Morgan, I. R.; Yazici, A.; Pyne, S. G. *Tetrahedron* **2008**, *64*, 1409–1419.

(73) Jin, S.-S.; Wang, H.; Zhu, T.-S.; Xu, M.-H. *Org. Biomol. Chem.* **2012**, *10*, 1764–1768.

(74) Lv, X.; Xiang, Q.; Zeng, Q. *Org. Prep. Proced. Int.* **2014**, *46*, 164–175.

(75) Klunder, J. M.; Posner, G. H. In *Comprehensive Organic Chemistry, Vol. 3*; Trost, B. M.; Fleming, I., Eds.; Pergamon Press, Oxford, **1991**; pp. 207–239.

(76) Mori, S.; Nakamura, E. In *Modern Organocopper Chemistry*; Krause, N., Ed.; Wiley-VCH Verlag GmbH & Co., **2002**; pp. 315–346.

(77) Vaillancourt, V.; Albizati, K. F. *J. Org. Chem.* **1992**, *57*, 3627–3631.

(78) Allen, C. F. H.; Beilfuss, H. R.; Burness, D. M.; Reynolds, G. A.; Tinker, J. F.; VanAllan, J. A. *J. Org. Chem.* **1959**, *24*, 779–787.

(79) Allen, C. F. H.; Reynolds, G. A.; Tinker, J. F.; Williams, L. A. *J. Org. Chem.* **1960**, *25*, 361–366.

(80) Williams, L. A. *J. Chem. Soc.* **1961**, 3046–3052.

(81) Reimlinger, H.; Peiren, M. A. *Chem. Ber.* **1970**, *103*, 3266–3277.

(82) Beckett, A. H.; Spickett, R. G. W.; Wright, S. H. B. *Tetrahedron* **1968**, *24*, 2839–2850.

(83) Yamamoto, Y. *Chem. Rev.* **2008**, *108*, 3199–3222.

(84) Schäfer, C.; Miesch, M.; Miesch, L. *Chem. Eur. J.* **2012**, *18*, 8028–8031.

(85) Li, S.; Li, Z.; Yuan, Y.; Li, Y.; Zhang, L.; Wu, Y. *Chem. Eur. J.* **2013**, *19*, 1496–1501.

(86) Kirmse, W. *Angew. Chem. Int. Ed.* **2004**, *43*, 1767–1769.

(87) De Frémont, P.; Marion, N.; Nolan, S. P. *Coord. Chem. Rev.* **2009**, *253*, 862–892.

(88) Rice, F. O.; Glaserbrook, A. L. *J. Am. Chem. Soc.* **1934**, *56*, 2381–2383.

(89) Enders, D.; Niemeier, O.; Henseler, A. *Chem. Rev.* **2007**, *107*, 5606–5655.

(90) Nelson, D. J.; Nolan, S. P. In *N-Heterocyclic Carbenes: Effective Tools for Organometallic Synthesis*; Nolan, S. P., Ed.; Wiley-VCH Verlag GmbH & Co., **2014**; pp. 1–22.

(91) Hopkinson, M. N.; Richter, C.; Schedler, M.; Glorius, F. *Nature* **2014**, *510*, 485–496.

(92) Bourissou, D.; Guerret, O.; Gabbaï, F. P.; Bertrand, G. *Chem. Rev.* **2000**, *100*, 39–91.

(93) Hahn, F. E.; Jahnke, M. C. *Angew. Chem. Int. Ed.* **2008**, *47*, 3122–3172.

(94) Doering, W. von E.; Hoffmann, K. A. *J. Am. Chem. Soc.* **1954**, *76*, 6162–6165.

(95) Fischer, E. O.; Maasböl, A. *Angew. Chem. Int. Ed.* **1964**, *3*, 580–581.

(96) Igau, A.; Grutzmacher, H.; Baceiredo, A.; Bertrand, G. *J. Am. Chem. Soc.* **1988**, *110*, 6463–6466.

(97) Arduengo, A. J.; Harlow, R. L.; Kline, M. *J. Am. Chem. Soc.* **1991**, *113*, 361–363.

(98) Wanzlick, H.-W. *Angew. Chemie Int. Ed.* **1962**, *1*, 75–80.

(99) Wanzlick, H.-W.; Schönherr, H.-J. *Angew. Chemie Int. Ed.* **1968**, *7*, 141–142.

(100) Öfele, K. *J. Organomet. Chem.* **1968**, *12*, 42–43.

(101) Hitchcock, P. B.; Lappert, M. F.; Pye, P. L.; Thomas, S. *J. Chem. Soc., Dalt. Trans.* **1979**, 1929–1942.

(102) Cardin, D. J.; Cetinkaya, B.; Lappert, M. F. *Chem. Rev.* **1972**, *72*, 545–574.

(103) Nelson, D. J.; Nolan, S. P. *Chem. Soc. Rev.* **2013**, *42*, 6723–6753.

(104) Pauling, L. *J. Chem. Soc., Chem. Comm.* **1980**, 688–689.

(105) Böhm, V. P. W.; Herrmann, W. A. *Angew. Chemie Int. Ed.* **2000**, *39*, 4036–4038.

(106) Lemal, D. M.; Lovald, R. A.; Kawano, K. I. *J. Am. Chem. Soc.* **1964**, *86*, 2518–2519.

(107) Winberg, H. E.; Carnahan, J. E.; Coffman, D. D.; Brown, M. *J. Am. Chem. Soc.* **1965**, *87*, 2055–2056.

(108) Denk, M. K.; Hatano, K.; Ma, M. *Tetrahedron Lett.* **1999**, *40*, 2057–2060.

(109) Hahn, F. E.; Wittenbecher, L.; Van, D. Le; Fröhlich, R. *Angew. Chemie Int. Ed.* **2000**, *39*, 541–544.

(110) Liu, Y.; Lindner, P. E.; Lemal, D. M. *J. Am. Chem. Soc.* **1999**, *121*, 10626–10627.

(111) Liu, Y.; Lemal, D. M. *Tetrahedron Lett.* **2000**, *41*, 599–602.

(112) Kirmse, W. *Angew. Chem. Int. Ed.* **2010**, *49*, 8798–8801.

(113) Alder, R. W.; Blake, M. E.; Chaker, L.; Harvey, J. N.; Paolini, F.; Schütz, J. *Angew. Chem. Int. Ed.* **2004**, *43*, 5896–5911.

(114) Jahnke, M. C.; Hahn, F. E. In *N-Heterocyclic Carbenes: From Laboratory Curiosities to Efficient Synthetic Tools*; Díez-González, S., Ed.; RSC Publishing, **2011**; pp. 1–41.

(115) Arduengo, A. J.; Goerlich, J. R.; Marshall, W. J. *J. Am. Chem. Soc.* **1995**, *117*, 11027–11028.

(116) Herrmann, W. A.; Köcher, C. *Angew. Chemie Int. Ed.* **1997**, *36*, 2162–2187.

(117) Heinemann, C.; Mu, T.; Apeloig, Y. *J. Am. Chem. Soc.* **1996**, *118*, 2023–2038.

(118) Sauers, R. R. *Tetrahedron Lett.* **1996**, *37*, 149–152.

(119) Tafipolsky, M.; Scherer, W.; Öfele, K.; Artus, G.; Pedersen, B.; Herrmann, W. A.; McGrady, G. S. *J. Am. Chem. Soc.* **2002**, *124*, 5865–5880.

(120) Arduengo, A. J.; Dias, H. V. R.; Harlow, R. L.; Kline, M. *J. Am. Chem. Soc.* **1992**, *114*, 5530–5534.

(121) Breslow, R. *J. Am. Chem. Soc.* **1958**, *80*, 3719–3726.

(122) Arduengo, A. J.; Dias, H. V. R.; Dixon, D. A.; Harlow, R. L.; Klooster, W. T.; Koetzle, T. F. *J. Am. Chem. Soc.* **1994**, *116*, 6812–6822.

(123) Arduengo, A. J.; Dixon, D. A.; Kumashiro, K. K.; Lee, C.; Power, W. P. *J. Am. Chem. Soc.* **1994**, *116*, 6361–6367.

(124) Boehme, C.; Frenking, G. *J. Am. Chem. Soc.* **1996**, *118*, 2039–2046.

(125) Dröge, T.; Glorius, F. *Angew. Chem. Int. Ed.* **2010**, *49*, 6940–6952.

(126) Bantreil, X.; Nolan, S. P. *Nat. Protoc.* **2011**, *6*, 69–77.

(127) Benhamou, L.; Chardon, E.; Lavigne, G.; Bellemin-Laponnaz, S.; César, V. *Chem. Rev.* **2011**, *111*, 2705–2733.

(128) Kuhn, N.; Kratz, T. *Synthesis* **1993**, *6*, 562–562.

(129) Otto, M.; Conejero, S.; Canac, Y.; Romanenko, V. D.; Rudzevitch, V.; Bertrand, G. *J. Am. Chem. Soc.* **2004**, *126*, 1016–1017.

(130) Nyce, G. W.; Csihony, S.; Waymouth, R. M.; Hedrick, J. L. *Chem. Eur. J.* **2004**, *10*, 4073–4079.

(131) Voutchkova, A. M.; Feliz, M.; Clot, E.; Eisenstein, O.; Crabtree, R. H. *J. Am. Chem. Soc.* **2007**, *129*, 12834–12846.

(132) Nyce, G. W.; Glauser, T.; Connor, E. F.; Möck, A.; Waymouth, R. M.; Hedrick, J. L. *J. Am. Chem. Soc.* **2003**, *125*, 3046–3056.

(133) Herrmann, W. a. *Angew. Chem. Int. Ed.* **2002**, *41*, 1290–1309.

(134) Crabtree, R. H. *J. Organomet. Chem.* **2005**, *690*, 5451–5457.

(135) Crudden, C. M.; Allen, D. P. *Coord. Chem. Rev.* **2004**, *248*, 2247–2273.

(136) Kühl, O. In *Functionalised N-Heterocyclic Carbene Complexes*; Kühl, O., Ed.; John Wiley & Sons, Ltd, **2010**; pp. 7–37.

(137) Díez-González, S.; Nolan, S. P. *Coord. Chem. Rev.* **2007**, *251*, 874–883.

(138) Scholl, M.; Ding, S.; Lee, C. W.; Grubbs, R. H. *Org. Lett.* **1999**, *1*, 953–956.

(139) Kingsbury, J. S.; Harrity, J. P. A.; Bonitatebus, P. J.; Hoveyda, A. H.; Hill, C.; September, R. V. *J. Am. Chem. Soc.* **1999**, *121*, 791–799.

(140) Nasielski, J.; Hadei, N.; Achonduh, G.; Kantchev, E. A. B.; O'Brien, C. J.; Lough, A.; Organ, M. G. *Chem. Eur. J.* **2010**, *16*, 10844–10853.

(141) Kantchev, E. A. B.; O'Brien, C. J.; Organ, M. G. *Angew. Chem. Int. Ed.* **2007**, *46*, 2768–2813.

(142) Vougioukalakis, G. C.; Grubbs, R. H. *Chem. Rev.* **2010**, *110*, 1746–1787.

(143) Curran, D. P.; Solovyev, A.; Makhlouf Brahmi, M.; Fensterbank, L.; Malacria, M.; Lacôte, E. *Angew. Chem. Int. Ed. Engl.* **2011**, *50*, 10294–10317.

(144) Murphy, L. J.; Robertson, K. N.; Masuda, J. D.; Clyburne, J. A. C. In *N-Heterocyclic Carbenes: Effective Tools for Organometallic Synthesis*; Nolan, S. P., Ed.; Wiley-VCH Verlag GmbH & Co., **2014**; pp. 427–498.

(145) Kuhn, N.; Alsheikh, a. *Coord. Chem. Rev.* **2005**, *249*, 829–857.

(146) Dyker, C. A.; Bertrand, G. *Science* **2008**, *321*, 1050–1051.

(147) Wang, Y.; Xie, Y.; Wei, P.; King, R. B.; Schaefer, H. F.; von R Schleyer, P.; Robinson, G. H. *Science* **2008**, *321*, 1069–1071.

(148) Fensterbank, L.; Malacria, M.; Curran, D. P. *J. Am. Chem. Soc.* **2008**, *130*, 10082–10083.

(149) Kolychev, E. L.; Bannenberg, T.; Freytag, M.; Daniliuc, C. G.; Jones, P. G.; Tamm, M. *Chem. Eur. J.* **2012**, *18*, 16938–16946.

(150) Fuchter, M. J. *Chem. Eur. J.* **2010**, *16*, 12286–12294.

(151) Marion, N.; Díez-González, S.; Nolan, S. P. *Angew. Chem. Int. Ed.* **2007**, *46*, 2988–3000.

(152) Enders, D.; Niemeier, O.; Henseler, A. *Chem. Rev.* **2007**, *107*, 5606–5655.

(153) Ukai, T.; Tanaka, R.; Dokawa, T. *J. Pharm. Soc. Jpn.* **1943**, *63*, 269–300.

(154) Lapworth, A. *J. Chem. Soc., Trans* **1904**, *85*, 1206–1214.

(155) Berkessel, A.; Elfert, S.; Yatham, V. R.; Neudörfl, J.-M.; Schlörer, N. E.; Teles, J. H. *Angew. Chem. Int. Ed.* **2012**, *51*, 12370–12374.

(156) Bugaut, X.; Glorius, F. *Chem. Soc. Rev.* **2012**, *41*, 3511–3522.

(157) Grossmann, A.; Enders, D. *Angew. Chemie Int. Ed.* **2011**, n/a–n/a.

(158) Biju, A. T.; Kuhl, N.; Glorius, F. *Acc. Chem. Res.* **2011**, *44*, 1182–1195.

(159) Ryan, S. J.; Candish, L.; Lupton, D. W. *Chem. Soc. Rev.* **2013**, *42*, 4906–4917.

(160) Stetter, H.; Rämsch, R. Y.; Kuhlmann, H. *Synthesis* **1976**, *11*, 733–735.

(161) Matsumoto, T.; Ohishi, M.; Inoue, S. *J. Org. Chem.* **1985**, *50*, 603–606.

(162) Sheehan, J. C.; Hunneman, D. H. *J. Am. Chem. Soc.* **1966**, *88*, 3666–3667.

(163) Enders, D.; Kallfass, U. *Angew. Chem. Int. Ed.* **2002**, *41*, 1743–1745.

(164) Stetter, H. *Angew. Chemie Int. Ed.* **1976**, *15*, 639–712.

(165) Christmann, M. *Angew. Chem. Int. Ed.* **2005**, *44*, 2632–2634.

(166) Bode, J. W. *Nat. Chem.* **2013**, *5*, 813–815.

(167) De Sarkar, S.; Biswas, A.; Samanta, R. C.; Studer, A. *Chem. Eur. J.* **2013**, *19*, 4664–4678.

(168) Mahatthananchai, J.; Bode, J. W. *Acc. Chem. Res.* **2014**, *47*, 696–707.

(169) Zeitler, K. *Angew. Chem. Int. Ed. Engl.* **2005**, *44*, 7506–7510.

(170) Chan, A.; Scheidt, K. A. *Org. Lett.* **2005**, *7*, 905–908.

(171) Chen, S.; Hao, L.; Zhang, Y.; Tiwari, B.; Chi, Y. R. *Org. Lett.* **2013**, *15*, 5822–5825.

(172) Hao, L.; Chen, S.; Xu, J.; Tiwari, B.; Fu, Z.; Li, T.; Lim, J.; Chi, Y. R. *Org. Lett.* **2013**, *15*, 4956–4959.

(173) Fu, Z.; Xu, J.; Zhu, T.; Leong, W. W. Y.; Chi, Y. R. *Nat. Chem.* **2013**, *5*, 835–839.

(174) Zhang, B.; Feng, P.; Cui, Y.; Jiao, N. *Chem. Commun.* **2012**, *48*, 7280–7282.

(175) Uno, T.; Inokuma, T.; Takemoto, Y. *Chem. Commun.* **2012**, *48*, 1901-1903.

(176) Samanta, R. C.; De Sarkar, S.; Fröhlich, R.; Grimme, S.; Studer, A. *Chem. Sci.* **2013**, *4*, 2177.

(177) Thomson, J. E.; Rix, K.; Smith, A. D. *Org. Lett.* **2006**, *8*, 3785–3788.

(178) Bode, J. W.; Sohn, S. S. *J. Am. Chem. Soc.* **2007**, *129*, 13798–13799.

(179) Guin, J.; De Sarkar, S.; Grimme, S.; Studer, A. *Angew. Chem. Int. Ed.* **2008**, *47*, 8727–8730.

(180) Zhao, Y.-M.; Cheung, M. S.; Lin, Z.; Sun, J. *Angew. Chem. Int. Ed.* **2012**, *51*, 10359–10363.

(181) Douglas, J.; Ling, K. B.; Concellón, C.; Churchill, G.; Slawin, A. M. Z.; Smith, A. D. *Eur. J. Org. Chem.* **2010**, 5863–5869.

(182) He, M.; Struble, J. R.; Bode, J. W. *J. Am. Chem. Soc.* **2006**, *128*, 8418–8420.

(183) Davies, A. T.; Taylor, J. E.; Douglas, J.; Collett, C. J.; Morrill, L. C.; Fallan, C.; Slawin, A. M. Z.; Churchill, G.; Smith, A. D. *J. Org. Chem.* **2013**, *78*, 9243–9257.

(184) Davies, A. T.; Pickett, P. M.; Slawin, A. M. Z.; Smith, A. D. *ACS Catal.* **2014**, *4*, 2696–2700.

(185) Taylor, J. E.; Daniels, D. S. B.; Smith, A. D. *Org. Lett.* **2013**, *15*, 6058–6061.

(186) Duguet, N.; Campbell, C. D.; Slawin, A. M. Z.; Smith, A. D. *Org. Biomol. Chem.* **2008**, *6*, 1108–1113.

(187) Zhang, Y.-R.; He, L.; Wu, X.; Shao, P.-L.; Ye, S. *Org. Lett.* **2008**, *10*, 277–280.

(188) Douglas, J.; Churchill, G.; Smith, A. *Synthesis* **2012**, *44*, 2295–2309.

(189) Kaeobamrung, J.; Kozlowski, M. C.; Bode, J. W. *Proc. Natl. Acad. Sci. U. S. A.* **2010**, *107*, 20661–20665.

(190) Nair, V.; Vellalath, S.; Babu, B. P. *Chem. Soc. Rev.* **2008**, *37*, 2691–2698.

(191) Struble, J. R.; Kaeobamrung, J.; Bode, J. W. *Org. Lett.* **2008**, *10*, 957–960.

(192) Morrill, L. C.; Smith, A. D. *Chem. Soc. Rev.* **2014**, *43*, 6214–6226.

(193) Carbenes, N.; Kano, T.; Sasaki, K.; Maruoka, K. *Org. Lett.* **2005**, *7*, 2004–2006.

(194) Sun, X.; Ye, S.; Wu, J. *Eur. J. Org. Chem.* **2006**, 4787–4790.

(195) Chiang, P.-C.; Rommel, M.; Bode, J. W. *J. Am. Chem. Soc.* **2009**, *131*, 8714–8718.

(196) Zhang, J.; Xing, C.; Tiwari, B.; Chi, Y. R. *J. Am. Chem. Soc.* **2013**, *135*, 8113–8116.

(197) Reynolds, N. T.; Read de Alaniz, J.; Rovis, T. *J. Am. Chem. Soc.* **2004**, *126*, 9518–9519.

(198) Chow, K. Y.-K.; Bode, J. W. *J. Am. Chem. Soc.* **2004**, *126*, 8126–8127.

(199) Vora, H. U.; Wheeler, P.; Rovis, T. *Adv. Synth. Catal.* **2012**, *354*, 1617–1639.

(200) Sohn, S. S.; Bode, J. W. *Org. Lett.* **2005**, *7*, 3873–3876.

(201) Ling, K. B.; Smith, A. D. *Chem. Commun.* **2011**, *47*, 373–375.

(202) Sohn, S. S.; Bode, J. W. *Angew. Chem. Int. Ed.* **2006**, *45*, 6021–6024.

(203) Reynolds, N. T.; Rovis, T. *J. Am. Chem. Soc.* **2005**, *127*, 16406–16407.

(204) Thai, K.; Wang, L.; Dudding, T.; Bilodeau, F.; Gravel, M. *Org. Lett.* **2010**, *12*, 5708–5711.

(205) Li, G.-Q.; Li, Y.; Dai, L.; You, S. *Org. Lett.* **2007**, *9*, 3519–3521.

(206) Li, G.-Q.; Li, Y.; Dai, L.-X.; You, S.-L. *Adv. Synth. Catal.* **2008**, *350*, 1258–1262.

(207) Vora, H. U.; Rovis, T. *J. Am. Chem. Soc.* **2007**, *129*, 13796–13797.

(208) Gondo, C.; Bode, J. *Synlett* **2013**, *24*, 1205–1210.

(209) Binanzer, M.; Hsieh, S.-Y.; Bode, J. W. *J. Am. Chem. Soc.* **2011**, *133*, 19698–19701.

(210) Owen, T. C.; Richards, A. *J. Am. Chem. Soc.* **1987**, *109*, 2520–2521.

(211) De Sarkar, S.; Grimme, S.; Studer, A. *J. Am. Chem. Soc.* **2010**, *132*, 1190–1191.

(212) Miyashita, A.; Suzuki, Y.; Nagasaki, I.; Ishiguro, C.; Iwamoto, K.; Higashino, T. *Chem. Pharm. Bull.* **1997**, *45*, 1254–1258.

(213) Chiang, P.-C.; Kim, Y.; Bode, J. W. *Chem. Commun.* **2009**, 4566–4568.

(214) Iwahana, S.; Iida, H.; Yashima, E. *Chem. Eur. J.* **2011**, *17*, 8009–8013.

(215) Lu, S.; Poh, S. B.; Zhao, Y. *Angew. Chem. Int. Ed.* **2014**, *53*, 11041–11045.

(216) Greene, T. W.; Wuts, P. G. M. In *Protective Groups in Organic Synthesis*; John Wiley & Sons, Inc., **1999**; pp. 494–653.

(217) Amarnath, V.; Broom, A. D. *Chem. Rev.* **1977**, *77*, 183–217.

(218) Minami, I.; Ohashi, Y.; Shimizu, I.; Tsuji, J. *Tetrahedron Lett.* **1985**, *26*, 2449–2452.

(219) Tseng, C. C.; Paisley, S. D.; Goering, H. L. *J. Org. Chem.* **1986**, *51*, 2884–2891.

(220) Okamoto, S.; Tominaga, S.; Saino, N.; Kase, K.; Shimoda, K. *J. Organomet. Chem.* **2005**, *690*, 6001–6007.

(221) Tseng, C. C.; Yen, S.-J.; Goering, H. L. *J. Org. Chem.* **1986**, *51*, 2892–2895.

(222) Denmark, S. E.; Marble, L. K. *J. Org. Chem.* **1990**, *55*, 1984–1986.

(223) Dong, X.; Zhao, Y.-M.; Sun, J. *Synlett* **2013**, *24*, 1221–1224.

(224) Dong, X.; Sun, J. *Org. Lett.* **2014**, *16*, 2450–2453.

(225) Chen, X.-Y.; Xia, F.; Cheng, J.-T.; Ye, S. *Angew. Chem. Int. Ed.* **2013**, *52*, 10644–10647.

(226) Pappo, R.; Allen, D. S.; Lemieux, R. U.; Johnson, W. S. *J. Org. Chem.* **1956**, *21*, 478–479.

(227) Robinson, A.; Aggarwal, V. K. *Angew. Chem. Int. Ed.* **2010**, *49*, 6673–6675.

(228) Sharpless, K. B.; Amberg, W.; Bennani, Y. L.; Crispino, G. A.; Hartung, J.; Jeong, K.-S.; Kwong, H.-L.; Morikawa, K.; Want, Z.-M.; Xu, D.; Zhang, X.-L. *J. Org. Chem.* **1992**, *57*, 2768–2771.

(229) Mahatthananchai, J.; Bode, J. W. *Chem. Sci.* **2012**, *3*, 192.

(230) Collett, C. J.; Massey, R. S.; Maguire, O. R.; Batsanov, A. S.; O'Donoghue, A. C.; Smith, A. D. *Chem. Sci.* **2013**, *4*, 1514.

(231) Massey, R. S.; Collett, C. J.; Lindsay, A. G.; Smith, A. D.; Donoghue, A. C. O. *J. Am. Chem. Soc.* **2012**, *134*, 20421–20432.

(232) Kerr, M. S.; Alaniz, J. R. De; Rovis, T. *J. Org. Chem.* **2005**, *70*, 5725–5728.

(233) Brown Ripin, D. H. In *Practical Synthetic Organic Chemistry*; Caron, S., Ed.; John Wiley & Sons, Inc., **2011**; pp. 771–804.

(234) Martin, G.; Mäki-Arvela, P.; Murzin, D. Y.; Salmi, T. *Catal. Sci. Technol.* **2014**, *4*, 170.

(235) Cox, B. G. *Acids and Bases: Solvent Effects on Acid–Base Strength*; First.; Oxford University Press: Oxford, **2013**; pp. 111–116.

(236) Aresta, M.; Quaranta, E. *Tetrahedron* **1992**, *48*, 1515–1530.

(237) Vaidyanathan, R.; Kalthod, V. G.; Ngo, D. P.; Manley, J. M.; Lapekas, S. P. *J. Org. Chem.* **2004**, *69*, 2565–2568.

(238) Aresta, M.; Dibenedetto, A. *Chem. Eur. J.* **2002**, *8*, 685–690.

(239) Aresta, M.; Quaranta, E. *Tetrahedron Lett.* **1991**, *47*, 9489–9502.

(240) Ram, S.; Ehrenkaufer, R. E. *Tetrahedron Lett.* **1985**, *26*, 5367–5370.

(241) Dean, C. S.; Tarbell, D. S. *J. Org. Chem.* **1971**, *36*, 1180–1183.

(242) Ram, S.; Ehrenkaufer, R. E.; Jewett, D. M. *Appl. Radiat. Isot.* **1986**, *37*, 391–395.

(243) Woodman, E. K.; Chaffey, J. G. K.; Hopes, P. A.; Hose, D. R. J.; Gilday, J. P. *Org. Process Res. Dev.* **2009**, *13*, 106–113.

(244) McCusker, E. O.; Scheidt, K. A. *Angew. Chem. Int. Ed.* **2013**, *52*, 13616–13620.

(245) Dell'Amico, D. B.; Calderazzo, F.; Labella, L.; Marchetti, F.; Pampaloni, G. *Chem. Rev.* **2003**, *103*, 3857–3898.

(246) Hampe, E. M.; Rudkevich, D. M. *Tetrahedron* **2003**, *59*, 9619–9625.

(247) Xu, H.; Rudkevich, D. M. *J. Org. Chem.* **2004**, *69*, 8609–8617.

(248) Danckwerts, P. V. *Chem. Eng. Sci.* **1979**, *34*, 443–446.

(249) George, M.; Weiss, R. G. *J. Am. Chem. Soc.* **2001**, *123*, 10393–10394.

(250) Hoerr, C. W.; Harwood, H. J.; Ralston, A. W. *J. Org. Chem.* **1944**, *9*, 201–210.

(251) Denning, D. M.; Falvey, D. E. *J. Org. Chem.* **2014**, *79*, 4293–4299.

(252) Halland, N.; Braunton, A.; Bachmann, S.; Marigo, M.; Jørgensen, K. A. *J. Am. Chem. Soc.* **2004**, *126*, 4790–4791.

(253) Beshara, C. S.; Hall, A.; Jenkins, R. L.; Jones, T. C.; Parry, R. T.; Thomas, S. P.; Tomkinson, N. C. O. *Chem. Commun.* **2005**, 1478–1480.

(254) Hassner, A.; Reuss, R. H.; Pinnick, H. W. *J. Org. Chem.* **1975**, *40*, 3427–3429.

(255) Gruber, J. M.; Rubottom, G. M. *Tetrahedron Lett.* **1978**, *47*, 4603–4604.

(256) Rubottom, G. M.; Gruber, J. M. *J. Org. Chem.* **1978**, *43*, 1599–1602.

(257) Barbier, P.; Benezra, C. *J. Org. Chem.* **1983**, *48*, 2705–2709.

(258) Kern, W.; Spiteller, G. *Tetrahedron* **1996**, *52*, 4347–4362.

(259) Zhu, Y.; Shu, L.; Tu, Y.; Shi, Y. *J. Org. Chem.* **2001**, *66*, 1818–1826.

(260) Crandall, J. K.; Batal, D. J.; Lin, F.; Reix, T.; Nadol, G. S.; Ng, R. A. *Tetrahedron* **1992**, *48*, 1427–1448.

(261) Crandall, J. K.; Rambo, E. *Tetrahedron* **2002**, *58*, 7027–7036.

(262) Cheshev, P.; Marra, A.; Dondoni, A. *Carbohydr. Res.* **2006**, *341*, 2714–2716.

(263) Boons, G.-J. In *Organic Synthesis with Carbohydrates*; Sheffield Academic Press: Sheffield, **2000**; pp. 1–24.

(264) Fraser-Reid, B. *Acc. Chem. Res.* **1975**, *8*, 192–201.

(265) Inch, T. D. *Tetrahedron* **1984**, *40*, 3161–3213.

(266) Ferrier, R. J.; Middleton, S. *Chem. Rev.* **1993**, *93*, 2779–2831.

(267) Mukaiyama, T.; Suzuki, K.; Yamada, T.; Tabusa, F. *Tetrahedron* **1990**, *46*, 265–276.

(268) Hanessian, S. *Acc. Chem. Res.* **1979**, *925*, 159–165.

(269) Nicolaou, K. C.; Mitchell, H. J. *Angew. Chemie Int. Ed.* **2001**, *40*, 1576–1624.

(270) Verheyden, J. P. H.; Richardson, A. C.; Bhatt, R. S.; Grant, B. D.; Fitch, W. L.; Moffatt, J. G. *Pure Appl. Chem.* **1978**, *50*, 1363–1383.

(271) Jones, R. A; Davidson, R.; Tran, A. T.; Smith, N.; Carmen Galan, M. *Carbohydr. Res.* **2010**, *345*, 1842–1845.

(272) Brito-Arias, M. In *Synthesis and Characterization of Glycosides*; Springer Science+Business Media, LLC, **2010**; pp. 1–67.

(273) Levy, D. E. In *The Organic Chemistry of Sugars*; Levy, D. E.; Fügedi, P., Eds.; CRC Press, **2006**; pp. 269–348.

(274) Isbell, H. S.; Frush, H. L. *J. Org. Chem.* **1968**, *23*, 1309–1319.

(275) Shu, L.; Shen, Y.-M.; Burke, C.; Goeddel, D.; Shi, Y. *J. Org. Chem.* **2003**, *68*, 4963–4965.

(276) Hassner, A.; Namboothiri, I. *Organic Syntheses Based on Name Reactions*; Third.; Elsevier Ltd: Oxford, **2012**.

(277) Liu, Y.; Chai, W.; Childs, R. A.; Feizi, T. *Methods Enzymol.* **2006**, *415*, 326–340.

(278) Liu, Y.; Feizi, T.; Campanero-Rhodes, M. A.; Childs, R. A.; Zhang, Y.; Mulloy, B.; Evans, P. G.; Osborn, H. M. I.; Otto, D.; Crocker, P. R.; Chai, W. *Chem. Biol.* **2007**, *14*, 847–859.

(279) Liu, Y.; Palma, A. S.; Feizi, T. *Biol. Chem.* **2009**, *390*, 647–656.

(280) Bestmann, H. J.; Angerer, J. *Tetrahedron Lett.* **1969**, *41*, 3665–3666.

(281) Pougny, J.-R.; Nassr, M. A. M.; Sinaÿ, P. *J. Chem. Soc. Chem. Commun.* **1981**, 375–376.

(282) Railton, C. J.; Clive, D. L. J. *Carbohydr. Res.* **1996**, *281*, 69–77.

(283) Popsavin, V.; Grabež, S.; Popsavin, M.; Krstić, I.; Kojić, V.; Bogdanović, G.; Divjaković, V. *Tetrahedron Lett.* **2004**, *45*, 9409–9413.

(284) Aucagne, V.; Tatibouët, A.; Rollin, P. *Tetrahedron* **2004**, *60*, 1817–1826.

(285) Boschetti, A.; Nicotra, F.; Panza, L.; Russo, G. *J. Org. Chem.* **1988**, *53*, 4181–4185.

(286) He, M.; Beahm, B. J.; Bode, J. W. *Org. Lett.* **2008**, *10*, 3817–3820.

(287) Balmond, E. I.; Coe, D. M.; Galan, M. C.; McGarrigle, E. M. *Angew. Chem. Int. Ed.* **2012**, *51*, 9152–9155.

(288) Bellucci, G.; Catelani, G.; Chiappe, C.; D'Andrea, F.; Grigo, G. *Tetrahedron: Asymmetry* **1997**, *8*, 765–773.

(289) Fulmer, G. R.; Miller, A. J. M.; Sherden, N. H.; Gottlieb, H. E.; Nudelman, A.; Stoltz, B. M.; Bercaw, J. E.; Goldberg, K. I. *Organometallics* **2010**, *29*, 2176–2179.

(290) Lerebours, R.; Wolf, C. *J. Am. Chem. Soc.* **2006**, *128*, 13052–13053.

(291) Kleeberg, C.; Dang, L.; Lin, Z.; Marder, T. B. *Angew. Chemie* **2009**, *121*, 5454–5458.

(292) Lee, Y. S.; Park, J. H.; Kim, M. H.; Seo, S. H.; Kim, H. J. *Arch. Pharm. Chem. Life Sci.* **2006**, *339*, 111–114.

(293) Arcelli, A.; Bongini, A.; Porzi, G.; Rinaldi, S. *J. Phys. Org. Chem.* **2012**, *25*, 132–141.

(294) Player, M. R.; Huang, H.; Huaping, H. US 2007/0060578 A1, **2007**.

(295) Caturla, F.; Jiménez, J.-M.; Godessart, N.; Amat, M.; Cárdenas, A.; Soca, L.; Beleta, J.; Ryder, H.; Crespa, M. I. *J. Med. Chem.* **2004**, *47*, 3874–3886.

(296) Plobeck, N.; Powell, D. *Tetrahedron: Asymmetry* **2002**, *13*, 303–310.

(297) Reiter, J.; Pongó, L.; Dyortsák, P. *Tetrahedron* **1987**, *43*, 2497–2504.

(298) Reiter, J.; Pongó, L.; Dvortsák, P. *J. Heterocycl. Chem.* **1987**, *24*, 1149–1154.

(299) Williams, L. A. *J. Chem. Soc.* **1962**, 2222–2228.

(300) Lin, H.; Liu, Y.; Wu, Z.-L. *Chem. Commun.* **2011**, *47*, 2610–2612.

(301) Verhé, R.; De Kimpe, N.; De Buyck, L.; Tilley, Ma.; Schamp, N. *Tetrahedron* **1980**, *36*, 131–142.

(302) Vora, H. U.; Rovis, T. *J. Am. Chem. Soc.* **2010**, *132*, 2860–2861.

(303) Armarengo, W. L. F.; Chai, C. L. L. *Purification of Laboratory Chemicals*; Sixth.; Butterworth-Heinemann Ltd., **2009**.

(304) Wong, L. S.; Chan, B.; Tan, E. W. *Tetrahedron Lett.* **2000**, *41*, 2671–2674.

(305) Stevens, C. L.; Dittmer, H.; Kovacs, J. *J. Am. Chem. Soc.* **1963**, *85*, 3394–3396.

(306) Suzuki, K.; Okano, K.; Nakai, K.; Terao, Y.; Sekiya, M. *Synthesis* **1983**, *9*, 723–725.

(307) Ahlsten, N.; Bermejo Gómez, A.; Martín-Matute, B. *Angew. Chem. Int. Ed.* **2013**, *52*, 6273–6276.

(308) Kunishima, M.; Yamamoto, K.; Watanabe, Y.; Hioki, K.; Tani, S. *Chem. Commun.* **2005**, 2698–7000.

(309) Nambu, H.; Hata, K.; Matsugi, M.; Kita, Y. *Chem. Eur. J.* **2005**, *11*, 719–727.

(310) Liu, M.-Z.; Fan, H.-N.; Guo, Z.-W.; Hui, Y.-Z. *Carbohydr. Res.* **1996**, *290*, 233–237.

(311) Schmidt, R. R.; Effenberger, G. *Carbohydr. Res.* **1986**, *171*, 59–79.